



TECHNISCHE UNIVERSITÄT MÜNCHEN

Integrative Research Center Campus Straubing für Biotechnologie und Nachhaltigkeit

Characterization of Biomimetic Nicotinamide Cofactors and Optimization of Enzymatic Regeneration Processes

Claudia Nowak

Vollständiger Abdruck der von der promotionsführenden Einrichtung Campus Straubing für Biotechnologie und Nachhaltigkeit der Technischen Universität München zur Erlangung des akademischen Grades eines

Doktors der Naturwissenschaften (Dr. rer. nat.)

genehmigten Dissertation.

Vorsitzender: Prof. Dr. Matthias Gaderer

Prüfer der Dissertation: 1. Prof. Dr. Volker Sieber
2. Prof. Dr. Cordt Zollfrank

Die Dissertation wurde am 18.06.2019 bei der Technischen Universität München eingereicht und von der promotionsführenden Einrichtung Campus Straubing für Biotechnologie und Nachhaltigkeit am 28.10.2019 angenommen.

Table of Contents

Summary	4
List of Publications.....	6
1 Introduction	7
1.1 Nicotinamide Cofactors – Natural and Biomimetic Derivatives	7
1.1.1 Oxidation and Reduction	7
1.1.2 Natural Nicotinamide Cofactors	8
1.1.3 Whole Cell Catalysis vs. Cell-free Catalysis	11
1.1.4 Application of Nicotinamide-Dependent Oxidoreductases in Biotechnology	12
1.1.5 Development of Biomimetic Cofactors	16
1.1.6 Biocatalysis Using Biomimetic Cofactors.....	18
1.2 Enzymatic Cofactor Regeneration.....	23
1.2.1 Cofactor Regeneration	23
1.2.1.1 Enzyme-coupled Cofactor Regeneration.....	23
1.2.1.2 Substrate-coupled Cofactor Regeneration.....	25
1.2.1.3 Reaction-internal Cofactor Regeneration.....	26
1.2.2 Glucose Dehydrogenase from <i>Sulfolobus solfataricus</i>	26
1.2.3 NADH Oxidase.....	28
1.3 Scope of Work.....	30
2 Material and Methods.....	31
2.1 Material.....	31
2.1.1 Equipment.....	31
2.1.2 Software and Databases.....	33
2.1.3 Chemicals	34
2.1.4 Enzymes.....	37
2.1.5 Kits and Standards	38
2.2 Media and Solutions	38
2.2.1 Media	38
2.2.2 Antibiotics	39
2.3 Bacterial Strains	39
2.4 Plasmids.....	40
2.5 Methods.....	41
2.5.1 Microbiological and Molecular Biological Methods.....	41
2.5.1.1 Measurement of the Optical Density of a Cell Suspension.....	41
2.5.1.2 Preparation of Chemically Competent Cells	41
2.5.1.3 Preparation of Chemically Competent - NEB Turbo	41
2.5.1.4 Transformation of Chemically Competent Cells.....	42
2.5.1.5 Preparation of Electro Competent Cells.....	42
2.5.1.6 Transformation of Electro Competent Cells	42
2.5.1.7 Calculation of Transformation Efficiency.....	43
2.5.1.8 Plasmid Extraction	43
2.5.1.9 Measurement of Plasmid Concentration	43
2.5.1.10 Agarose Gel Electrophoresis	43
2.5.1.11 Sequencing of DNA Fragments	44

2.5.2	Protein Analytics and Purification.....	44
2.5.2.1	Determination of Protein Concentration Using UV Spectroscopy.....	44
2.5.2.2	Determination of Protein Concentration Using the Bradford Assay.....	44
2.5.2.3	SDS Polyacrylamide Gel Electrophoresis.....	44
2.5.2.4	Cell Disruption by Sonication.....	45
2.5.3	Chemical Methods.....	46
2.5.3.1	Reaction Control During Chemical Synthesis of the Biomimetic Cofactors.....	46
2.5.3.2	NMR Analysis.....	46
3	Results.....	47
3.1	Regeneration of Oxidized Biomimetic Cofactors by NADH Oxidase from <i>Lactobacillus pentosus</i>.....	47
3.1.1	A water-forming NADH oxidase from <i>Lactobacillus pentosus</i> suitable for the regeneration of synthetic biomimetic cofactors.....	47
3.1.2	Characterization of Biomimetic Cofactors According to Stability, Redox Potentials, and Enzymatic Conversion by NADH Oxidase from <i>Lactobacillus pentosus</i>	58
3.2	Enzymatic Reduction of Nicotinamide Biomimetic Cofactors Using an Engineered Glucose Dehydrogenase: Providing a Regeneration System for Artificial Cofactors	66
4	Discussion and Prospects	75
4.1	Characterization and Optimization of Enzymes	75
4.1.1	NADH Oxidase from <i>Lactobacillus pentosus</i>	75
4.1.2	Glucose Dehydrogenase from <i>Sulfolobus solfataricus</i>	77
4.2	Characterization and Optimization of Biomimetic Cofactors.....	79
4.3	Optimization of the Reaction/Regeneration Process	81
5	References.....	83
6	Appendix	93
6.1	Supporting Information - A water-forming NADH oxidase from <i>Lactobacillus pentosus</i> suitable for the regeneration of synthetic biomimetic cofactors	93
6.2	Supporting Information - Characterization of Biomimetic Cofactors According to Stability, Redox Potentials, and Enzymatic Conversion by NADH Oxidase from <i>Lactobacillus pentosus</i>	97
6.3	Supporting Information - Enzymatic Reduction of Nicotinamide Biomimetic Cofactors Using an Engineered Glucose Dehydrogenase: Providing a Regeneration System for Artificial Cofactors	109
6.4	NMR of Biomimetic Cofactors	144
6.5	List of Enzymes Additionally Investigated for the Activity with Biomimetic Cofactors	148
7	Abbreviations.....	149
8	List of Figures	154
9	List of Tables.....	156
	Curriculum vitae	157

Summary

The optimization of biotechnological processes is of interest in order to create alternative synthetic pathways to so far petroleum-based products (ERICKSON et al. 2012; SHELDON & WOODLEY 2018). For the synthesis of high-value products, oxidoreductases might be used, but the fact that they are cofactor dependent needs to be considered in process design. Hence, efficient biocatalysis involving these enzymes is usually based on a combined reaction/regeneration process or designed as a pathway that is redox balanced. However, the cofactor remains a cost-pushing factor. Thus, the development of biomimetic cofactors, which are cheaper than their natural counterparts (nicotinamide cofactors - NAD(P)/H) and which can easily be synthesized, and the efficient use of these molecules in enzymatic catalysis would further increase the applicability of products synthesized *via* green chemistry (GEDDES et al. 2016).

However, various disadvantages that restrict the extensive use of synthetic cofactors need to be overcome like the strongly restricted number of enzymes available for biomimetic catalysis as well as the stability of the biomimetic molecules, especially of the reduced forms. In the cell-free processes involving biomimetic cofactors described so far, recycling of these synthetic molecules was performed with metal catalysts (OKAMOTO et al. 2016).

Within this work, two enzymatic regeneration systems, namely NADH oxidase from *Lactobacillus pentosus* (*LpNox*) and glucose dehydrogenase from *Sufolebus solfataricus* (*SsGDH*), were described for the conversion of totally synthetic biomimetic cofactors that contain a nicotinamide moiety, an alkyl chain, and in some instances a phenyl group.

Several known biomimetic cofactors and variations thereof were tested. During characterization of these biomimetic cofactors, the molecule containing an ethyl chain between the nicotinamide moiety and phenyl group was found to be as stable as the natural nicotinamide cofactors NAD(P)H. However, further improvements in stability and solubility are also needed to further increase their applicability.

The flavin dependent *LpNox* was found to be able to oxidize all tested biomimetics after *in vitro* loading of the enzyme with FAD. Here, the side product water was formed. Free FAD was also able to convert the biomimetics, however, the by-product hydrogen peroxide was detected instead. Depending on the recycling strategy, *LpNox* or free FAD can be used for the regeneration of the tested oxidized biomimetics differing in side product formation. However, *LpNox* holds the potential to be evolvable.

Furthermore, *SsGDH* was shown to reduce the totally synthetic cofactors, which contain a phenyl group. Enzyme engineering was performed to increase the reaction rates and also to get more information on the binding of the biomimetic cofactors in the cofactor binding site. Two of the seven investigated positions were found to increase activity. The combination of these single variants resulted in an enzyme with a ten-fold higher activity compared to the wild-type enzyme. Exchange of the nonpolar and large isoleucine with a smaller and more polar threonine in Ile192Thr, which could also act as a hydrogen donor and acceptor, supported binding interactions in combination with the mutation Val306Ile. With this *SsGDH* variant and the enoate reductase from *Thermus scotoductus* (*TsER*), the applicability of biomimetic cofactors in a biocatalytic reaction/regeneration process was shown. However, both enzymes still have a high preference for the natural cofactors, which disturbs a process that is supposed to be based on synthetic cofactors. Thus, an additional trap for NAD(P)/H needed to be included to get the desired process run solely based on the conversion of biomimetic

cofactors. Overall, further improvement of both enzymes is needed to reduce the preference for the natural cofactors and simultaneously increase the activity with the biomimetics.

List of Publications

Nowak, Claudia; Beer, Barbara Caroline; Pick, André; Roth, Teresa; Lommes, Petra and Sieber, Volker (2015): A water-forming NADH oxidase from *Lactobacillus pentosus* and its potential application in the regeneration of synthetic biomimetic cofactors. In: *Frontiers in Microbiology*, Vol. **6**, S. 957, DOI: 10.3389/fmicb.2015.00957.

Nowak, Claudia; Pick, André; Lommes, Petra and Sieber, Volker (2017): Enzymatic Reduction of Nicotinamide Biomimetic Cofactors Using an Engineered Glucose Dehydrogenase: Providing a Regeneration System for Artificial Cofactors. In: *ACS Catalysis*, Vol. **7**, 8, S. 5202-5208, DOI: 10.1021/acscatal.7b00721.

Nowak, Claudia; Pick, André; Csepei, Lénárd-István and Sieber, Volker (2017): Characterization of Biomimetic Cofactors According to Stability, Redox Potentials, and Enzymatic Conversion by NADH Oxidase from *Lactobacillus pentosus*. In: *ChemBioChem*, Vol. **18**, 19, S. 1944-1949, DOI: 10.1002/cbic.201700258.

Zachos, Ioannis; **Nowak, Claudia** and Sieber, Volker (2019): Biomimetic cofactors and methods for their recycling. In: *Current Opinion in Chemical Biology*, Vol. **49**, S. 59-66, DOI:10.1016/j.cbpa.2018.10.003.

1 Introduction

1.1 Nicotinamide Cofactors – Natural and Biomimetic Derivatives

1.1.1 Oxidation and Reduction

Since the end of the 18th century, the chemical community had defined combustion as any reaction involving oxygen. Following this, Antoine-Laurent Lavoisier defines such a reaction as oxidation, whereas a reaction, in which a chemical compound releases oxygen, as reduction. In a redox reaction, a combination of oxidation and reduction, oxygen is transferred from one reactant to the other (according to the definition of Antoine-Laurent Lavoisier) (ACS). Nowadays, oxidation and reduction are defined based on the level of electron movement, which also include reactions that do not involve oxygen. Accordingly, oxidations and reductions are reactions, in which electrons are removed from the atom or added to the atom, respectively. Thus, the valence of the atom is changed resulting in an oxidized or reduced state. However, this definition may not be completely suitable for organic compounds, as these molecules normally remain without a charge after oxidation or reduction. Organic molecules that undergo such reactions perform a two electron or multiple electron transfer for keeping the electrons paired. Even after oxidation or reduction, atoms like carbon, hydrogen, or oxygen remain without a charge, whereas nitrogen or sulfur for example, are more likely to adopt a valence after redox reactions (HAMILTON 2009).

Enzymes, namely oxidoreductases (enzyme class [EC] 1), catalyze the oxidation and reduction of several organic compounds. Looking at the natural metabolic pathways, oxidoreductases participate, among others, in the overall conversion of D-glucose to pyruvate in glycolysis, that is the conversion of glyceraldehyde 3-phosphate to 1,3-bisphosphoglycerate with glyceraldehyde 3-phosphate dehydrogenase or catalyze various steps in the citric acid cycle, i.e. isocitrate dehydrogenase, malate dehydrogenase, succinate dehydrogenase (VOET et al. 2002). Advantages of oxidoreductase catalyzed reactions include high selectivity and stereospecificity as well as high reaction rates under mild conditions (MAY & PADGETTE 1983). Generally, oxidoreductases are dependent on cofactors that are defined as “*any non-protein substance required for a protein to be catalytically active. Some cofactors are inorganic, such as the metal atoms zinc, iron, and copper in various oxidation states. Others, such as most vitamins, are organic. Cofactors are generally either bound tightly to active sites, or may bind loosely with the enzyme. They may also be important for structural integrity, i.e. if they are not present, the enzyme does not fold properly or becomes unstable*” (RICHTER 2013; UNIPROT Last modified December 5, 2014). Organic cofactors for example are adenosine-5' phosphate, adenosine-5' diphosphate, adenosine-5' triphosphate, vitamins and their derivatives, flavin mononucleotide (FMN), flavin adenine dinucleotide (FAD), nicotinamide adenine dinucleotide (oxidized/reduced state), or nicotinamide adenine dinucleotide phosphate (oxidized/reduced state) (WU et al. 2013). Among these, flavin cofactors remain in the active site of the enzyme during catalysis and are self-regenerating. In contrast, nicotinamide or adenosine cofactors bind to the enzyme during the catalytic cycle, provide their functional group for the conversion of the substrate to the product and are released thereafter. Hence, these cofactors are not self-regenerating and need to be added in stoichiometric amounts in a cell-free reaction system (RICHTER 2013; ZHAO & VAN DER DONK 2003).

1.1.2 Natural Nicotinamide Cofactors

Nicotinamide cofactors are among the most common electron carrier molecules in nature and perform the transfer of a hydride - one proton with two electrons. Nicotinamide cofactors include nicotinamide adenine dinucleotide (NAD^+), dihydro nicotinamide adenine dinucleotide (NADH), nicotinamide adenine dinucleotide phosphate (NADP^+), and dihydro nicotinamide adenine dinucleotide phosphate (NADPH). In living cells, NAD^+ is mostly used for catabolic reactions, whereas NADPH can be found in anabolic processes. They are composed of a nicotinamide moiety connected with a ribose, a pyrophosphate, and an adenosine. In comparison to NAD/H , NADP/H is phosphorylated at C2 of the riboside (VOET et al. 2002) (Figure 1 A). These molecules can act as electron donor (NAD(P)H) or acceptor (NAD(P)^+) by reversibly releasing or accepting a hydride at C4 of the nicotinamide ring, respectively (PAUL et al. 2014a) (Figure 1 B).

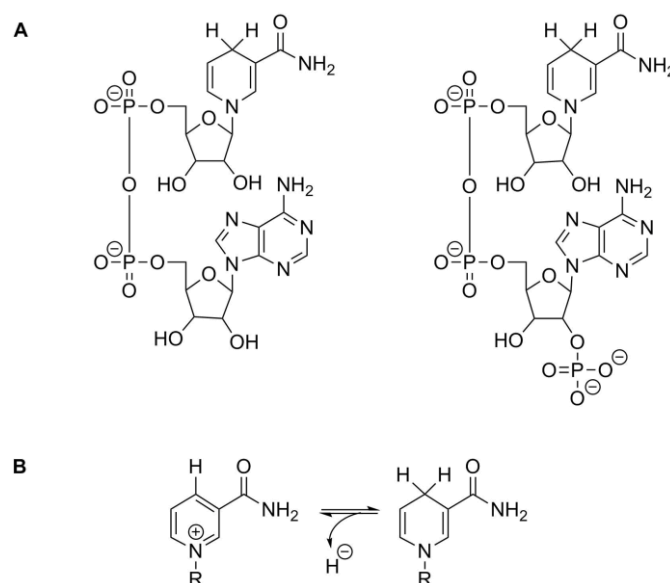


Figure 1: **A)** The natural nicotinamide cofactors, NADH and NADPH , are composed of a nicotinamide moiety, a ribose, a pyrophosphate, and an adenosine. NADP/H is phosphorylated at C2 of the riboside compared to NAD/H . **B)** The C4 of the nicotinamide moiety releases or accepts the hydride, respectively.

In the 1970s, Rossmann *et al.* compared four crystal structures of NAD(P)/H dependent enzymes resulting in the assumption that the tertiary structure of the nicotinamide cofactor binding domain is highly conserved. Furthermore, a structural motif containing β -sheets and α -helices, nowadays called the Rossmann fold, was described (pattern: $\beta\alpha\beta\alpha\beta$, Figure 2). The region around 30 to 35 amino acids counting from beginning of the pattern was defined as the fingerprint region due to its high similarity. This region is characterized by a phosphate binding sequence (GXGXG), small hydrophobic amino acids (in six positions), a negatively charged amino acid at the end of the motif, and a positively charged amino acid at the beginning of the motif. Overall, in a classical cofactor binding domain, NAD(P)/H was found to bind in an extended conformation and similar orientation including hydrogen bonds and van der Waals interactions (Figure 2). Accordingly, the substrate is bound in the substrate binding domain in an orientation, so that it is in close proximity to NAD(P)/H . Variations in enzymatic mechanisms are caused by different cofactor conformations, particular substrate positioning in the

enzyme and the amino acid composition (BELLAMACINA 1996; ROSSMANN 1976; ROSSMANN et al. 1974).



Figure 2: The Rossmann fold of glucose dehydrogenase from *Sulfolobus solfataricus* (MILBURN et al. 2006) contains three β -sheets and two α -helices (green colour). The first three β -sheets are connected by α -helices. Additionally, this pattern is duplicated. The GXGXXG motif is highlighted in yellow. Additionally, NAD(P)/H binds an extended conformation and the orientation including hydrogen bonds and van der Waals interactions is similar in a classical cofactor binding domain.

Looking at the chemical stability of NAD(P)/H, early experiments already showed that NAD(P)H is degraded under acidic conditions, whereas NAD(P)⁺ is not affected. However, under alkaline conditions, NAD(P)H molecules remain stable and NAD(P)⁺ is decomposed (ADLER et al. 1936; VON EULER et al. 1936; WARBURG et al. 1935). During acid catalyzed decomposition of NAD(P)H, the C5 atom of the 5,6-double bond is protonated following nucleophilic attack of the corresponding imine (OPPENHEIMER & KAPLAN 1974; WONG & WHITESIDES 1981) (Figure 3 A). Alkali treatment of NAD(P)⁺ leads to hydrolysis of the nicotinamide-ribose bond caused by the nucleophilic attack of the hydroxide. Nicotinamide is good leaving group, the reaction is strongly thermodynamically favored and the resulting oxocarbenium intermediate is considerably stable (KAPLAN et al. 1951; OPPENHEIMER 1994) (Figure 3 B). The cleavage of pyrophosphate results in adenylic acid and its release was only detected after primary cleavage of the nicotinamide-ribose linkage during alkali treatment (KAPLAN et al. 1951). Additional research also showed the formation of 2-hydroxy-3-pyridine carboxaldehyde after incubation of NAD⁺ under alkaline conditions due to addition of the hydroxide to the nicotinamide ring following ring opening, elimination, and recyclization (GUILBERT & JOHNSON 1971; GUILBERT & JOHNSON 1977; JOHNSON & MORRISON 1970) (Figure 3 B).

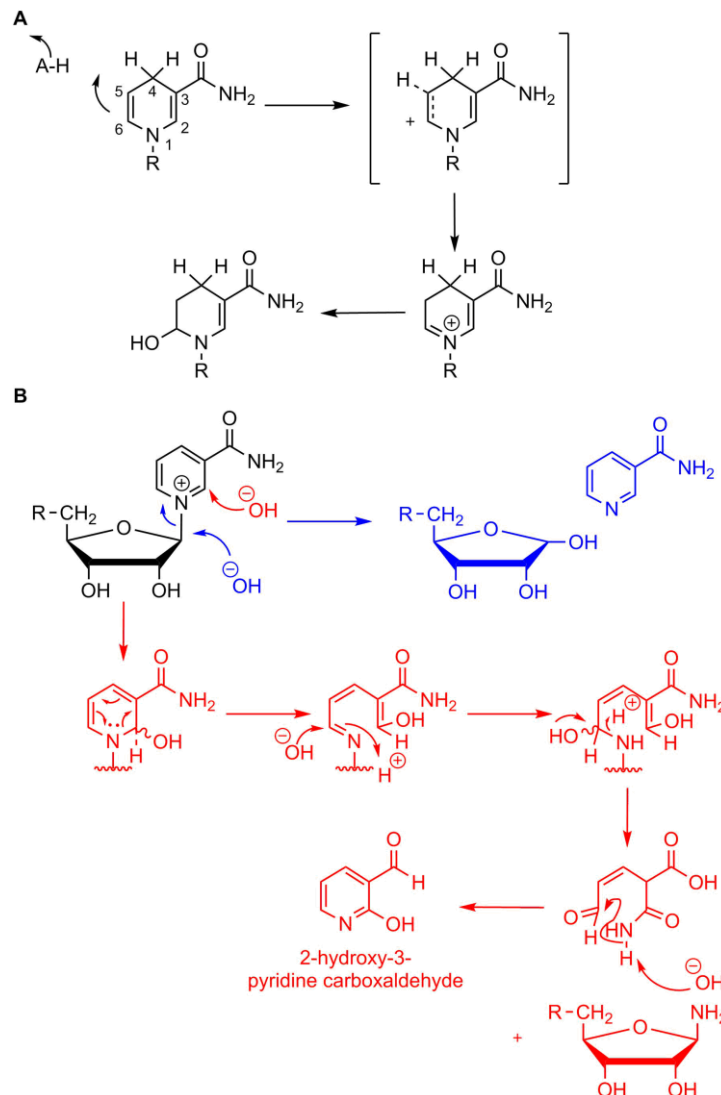


Figure 3: **A**) Acid catalyzed decomposition of NAD(P)H. **B**) Degradation of NAD(P)⁺ under alkaline conditions. (HENTALL et al. 2001; OPPENHEIMER 1982; OPPENHEIMER 1994; OPPENHEIMER & KAPLAN 1974)

In addition to the acid catalyzed degradation of NAD(P)H, Lowry *et al.* found that the reduced nicotinamide cofactors are converted to the oxidized forms after storage for a longer period of time depending on the time of storage, pH values, temperature, and cofactor concentration (LOWRY et al. 1961). A solution of 40 mM NADH was stable at -20 °C at pH values ranging from 9.1 to 12.7, but degradation was found at 4 °C in the more alkaline range. But a solution of 0.4 mM NADH was more stable at 4 °C compared to the degradation at -20 °C (pH > 10.5). According to the explanation of Lowry and coworkers, the oxidation at the higher pH values was catalyzed by impurities in the NADH solution or NADH itself. In addition, these impurities would be concentrated in the liquid phase at -20 °C and would increase the oxidation in the 0.4 mM solution. Due to precipitation, NADH molecules in the 40 mM solution are more protected.

Colowick *et al.* also observed that the rate of decomposition of the natural nicotinamide cofactor is different in various buffers (pH 7.5) resulting in an increased rate of hydrolysis when phosphate or citrate buffer was used (three- to four-fold). This rate of hydrolysis remained unchanged when incubated in Tris(hydroxymethyl)aminomethan (Tris) and acetate buffer compared to an unbuffered

solution (COLOWICK *et al.* 1951). Anderson *et al.* verified the various effects of buffers on the nicotinamide cofactors. The results showed that while using Tris, imidazole, or glycylglycine buffer the rate of hydrolysis was lowest compared to phosphate buffer, where the highest amount of degradation could be detected. Overall, the same products of degradation were detected in all buffers (ANDERSON & ANDERSON 1963). Following this, Alivisatos *et al.* described a mechanism of NADH and phosphate interaction, which was verified by absorption measurements. The 5,6-double bond interacts with the phosphate by forming a charge transfer complex resulting in the decomposition of the nicotinamide cofactor including the addition of a phosphate group on the 5,6-double bond (ALIVISATOS *et al.* 1964) (Figure 4).

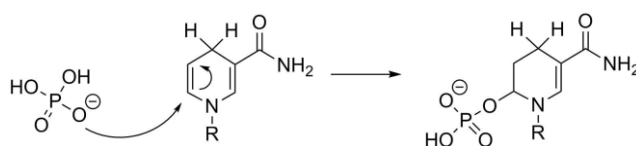


Figure 4: Interaction of NADH with phosphate (from the buffer) following cofactor degradation. (ALIVISATOS *et al.* 1964)

Generally, most research has focused on NADH degradation. Lowry *et al.* found that the degradation of NADPH was about 80% faster than the decomposition of NADH (30 °C, pH 2 to 4.5). However, an explanation for this increased instability was not provided taking into account that NADH and NADPH only differ in a phosphate group at the ribose of the adenosine (LOWRY *et al.* 1961).

1.1.3 Whole Cell Catalysis vs. Cell-free Catalysis

In an economical process design, the properties of the biocatalysts as well as of the nicotinamide cofactors need to be considered. Generally, whole cell biocatalysis and cell-free biocatalysis are available options for the production of various value-added fine or bulk compounds.

The advantage of whole-cell biocatalysis is that all compounds are naturally regenerated and reproduced in a closed reaction system. However, limitations might also occur regarding the cofactor supply or regeneration, when the reaction of interest is too fast. Nevertheless, the efficiency of whole cell biocatalysis is increased due to the stabilization of the enzyme and the cofactor even under harsh conditions to the protective nature of the cell (LIN & TAO 2017). Anyhow, side pathways in the cell leading to undesired products may also be present.

The use of crude cell extracts or purified enzymes in a cell-free approach eliminates undesired side reaction pathways, since the biosynthesis is performed outside of the cell while just using the enzyme(s) and single reaction components. Due to the simplicity of the system, new reaction routes can easily be designed including a simplified reaction control (ROLLIN *et al.* 2013; ZHANG 2010).

Considering industrial reactions involving oxidoreductases, the supply of cofactor plays an important role when creating biotechnological processes in an economical and efficient manner, as 80% of the described oxidoreductases need NAD/H and 10% of these biocatalysts require NADP/H. The addition of stoichiometric amounts of cofactor in cell-free synthesis is far too expensive due to the high cost of NAD(P)/H (Table 1) and its instability (discussed in section 1.1.2). Thus, an efficient regeneration system needs to be included in the reaction setup, which among other concerns, considers the chemical

instability of the nicotinamide cofactors (WU et al. 2013), inhibitory effects, removal of side products (PAUL et al. 2014a), and may also be used multiple times (WU et al. 2013).

Table 1: Overview on costs of NAD(P)/H (obtained from Carl Roth GmbH & Co. KG online on 10.11.2018).

Nicotinamide cofactor	Prize
NAD ⁺	12,70 €/mol
NADH	23,34 €/mol
NADP ⁺	88,58 €/mol
NADPH	491,71 €/mol

1.1.4 Application of Nicotinamide-Dependent Oxidoreductases in Biotechnology

The advantages of a particular reaction catalyzed by oxidoreductases might be high reaction rates, wide substrate range, high regio-, stereo- and enantioselectivity, mild reaction conditions, possibility of overexpression of the biocatalyst, optimization of activity by directed evolution, simple reaction system, “green” process design, and low waste products. Generally, the use of biocatalysis represents a green and sustainable technology. The biobased industrial synthesis of for example pharmaceutical ingredients was empowered by advancements in protein engineering for the optimization of the biocatalysts, the development of synthetic reactions routes that could not be found in nature or substrate, medium, and reactor engineering, all to further increase the reaction and economic efficiency. Thus, the sustainability of a biocatalytic reaction is improved (SHELDON & WOODLEY 2018).

Overall, there are some examples for efficient biocatalysis using oxidoreductases. Nicotinamide dependent, flavin containing Baeyer-Villiger monoxygenases were for instance used for the conversion of ketones into the corresponding esters or lactones, respectively (Figure 5). Within this process, dynamic kinetic resolution was applied, which is normally used in the scope of hydrolase catalyzed reactions. Various α -alkyl- β -esters were converted in an enantioselective oxidation including base catalyzed racemization to the corresponding (S)-diesters. Conversions of close to 100% and high stereoselectivities were achieved (enantiomeric excess [*ee*] > 99%). After acid hydrolysis, the α -hydroxy esters were obtained in yields of about 60% to 85% with high optical purity and may be used as a compound for bioactive drugs (RIOZ-MARTINEZ et al. 2011).

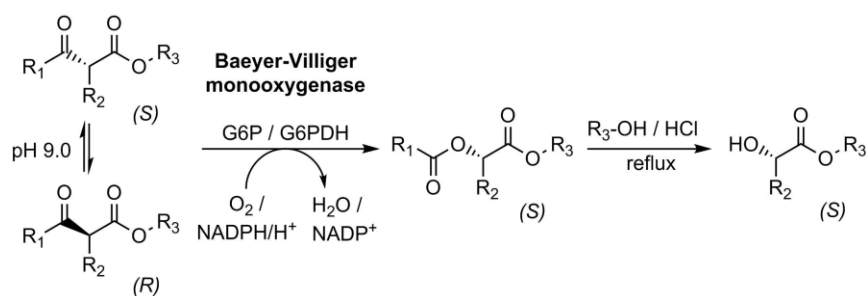


Figure 5: Dynamic kinetic resolution applying a Baeyer-Villiger monoxygenase for the synthesis of α -hydroxy esters. Cofactor regeneration was achieved with glucose-6-phosphate (G6P) and glucose-6-phosphate dehydrogenase (G6PDH). (RIOZ-MARTINEZ et al. 2011; SIMON et al. 2013)

A lot of attention has been given to alcohol dehydrogenases for the synthesis of chiral alcohols using their large availability and high stereospecificity (DE WILDEMAN et al. 2007). Alcohol dehydrogenase catalyzed asymmetric reductions of ketones are dependent on nicotinamide cofactors that may be recycled using various regeneration techniques.

The cholesterol lowering drug atorvastatin was synthesized by the reduction of ethyl 4-chloro-3-oxobutanoate catalyzed by alcohol dehydrogenase ($ee > 99\%$, isolated yield 95%, substrate concentration $160 \text{ g}\cdot\text{L}^{-1}$), followed by the replacement of chlorine with a cyano moiety using halohydrin dehalogenase and various steps finally leading to the desired product (Figure 6). Cofactor regeneration was achieved by the integration of a D-glucose/glucose dehydrogenase system (MA et al. 2010).

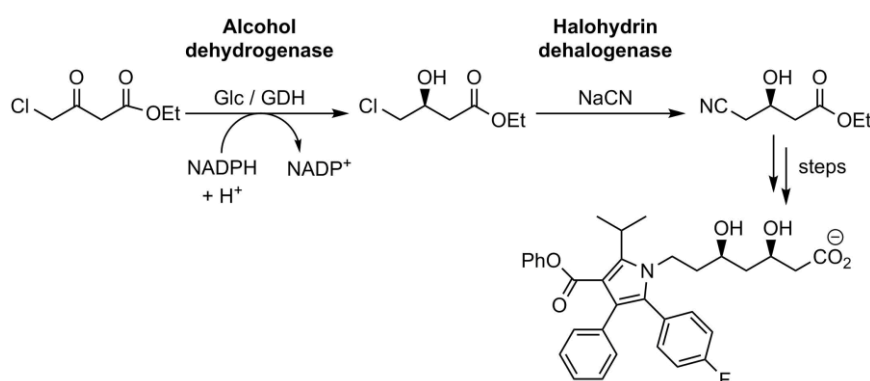


Figure 6: Alcohol dehydrogenase catalyzed redox reaction for the introduction of an alcohol group in the overall synthesis to atorvastatin. Cofactor regeneration was achieved with D-glucose (Glc) and glucose dehydrogenase (GDH). (MA et al. 2010; SIMON et al. 2013)

Another example is the synthesis of (R)-tetrahydrothiophene-3-ol that is an intermediate in the production of the potent antibacterial agent sulopenem (Figure 7). Within this process, an engineered alcohol dehydrogenase catalyzed the conversion of the corresponding ketone to (R)-tetrahydrothiophene-3-ol. At a substrate concentration of $100 \text{ g}\cdot\text{L}^{-1}$, a quantitative conversion was achieved within 24 hours as well as a stereoselectivity of $ee > 99$ (LIANG et al. 2010).

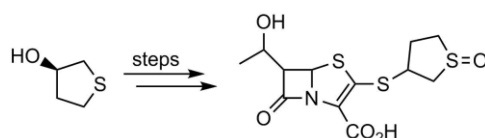


Figure 7: Alcohol dehydrogenase dependent reaction to (R)-tetrahydrothiophene-3-ol for the overall synthesis of sulopenem. (LIANG et al. 2010; SIMON et al. 2013)

Flavin and nicotinamide dependent Old Yellow Enzymes (OYE) catalyze the reduction of activated C=C bonds as in α,β -unsaturated carbonyls, nitroalkenes, esters, nitriles, or lactones. They were applied in the O-allyl- and O-benzyl-2-hydroxymethylacrylate reduction leading to (R)-configured Roche ester, which may be used as a precursor for vitamins (e.g. α -tocopherol) and antibiotics (e.g. calcimycin, palinurin, rapamycin, 13-deoxytedanolide dictyostatin) (Figure 8). For instance, the enzyme xenobiotic reductase A synthesized a Roche ester with a conversion of 97% and a high stereoselectivity ($ee > 99\%$) (STUECKLER et al. 2010).

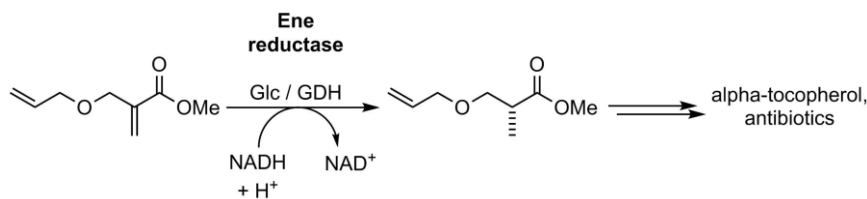


Figure 8: Ene reductase catalyzed reaction for the overall synthesis of α -tocopherol or antibiotics. Cofactor regeneration was achieved with D-glucose (Glc) and glucose dehydrogenase (GDH). (SIMON et al. 2013; STUECKLER et al. 2010)

Most enzymatic reactions in organic synthesis consist only of one or two enzyme-catalyzed steps. However, multistep reactions including a higher number of enzymes are progressively developed (GUTERL et al. 2012). Such cascade reactions are characterized by a one pot reaction that combines numerous single reaction steps without isolation of intermediates (KROUTIL & RUEPING 2014).

Sattler and coworkers showed the amination of primary alcohols using such an approach (Figure 9). In the first step, an alcohol was converted to an aldehyde catalyzed by NAD⁺-consuming alcohol dehydrogenase from *Bacillus stearothermophilus*. Afterwards, the aldehyde was aminated by a ω -transaminase from *Chromobacterium violaceum* using L-alanine (L-Ala) as the amine donor. Regeneration of L-alanine as well as NAD⁺ was simultaneously done by an alanine dehydrogenase (AlaDH), thus, connecting the oxidation and the reductive amination. Additionally, deamination was performed in a preparative scale (174 mg of substrate) leading to 94% conversion and 70% isolated yield. Generally, the resulting amines may be used as building blocks in the chemical industry for the production of polymers or dyes and represent intermediates for various industrial applications (SATTLEL et al. 2012).

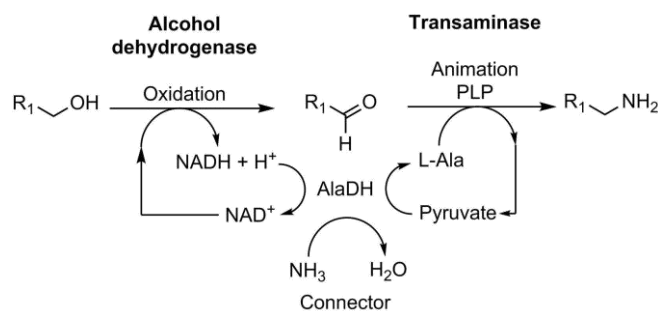


Figure 9: One pot reaction combining various enzymes for the bioamination of primary alcohols. The coenzyme pyridoxal 5'-phosphate (PLP) need to be additionally added for the animation reaction. (SATTLEL et al. 2012)

Another artificial reaction cascade showed the conversion of D-glucose *via* pyruvate (4-enzyme-catalysis) resulting in either isobutanol or ethanol (Figure 10). Phosphorylation requirements were not necessary and the overall process is redox balanced with respect to NAD⁺. Synthesis of ethanol requires a set of six enzymes demonstrating that conversion of 25 mM D-glucose using 5 mM NAD⁺ in 19 h leads to 28.7 mM ethanol (molar yield: 57.4%). For the production of isobutanol, a combination of nine biocatalysts is necessary. It was shown that 10.3 mM isobutanol could be produced starting from 19.1 mM D-glucose in 23 h representing a molar yield of 53% (GUTERL et al.

2012). The process was run at 50 °C. Hence, instability of the reduced cofactor NADH was also noticed following accumulation of the intermediate acetaldehyde (STEFFLER 2014).

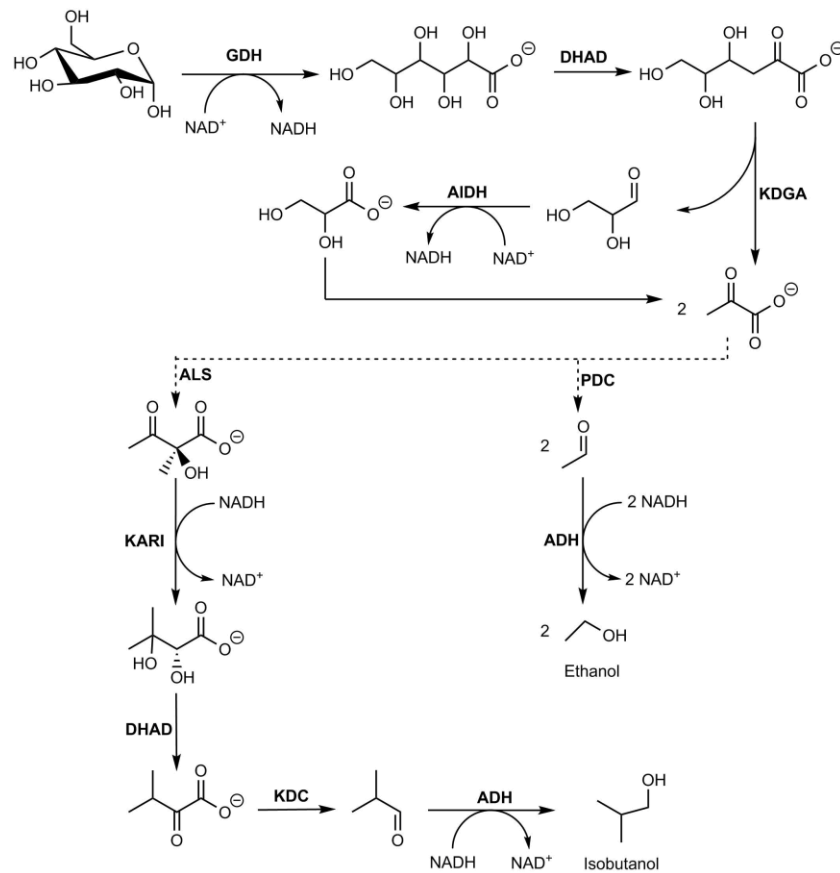


Figure 10: Multi-step reaction cascade for the overall synthesis of ethanol or isobutanol, respectively. The following enzymes were used: glucose dehydrogenase (GDH), dihydroxy acid dehydratase (DHAD), 2-keto-3-desoxygluconate aldolase (KDGA), glyceraldehyde dehydrogenase (AIDH), pyruvate decarboxylase (PDC), alcohol dehydrogenase (ADH), acetolactate synthase (ALS), ketolacid reductoisomerase (KARI), and 2-ketoacid decarboxylase (KDC). (GUTERL et al. 2012)

Furthermore, the *in vitro* synthesis of α -ketoglutarate, which may be used for medical treatment or as a chemical building block (Figure 11), using a set of five enzymes including an enzyme for cofactor regeneration resulted in the conversion of $10 \text{ g}\cdot\text{L}^{-1}$ of the starting material glucuronate with a yield of 92% α -ketoglutarate within 5 h. A productivity of $2.8 \text{ g}\cdot\text{L}^{-1}\cdot\text{h}^{-1}$ was achieved (BEER et al. 2017).

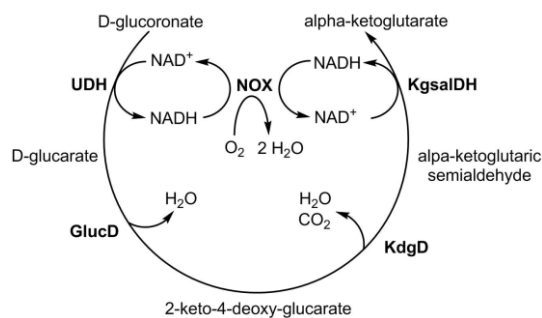


Figure 11: Multistep synthesis combining various enzymes for the synthesis of α -ketoglutarate. The following enzymes were used: uronate dehydrogenase (UDH), glucarate dehydratase (GlucD), 5-keto-4-deoxyglucarate dehydratase (KdgD), aldehyde dehydrogenase (KgsalDH), and NADH oxidase (NOX). (BEER et al. 2017)

In conclusion, there are numerous possibilities for the use of cofactor-dependent reactions available including enzymes from commercial sources and non-commercial sources, or even new biocatalysts, thus, cofactor dependence must not be a major drawback in “green” biocatalysis. An example for a commercial source is the protein engineering company Codexis, which offers complete screening kits, among others, for the reduction of ketones, diketones, and keto esters (CODEXIS 2018).

1.1.5 Development of Biomimetic Cofactors

As described previously, natural cofactors have some drawbacks and are expensive in a cell-free process. In an attempt to reduce process operation costs, the research was focused on artificial cofactors (i.e. biomimetics).

In the beginning of the 20th century, the existence of NAD(P)/H was first recognized by Harden and coworkers in reactions catalyzed by yeast juice (HARDEN & YOUNG 1906a; HARDEN & YOUNG 1906b). Thereafter, the molecules were isolated and purified, and the structure of NAD(P)/H was determined (VON EULER et al. 1936; WARBURG & CHRISTIAN 1931; WARBURG et al. 1935). Within this time, the release or acceptance of the hydride at C4 of the nicotinamide ring was also discovered including differences in absorption comparing the oxidized and reduced form (WARBURG & CHRISTIAN 1936).

In 1937, Karrer and coworkers synthesized a set of totally synthetic nicotinamide analogues (Figure 12) for the very first time to get a better understanding of the chemical properties of NAD(P)/H and their interactions with enzymes (KARRER & STARE 1937).

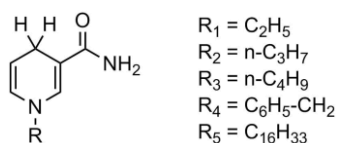


Figure 12: Biomimetic cofactors synthesized in the beginning of the 20th century. (KARRER & STARE 1937)

To clearly demonstrate the hydrogen transfer of the C4 of the dihydro nicotinamide ring in enzymatic and non-enzymatic reactions, Mauzerall *et al.* synthesized deuterated 1-benzyl-1,4-dihydro nicotinamide (BNAH) variants. As a result, it was shown that neither the deuterium of the 2-position

nor the deuterium of the 6-position of the dihydro nicotinamide ring was transferred during reduction of malachite green (MAUZERALL & WESTHEIMER 1955). Only the transfer of the deuterium at the 4-position to the substrate could be detected. These discoveries were further supported by the results obtained *via* nuclear magnetic resonance (NMR) spectrometry using N-methyl-1,4-dihydro nicotinamide (MNAH) as a biomimetic cofactor (HUTTON & WESTHEIMER 1958). The results were expanded during the mid-20th century (EISNER & KUTHAN 1972; WESTHEIMER 1962).

Today's synthesis of synthetic biomimetic cofactors is based on the descriptions of the early 20th century (KNAUS et al. 2015; OKAMOTO et al. 2016; PAUL et al. 2013). The oxidized form can be prepared from nicotinamide and the desired alkyl-phenyl halide (e.g. benzyl chloride) followed by the reduction with sodium dithionite to obtain the reduced biomimetic cofactor (Figure 13).

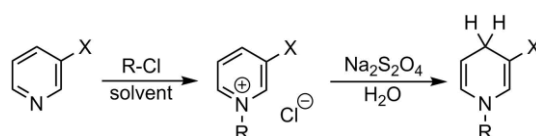


Figure 13: General synthesis of oxidized and reduced biomimetic cofactors. (PAUL et al. 2013)

Furthermore, semi-synthetic cofactors were also developed. They are structurally very similar to the natural nicotinamide cofactors compared to the totally synthetic biomimetics described above. In the 1950s, Kaplan and coworkers prepared a set of semisynthetic biomimetics (e.g. 3-acetylpyridine or pyridine-3-aldehyde analogue of NADH) using pig brain NADase, a NAD⁺ glycohydrolase that catalyzes ADP-ribose transfer, for synthesis (KAPLAN & CIOTTI 1954; KAPLAN & CIOTTI 1956) and showed their activities with various oxidoreductases like yeast alcohol dehydrogenase or horse liver alcohol dehydrogenase (HLADH) (KAPLAN et al. 1956; WEBER & KAPLAN 1956). Further research on this topic was done using cofactors with variations at position 3 of the nicotinamide part concluding that the replacement of this group without loss of cofactor activity in different dehydrogenases is indeed possible (Figure 14). Additionally, it was stated that every variation on the nicotinamide part could have a great influence on the overall reactivity including steric effects. HLADH was active with all the biomimetics tested (ANDERSON et al. 1959; ANDERSON & KAPLAN 1959). Ansell and coworkers presented various synthetic cofactors containing the triazine ring, a dibenzene sulphonic acid unit or/and sulfonic acid groups and showed the activity with HLADH and other dehydrogenases (ANSELL et al. 1999a).

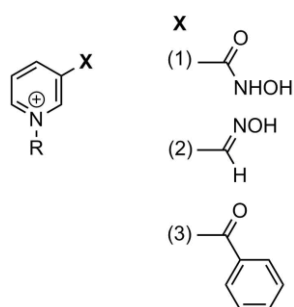


Figure 14: Investigation of various semi-synthetic nicotinamide cofactors with variations at C3 of the nicotinamide ring. (ANDERSON et al. 1959)

Slama *et al.* synthesized carba nicotinamide adenine dinucleotide (carba NAD), by replacing the ribotide oxygen with a methylene, in order to find the relationship between the ribonucleotide part and the enzymatic activity (Figure 15). The pyridinium carbon bond was supposed to be more stable, all other properties were similar to that of NAD⁺ and enzyme activity could be detected for yeast alcohol dehydrogenase and HLADH (SLAMA & SIMMONS 1988; SLAMA & SIMMONS 1989). F.Hoffmann-La Roche AG and Roche Diagnostics GmbH used this cofactor for the stabilization of enzymes by storing the enzymes along with these stable biomimetics for the application in biochemical detection methods and reagent kits (HOENES *et al.* 2007; ROCHE 2009).

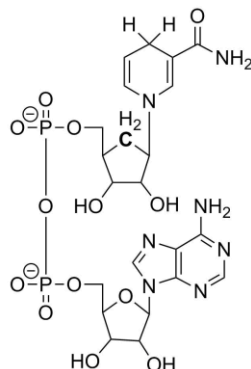


Figure 15: By replacing the ribotide oxygen with a methylene, the more stable biomimetic carba NAD was designed. (SLAMA & SIMMONS 1988; SLAMA & SIMMONS 1989)

In summary, the totally synthetic as well as semi-synthetic biomimetic cofactors have been used to understand the reactions in which NAD(P)/H dependent oxidoreductases are involved following the application in biocatalysis.

1.1.6 Biocatalysis Using Biomimetic Cofactors

Until now, several processes regarding biomimetic nicotinamide cofactors have been described in biocatalysis in order to reduce process costs, to increase cofactor stability towards hydrolysis (in acids and base), as well as to show novel enzyme activity. Additionally, biomimetic cofactors hold the potential to be readily available due to their simple synthesis (KARA *et al.* 2014).

During the 1990s, various groups started working with NAD(P)/H analogues. Most of these cofactors were derived from triazine dyes. They were supposed to be more stable than NAD(P)/H and activities with HLADH were presented (ANSELL *et al.* 1997; ANSELL *et al.* 1999b; BURTON *et al.* 1996; DILMAGHANIAN *et al.* 1997; MCLOUGHLIN & LOWE 1997). The most active one, namely 1-(4'-(4''-acetamido-3''-sulphoanilino)-2'-sulphoanilino)-3-amino-5-(3'carboxamidopyridino)-2,4,6-sym-triazine (Figure 16), showed 4% of the residual activity for HLADH oxidation of n-butanol compared to the natural nicotinamide cofactor (ANSELL *et al.* 1999a; ANSELL *et al.* 1999b).

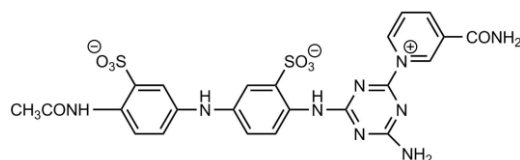


Figure 16: Synthetic cofactor developed by Ansell and coworkers that was most active with HLADH. (ANSELL et al. 1999a; ANSELL et al. 1999b)

Further work on HLADH was done by Lo *et al.* using totally synthetic biomimetics for the synthesis of chiral alcohols (LO & FISH 2002). The conversion of 4-phenyl-2-butanone with 1-benzylnicotinamide (BNA⁺) triflate (OTf) and HLADH including a rhodium based recycling system [Cp**Rh*(bpy)-(H₂O)]OTf₂ resulted in a turnover frequency of 30 d⁻¹ (Figure 17).

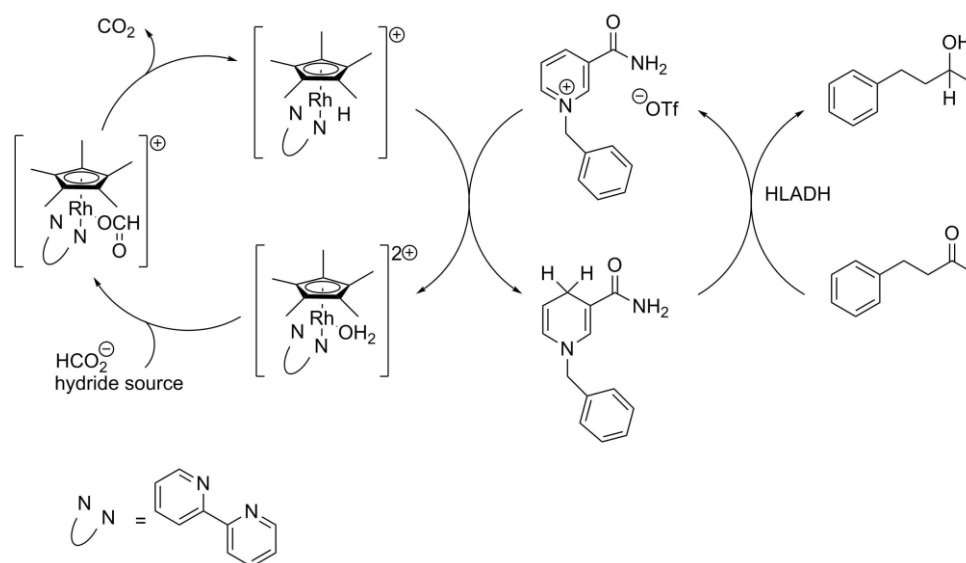


Figure 17: Process developed by Lo and Fish using a HLADH catalyzed reaction for the synthesis of a chiral alcohol. (LO & FISH 2002)

However, latest research questioned these findings since the conversion of BNAH with HLADH could not be reproduced. Probably, activity was initially caused by impurities of the enzymatic preparations with natural cofactors (PAUL & HOLLMANN 2016). The natural cofactors are still preferred by HLADH and only small amounts of NAD(P)/H were sufficient to lead to false positive results by feigning acceptance of the biomimetic cofactor.

In the subsequent years, BNA/H was often the cofactor of choice. Lutz *et al.* described the regioselective hydroxylation of 2-hydroxybiphenyl using the FAD-dependent enzyme 2-hydroxybiphenyl 3-monooxygenase (LUTZ et al. 2004). Although the activity was lower with the biomimetic compared to the natural cofactor, the simple chemical synthesis and improved hydride transfer from BNAH to FAD were advantageous (WU et al. 2013). However, the Michaelis–Menten constant (K_m), which describes the substrate concentration at which half of the maximum reaction rate (v_{max}) is reached, was increased 130-fold for BNAH compared to that of NADH. During the reaction, flavin reduction and substrate hydroxylation was also noticed leading to hydrogen peroxide (H₂O₂) formation (KARA et al. 2014).

Ryan *et al.* presented other activities with FAD-dependent enzymes: cytochrome P450 from *Bacillus megaterium* (P450 BM-3) and from *Pseudomonas putida* (P450cam) (Figure 18). While no activity could be detected for wild-type enzyme P450 BM-3, the mutant enzyme P450 BM-3 R966D/W1046S showed an initial rate of $23.3 \text{ nmol}\cdot\text{s}^{-1}$ per mg of P450 BM-3 in the hydroxylation of p-nitrophenoxydecanoic acid with BNAH (MAURER *et al.* 2005; RYAN *et al.* 2008). Mutation in P450cam resulted in only small variations of initial rates. A non-enzymatic cofactor regeneration approach using the rhodium catalyst was also included in the reaction. Generally, cytochrome P450 enzymes are interesting due to their broad substrate range, oxidation activity at unreactive carbon hydrogen bonds, and high regio- and enantioselectivity (RYAN *et al.* 2008). These reactions can chemically only be done with great effort (GROGAN 2011). Thus, P450 enzymes are industrially used in the production of various drugs like chemotherapeutic substances (JENNEWEIN *et al.* 2001), antibiotics (SHAFIEE & HUTCHINSON 1987), and steroids (FUJII *et al.* 2009).

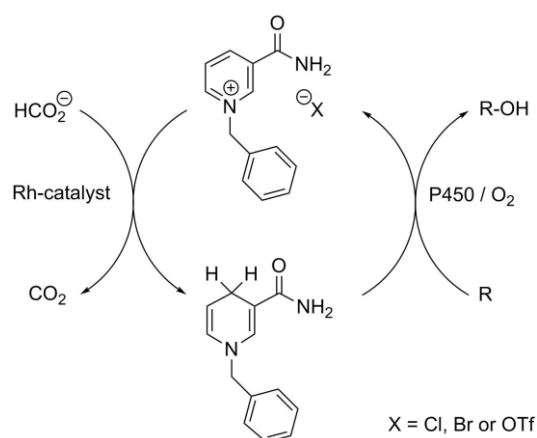


Figure 18: The P450 mutant was able to use BNAH as the cofactor. Regeneration was done with a rhodium catalysts. (RYAN *et al.* 2008)

Furthermore, a bioorthogonal system for the oxidative decarboxylation of L-malate was created by Ji *et al.* (JI *et al.* 2011). Mutant libraries of malic enzyme from *Escherichia coli* (*E.coli*) were screened with a biomimetic cofactor, in which the adenine of NAD/H is replaced by flucytosine, and with a defluorinated version of that cofactor. Enzyme engineering resulted in the double mutant malic enzyme L310R/Q401C that showed higher activity with the synthetic cofactors compared to wild-type enzyme and activity with the natural cofactor was also significantly decreased.

Application in bioelectrocatalysis of the minimal biomimetic nicotinamide mononucleotide in an immobilized system was investigated by Campbell *et al.* (CAMPBELL *et al.* 2012). Although enzyme turnover rate of alcohol dehydrogenase K249G/H255R from *Pyrococcus furiosus* decreased with the usage of artificial cofactors, increase in performance in the immobilized system was observed.

In 2013, Paul *et al.* demonstrated the asymmetric reduction of conjugated C=C double bonds with enoate reductase from *Thermus scotoductus* (*TsER*) using various synthetic biomimetic cofactors, which differ in the amide group as well as in the residue attached to the nitrogen (position 1) of the nicotinamide ring (Figure 19). Overall, equal or higher conversion was achieved compared to NAD(P)/H without loss of selectivity (PAUL *et al.* 2013).

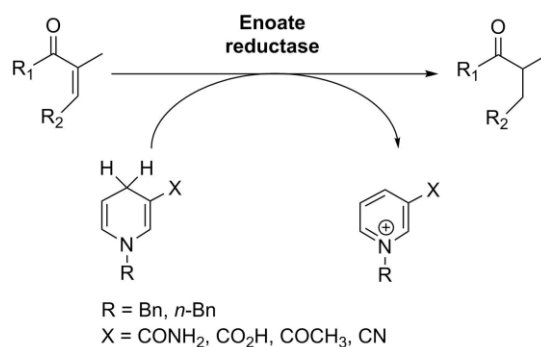


Figure 19: Conversion of various biomimetic cofactors by enoate reductase. (PAUL et al. 2013)

Another approach using BNAH was shown by the same group. Hydrogen peroxide was generated *in situ* by the reaction of BNAH with flavin mononucleotide. Formation of H₂O₂ was controlled by varying the concentrations of these two components. On coupling the reaction with H₂O₂ consuming enzymes such as P450_{Bsβ} CYP152A1 from *Bacillus subtilis* and P450_{C1β} from *Clostridium acetobutylicum*, conversion of myristic acid to 2- and 3-hydroxymyristic acid products was achieved (PAUL et al. 2014b). The combination of BNAH, FAD, and styrene monooxygenase StyA1 from *Rhodococcus opacus* 1CP resulted in enantioselective epoxidation of various styrene derivatives (Figure 20). By using this system, the reaction could be simplified since the addition of a NADH regeneration system and the enzyme StyB were not necessary resulting in a compressed electron transport chain (PAUL et al. 2015). A regeneration system for BNAH was not included in the process.

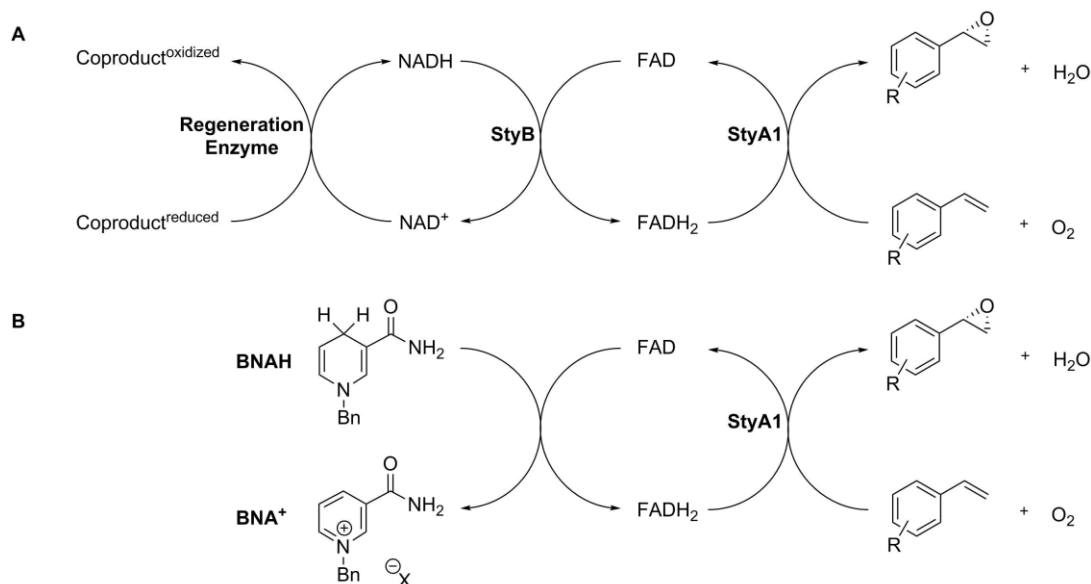


Figure 20: Comparison of styrene catalyzed reactions using NADH or BNAH as cofactor, respectively. (PAUL et al. 2015)

Further research showed that by co-crystallization of a xenobiotic reductase A of *Pseudomonas putida* (PDB: 5CPL) with the natural cofactor as well as various biomimetics, the amino acid Trp302 adopts a different conformation depending on the size of the cofactor (KNAUS et al. 2015). Thus, for the smaller biomimetics the volume of the active site is reduced (Figure 21). Furthermore, stacking

interactions between the isoalloxazine ring of the flavin cofactor, the amino acids His181, His178, as well as Cys25 with the nicotinamide ring were noticed. A range of ene reductases from the Old Yellow Enzyme Family that showed activity with the biomimetics were also presented in the work, indicating a broad applicability of biomimetics.

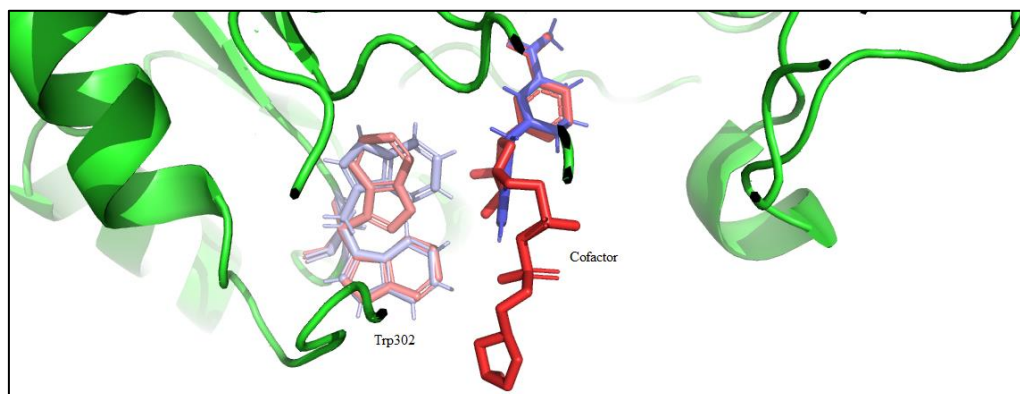


Figure 21: Variation of Trp302 position depending on the size of the cofactor. The conformation for the natural cofactors is indicated in red and for the biomimetic cofactor (BNA/H) is colored in blue. (KNAUS et al. 2015)

Comparing Class I ene reductases (classical OYEs from plants or bacteria) with the closely related Class II ene reductases (classical OYEs from fungal origin), it was found that biomimetic cofactors were converted better than the natural cofactors when Class I enzymes were used, however, enzymes in Class II did not accept biomimetics. In addition to Class I ene reductases, enzymes in Class III (thermophilic-like or mesophilic OYEs from bacteria) were also able to convert carboxy and nitrile substituted biomimetics most efficiently (SCHOLTISSEK et al. 2017).

Riedel *et al.* presented the activity of another ene reductase from *Rhodococcus opacus* 1CP, which preferred NADPH over NADH and BNAH, with BNAH's activity being intermediate compared to the natural cofactors (RIEDEL et al. 2015). Recently, Löw and coworkers described the activity of a NAD(P)H-dependent 2-cyclohexen-1-one reductase from *Zymomonas mobilis* with a cofactor containing a N-substituted 4-hydroxy-phenyl residue that increased v_{\max} six-fold compared to NADH. Overall, it was shown that the substrate scope can depend on the choice of the cofactor regarding its molecular size (LOW et al. 2016).

In addition to the aforementioned reactions, the stabilities of natural as well as biomimetic cofactors are still an important factor. Hentall *et al.* prepared biomimetic cofactors containing a methyl group at the nicotinamide ring (HENTALL et al. 2001). As a result, it was noticed that the methyl group at the 5-position conferred an increased stability in aqueous buffer since the 5,6-double bond was well protected against protonation (steric hindrance). In contrast, the methyl substituent at the 6-position led to a lower stability probably due to electronic effects.

In situ regeneration of biomimetic nicotinamide cofactors remains an unsolved problem. So far, only inorganic systems have been described, which include the use of a rhodium complex as catalyst and formate as reducing agent. However, interactions with biocatalysts lead to the deactivation of the enzyme as well as of the regeneration complex (LUTZ et al. 2004; POIZAT et al. 2010; RYAN et al. 2008). Another approach was addressed by Okomato *et al.* using artificial metalloproteins that are

based on streptavidin variants and a biotinylated iridium cofactor (OKAMOTO et al. 2016). These components were coupled with an enoate reductase for the reduction of N-ethyl-2-methylmaleimide. As a result, total turnover numbers of 2000 were reached.

Another limitation that needs to be overcome is the proper binding of the biomimetic analogues in the cofactor binding site by considering structural changes during catalysis as well. Due to the big structural differences between the purely synthetic and the natural cofactors, most binding interaction may not be formed, which resulted in high K_m values and low reaction rates (ANSELL & LOWE 1999; CAMPBELL et al. 2012; KARA et al. 2014; LO & FISH 2002).

However, as indicated by Rollin *et al.*, the use of biomimetic cofactors holds the potential for decreasing the prizes for biocatalytic processes. Based on these calculations, BNA^+ may cost only about 1% compared to the prize of $NADP^+$ (ROLLIN et al. 2013).

1.2 Enzymatic Cofactor Regeneration

A high number of industrially relevant biotransformations can be performed with cofactor dependent oxidoreductases. To overcome economic and practical challenges associated with the use of cofactors, various *in situ* regeneration systems have been developed, especially for NAD^+ , $NADP^+$, $NADH$, or $NADPH$, respectively, thereby creating a broad range of opportunities for efficient reaction/regeneration processes (even at an industrial scale) (KARA et al. 2014). In all cost-efficient processes, the integration of the cofactor regeneration system is of utmost importance since the stoichiometric use of natural nicotinamide cofactors is very expensive. Such a regeneration reaction (enzymatic, chemical, photochemical, and electrochemical) should be kinetically as well as thermodynamically favored and the co-substrate, co-intermediate, co-product, or co-enzyme should not interfere with one of the components of the reaction of interest. The downstream processing should not be affected, too. Generally, all components of the regeneration system should be cheap, readily available, stable, and easily separable from the reaction pot (HUMMEL & GRÖGER 2014).

1.2.1 Cofactor Regeneration

According to the principle of Le Chatelier and Braun, if in a chemical reversible system the equilibrium is subjected to a change in temperature, pressure, or concentration, the chemical system (i.e. equilibrium) will be shifted to partially undo this perturbation in order to oppose the stress (BRAUN 1887; BRAUN 1888; LE CHATELIER 1884). Generally, the various principles of cofactor regeneration follow the idea of a change in the reaction equilibrium as defined at the end of the 19th century.

1.2.1.1 Enzyme-coupled Cofactor Regeneration

In an enzyme-coupled approach, a second independent reaction containing an additional substrate and enzyme performing an ideally irreversible reaction is included in the process (HUMMEL & GRÖGER 2014) (Figure 22 A).

Glucose dehydrogenase, which accepts NAD^+ as well as $NADP^+$ as cofactor, is commonly used in an enzyme-coupled approach. The enzyme has a high specific activity, is stable and the substrate D-glucose is cheap and readily available. For example, cofactor regeneration with glucose

dehydrogenase from *Bacillus megaterium* was used in a two-step synthesis to actinol starting from ketoisophorone catalyzed by the Old Yellow Enzyme from *Saccharomyces cerevisiae* and the levodione reductase from *Corynebacterium aquaticum* (WADA et al. 2003) (Figure 22 B). However, co-product isolation may be more complicated or time-consuming compared to formate dehydrogenase (FDH) catalyzed reactions (HUMMEL & GRÖGER 2014).

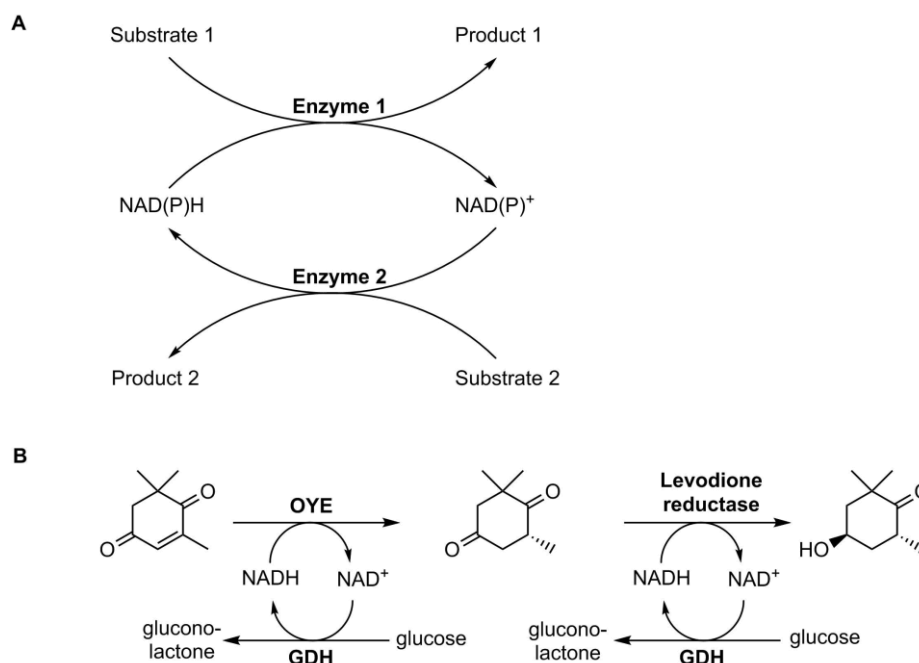


Figure 22: **A**) Scheme of an enzyme-coupled cofactor regeneration. **B**) Application of GDH for the cofactor regeneration in the overall synthesis to actinol. (HUMMEL & GRÖGER 2014; WADA et al. 2003)

One of the first systems established using enzyme-coupled cofactor regeneration was the addition of FDH for the regeneration of NADH in the production of *tert* L-leucine from trimethylpyruvic acid by a leucine dehydrogenase (LeuDh) (Figure 23). Because of the high yield and optical purity, the process was even used at an industrial ton scale (GRÖGER et al. 2012; SHAKED & WHITESIDES 1980).

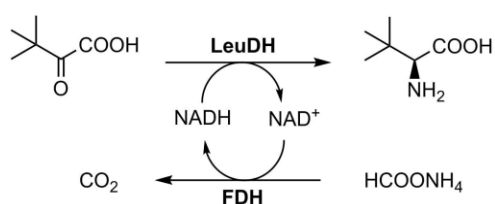


Figure 23: Synthesis of *tert* L-leucine from trimethylpyruvic acid by LeuDh. FDH was used for cofactor regeneration. (GRÖGER et al. 2012; SHAKED & WHITESIDES 1980)

Due to the irreversibility of formate dehydrogenase catalyzed reactions, high amounts of NADH are available for the reaction of interest, thus, conversion to trimethylpyruvic acid was not limited by the cofactor availability. Accordingly, the reaction equilibrium is favorable for product formation. Conversion of cheap and harmless formate by commercially available formate dehydrogenase leads to carbon dioxide, which being a gas, can be easily removed from the system. However, a limitation of

the system is the low specific activity (4-6 U*mg⁻¹) and the cofactor specificity for NAD/H (HUMMEL & GRÖGER 2014).

Other enzymes that have successfully been used in this approach are for example glucose-6-phosphate dehydrogenase (especially for NADPH regeneration) or phosphite dehydrogenase (JOHANNES et al. 2007). Additionally, reaction/regeneration processes were described in which two valuable substances were produced like the reduction of xylose to xylitol under NADH consumption by xylose reductase and reaction of glycerol and NAD⁺ to dihydroxyacetone catalyzed by glycerol dehydrogenase (ZHANG et al. 2011). Xylitol may be used in the food and chemical industry (WINKELHAUSEN & KUZMANOVA 1998) and dihydroxyacetone is a specialty chemical coming from glycerol, a biodiesel by-product (ENDERS et al. 2005; LEVY 1992).

For the regeneration of oxidized cofactors, NADH oxidase might be used. These flavo-enzymes oxidize NAD(P)H to NAD(P)⁺ while molecular oxygen is reduced to hydrogen peroxide or water. The water-forming NADH oxidases are mostly preferred as even small amounts of hydrogen peroxide can harm enzymes in processes (HERNANDEZ et al. 2012). Riebel *et al.* combined the alcohol dehydrogenase from *Lactobacillus brevis* with the recycling enzyme NADH oxidase from *Lactobacillus sanfranciscensis* for the production (S)-phenylethanol from acetophenone from racemic phenylethanol (RIEBEL et al. 2003).

1.2.1.2 Substrate-coupled Cofactor Regeneration

Another possibility is the use of the same enzyme for the reaction and regeneration process (substrate-coupled approach) (Figure 24 A). While synthesizing the desired chiral alcohol, the solvent stable alcohol dehydrogenase from *Thermoanaerobacter brockii* (TBADH) also catalyzed the conversion of inexpensive 2-propanol to acetone for cofactor regeneration (KEINAN et al. 1987) (Figure 24 B). The catalytic equilibrium can be influenced by imbalances in the thermodynamic equilibrium (HUMMEL & GRÖGER 2014). Activity will be further increased when the cofactor is directly attached to the enzyme following reduced cofactor concentration, thereby decreasing process costs (MANSSON et al. 1978). However, two reactions compete for the same active site of an enzyme implying that the reactions need to be adjusted properly. Another advantage is that, 2-propanol as an organic solvent may also increase solubility of water-insoluble substances (HUMMEL & GRÖGER 2014).

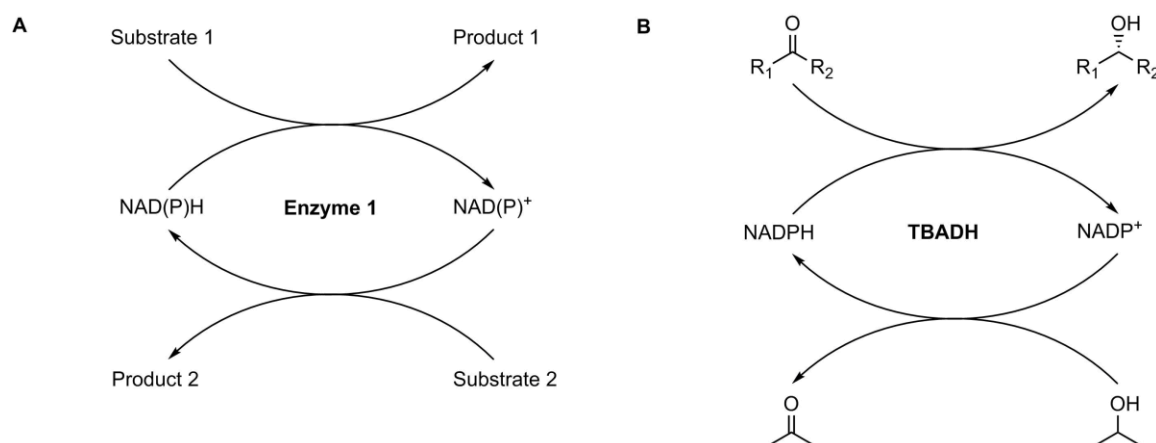


Figure 24: **A)** Scheme of a substrate-coupled cofactor regeneration. **B)** Synthesis of the desired chiral alcohol and acetone in the regeneration reaction using an ADH as production as well as regeneration enzyme. (HUMMEL & GRÖGER 2014; KEINAN et al. 1987)

1.2.1.3 Reaction-internal Cofactor Regeneration

In addition to the methods described above, there is also an opportunity to integrate the regeneration process within the course of a reaction in the scope of closed loop reactions including hydrogen borrowing (Figure 25); e.g the conversion of D-glucose to ethanol or isobutanol using NAD⁺ consuming enzymes (glucose dehydrogenase and aldehyde dehydrogenase) as well as NAD⁺ forming reactions (catalyzed by ketolacid reductoisomerase and alcohol dehydrogenase) (see section 1.1.4) (GUTERL et al. 2012). Thus, no addition of an “artificial” reaction system is necessary, hence, simplifying the reaction system and reducing process costs (HUMMEL & GRÖGER 2014).

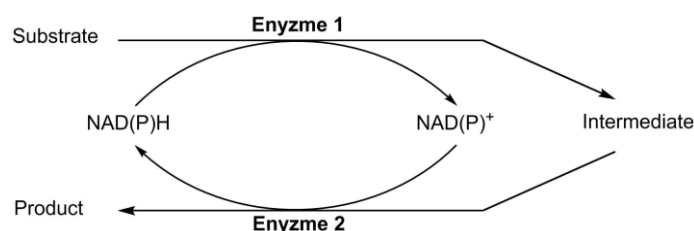


Figure 25: Scheme of a reaction-internal cofactor regeneration. (HUMMEL & GRÖGER 2014)

However, as described in section 1.1.6, none of these methods is available for the regeneration of biomimetic nicotinamide cofactors.

1.2.2 Glucose Dehydrogenase from *Sulfolobus solfataricus*

Glucose dehydrogenase from *Sulfolobus solfataricus* (SsGDH, EC 1.1.1.47) was first described by Giardina *et al.* in 1986. The enzyme from the thermoacidophilic archaeobacterium converts both natural nicotinamide cofactors NAD⁺ and NADP⁺ while oxidizing various monosaccharides (Figure 26).

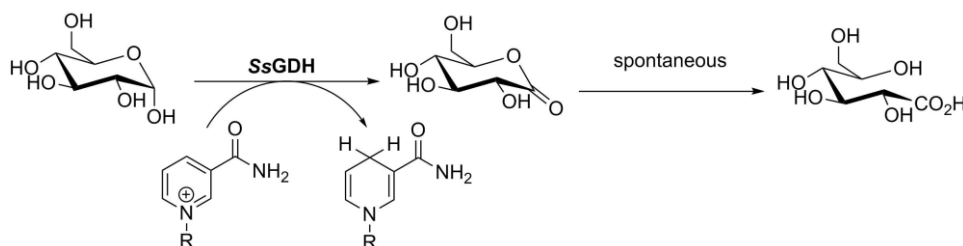


Figure 26: SsGDH catalyzed reaction using D-glucose as substrate with NAD(P)⁺ as cofactor. (MILBURN et al. 2006)

The optimal conditions of pH and temperature for maximum activity for this enzyme were pH 8 and 77 °C, respectively. It is worth mentioning that SsGDH is stable in various organic solvents. Furthermore, 20% of the activity at 37 °C could be obtained compared to that at 77 °C, which is advantageous as most extreme thermophiles are almost inactive at this reaction temperature (GIARDINA et al. 1986).

Activity could also be determined with D-galactose (C4 epimer of D-glucose) but not with D-allose or D-mannose, with D-xylose (pentose with identical configuration as D-glucose) as well as with L-arabinose (C4 epimer of D-xylose), thus, SsGDH appears to have a preference for the D-glucose-specific stereo-configuration at C2 and C3 but the configuration of C4 may vary. Very little activity could be detected with D-glucosamine and 2-deoxy-D-glucose. Other good substrates are 6-deoxy-D-glucose and D-fucose (Figure 27). The kinetic parameters were determined at 70 °C for D-glucose with NAD⁺ as cofactor (K_m 1.50 ± 0.05 mM, v_{max} 110 ± 5 U*mg⁻¹, catalytic constant [k_{cat}] 74.9 s⁻¹, catalytic efficiency [k_{cat}/K_m] 49.9 s⁻¹*mM⁻¹) and with NADP⁺ as cofactor (K_m 1.30 ± 0.05 mM, v_{max} 70 ± 2 U*mg⁻¹, k_{cat} 47.7 s⁻¹, k_{cat}/K_m 36.7 s⁻¹*mM⁻¹) (LAMBLE et al. 2003).

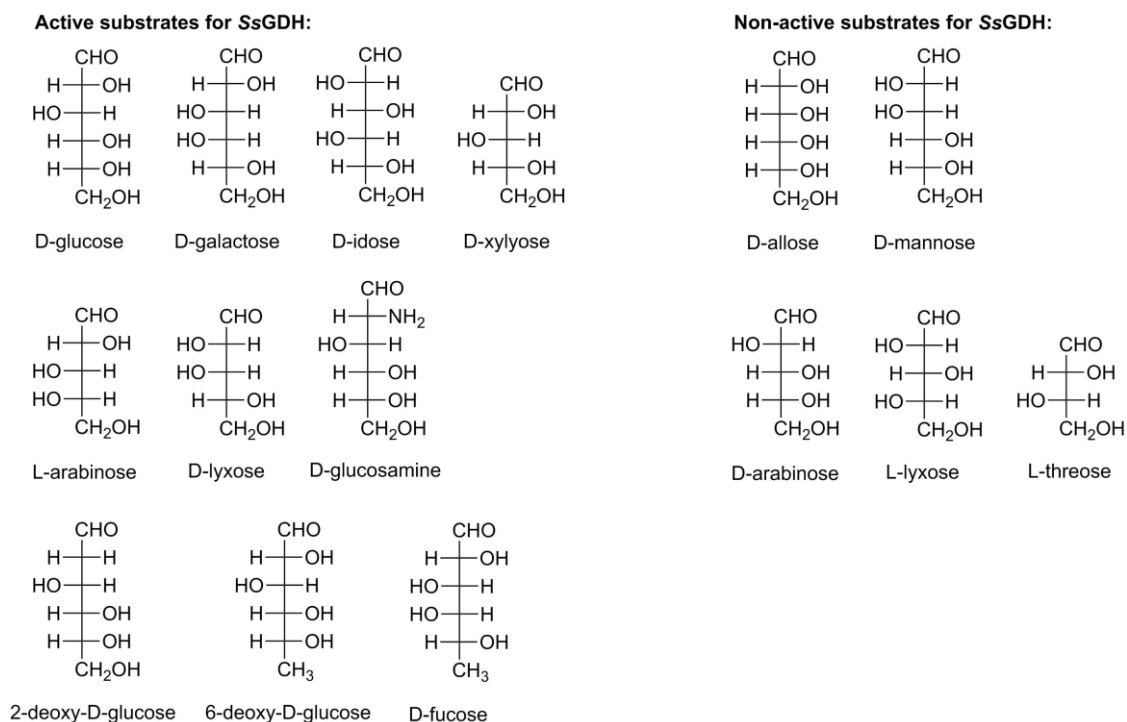


Figure 27: Various sugars for which an activity with SsGDH was tested. (LAMBLE et al. 2003)

In addition, the enzyme was assigned to medium-chain alcohol/polyol dehydrogenase/reductase branch of the superfamily of pyridine-nucleotide-dependent alcohol/polyol/sugar dehydrogenases (LAMBLE et al. 2003). This group is characterized by a chain length of 350-375 bp, consists of a zinc-binding site, and a nucleotide binding site preferring NAD^+ or NADP^+ (WIERENGA et al. 1985). Crystallographic studies identified *SsGDH* as a 164 kDa homotetramer (THEODOSSIS et al. 2005), containing a nucleotide-binding domain (residues 190-308) and a catalytic domain (residues 309-366) per subunit. The nucleotide-binding domain consists of a Rossmann fold including six parallel strands and the GXGXXG nucleotide-binding motif (residues 188-193) is situated between the catalytic and nucleotide-binding domain. The natural nicotinamide cofactor binds a linear conformation in the nucleotide-binding domain performing π - π stacking interactions of the nicotinamide ring with Phe277 and Phe279. Leu305, Phe277, and Asn307 also interact with the amid group of the nicotinamide. Ile192, as part of the GXGXXG motif, gets in contact with the phosphate group closest to the nicotinamide ring as well as Lys354 (part of the catalytic domain) with the phosphate nearest to the adenosine ring. Further interactions with the adenosine part of the natural cofactor were observed for Thr189 and Asn211. In case of NADP^+ as the cofactor, Arg213 and Asn211 interact with the additional phosphorous or oxygen linked to the phosphate, respectively. Additionally, Arg212 moves to avoid steric hindrances and stacks against the adenosine ring. Asn211 is also described to act as an indicator for NADP^+ specificity (PDB: 2cd9, 2cda, 2cdb, 2cdc) (MILBURN et al. 2006).

The enzyme *SsGDH* was applied in a cell-free reaction cascade starting from D-glucose to produce the industrially-relevant chemicals ethanol and/or isobutanol as a renewable alternative to petroleum-based products (GUTERL et al. 2012). Generally, *SsGDH* and other glucose dehydrogenases were used in various reaction/regeneration processes (see section 1.2.1.1), however, their activity is limited to the natural nicotinamide cofactors as conversion of biomimetic cofactors has so far never been shown.

1.2.3 NADH Oxidase

NADH oxidases (EC 1.6.3.4) convert NAD(P)H to NAD(P)^+ representing an enzymatic regeneration system (Figure 28). They are flavoproteins containing FMN or FAD as cofactor closely bound in the enzyme. During catalysis, the side products, either water (in a four electron reduction) or hydrogen peroxide (in a two electron reduction), respectively, were formed. Subsequently, the enzymes were classified according to the side products (GEUEKE et al. 2003).

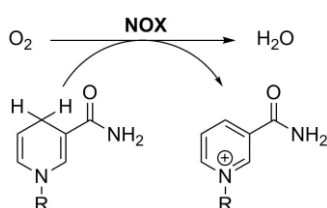


Figure 28: Water-forming NADH oxidase (NOX) catalyzed reaction with the cofactor NADH resulting in H_2O as side product.

Water-forming enzymes are found in *Lactobacillus brevis* (GEUEKE et al. 2003; HUMMEL & RIEBEL 2003), *Leuconostoc mesenteroides* (KOIKE et al. 1985), or *Enterococcus (Streptococcus) faecalis*

(ROSS & CLAIBORNE 1992), whereas enzymes from *Thermus thermophilus* (PARK et al. 1992) or *Amphibacillus xylanu* (NIIMURA et al. 1993) lead to hydrogen peroxide as side product.

The use of NADH oxidases is advantageous compared to other regeneration enzymes for oxidized cofactors like glutamate dehydrogenase or lactate dehydrogenase, as no by-products were formed that may lead to complications in the downstream processing.

Further, the water-forming enzymes may also be preferred since water does not interfere with the reaction and catalase need not be added to degrade hydrogen peroxide, as when hydrogen peroxide producing NADH oxidases are used (GEUEKE et al. 2003). Riebel *et al.* successfully applied water-producing NADH oxidase from *Lactobacillus sanfranciscensis* as a regeneration system for the production of acetophenone from racemic phenylethnaol in an enantiospecific oxidation catalyzed by (R)-alcohol dehydrogenase from *Lactobacillus brevis*. The activity was shown for NADH and NADPH as NADH oxidase from *Lactobacillus sanfranciscensis* accepts both cofactors. Wild-type (R)-alcohol dehydrogenase from *Lactobacillus brevis* prefers NADPH, however, the mutant G37D was able to convert NADH (RIEBEL et al. 2003). Crystallographic studies of NADH oxidase from *Lactobacillus sanfranciscensis* (PDB: 2CDU) indicated a FAD binding domain, a NAD(P)H binding domain, and a dimerization domain. The first two domains, which adopt a Rossmann conformation, were highly conserved along with the redox-active cysteine, which were significantly involved in a catalytic cycle (LOUNTOS et al. 2006). Tachon *et al.* discussed the essential role of FAD and showed that optimal activity was reached when fresh preparations of NADH oxidase from *Lactococcus lactis* were reactivated with cysteine and FAD (TACHON et al. 2011).

Overall, the activity of NADH oxidases has so far not been presented with biomimetic nicotinamide cofactors. If such processes were to be developed the fact that FMN or FAD is an essential part of such enzymes needs to be considered. The flavin molecules were also described to convert biomimetics without the contribution of any enzyme (PAUL et al. 2015).

1.3 Scope of Work

The optimization of biotechnological processes holds a high potential for the future. In this context, it was the overall aim of this work to develop synthetic nicotinamide cofactors and conduct their enzymatic conversion. Oxidoreductases, which need nicotinamide cofactors as redox equivalents, catalyze industrially relevant reactions with a high selectivity and stereospecificity including high reaction rates under mild conditions. Since the natural nicotinamide cofactors are instable and expensive leading to increased process costs, the use of stable and easy to synthesize synthetic molecules may be advantageous.

To overcome the instability of the natural nicotinamide cofactors NAD(P)/H, in a first step, well-known biomimetic cofactors should be synthesized following published synthesis routes, characterized according to their stability in various buffers, at various pH values and temperatures, and methods for analysis should be developed. Based on these results, new cofactors should be synthesized in order to create molecules with improved properties compared to NAD(P)/H as well as to the well-known biomimetics.

In addition, enzymatic regeneration systems for these biomimetics should be established. For this, various enzymes should be screened for their activity with the synthesized biomimetic cofactors. The resulting active biocatalysts should be characterized and optimized reaction parameters should be found. Using these data and all available information from literature, a high-throughput platform to perform enzyme engineering should be developed. This allows studying the coordination and binding of the biomimetics in the cofactor binding site, as well as increasing the enzymatic activity with the biomimetics by site directed mutagenesis. Finally, the proof-of-concept of successfully using biomimetic cofactors in a biocatalytic process should be shown along with suitable detection methods.

2 Material and Methods

2.1 Material

2.1.1 Equipment

Table 2: Listing of the equipment used in this work.

Equipment	Manufacturer
Autoclave	Thermo Scientific (Ulm) Varioklav 135S
Centrifuge	Thermo Scientific (Ulm) Sorvall RC-6 Plus equipped with rotor F10-6x500y (Piramoon Technologies Inc (Santa Clara)), rotor F9-4x1000y (Piramoon Technologies Inc (Santa Clara)), rotor SH-3000 (Thermo Scientific (Ulm)) and Rotor SS-34 (Thermo Scientific (Ulm)); Thermo Scientific (Ulm) Fresco 21 Centrifuge
Clean bench	Thermo Scientific (Ulm) MSC Advantage
Incubation chamber	Binder (Tuttlingen) Klimaschrank KBF 240 E5.1/C
Drying oven	Thermo Scientific (Ulm) Function Line T12 and B12
Electroporator	Bio-Rad Laboratories GmbH (München) MicroPulser™
Freezer -20 °C	Liebherr-Hausgeräte (Ochsenhausen)
Freezer -80 °C	Thermo Scientific (Ulm) Forma 906 -86 °C ULT
Gas chromatography (GC)	Thermo Scientific (Ulm) Trace GC 2000 with Ultra Trace
Autosampler	Thermo Scientific (Ulm) TriPlus Autosampler
Mass-spectrometer (MS)	Thermo Scientific (Ulm) Ultra Trace DSQ II
Columns	Restek GmbH (Bad Homburg) Stabilwax® (30 m, diameter 0.25 mm, film 0.25 µm); SGE Analytical Science (Milton Keynes) BPX-5 (30 m, diameter 0.25 mm, film 0,25 µm)
Gel electrophoresis	Bio-Rad (München)
Agarose electrophoresis	Bio-Rad (München) Mini-Sub Cell GT System
SDS electrophoresis	Bio-Rad (München) Mini-PROTEAN® Tetra Cell; Bio-Rad (München) Mini-Protean® 3Multi-Casting Chamber
Power supply	Bio-Rad (München) PowerPAC™ Basic
Documentation	Intas Science Imaging Instruments GmbH (Göttingen) Gel iX Imager
Syringe	Hamilton AG (Bonaduz) syringe 25 µL
Heating block	Analytik Jena AG (Jena) Thermostat Tmix
High pressure cell disruptor	Constant Systems (Daventry) Cell Disruption System Basic Z
Homogenizer	IKA (Staufen) Ultra Turrax T18 basic
Incubator	Infors AG (Bottmingen/Basel) HAT Minitron, Thermo Scientific (Ulm) MaxQ 2000
Magnetic stirrer	Thermo Scientific (Ulm) Variomag Telesystem; VWR (Darmstadt) VMS-C7, Heidolph (Schwabach) MR 3001 K
Microplate shaker	Edmund Bühler (Hechingen) TiMix 5 control and TH 15

Equipment	Manufacturer
Microwave	ECG (Prag) MH 25 ED
Multichannel pipette	Eppendorf AG (Hamburg) Research pro 8x1200 µL and 12x300 µL; BRAND (Wertheim) Transferpette® S-8 electronic 5-50 µL, 10-100 µL; BRAND (Wertheim) Transferpette® S-12 electronic 20-200 µL
Nanophotometer	IMPLEN (Westlake Village) Nanophotometer P-class
NMR spectroscopy	JEOL ECS 400 (Jeol Ltd. (Akishima))
pH-Meter and electrode	Mettler-Toledo (Gießen) Five Easy™ and Five Go™; InLab® Expert Pro pH 0-14 (0-100 °C) and InLab® Micro Pro pH 0-14 (0-100 °C)
Pipettes	BRAND (Wertheim) Transferpette® S 0.1-10 µL, 1-10 µL, 10-100 µL, 100-1000 µL, 1000-10000 µL, 500-5000 µL
Scale	Satorius (Göttingen) TE1502S and TE6101
Special accuracy scale	Ohaus Europe (Nänikon), Pioneer™
Protein purification system	GE Healthcare Europe GmbH (Freiburg) ÄKTA™ purifier
Pump	GE Healthcare Europe GmbH (Freiburg) P-900
Sample pump	GE Healthcare Europe GmbH (Freiburg) UP-900
Control device	GE Healthcare Europe GmbH (Freiburg) UPC-900
Columns	GE Healthcare Europe GmbH (Freiburg) HisTrap FastFlow 5 mL and HiTrap 26/10 Desalting
Rocking platform	VWR (Darmstadt)
Spectrophotometer	Thermo Scientific (Ulm) Varioskan Flash and Multiskan; BioTek (USA) Epoch2 Spektrophotometer
Desk centrifuge	Thermo Scientific (Ulm) Heraeus Fresco 21
Thermo cycler	Bio-Rad (München) MyCycler™ Thermal Cycler; MJ Mini™ Personal Cycler and CFX96 Touch
Ultra high performance liquid chromatography (UHPLC)	Dionex (Idstein) UltiMate 3000RS
Degasser	Dionex (Idstein) SRD 3400
Pump module	Dionex (Idstein) HPG 3400RS
Autosampler	Dionex (Idstein) WPS 3000TRS
Column compartment	Dionex (Idstein) TCC 3000RS
Diode array detector	Dionex (Idstein) DAD 3000RS
High capacity ion trap	Bruker Daltonics (Bremen) HCT
Columns	Deutsche Metrohm GmbH (Filderstadt) Metrosep A Supp 10-250/4.0, 250 mm, particle size 4.6 µm; Macherey-Nagel (Düren) Gravity C18, 100 mm length, 2 mm i.d.; 1.8 µm particle size
Ultrapure water system	ELGA LabWater (Celle) PURELAB classic
Ultrasonic bath	VWR International GmbH (Darmstadt) Ultrasonic Cleaner

Equipment	Manufacturer
Ultrasonic	Hielscher (Teltow) UIS250 L with sonotrode „VialTweeter“ and sonotrode LS24d10
Ultraviolet (UV) cabinet	CAMAG (Berlin) UV INSPECTION 022.9070
Vacuum pump	VACUUBRAND GmbH & Co. KG (Wertheim) PC 2004 VARIO
Vortexer	Scientific Industries (Bohemia) Vortex Genie 2
Water bath	JULABO (Seelbach) ED-33

2.1.2 Software and Databases

Table 3: Listing of the software and databases used in this work.

Product	Manufacturer	Application
3D Ligand Site	Imperial College London, http://www.sbg.bio.ic.ac.uk/3dligandsite/	Prediction of ligand binding sites
BioEdit	Tom A. Hall	Sequence alignment editor
Basic Local Alignment Search Tool (BLAST)	National Center for Biotechnology Information, https://blast.ncbi.nlm.nih.gov/	Sequence alignments
ChemDraw Ultra	Perkin Elmer Informatics (USA)	Drawing and 3D view of chemical structures
Chromleon	Dionex (Idstein)	Data analyzing UHPLC and HPLC
Clone Manager 6	Scientific & Educational Software (USA)	Sequence alignment editor
Clustal Omega	EMBL-EBI, https://www.ebi.ac.uk/Tools/msa/clustalo/	Sequence alignments
DataAnalysis Delta™	Bruker (Bremen)	MS-data analysis
GATC™ Viewer	Jeol Ltd. (Akishima)	NMR analysis software
HyStar	GATC Biotech AG (Konstanz)	Sequence alignment editor
Library Editor	Bruker (Bremen)	System control
NCBI	Bruker (Bremen)	Spectra database
RCSB Protein Data Bank (PDB)	National Center for Biotechnology Information, https://www.ncbi.nlm.nih.gov/	Supply of biomedical and genomic information
Protein Homology / analogY Recognition Engine V 2.0 (PHYRE ²)	National Science Foundation, National Institutes of Health, and US Department of Energy, https://www.rcsb.org/	3D shapes of proteins and complexes
	Imperial College London, http://www.sbg.bio.ic.ac.uk/phyre2/html/page.cgi?id=index	Prediction of protein structure

Product	Manufacturer	Application
PRALINE multiple sequence alignment	University of Amsterdam, http://www.ibi.vu.nl/programs/pralinewww/	Sequence alignments
ProtParam tool (ExPaSy)	ETH Zürich, Swiss Institute of Bioinformatics https://web.expasy.org/protparam/	Protein characterization
PyMOL v1.3r1 edu	DeLano Scientific LLC (USA)	Crystal structure analysis
ScanIt	Thermo Scientific (Ulm)	Spectrophotometer control software
Gen5 Data Analysis software	Biotek (USA)	Spectrophotometer control software
SciFinder	Chemical Abstract Service (CAS), https://scifinder.cas.org/scifinder	Literature research
SigmaPlot 11.0	Systat Software (Erkrath)	Analysis of enzymatic kinetic parameters
QuantAnalysis	Bruker (Bremen)	Quantification of MS-data
Web of knowledge	Thomson Reuters	Literature Research
Xcalibur	Thermo Scientific	Analysis of GC data
Yet Another Scientific Artificial Reality Application (YASARA)	YASARA Biosciences GmbH (Austria)	Crystal structure analysis

2.1.3 Chemicals

All chemicals were of analytical or biochemical purity and ordered from Alfa Aesar, AppliChem GmbH, Biochemical, Bio-Rad, Biozym Scientific GmbH, Bode Chemie GmbH, Carl Roth GmbH & Co. KG (Carl Roth), Fluka, GE Healthcare Europe GmbH, Gerbu Biotechnik GmbH, Life Technologies GmbH, Macherey-Nagel, Merck KGaA PorLab, Rapidozym, Serva Electrophoresis GmbH (Serva), Sigma-Aldrich, VWR International GmbH (VWR), and Wako Chemicals GmbH.

Table 4: Overview of chemicals used in this work in detail.

Name of Reagent	Manufacturer	Order Number
(2-Chloroethyl)benzene	Alfa Aesar	L04891
(3-Bromopropyl)benzene	Alfa Aesar	A14050.22
1-Phenyl-3-methyl-5-pyrazolone	Sigma-Aldrich	M70800
2-Methylbutanal	Sigma-Aldrich	W269107
2-Pentanol	Sigma-Aldrich	P8017
2-Pentanone	Sigma-Aldrich	68950
3-Phenylpropanal	Sigma-Aldrich	W288705-SAMPLE-K
5,10,15,20-Tetrakis-(4-sulfonatophenyl)-porphyrin-Fe[III] chloride	PorLab	PL00832617

Name of Reagent	Manufacturer	Order Number
Acetic acid	Sigma-Aldrich	338826
Acetic acid, 100%	Carl Roth	6755.1
Acetonitrile LC-MS	VWR	83640320
Acetophenone	Sigma-Aldrich	A10701
Acrylamid-Bisacrylamidstammlösung Rotiphorese Gel 30	Carl Roth	3029
Agar	Carl Roth	5210.2
Agarose Serva Wide Range	Serva	11406.03
Ammonium persulfate	Merck KGaA	1012010500
Ammonium solution	Carl Roth	P093.1
Ammonium sulfate	AppliChem GmbH	A1032,5000
Ampicillin sodium	Carl Roth	K029.2
Benzyl chloride	Sigma-Aldrich	185558
Bromophenol blue	Merck KGaA	1.081.220.005
<i>tert</i> -Butyl methyl ether	Carl Roth	6746.4
Calcium chloride	Carl Roth	A119.1
Calcium L-lactate pentahydrate	Carl Roth	4071.2
Chloramphenicol	Sigma-Aldrich	C0378
Chloroform-d1	Carl Roth	AE59.1
Cinnamaldehyde	Sigma-Aldrich	W228613
Coomassie Brilliant Blue G250	Sigma-Aldrich	27815
Coomassie Brilliant Blue R250	Biochemical	443283M
Cyclohexanone	Sigma-Aldrich	29140
DA-64	Wako Chemicals GmbH	043-22351
DC-Kunststoffplatten, Kieselgel 60 mit UV Indikator	Merck KGaA	1.05750.0001
Dichloromethane	Carl Roth	8424.3
Diethyl ether	Carl Roth	5920.3
Dihydro nicotinamide adenine dinucleotide	Carl Roth	AE12.3
Dihydro nicotinamide adenine dinucleotide phosphate	Carl Roth	AE14.2
Dimethyl sulfoxide	Carl Roth	4720.1
Dimethylsulfoxide-d ₆	Carl Roth	AE56.1
Dipotassium phosphate	Carl Roth	P749.3
Disodium hydrogen phosphate	Carl Roth	P030.3
Dithiothreitol	Carl Roth	6908.2
dNTPs (mix)	Rapidozym	GEN_011_M10
Ethanol absolut	VWR	20821.321
Ethanol denatured	VWR	85033.460DB
Ethidium bromide 1% Lösung	Carl Roth	2218.4

Name of Reagent	Manufacturer	Order Number
Ethyl acetate	Merck KGaA	1.096.232.500
Ethylenediaminetetraacetic acid	Carl Roth	8040.2
Flavin adenine dinucleotide	Carl Roth	5581.4
Formic acid	Sigma-Aldrich	SZE90980
Gluconate	Sigma-Aldrich	S2054
D-Glucose-6-phosphate disodium salt hydrate	Sigma-Aldrich	G7250
D-Glucose monohydrate	Serva	22720.02
Glycerine	Carl Roth	7530.4
Glycerol	Carl Roth	3783.2
Glycine	Carl Roth	3790.2
HEPES	Carl Roth	HN78.3
Horseradish peroxidase	Sigma-Aldrich	P6782-50MG
Hydrochloric acid, 37%	Carl Roth	4625.1
Hydrogen peroxide	Carl Roth	CP26.1
Imidazole	Merck KGaA	1047160250
Isopropyl- β -D-thiogalactoside	Carl Roth	CN08.3
Kanamycin sulfate	Carl Roth	T832.3
Ketoisophorone	Sigma-Aldrich	329517
Lactose monohydrate	Carl Roth	6868.1
Lysozyme	Carl Roth	8259.3
Magnesium chloride-6-hydrate	Carl Roth	2189.1
Magnesium sulfate-7-hydrate	Merck KGaA	1.058.861.000
Manganese(II) chloride	VWR	1.05927-0100
Methanol LC-MS	VWR	83.638.320
Methyl iodide	VWR	25.596.154
Mehtyl-but-2-enal	Sigma-Aldrich	W340707
β -Mercaptoethanol	Merck KGaA	805.740.250
MOPS	Carl Roth	6979.4
Nicotinamide	Alfa Aesar	A15970
Nicotinamide adenine dinucleotide	Carl Roth	AE11.3
Nicotinamide adenine dinucleotide phosphate	Carl Roth	AE13.3
Oleic acid	Sigma-Aldrich	1008
Phenol	VWR	20.599.231
Potassium acetate	Carl Roth	4986.1
Potassium chloride	Carl Roth	6781.1
Potassium dihydrogen phosphate	Carl Roth	3904.3
Potassium hydroxide	Carl Roth	6751.2
Propan-2-ol	Carl Roth	7343.1

Name of Reagent	Manufacturer	Order Number
Roti® Phenol	Carl Roth	0038.3
Sodium bicarbonate	Sigma-Aldrich	S6014
Sodium carbonate	Carl Roth	8563.1
Sodium chloride	Carl Roth	P029.3
Sodium citrate dihydrate	VWR	27.830.294
Sodium dihydrogen phosphate	Fluka	71496
Sodium dithionite	Sigma-Aldrich	71699
Sodium dodecyl sulfate	Serva	20760.02
Sodium formate	Merck KGaA	106443
Sodium hydroxide	Carl Roth	6771.2
Sodium pyruvate	Carl Roth	8793.1
Sodium sulfate	Carl Roth	8560.2
Tetramethylethylenediamine	VWR	M146
N-Trimethylsilyl-N-methyl trifluoroacetamide	Macherey-Nagel	REF7012270.510
Tris	Carl Roth	AE15.2
Tryptone	Carl Roth	8952.5
Water-d ₂	Carl Roth	HN81.2
Yeast extract	Carl Roth	2363

2.1.4 Enzymes

Table 5: Listing of enzymes used in this work.

Enzyme	Manufacturer
PhuUltra High-Fidelity DNA polymerase	Agilent (Waldbronn)
DpnI	New England Biolabs GmbH (Frankfurt am Main)
DNaseI	Serva (Heidelberg)
Lysozym	Carl Roth (Karlsruhe)
Formate dehydrogenase from <i>Candida boidinii</i> (order number F8649)	Sigma-Aldrich (Deisenhofen)
Glucose-6-phosphate dehydrogenase from baker's yeast (<i>S. cerevisiae</i>) (order number g6378)	Sigma-Aldrich (Deisenhofen)
Glucose dehydrogenase from <i>Thermoplasma</i> <i>acidophilum</i> (order number g5909)	Sigma-Aldrich (Deisenhofen)
Alcohol dehydrogenase equine (order number 55689)	Sigma-Aldrich (Deisenhofen)

2.1.5 Kits and Standards

Table 6: Listing of kits and standards used in this work.

Kits and Standards	Manufacturer
GeneJET™ Plasmid Miniprep Kit	Thermo Scientific (Ulm)
Roti®-Nanoquant Kit	Carl-Roth GmbH & Co. KG (Karlsruhe)
2-Log DNA Ladder	New England Biolabs GmbH (Frankfurt am Main)
PageRuler unstained Protein Ladder	Fermentas (St- Leon-Rot)

2.2 Media and Solutions

All media, buffer, and other solutions were autoclaved at 121 °C and 2 bar for 20 min. All components that were heat sensitive were filtered through a sterile syringe filter holder (0.2 µm, VWR). All components of salt containing media were autoclaved separately. For the preparation of agar plates, 1.5% agar was added to the media before autoclaving. After cooling of the media/agar media, the pre-sterile filtered antibiotic was added. All media and solutions were prepared using purified water (ddH₂O). They were stored at room temperature, if not otherwise specified.

2.2.1 Media

LB media (BERTANI 1951)

- 0.5% (w/v) yeast extract
- 1.0% (w/v) sodium chloride
- 1.0% (w/v) tryptone

LB-low media

- 0.5% (w/v) yeast extract
- 0.5% (w/v) sodium chloride
- 1.0% (w/v) tryptone

Solution pH was adjusted to pH 7.

SOB media

- 0.5% (w/v) yeast extract
- 0.5% (w/v) sodium chloride
- 2.0% (w/v) tryptone

After autoclaving 10 mM magnesium sulfate, 10 mM magnesium chloride and 2.5 mM potassium chloride (all sterilized by filtration) were added.

SOC media

Preparation similar to SOB media but 20 mM D-glucose (autoclaved separately) was added after cooling.

Auto induction media (STUDIER 2005)

ZY media	10 g (w/v) tryptone and 5 g (w/v) yeast extract were solved in 925 mL H ₂ O
50x5052 solution	25% (w/v) glycerin, 2.5% (w/v) D-glucose monohydrate, 10% lactose monohydrate
20xNPS solution	6.6% (w/v) ammonium sulfate, 13.6% (w/v) potassium phosphate, 14.2% sodium hydrogen phosphate
1 M magnesium sulfate	

All solutions were prepared and autoclaved separately and combined as follows (total volume 1 L):

Component	Volume (mL)	Final Concentration
ZY media	928	
1 M magnesium sulfate	1	1 mM
50x5052	20	1x
20xNPS	50	1x

The antibiotics were added after cooling to a final concentration of 100 $\mu\text{g}\cdot\text{mL}^{-1}$ kanamycin, 100 $\mu\text{g}\cdot\text{mL}^{-1}$ ampicillin, and 34 $\mu\text{g}\cdot\text{mL}^{-1}$ chloramphenicol.

2.2.2 Antibiotics

All stock solutions of the corresponding antibiotics were filtered through a sterile syringe filter holder (0.2 μm , VWR) and aliquots were stored at -20 °C.

Table 7: Listing of antibiotics used in this work.

Antibiotic	Stock Solution
Ampicillin stock solution (1000x)	100 $\text{mg}\cdot\text{mL}^{-1}$ ampicillin sodium salt
Kanamycin stock solution (1000x)	30 $\text{mg}\cdot\text{mL}^{-1}$ kanamycin sulfate or 100 $\text{mg}\cdot\text{mL}^{-1}$ kanamycin sulfate
Chloramphenicol stock solution (1000x)	34 $\text{mg}\cdot\text{mL}^{-1}$ chloramphenicol

2.3 Bacterial Strains

Different *E.coli* strains were used for the cloning and expression of various proteins in this work. *E.coli* XL1-Blue, *E.coli* DH5 α , and NEB Turbo were used for cloning experiments and *E.coli* BL21(DE3) was used for expression.

Table 8: Listing of bacterial strains that were used in this work.

Strain	Genotype	Manufacturer
<i>E.coli</i> XL1-Blue	<i>recA1 endA1 gyrA96 thi-1 hsdR17 supE44 relA1 lac</i> [F' <i>proAB lacIqZΔM15 Tn10</i> (Tet ^R)]	Stratagene (Heidelberg)
<i>E.coli</i> DH5α	F- <i>endA1 glnV44 thi-1 recA1 relA1 gyrA96 deoR nupG Φ80dlacZΔM15 Δ(lacZYA-argF)U169, hsdR17(rK-mK+), λ-</i>	Life Technologies (Darmstadt)
NEB Turbo	F' <i>proA⁺B⁺ lacI^q Δ(lacZ) M15/fhuA2 Δ(lac-proAB) glnV gal R(zgb-210::Tn10)Tet^S endA1 thi-1 Δ(hsdS-mcrB)5</i>	New England Biolabs GmbH (Frankfurt am Main)
<i>E.coli</i> BL21(DE3)	F <i>ompT gal dcm hsdS_B(r_B⁻ m_B⁻) λ(DE3)</i>	Novagen/Merck (Darmstadt)

2.4 Plasmids

Various plasmids were used throughout this work and they were stored at -20 °C prior to use.

Table 9: Listing of plasmids used in this work.

Plasmid	Size	Description	Reference
pET28a (CBR_P_004)	5369	Kan ^R ColeI P _{lac} lacZ' <i>lacI</i> , gene expression vector with T7-expression system under the control of a lac-operator	Novagen/Merck (Darmstadt)
pCBRHis-CHis-GDH2 (CBR_P_133)	6356	ColeI LacZ' KanR PT17 Plac	(GUTERL et al. 2012; STEFFLER 2014)
pET28a-NHis-nox-L.p.	6655	Kan ^R , <i>nox</i> from <i>Lactobacillus pentosus</i> , cloned via restriction sites <i>NdeI</i> and <i>XhoI</i>	Generated by Wolfgang Ott

Other plasmids used in this work were previously designed at the Chair of Chemistry of Biogenic Resources (Technical University of Munich) according to the original protocols; for instance, the plasmids for glucose dehydrogenase E170K/Q252L of *Bacillus subtilis* (VAZQUEZ-FIGUEROA et al. 2007), glucose dehydrogenase IV from *Bacillus megaterium* (NAGAO et al. 1992), lactate dehydrogenase from *Geobacillus stearothermophilus* (MÜLLER 2013), and Cytochrome P450 BM-3 R966D/W1046S from *Bacillus megaterium* (BORST 2016; RYAN et al. 2008).

2.5 Methods

Partly the methods are derivatives or one-to-one repetitions taken from the standard operating procedures of the Chair of Chemistry of Biogenic Resources (Technical University of Munich).

2.5.1 Microbiological and Molecular Biological Methods

2.5.1.1 Measurement of the Optical Density of a Cell Suspension

Optical density (OD) of cell suspensions were measured in plastic cuvettes at 600 nm (volume 1 mL). The corresponding media was used for blank measurements. Values higher than OD=1 were diluted to minimize the measurement error. An OD₆₀₀ of 1 corresponds to approximately 3.2×10^8 cells*mL⁻¹ (for *E.coli*).

2.5.1.2 Preparation of Chemically Competent Cells

Solutions:

50 mM calcium chloride (sterile)

85% (v/v) 50 mM calcium chloride mixed with 15% (v/v) glycerin (sterile)

A pre culture was done on 5 mL of LB media with the desired *E.coli* strain. The main culture (100 mL LB media) was inoculated to OD₆₀₀=0.1 and incubated at 37 °C and 150 rpm to OD₆₀₀=0.5-0.6. After centrifugation (4500 rpm, 15 min, 4 °C), the cells were resuspended with 50 mL ice cold 50 mM calcium chloride and incubated on ice for 60 min. Afterwards, the resulting suspension was centrifuged (4500 rpm, 15 min, 4 °C), the cells were resuspended with 10 mL solution of 85% (v/v) 50 mM calcium chloride and 15% (v/v) glycerin. The mixture was once again incubated on ice for 60 min. Finally, aliquots of 100 µL in 1.5 mL reaction tubes were prepared, frozen in liquid nitrogen and stored at -80 °C until further use.

2.5.1.3 Preparation of Chemically Competent - NEB Turbo

Solutions:

TFB I 100 mM potassium chloride

50 mM manganese(II) chloride

30 mM potassium acetate

10 mM calcium chloride

15% (v/v) glycerin

TFB II 100 mM Tris-HCl pH 7.0

10 mM potassium chloride

75 mM calcium chloride

15% (v/v) glycerin

Both stock solutions (TFB I and TFB II) were prepared and autoclaved separately and stored at 4 °C. The buffers were always prepared prior to utilization.

Chemically competent NEB Turbo cells were prepared according to Inoue *et al.* (INOUE *et al.* 1990). The main culture (1 L LB media) was inoculated with the over night culture (50 mL, 37 °C) to an OD₆₀₀ of 0.1 and incubated at 37 °C and 150 rpm to OD₆₀₀ of 0.6. Afterwards the cells were cooled for 15 min on ice and harvested (4 °C, 10 min, 400 rpm) in a sterile vessel. The cell pellet was gently resuspended with 100 mL ice cold TFB I buffer and again centrifuged at 4 °C and 4000 rpm for 10 min. The resulting pellet was resuspended on ice in 10 mL TDB II buffer und transferred (100 µL) in sterile 1.5 mL reaction tubes. The aliquots were frozen in liquid nitrogen and stored at -80 °C.

2.5.1.4 Transformation of Chemically Competent Cells

For chemical transformation of *E.coli*, 0.5 µL of plasmid was transferred to 100 µL cells. This mixture was incubated for 30 min on ice, after which, a heat step was performed at 42 °C for 45 s and a further 5 min incubation on ice. SOC media (500 µL) was added and the mixture was incubated for 1.5 h at 37 °C and finally plated on LB-agar plates (100 µL) containing the corresponding antibiotic and incubated over night at 37 °C.

2.5.1.5 Preparation of Electro Competent Cells

Solutions:

10% (w/v) glycerin (sterile)

ddH₂O (sterile)

LB-low media (5 mL) was inoculated with a single colony from the corresponding *E.coli* strain over night (37 °C, 150 rpm). Main culture (100 mL LB-low media) was inoculated to OD₆₀₀ of 0.1 and incubated at 37 °C and 150 rpm until OD₆₀₀ of 0.5-0.6. Then, it was cooled on ice for 15 min, transferred into two falcons and centrifuged (3500 x g-force, 15 min, 4 °C). The cell pellets were resuspended in 10 mL ddH₂O and filled up to 50 mL with ddH₂O. After 3 times of gently inverting, the cells were again centrifuged (3500 x g-force, 15 min, 4 °C) and afterwards resuspended with 10 mL 10% (v/v) glycerin. Furthermore, it was filled up to 50 mL with 10% (w/v) glycerin. After gently inverting and centrifugation (3500 x g-force, 15 min, 4 °C), the pellets were combined and finally resuspended in 300 µL 10% (w/v) glycerin. The optical density of the suspension was adjusted to a value of 50 with 10% (w/v) glycerin. The competent cells were aliquoted (70 µL) in 1.5 mL reaction tubes, frozen in liquid nitrogen and stored at -80 °C.

2.5.1.6 Transformation of Electro Competent Cells

For transformation of competent *E.coli* cells (70 µL, previously thawed on ice), 1.5 µL-10 µL plasmid containing only low salt concentrations were added to the cells and mixed gently. After incubation on ice (5 min), the solution was transferred to an electroporation cuvette (1 mm cuvette). Immediately after, an electric pulse (1.8 kV, 1 pulse for 5 ms) was given, 900 µL SOC media was added to the electroporation cuvette and the solution incubated for 1 h at 37 °C and 150 rpm. Then 100 µL of the cell suspension (diluted or non-diluted) were spread on agar plates containing the corresponding antibiotic and incubated at 37 °C over night.

2.5.1.7 Calculation of Transformation Efficiency

For calculation of transformation efficiency, the competent *E.coli* strain was transformed with 1 ng of plasmid DNA. After incubation at 37 °C different dilutions were spread on agar plates and incubated at 37 °C over night. Calculation of transformation efficiency was done using the following formula:

$$T_E = \frac{n_{Colonies} * f}{m_{DNA}}$$

with

T_E	Transformation efficiency (colonies per μg DNA)
$n_{Colonies}$	Number of colonies on an agar plate
f	Dilution factor
m_{DNA}	DNA used for transformation in μg .

2.5.1.8 Plasmid Extraction

For plasmid-DNA isolation and purification from *E.coli*, the GeneJET™ Plasmid Miniprep Kit was used following the manufacturer's specifications: the cells were resuspended, lysed, and neutralized. After binding of the DNA to the column, it was washed and finally the purified DNA was eluted. Elution was done with ddH₂O in two steps (1st step: 30 μL , 2nd step: 20 μL). Plasmids were stored at -20 °C.

2.5.1.9 Measurement of Plasmid Concentration

DNA concentration was measured photometrically at 260 nm in a nanophotometer. Calculation was done according to the Lambert-Beer Law indicating that an extinction of 1.0 at 260 nm and a thickness of 1 cm refers to double stranded DNA concentration of 50 $\mu\text{g} * \text{mL}^{-1}$. A DNA solution was considered as pure when there is no extinction higher than 300 nm and the value A_{260}/A_{280} is at least 1.8 (MÜLHARDT 2009).

2.5.1.10 Agarose Gel Electrophoresis

Solutions:

1% (w/v) agarose solution

5 g agarose was boiled in 500 mL 1xTAE buffer [Tris-Acetate-EDTA] and stored at 60 °C

50x TAE buffer

2 M Tris; 0.05 M ethylenediaminetetraacetic acid (EDTA) and 57.1 mL pure acetic acid were dissolved in ddH₂O (final volume 1 L)

10 $\text{mg} * \text{mL}^{-1}$ ethidium bromide (1000x)

For gel staining, 500 mL 1xTAE buffer containing 0.01 $\text{mg} * \text{mL}^{-1}$ ethidium bromide was used

Destaining solution

500 mL 1xTAE buffer

6x loading dye

10 mM Tris pH 7.6, 60 mM EDTA, 60% glycerol (v/v), 0.03% (w/v) bromophenol blue, 0.03% (w/v) xylene cyanol

While using 1% (w/v) agarose gels, the DNA fragments were separated by electrophoresis according to their length. Gels were prepared using gel chambers with an appropriate sample comb. DNA

solutions were mixed with loading dye to a final concentration of 1x and pipetted into the sample pockets. The electrophoresis was run at 110 V for 25 min. The DNA in the gel was stained with ethidium bromide (15 min) and background stains were reduced by destaining for another 15 min. Documentation was performed under UV light (SHARP et al. 1973) using the INTAS, Gel iX Imager. For reference, a DNA standard from New England Biolabs GmbH (2-Log DNA Ladder) was used.

2.5.1.11 Sequencing of DNA Fragments

Sequencing of DNA was performed by GATC Biotech (Cologne).

2.5.2 Protein Analytics and Purification

2.5.2.1 Determination of Protein Concentration Using UV Spectroscopy

Protein concentrations of non-FAD dependent enzymes were measured using UV spectroscopy with a nanophotometer. The ProtParam tool (ExPASy) was used for calculation of the molecular weight and extinction coefficient. Thus, the absorption of tryptophan, tyrosine and cysteine (disulfide bridges) between 250 nm and 300 nm is considered. Accordingly, the extinction coefficient is calculated by this equation (PACE et al. 1995):

$$\epsilon_{280} = \sum Trp * 5500 + \sum Tyr * 1490 + \sum Cys * 125$$

The protein concentration is then calculated using the Lambert-Beer law:

$$c = \frac{A_{280}}{d * \epsilon_{280}} * MW$$

with

c	Concentration in mg/mL
A_{280}	Absorption at 280 nm
d	Optical Path Length in cm
ϵ_{280}	Extinction Coefficient in $M^{-1} * cm^{-1}$
MW	Molecular Weight in $g * mol^{-1}$

Absorption above 300 nm is caused by light scattering and serves as an indication for protein aggregates.

2.5.2.2 Determination of Protein Concentration Using the Bradford Assay

The determination of the protein concentration with the Bradford Assay (BRADFORD 1976) followed the instructions of the manufacturer.

2.5.2.3 SDS Polyacrylamide Gel Electrophoresis

The sodium dodecyl sulphate polyacrylamide gel electrophoresis (SDS-PAGE) was done using the protocol of Laemmli (LAEMMLI 1970).

Solutions:

Ammonium persulfate (APS) stock solution, 10%

10% (w/v) APS were solved in ddH₂O and stored at 4 °C

Coomassie staining solution

0.2% (w/v) Coomassie Brilliant Blue G250 + R250, 50% (v/v) ethanol, 10% (v/v) pure acetic acid; The solution was stirred for 3 h before filtration and stored protected from light at room temperature.

4x SDS-PAGE separating gel buffer

0.8% (w/v) SDS, 1.5 M Tris-HCl pH 8.8; The pH was adjusted with 37% (v/v) hydrochloric acid.

4x SDS-PAGE stacking gel buffer

0.8% (w/v) SDS, 0.5 M Tris-HCl, pH 6.8; The pH was adjusted with 37% (v/v) hydrochloric acid.

10x SDS-PAGE buffer

1% (w/v) SDS, 0.25 M Tris, 1.92 M glycine; The resulting pH of 8.5 must not be changed.

5x SDS loading dye

50% (v/v) glycerol, 12.5% (v/v) β -mercaptoethanol, 7.5% (w/v) SDS, 0.25 M Tris, 0.25 g/L bromophenol blue, pH 6.8; The pH was adjusted with 37% (v/v) hydrochloric acid.

	Separation gel (80 mL) (12%)	Stacking gel (40 mL) (5%)
Acrylamide/bisacrylamide solution (40% (w/v); 37.5:1)	24 mL	5.2 mL
Separation/stacking gel buffer	20 mL	10 mL
ddH ₂ O	34.32 mL	23.96 mL
SDS (10% (w/v))	800 μ L	400 μ L
The polymerization was initiated with		
Tetramethylethylenediamine	80 μ L	40 μ L
APS (10% (w/v))	800 μ L	400 μ L

Samples were first diluted with water, if necessary, and mixed with 5x loading dye to give a final concentration of 1x. After heating at 95 °C for 5 min, they were spun (21.000 x g-force, 10 s) and could then be stored at 4 °C for several days. In the latter case, the samples were heated and centrifuged again before 5 to 15 μ L were applied to the gel using a microliter syringe and the electrophoresis was run at a constant current of 30 mA per gel for about 50 min. For detection of proteins, the gels were first stained with Coomassie Brilliant Blue for 15 min, whereas the detection limit lies around 0.2-0.5 μ g*(mm²)⁻¹. For a first analysis, the gels destained in boiling water (microwave, three times) and afterwards the gels were further destained in water at room temperature overnight. Here, a paper towel was added to bind the dye.

2.5.2.4 Cell Disruption by Sonication

In binding buffer resuspended expression cultures were disrupted by sonication while cooled on ice: 80% amplitude, 0.6 ms pulse, 3x10 min. The soluble fraction was obtained by centrifugation (14.000 x g-force, 45 min, 4 °C).

2.5.3 Chemical Methods

2.5.3.1 Reaction Control During Chemical Synthesis of the Biomimetic Cofactors

Thin layer chromatography was used to control the progress of the synthesis of the biomimetic cofactors (SCHELHORN 2004). The mobile phase contained 12.6 mL ethyl acetate, 1.4 mL methanol, and 625 μ L 32% ammonia. Silica gel 60 plates with UV indicator from Merck KGaA (Darmstadt) were used. The products could be visualized by the fluorescence indicator using UV light.

2.5.3.2 NMR Analysis

For NMR analysis, 10-20 mg of the synthesized biomimetic cofactor were diluted with 800 μ L of the corresponding solvent. Evaluation was done using the δ -scale (in ppm) for chemical shifts. Calibration was done on different significant signals:

Table 10: Chemical solvents used for NMR analysis with significant signals including tetramethylsilane (TMS) at 0 ppm or trimethylsilylpropanoic acid (TSP) at 0 ppm.

Solvents	Delta- ¹ H [ppm] (multiplicity)	Water peak- ¹ H [ppm]	Delta- ¹³ C [ppm] (multiplicity)
Chloroform-d ₁	7.26 (1)	1.55	77.0 (3)
Water-d ₂	4.67 (1)	-	-
Dimethylsulfoxide-d ₆	2.49 (5)	3.30	39.7 (7)

3 Results

3.1 Regeneration of Oxidized Biomimetic Cofactors by NADH Oxidase from *Lactobacillus pentosus*

3.1.1 A water-forming NADH oxidase from *Lactobacillus pentosus* suitable for the regeneration of synthetic biomimetic cofactors

In this publication, a novel water-forming, FAD-dependent NADH oxidase from *Lactobacillus pentosus* (*LpNox*) was characterized and cofactor recycling with biomimetic as well as natural cofactors was described. The use of cheap synthetic cofactors may additionally allow reduction of process costs, however, regeneration of biomimetic cofactors was limited to chemical and electrochemical methods.

First characterization of *LpNox* showed that the heterologous overexpressed enzyme only contained 13% FAD that resulted in a decreased specific activity ($7.9 \text{ U}\cdot\text{mg}^{-1}$ with NADH). After *in vitro* incubation of *LpNox* with FAD at 37°C and subsequent desalting to remove unbound FAD, the flavin content of the enzyme was increased to 95% resulting a specific activity with NADH of $50.1 \text{ U}\cdot\text{mg}^{-1} \pm 1.9 \text{ U}\cdot\text{mg}^{-1}$. The highest activity was detected at pH 7.0 in potassium phosphate buffer, between 35°C and 40°C and the kinetic parameters for NADH were a K_M of $17.9 \mu\text{M} \pm 3 \mu\text{M}$ and k_{cat} of 43.4 s^{-1} . Furthermore, *LpNox* was characterized regarding its activity with the biomimetic cofactors MNAH and BNAH: kinetic measurements revealed K_M for MNAH $1.6 \text{ mM} \pm 0.5 \text{ mM}$ with k_{cat} 0.14 s^{-1} and K_M for BNAH $1.3 \text{ mM} \pm 0.4 \text{ mM}$ with k_{cat} 0.17 s^{-1} .

Apart from the enzymatic recycling, which gives H_2O as a by-product by transferring four electrons onto oxygen, unbound FAD can also catalyze the oxidation of biomimetic cofactors. Here, a two electron process takes place yielding H_2O_2 instead. Thus, measurement of only trace amounts of H_2O_2 after MNAH/BNAH conversion with *LpNox* confirmed the enzymatic reaction. Accordingly, after reaction of MNAH or BNAH with FAD, high concentrations of H_2O_2 were detected. Reaction of both, *LpNox* and FAD, were of comparable activity. Taking into account that large concentrations of H_2O_2 can damage enzyme and substrates involved in the biocatalytic process, the use of *LpNox* may be the superior choice regarding side products and the biocatalysts also holds the potential to be evolvable.

The authors, Claudia Nowak and Barbara Beer, contributed equally to this publication and both wrote the manuscript. Claudia Nowak designed and conducted all experiments regarding the biomimetic cofactors among others including cofactor synthesis, assay development, conversion of biomimetics with *LpNox* and FAD, and measurement of side reaction products. Barbara Beer designed and conducted all experiments regarding general characterization of *LpNox* among others including activation of the enzyme, measurement of thermal stability, and total turnover number. André Pick supported in designing the experiments and proof-read the manuscript. Teresa Roth assisted on experiments with natural cofactors. Petra Lommes supported synthesis of biomimetic cofactors. Claudia Nowak and Barbara Beer designed the research project and experimental approach guided by Volker Sieber.

Supporting Information to this manuscript can be found in the appendix.

A water-forming NADH oxidase from *Lactobacillus pentosus* suitable for the regeneration of synthetic biomimetic cofactors

Claudia Nowak ¹, Barbara Beer ¹, André Pick, Teresa Roth, Petra Lommes, and Volker Sieber

Frontiers in Microbiology
2015

Open Source
DOI:10.3389/fmicb.2015.00957

¹ These authors have contributed equally to this work.



A water-forming NADH oxidase from *Lactobacillus pentosus* suitable for the regeneration of synthetic biomimetic cofactors

Claudia Nowak[†], Barbara Beer[†], André Pick, Teresa Roth, Petra Lommes and Volker Sieber*

Chair of Chemistry of Biogenic Resources, Straubing Centre of Science, Department Life Science Engineering, Technische Universität München, Straubing, Germany

OPEN ACCESS

Edited by:

Robert Kourist,
Ruhr-University Bochum, Germany

Reviewed by:

Frank Hollmann,
Delft University of Technology,
Netherlands
Matthias Höhne,
University of Greifswald, Germany

*Correspondence:

Volker Sieber,
Chair of Chemistry of Biogenic
Resources, Straubing Centre
of Science, Department Life Science
Engineering, Technische Universität
München, Schulgasse 16,
D-94315 Straubing, Germany
sieber@tum.de

[†]These authors have contributed
equally to this work.

Specialty section:

This article was submitted to
Microbiotechnology, Ecotoxicology
and Bioremediation,
a section of the journal
Frontiers in Microbiology

Received: 01 July 2015

Accepted: 28 August 2015

Published: 16 September 2015

Citation:

Nowak C, Beer B, Pick A, Roth T,
Lommes P and Sieber V (2015)
A water-forming NADH oxidase from
Lactobacillus pentosus suitable
for the regeneration of synthetic
biomimetic cofactors.
Front. Microbiol. 6:957.
doi: 10.3389/fmicb.2015.00957

The cell-free biocatalytic production of fine chemicals by oxidoreductases has continuously grown over the past years. Since especially dehydrogenases depend on the stoichiometric use of nicotinamide pyridine cofactors, an integrated efficient recycling system is crucial to allow process operation under economic conditions. Lately, the variety of cofactors for biocatalysis was broadened by the utilization of totally synthetic and cheap biomimetics. Though, to date the regeneration has been limited to chemical or electrochemical methods. Here, we report an enzymatic recycling by the flavoprotein NADH-oxidase from *Lactobacillus pentosus* (*LpNox*). Since this enzyme has not been described before, we first characterized it in regard to its optimal reaction parameters. We found that the heterologously overexpressed enzyme only contained 13% FAD. *In vitro* loading of the enzyme with FAD, resulted in a higher specific activity towards its natural cofactor NADH as well as different nicotinamide derived biomimetics. Apart from the enzymatic recycling, which gives water as a by-product by transferring four electrons onto oxygen, unbound FAD can also catalyze the oxidation of biomimetic cofactors. Here a two electron process takes place yielding H₂O₂ instead. The enzymatic and chemical recycling was compared in regard to reaction kinetics for the natural and biomimetic cofactors. With *LpNox* and FAD, two recycling strategies for biomimetic cofactors are described with either water or hydrogen peroxide as by-product.

Keywords: cofactor regeneration, H₂O-forming NADH oxidase, synthetic cofactors, biomimetic cofactors, *Lactobacillus pentosus*, flavin adenine dinucleotide, hydrogen peroxide

Introduction

The cell-free biocatalytic production of fine chemicals by oxidoreductases has continuously grown over the past years (Matsuda et al., 2009). When enzymes such as dehydrogenases that depend on the stoichiometric use of nicotinamide pyridine cofactors are involved, an integrated efficient recycling system is crucial to allow process operation under economic conditions (Weckbecker et al., 2010; Tauber et al., 2011). For a further increase of the profitability the variety of available cofactors for biocatalysis was recently broadened by the utilization of totally synthetic and cheap

biomimetics (Lutz et al., 2004; Ryan et al., 2008; Campbell et al., 2012; Paul et al., 2013). Hence, the cost for the cofactor in a cell-free process can be decreased enormously (Rollin et al., 2013). In most cases these biomimetic cofactors can easily be synthesized in one or two steps. First, the oxidized form is prepared within the reaction of nicotinamide and the corresponding alkyl halogenide. Subsequent reaction with sodium dithionite yields the reduced form of the derivative (Karrer and Stare, 1937; Mauzerall and Westheimer, 1955). Several biomimetics have been described in literature so far: 5-methyl-1,4-dihydro-*N*-benzylnicotinamide and 6-methyl-1,4-dihydro-*N*-benzylnicotinamide (Takeda et al., 1987; Hentall et al., 2001), *N*-methyl-1,4-dihydronicotinamide (MNAH) (Friedlos et al., 1992; Knox et al., 1995) and *N*-benzyl-1,4-dihydronicotinamide (BNAH) (Lutz et al., 2004; Ryan et al., 2008; Paul et al., 2013). Though, to date the regeneration of the oxidized biomimetic cofactors has been limited to chemical or electrochemical methods (Lutz et al., 2004; Ryan et al., 2008; Poizat et al., 2010; Kara et al., 2014). An enzymatic recycling system would have the advantage of being evolvable and thereby holds the potential of a most efficient recycling in the future. The main challenge researchers are facing at the moment lies in finding enzymes that have at least a minor activity with biomimetic cofactors. So far only a few examples are known from literature: Paul et al. (2013) showed that the enoate reductase from *Thermus scotoductus* could use BNAH to perform the asymmetric reduction of conjugated C=C double bonds. Another example is the hydroxylation of non-activated C-H bonds by cytochrome P450 BM-3 R966D/W1046S from *Bacillus megaterium* with BNAH instead of the natural cofactor 1,4-dihydro-nicotinamide adenine dinucleotide (NADH) or 1,4-dihydro-nicotinamide adenine dinucleotide phosphate (NADPH) (Ryan et al., 2008). Most of the enzymes described so far need a second cofactor like flavin adenine mononucleotide (FMN) or flavin adenine dinucleotide (FAD) to be active. These flavin derivatives act as a linker between substrate and nicotinamide pyridine cofactor and are supposed to facilitate the hydride transfer (Paul et al., 2014a). From this it can be concluded that also other enzymes carrying flavin adenine cofactors have the potential to accept biomimetic cofactors. In this context NADH oxidases, which are also flavo-enzymes that oxidize NAD(P)H to NAD(P)⁺ with simultaneous reduction of molecular oxygen to either hydrogen peroxide (H₂O₂) or water (H₂O), have attracted interest as suitable candidates for an efficient NAD⁺ cofactor recycling. In coupled enzyme reactions the four-electron reduction to benign H₂O is preferred over the two-electron reduction to H₂O₂, which, even in small amounts, can inactivate the enzymes of the production-regeneration cycle (Hernandez et al., 2012). The addition of catalase as a possible remedy increases the complexity of the system to the point where three enzymes have to be coupled and adjusted to their activity over time. Water-forming NADH oxidases are described from various *Cocci* and *Bacilli* species: *Enterococcus (Streptococcus) faecalis* (Schmidt et al., 1986), *Streptococcus pyogenes* (Gao et al., 2012), *Streptococcus mutans* (Higuchi et al., 1993), *Lactobacillus rhamnosus* (Zhang et al., 2012), *Lactobacillus brevis* (Geueke et al., 2003), *Lactococcus lactis* (Heux et al., 2006), *Lactobacillus sanfranciscensis* (Riebel et al., 2003) as well as from

Clostridium aminovalericum (Kawasaki et al., 2004) and from the hyperthermophile *Thermococcus profundus* (Jia et al., 2008). The sequence analysis of H₂O-forming NADH oxidases from different *Lactobacilli* reveals sequence identities with a putative NADH oxidase from *Lactobacillus pentosus* (LpNox) that range from 42.5% for the crystallographically defined NADH oxidases from *L. sanfranciscensis* (pdb identifier CDU2) (Lountos et al., 2006) to 46.3 and 87.2% for the NADH oxidases from *L. brevis* (Geueke et al., 2003) and *L. plantarum* (Park et al., 2011), respectively. In each case, the most highly conserved regions include the redox-active cysteine (Cys42 in all sequences) as well as the FAD and NAD(P)H binding domains (see Supplementary Figure S1). In the proposed reaction mechanism of H₂O-forming NADH oxidases the first NADP(H) transfers electrons onto FAD. FADH₂ reduces molecular oxygen to hydrogen peroxide, which is supposed to be trapped in the active site and motioned toward the thiolate moiety of Cys42. A nucleophilic attack of Cys42-S⁻ on H₂O₂ yields the first water molecule and generates the Cys42-SOH intermediate. The second NAD(P)H then reduces FAD, which transfers the electrons much faster onto Cys42-SOH than onto another oxygen. Thus, the sulfenic acid is converted back to the thiolate and the second water molecule is released.

Due to the high sequence similarity to crystallographically defined H₂O-forming NADH oxidases, we decided to investigate the putative NADH oxidase from *L. pentosus* MP-10 (LpNox) as a possible recycling enzyme in cell-free reactions. Furthermore, we tested the enzyme for the acceptance of the synthetic biomimetic cofactors MNAH and BNAH. The structures of all cofactors used are depicted in **Figure 1**. Interestingly, both LpNox and free FAD (Paul et al., 2014b, 2015) were capable of oxidizing the biomimetics and were therefore compared in regard of their kinetic parameters and the resultant by-products.

Materials and Methods

Reagents

All chemicals were purchased from Sigma-Aldrich, Merck or Carl Roth. All columns used for protein purification were from GE Healthcare (Munich, Germany).

Synthesis of the Oxidized Biomimetics

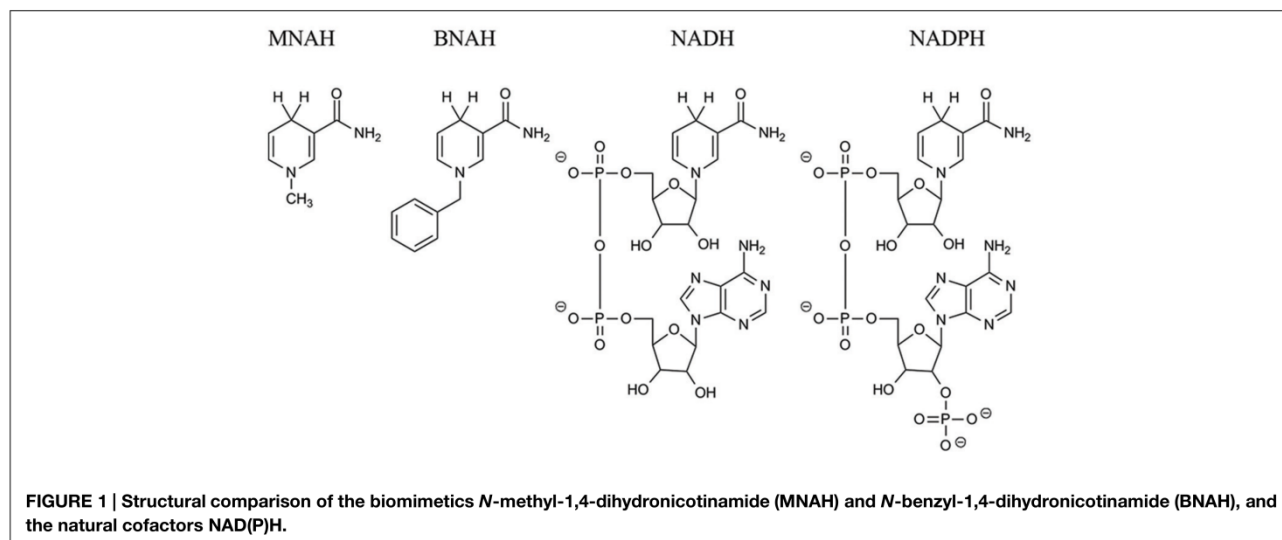
The synthesis was adapted from a former procedure (Karrer and Stare, 1937; Mauzerall and Westheimer, 1955).

MNA⁺

Nicotinamide (50 mmol) was dissolved in 30 mL methanol. Methyl iodide (150 mmol) was added and the reaction mixture was stirred for 27 h at room temperature. The yellow precipitate was filtered and washed twice with methanol. The crude product was recrystallized from 250 mL hot methanol. C₇H₉IN₂O; yellow solid; yield: 81%; ¹H NMR (400 MHz, DMSO) δ 9.3 (s, 1H), 9.0 (d, 1H), 8.8 (d, 1H), 8.5 (s, 1H), 8.2 (dd, 1H), 8.1 (s, 1H), 4.4 (s, 3H).

BNA⁺

Nicotinamide (120 mmol) was dissolved in 40 mL acetonitrile and heated to reflux. Benzyl chloride (120 mmol) was added



dropwise and the reaction mixture was stirred for further 12 h under reflux. After cooling to room temperature 120 mL diethyl ether was added, the precipitate was filtered and washed twice with diethyl ether. $C_{13}H_{13}ClN_2O$; white solid; yield: 86%; 1H NMR (400 MHz, D_2O) δ 9.2 (s, 1H), 8.9 (d, 1H), 8.8 (d, 1H), 8.1 (t, 1H), 7.4 (m, 5H), 5.8 (s, 2H).

Synthesis of the Reduced Biomimetics

The synthesis was adapted from a former procedure (Karrer and Stare, 1937; Mauzerall and Westheimer, 1955; Knox et al., 2000).

MNAH

MNA^+ (3.8 mmol) was dissolved in 250 mL water at 40°C under argon atmosphere. Sodium carbonate (24 mmol) and sodium bicarbonate (30 mmol) were added to the reaction mixture. Sodium dithionite (14 mmol) was added in portions and the mixture was stirred for further 30 min at 40°C. After cooling to room temperature an oily solid precipitated. The crude product was extracted three times with dichloromethane. The combined organic phases were washed once with water, dried over sodium sulfate and the solvent was removed by rotary evaporation. $C_7H_{10}N_2O$; yellow solid; yield: 25%; 1H NMR (400 MHz, $CDCl_3$) δ 7.0 (s, 1H), 5.7 (d, 1H), 5.4 (s, 2H), 4.7 (d, 1H), 3.1 (s, 2H), 2.9 (m, 3H).

BNAH

BNA^+ (20 mmol) was added to a solution of sodium bicarbonate (66 mmol) and sodium dithionite (60 mmol) at 50°C and stirred for 15 min. The reaction mixture was cooled to 0°C for another 15 min. The precipitating solid was then washed twice with 100 mL dichloromethane and dried over sodium sulfate. The crude product was recrystallized from water:ethanol (3:1) at 0°C for 2 h. $C_{13}H_{14}N_2O$; yellow solid; yield: 73%; 1H -NMR (400 MHz, $CDCl_3$), δ (ppm): 7.34–7.23 (m, 5H), 7.15–7.14 (d, 1H), 5.74–5.73 (dq, 1H), 5.40 (br s, 2H), 4.76–4.72 (m, 1H), 4.28 (s, 2H), 3.17–3.16 (m, 2H).

Cloning

For the cloning of the NADH oxidase (*LpNox*) from *L. pentosus* MP-10 (protein sequence GenBank™ CCB83530.1) genomic DNA was used as PCR template. It was isolated from cells of an overnight culture using the protocol of Chen and Kuo (1993). Three PCR reactions were performed to add an N-terminal, C-terminal or no His-Tag. For the N-terminal His-Tag the following primers were used: F-NheI-*nox-Lp* – GACAGGC TAGCATGAAAGTTATCGTAATTGGTTGTAC and R-XhoI-stop-*nox-Lp* – GCGACTCGAGTTATTCCGTCACCTTTTTCAGCC, for the C-terminal His-Tag: F-BsaI-*nox-Lp*-CACGGTC TCGCATGAAAGTTATCGTAATTGGTTGTAC and R-XhoI-*nox-Lp*-GCGACTCGAGTTCCGTCACCTTTTTCAGCCG and for no His-Tag: F-BsaI-*nox-Lp*-CACGGTCTCGCATGAAAGTT ATCGTAATTGGTTGTAC and R-XhoI-stop-*nox-Lp* – GCGA CTGAGTTATTCCGTCACCTTTTTCAGCC. The restriction enzyme recognition sites are underlined and the start and stop codon is marked in bold. The PCR products were purified and ligated into pET28a (Novagen, Darmstadt, Germany). The multiplication of the plasmid was performed with *E. coli* DH5 α (Stratagene, La Jolla, CA, USA) in LB medium containing 30 μ g/mL kanamycin.

Expression and Purification

The expression of each variant of *LpNox* was performed with *E. coli* BL21 (DE3) in 200 mL autoinduction media with 100 μ g/mL kanamycin (Studier, 2005). The preculture was incubated in 20 mL of LB medium with 30 μ g/mL kanamycin at 37°C overnight on a rotary shaker (180 rpm). Expression cultures were inoculated with a 1:100 dilution of overnight cultures. Incubation was performed for 3 h at 37°C followed by incubation for 21 h at 16°C.

Subsequently, there was a separation in the handling for the His-tagged enzymes and the one without His-Tag. The treatment for both His-tagged enzymes was the same. Cells were harvested by centrifugation and resuspended in 50 mM sodium phosphate buffer (pH 8.0, 20 mM imidazole, 500 mM

NaCl, and 10% glycerol). Crude extracts were prepared by the use of a Basic-Z Cell Disrupter (IUL Constant Systems), subsequent addition of $MgCl_2$ to a final concentration of 2.5 mM in combination with DNase I (1 $\mu g/mL$) and a following incubation for 20 min at room temperature to degrade DNA. The insoluble fraction of the lysate was removed by centrifugation (20,000 rpm for 40 min at 4°C). The supernatant was filtered through a 0.45 μm syringe filter and applied to an IMAC affinity resin column, 5 mL HisTrap™ FF, equilibrated with the resuspension buffer using the ÄKTA Purifier-system. The column was washed with five column volumes of resuspension buffer and eluted in a gradient of 10 column volumes from 0 to 100% elution buffer (50 mM sodium phosphate buffer pH 8.0, 500 mM imidazole, 500 mM NaCl, and 10% glycerol). Aliquots of eluted fractions were subjected to 12% SDS-Page described by Laemmli (1970). The molecular weight of the His-tagged LpNox was calculated to be 51.94 kDa using the ProtParam tool (Artimo et al., 2012). The fractions containing the eluted protein were pooled and the protein was desalted using a HiPrep™ 26/10 Desalting column which was preliminary equilibrated with 50 mM Tris-HCl pH 7.5. Aliquots of the light yellow protein solution were frozen in liquid nitrogen and stored at -80°C.

Cells containing the enzyme without His-Tag were harvested by centrifugation and resuspended in 50 mM potassium phosphate buffer pH 7.0. Crude extracts were prepared by the use of a Basic-Z Cell Disrupter (IUL Constant Systems), subsequent addition of $MgCl_2$ to a final concentration of 2.5 mM in combination with DNase I (1 $\mu g/mL$) and a following incubation for 20 min at room temperature to degrade DNA. The insoluble fraction of the lysate was removed by centrifugation (20,000 rpm for 40 min at 4°C). The supernatant was filtered through a 0.45 μm syringe filter and applied to an affinity resin column, 5 mL HiTrap Blue HP, equilibrated with the resuspension buffer using the ÄKTA Purifier-system. The column was washed with five column volumes of resuspension buffer and eluted in one step with elution buffer (50 mM potassium phosphate buffer pH 7.0 and 1.5 M KCl). Aliquots of the different fractions were subjected to 12% SDS-Page described by Laemmli (1970). The molecular weight was calculated to be 49.46 kDa.

Determination of Protein and FAD Concentration

The LpNox concentration was determined using a Bradford assay Roti®-nanoquant (Carl Roth) with BSA as standard. The FAD concentration was measured in microtiter plates at 450 nm and compared to a FAD standard (10–70 μM).

Enzyme Activation

The LpNox was incubated with an excess of FAD at 37°C for 15 min. After cooling the enzyme to 4°C precipitated protein was separated by centrifugation (20,000 rpm for 15 min at 4°C). Afterward unbound FAD was removed by size exclusion chromatography using a HiPrep™ 26/10 Desalting column, which had been preliminary equilibrated with 50 mM Tris-HCl pH 7.5. Aliquots of the protein were frozen in liquid nitrogen and stored at -80°C.

General Characterization of LpNox

All enzyme assays were performed in triplicate with 50 mM buffer at the desired pH, concentration of NADH and at the desired temperature. The absorption of NADH was measured in microtiter plates (Greiner, flat bottom) at 340 nm using a Multiskan or Varioskan spectrophotometer (Thermo Fisher Scientific).

The pH activity profile was obtained at 25°C with 0.3 mM NADH in 50 mM triple buffer containing $1/3$ sodium citrate, $1/3$ potassium phosphate and $1/3$ glycine. The pH values were adjusted with HCl or KOH from pH 5.0 to 10.0.

The optimum temperature was studied by adding the enzyme solution to the preheated reaction mixture containing 50 mM Tris-HCl pH 7.0 and 0.3 mM NADH. A temperature range of 25–50°C was chosen.

The thermostability (T_{50}^{30}) was studied by incubating the enzyme at various temperatures for 30 min in 50 mM Tris-HCl pH 7.0 with and without 5 mM DTT. The residual activity was measured at 37°C with 0.6 mM NADH.

The kinetic parameters of LpNox with NADH were investigated with a substrate range from 0.01 to 0.4 mM in 50 mM Tris-HCl pH 7.0. The calculation of Michaelis–Menten kinetics for determination of K_m and v_{max} was done with SigmaPlot 11.0 (Systat Software).

The total turnover number was calculated from k_{cat}/k_{deact} , whereas k_{deact} was obtained from incubating the enzyme at 37°C in 50 mM Tris-HCl pH 7.0 with and without 5 mM DTT. At certain time points the residual activity was measured with 0.3 mM NADH in the same buffer. The data points were fitted to an exponential decay equation using SigmaPlot 11.0 (Systat Software).

Characterization of the LpNox with the Biomimetic Cofactors

Stock solutions of MNAH/BNAH were dissolved in DMSO freshly before use and added to the assay to give a final DMSO concentration of 5%.

The activity of the LpNox was measured in triplicates with 0.5 mM biomimetic in 50 mM Tris-HCl pH 7.0 at 37°C. The decrease of the absorbance of MNAH/BNAH was followed at 358 nm. The activity of an equivalent concentration FAD with the biomimetics was determined similarly.

The kinetic constants for the biomimetic cofactors were determined in triplicate with a fluorescence measurement. A solution of 20 μl 2 M potassium hydroxide, 20 μl 20% acetophenone in DMSO, and 45 μl H₂O was prepared in a polypropylene fluorescence microtiter plate. The enzymatic reaction in 50 mM Tris-HCl pH 7.0 containing LpNox and substrate ranging from 0 to 8 mM was incubated at 37°C. Every 2–3 min a 5 μl sample from the enzymatic reaction was added to the solution. Then 90 μl 88% formic acid was added and it was incubated for 30 min at room temperature. The samples were measured at the following conditions: MNA⁺: excitation: 386 nm, emission: 446 nm; BNA⁺ excitation: 380 nm, emission: 438 nm (Zhang et al., 2011). For the calculation of concentrations a standard was used (0–0.8 mM oxidized cofactor). The calculation of Michaelis–Menten kinetics for

determination of K_m and v_{max} was done with Sigma-Plot 11.0 (Systat Software).

Quantification of H₂O₂

The H₂O₂ concentration was determined in a microtiter plate using 100 μ L of the activity assay containing 1 mM MNAH/BNAH/NADH and 6 μ M LpNox/FAD in 50 mM Tris-HCl pH 7.0, which was incubated for 5 h at 37°C, and 100 μ L detection reagent containing 50 μ M DA-64 and 0.2 U/mL horseradish peroxidase in 50 mM Tris-HCl pH 7.0. The absorbance was measured at 727 nm and the quantities were calculated by a standard curve (0–40 μ M).

Results

Enzyme Purification and Activation with FAD

The attempt to use the HiTrap Blue HP column for purification of the untagged enzyme was not successful. The complete enzyme was found in the flow through. However, both enzymes with N-terminal or C-terminal His-Tag were soluble and could be purified as a yellowish solution due to the bound FAD. No major impurities were detected by SDS-PAGE (Supplementary Figure S2) and 84 mg of N-terminal LpNox were obtained from 1 L of culture. There was no significant difference in the catalytic activity of both tagged enzymes and therefore all experiments were conducted using the N-terminal His-Tag enzyme.

The activity of NADH oxidases depends on the cofactor FAD, which binds to the enzymes when it is translated and folded in the producing organism. We found that the overexpression in *E. coli* can result in poor activity of the LpNox due to missing FAD: 1 mole of purified LpNox contained between 0.12 and 0.2 mol of FAD. But the LpNox could be loaded with FAD, when the enzyme was incubated with an excess amount of free FAD. The incubation of 157 μ M LpNox (containing 13% FAD) with 200 μ M FAD at 37°C for 15 min and subsequent desalting to remove unbound FAD, resulted in 60 μ M LpNox with 57 μ M FAD (95%). The specific activity was 7.9 U/mg before activation and 50.1 U/mg after loading. Overall, a sevenfold improvement in FAD content and a 6 fold increase in specific activity were achieved.

General Characterization

LpNox was investigated for its suitability as a regeneration enzyme. Therefore, it was tested under various conditions to determine influences on the activity (Figure 2).

pH, Buffer, and Temperature Effect

The pH profile showed a sharp peak at pH 7.0 with 70% residual activity at pH 6.0 and 8.0 (Figure 2A). The highest activity at pH 7.0 was measured in potassium phosphate buffer. But since potassium phosphate reduces cofactor stability (Rover et al., 1998), all further experiments were done in Tris-HCl pH 7.0 (92% activity compared to potassium phosphate; Figure 2B). The temperature optimum of LpNox was between 35 and 40°C. Overall, no strong temperature dependence could be detected during the first 5 min after starting the reaction (Figure 2C).

Kinetics and Reaction Product

From kinetic studies in 50 mM Tris-HCl pH 7.0 at 37°C, a K_m for NADH of 17.9 μ M \pm 3 μ M and a v_{max} of 50.1 \pm 1.9 U/mg ($k_{cat} = 43.4$ s⁻¹) for NADH were determined (Figure 2D). NADPH can be recognized as a substrate by LpNox, though the specific activity was only about 2% compared to NADH. Due to a conserved Cys residue at position 42 LpNox should be an H₂O-forming NADH oxidase. This hypothesis could be confirmed with an H₂O₂ assay, where less than 1% of the theoretical yield of hydrogen peroxide could be detected.

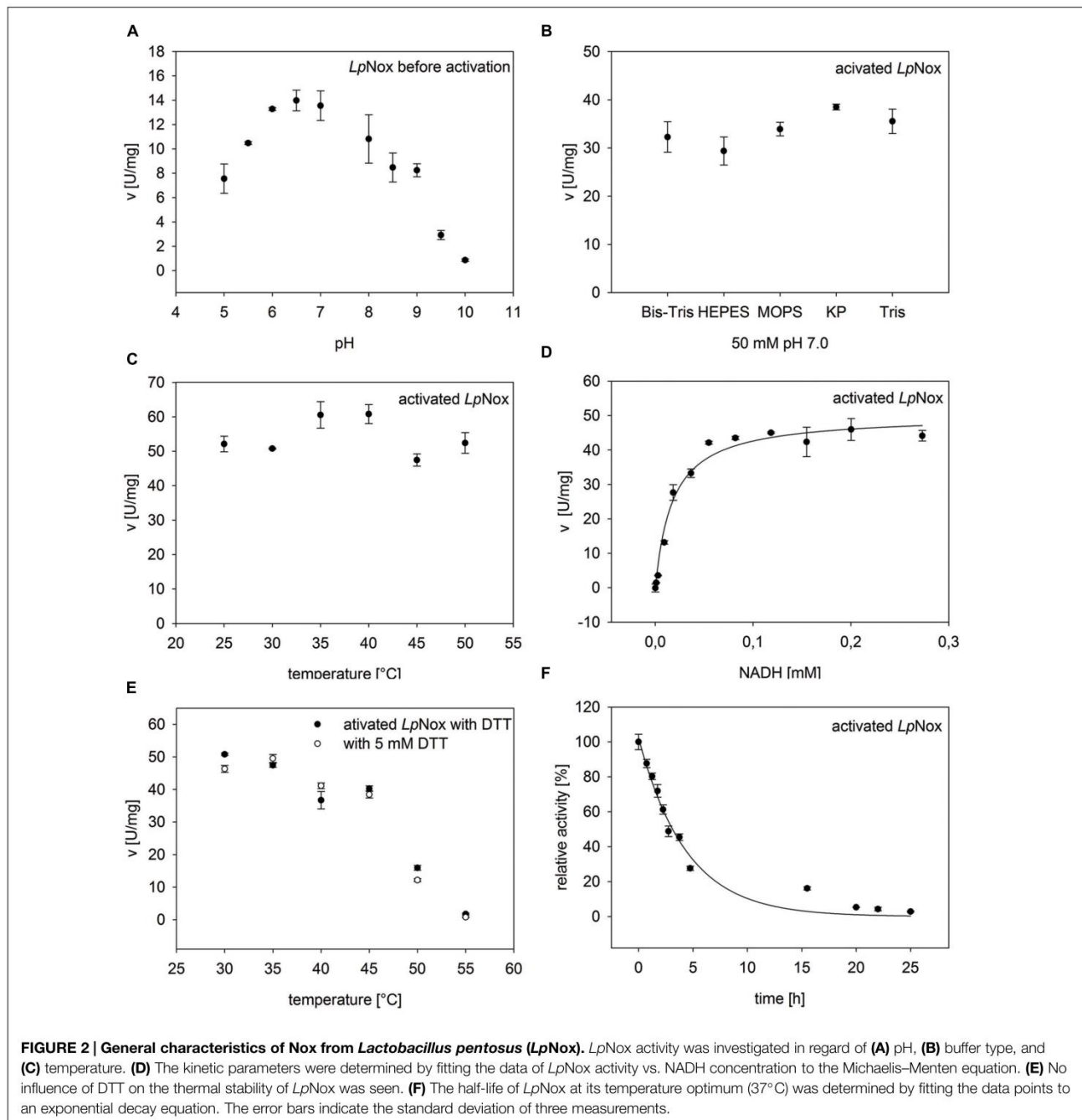
Thermal Stability and Total Turn Over

To determine the influence of temperature over a specific period of time, the thermal stability was tested by incubating the enzyme for 30 min at various temperatures and measuring the residual activity. The temperature, at which 50% of the activity was left compared to the activity before incubation (T_{50}^{30}), was 48.4°C. A similar result (48°C) was obtained when DTT was added to the enzyme during incubation (Figure 2E). The total turnover of an enzyme can be calculated from k_{cat}/k_{deact} . Therefore, the decrease in activity at 37°C until the enzyme was completely inactive was measured. The obtained values were fitted to an exponential function, giving a k_{deact} of 0.299 \pm 0.0237 h⁻¹ (Figure 2F). This resulted in a half-life of LpNox of 3 h and a total turnover number of 6.8 \times 10⁵. In order to see whether the loss of activity over time was due to a loss of FAD, the incubated enzyme solution was filtered (10 kDa cutoff). The flow through did not contain FAD, whereas the residue on the filter was yellow.

Activity with Biomimetic Cofactors

After the activation of the LpNox with FAD the activities with the biomimetic cofactors MNAH and BNAH could be increased by a factor of 4–6 (data not shown).

Recently, Paul et al. described the reaction of flavin mononucleotide (FMN) with the biomimetic cofactor BNAH under formation of H₂O₂ (Paul et al., 2014b, 2015). Accordingly, this chemical reaction was confirmed with FAD and the two biomimetics tested in this study (Table 1). In order to compare the enzymatic reaction to the reaction of free FAD, the turnover numbers (TON) were calculated with respect to the FAD content. With MNAH free FAD showed a slightly higher activity than the LpNox, while the activities with BNAH were equal. Since the LpNox is an FAD dependent enzyme the observed reaction could either be enzymatically or chemically catalyzed. To investigate this, the reaction products were determined. When incubating FAD with 1 mM of the biomimetic cofactors at 37°C for 5 h high quantities of H₂O₂ could be detected: 0.32 \pm 0.040 mM for MNAH and 0.50 \pm 0.018 mM for BNAH. In contrast, in the enzymatic reaction only small amounts of about 0.2 \times 10⁻³ mM (MNAH) and 2.6 \times 10⁻³ mM (BNAH) H₂O₂ were produced (Table 2). However, this could also be attributed to a possible catalase property of the LpNox. If LpNox is added after H₂O₂ production with free FAD, the concentration of hydrogen peroxide indeed decreases substantially but remains still significantly higher compared to the amount that was detected in the solely enzymatic reaction.



For the determination of the kinetic constants of *LpNox* with the biomimetic cofactors a fluorescence assay was used, because high concentrations of reduced cofactors exceed the maximal absorbance for photometric measurements. Both could be fitted to the Michaelis–Menten equation (Figure 3). K_m and v_{max} (k_{cat}) of both cofactors are in the same range with BNAH showing a slightly lower K_m and higher v_{max} than MNAH. Therefore, k_{cat}/K_m for BNAH is 1.4 higher than for MNAH (Table 3).

Discussion

General Applicability of *LpNox* for the Regeneration of Oxidized Cofactors

With the NADH oxidase from *L. pentosus* (*LpNox*), we identified a regeneration system for the natural cofactor NAD^+ as well as for the biomimetic cofactors MNA^+ and BNA^+ . After expression and purification in *E. coli*, more than 80% of the enzyme was present in the apo-form and did not contain the essential cofactor

TABLE 1 | Comparison of the turn over number (TON) of LpNox and FAD with the biomimetics.

Cofactor	TON of free FAD [min ⁻¹]	TON of LpNox [min ⁻¹]
MNAH	2.23 ± 0.15	1.31 ± 0.05
BNAH	0.97 ± 0.07	0.79 ± 0.01

The activities of the enzymatic and chemical catalyst were investigated with the biomimetics MNAH and BNAH in a photometric assay (358 nm). The activities were compared concerning the FAD content. The standard deviation was calculated from three measurements.

TABLE 2 | Measurement of the by-product H₂O₂.

Cofactor	FAD [mM H ₂ O ₂]	LpNox [mM H ₂ O ₂]	FAD/LpNox [mM H ₂ O ₂]
MNAH	0.32 ± 0.04	0.2*10 ⁻³ ± 0.1*10 ⁻³	16*10 ⁻³ ± 1*10 ⁻³
BNAH	0.51 ± 0.18	2.6*10 ⁻³ ± 0.9*10 ⁻³	25*10 ⁻³ ± 1*10 ⁻³

H₂O₂ concentrations in the reactions of FAD or LpNox with 1 mM of the biomimetics MNAH and BNAH were detected with DA-64 and horseradish peroxidase. Firstly either FAD or the enzyme was added to the cofactor. Secondly a combined approach was performed with addition of LpNox after 1 h. The standard deviation was calculated from three measurements.

FAD. Incubation of the enzyme with an excess amount of FAD and subsequent desalting resulted in fully activated LpNox that did not lose the FAD during desalting or the activity tests. This is similar to the procedure described by Jiang and Bommaris (2004) and Tóth et al. (2008) and obviates the need of adding FAD to the reaction mixture, which is also common (Jiang et al., 2005; Rocha-Martin et al., 2011). The disadvantage of the latter only becomes obvious when using the biomimetic cofactors, where this leads to the formation of hydrogen peroxide. The activated LpNox was investigated in regard of its possible application in cell-free reaction systems. Therefore, the effect of pH, buffers, temperature, the reducing agent DTT and the thermal stability were determined. The enzyme's optimal activity range was from pH 5.5 to 8.0, a common range for NAD(P)H oxidases (Higuchi et al., 1993; Jiang et al., 2005; Park et al., 2011). The upper limit is compatible with most dehydrogenases, so appropriate coupling seems feasible. The amount of H₂O₂ released by LpNox during turnover is so low that it can be regarded as a water-forming NADH oxidase (Jiang et al., 2005; Lountos et al., 2006; Park et al., 2011). Deactivation of

TABLE 3 | Comparison of kinetic parameters of the biomimetics with LpNox.

Cofactor	K _m [mM]	v _{max} [mU/mg _{LpNox}]	k _{cat} [s ⁻¹]	k _{cat} /K _m [s ⁻¹ mM ⁻¹]
MNAH	1.6 ± 0.5	166.0 ± 16.9	0.14	0.09
BNAH	1.3 ± 0.4	198.9 ± 19.8	0.17	0.13

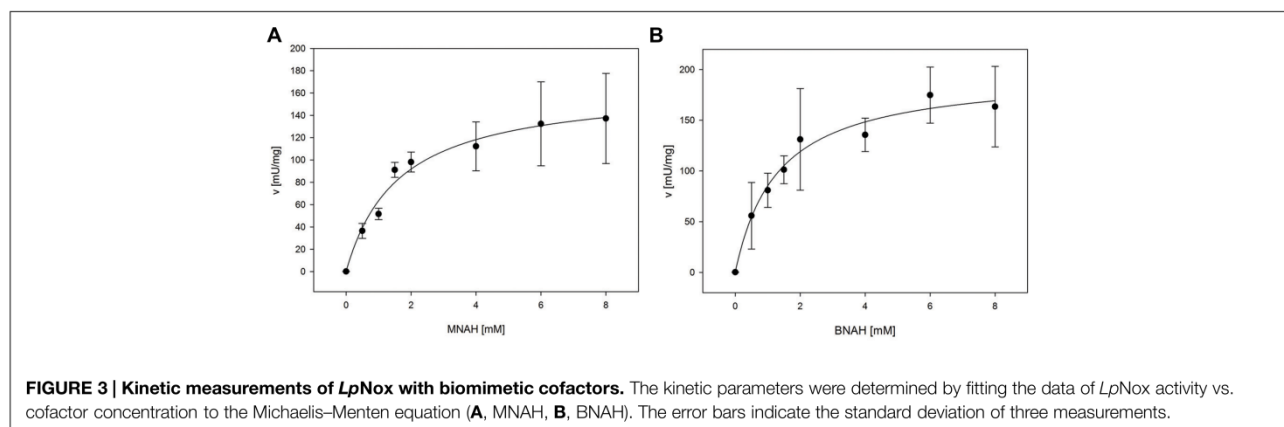
The enzymatic catalysis with MNAH and BNAH was characterized with a fluorescence assay. The kinetic parameters were determined by fitting the data of LpNox activity vs. cofactor concentration to the Michaelis–Menten equation. The standard deviation was calculated from three measurements.

NADH oxidases through over oxidation of the catalytically active Cysteine residue has been described among others for the Nox of *L. brevis* and could be avoided by adding a reducing agent such as DTT (Hummel and Riebel, 2003). For the LpNox no influence of DTT on activity or total turnover number was seen, neither positive nor negative. Together with the low influence of the buffer type on activity, this makes LpNox a flexible enzyme for coupled reactions. Room for improvement lies in the specific activity of LpNox, which is rather low compared to the H₂O-forming NADH oxidases from *Streptococcus pyogenes*: 344 U/mg (Gao et al., 2012) or *Lactobacillus brevis*: 116 U/mg (Hummel and Riebel, 2003). Also the rather low thermal stability at temperatures above 40°C could be improved by enzyme engineering.

Apart from NADH oxidases, an iron catalyzed oxidation of natural cofactors is possible (Maid et al., 2011). Here, also four electrons are transferred onto oxygen giving water as the by-product. Compared to the catalytic activity of LpNox, the metalloporphyrin is better in oxidizing NADPH (3.6 min⁻¹), but worse in oxidizing NADH (6.6 min⁻¹).

Enzyme-Catalyzed vs. FAD-Catalyzed Regeneration of Biomimetic Cofactors

LpNox and FAD are both capable of oxidizing the biomimetic cofactors MNAH and BNAH. The use of the catalyst decides on which by-product is formed. The chemical catalyst FAD produces H₂O₂ during the oxidation of the biomimetic proposedly by a two hydride transfer. However, in coupled redox reactions H₂O₂ should be avoided, since it can damage the



enzymes and substrates involved (Hernandez et al., 2012). The addition of a catalase would be possible, though this would add to the complexity of the system to the point where three catalysts (two enzymes and the chemical catalyst FAD) have to be matched. Therefore, using *LpNox* to regenerate biomimetic cofactors would be the superior choice over FAD, if it is optimized, e.g., by enzyme engineering. An exception is a case described by Paul et al. (2014b). Here the biomimetic cofactor BNAH plus FMN were used to specifically produce H₂O₂ *in situ* for the subsequent enzymatic reaction with a P450 peroxxygenase. For this kind of application, both biomimetic cofactors tested in our study would be suitable. Apart from the stated example, inhibitions in the biotransformation of interest by H₂O₂ can be avoided using the *LpNox* for cofactor regeneration instead. The conserved Cys residue at position 42 presumably acts as a second redox center. Therefore, in total a four electron transfer is achieved and innocuous water is produced. The kinetic experiments suggest that BNAH could be oxidized slightly more efficiently compared to MNAH. Because of the hydrophobic benzyl group in BNAH, the recognition and coordination in the cofactor binding site of *LpNox* is possibly better than for the smaller cofactor MNAH. Generally, the activity with free FAD is higher than with the enzyme. However, it has to be considered that the *LpNox* could be improved by enzyme engineering. If the interactions of the *LpNox* with the biomimetic cofactors could be increased, a more efficient catalysis might be obtained. In this way the amount of catalysts can be kept low while simultaneously the activity and effectivity is improved.

Conclusion

In conclusion, we found a H₂O-forming NADH oxidase from *L. pentosus* (*LpNox*) that is able to oxidize the natural cofactor NADH as well as the biomimetic cofactors MNAH

and BNAH. The enzyme is highly active between pH 6.0 and 8.0, is independent of the buffer type and DTT, and has a temperature optimum of 35–40°C. The K_m for NADH is 17.9 μM and k_{cat} is 43.4 s^{-1} , whereas for the biomimetic the K_m is 1.6 mM (1.3 mM) and k_{cat} is 0.14 s^{-1} (0.17 s^{-1}) for MNAH (BNAH). Furthermore, we compared the reaction rates of the enzyme with the reaction rate of free FAD. Although, the *LpNox* has a lower or equal rate as free FAD, the reaction products differ. In case of *LpNox* innocuous water is formed, while with free FAD hydrogen peroxide is obtained. Considering the future application of biomimetic cofactors in cell-free coupled reaction systems with other enzymes, hydrogen peroxide would be hazardous and henceforth, the use of *LpNox* would be favorable. In order to enhance the activity of *LpNox* towards the synthetic cofactors, enzyme engineering could be performed.

Acknowledgments

BB was funded by the Bavarian State Ministry of the Environment and Consumer Protection. CN was funded by the Bavarian State Ministry of Economic Affairs and Media, Energy and Technology. We are also grateful to Patrick Westermann for constructing the plasmid for the N-terminal variant. This work was supported by the German Research Foundation (DFG) and the Technische Universität München within the funding program Open Access Publishing.

Supplementary Material

The Supplementary Material for this article can be found online at: <http://journal.frontiersin.org/article/10.3389/fmicb.2015.00957>

References

- Artimo, P., Jonnalagedda, M., Arnold, K., Baratin, D., Csardi, G., de Castro, E., et al. (2012). ExPASy: SIB bioinformatics resource portal. *Nucleic Acids Res.* 40, W597–W603. doi: 10.1093/nar/gks400
- Campbell, E., Meredith, M., Minter, S. D., and Banta, S. (2012). Enzymatic biofuel cells utilizing a biomimetic cofactor. *Chem. Commun.* 48, 1898–1900. doi: 10.1039/c2cc16156g
- Chen, W. P., and Kuo, T. T. (1993). A simple and rapid method for the preparation of gram-negative bacterial genomic DNA. *Nucleic Acids Res.* 21, 2260. doi: 10.1093/nar/21.9.2260
- Friedlos, F., Jarman, M., Davies, L. C., Boland, M. P., and Knox, R. J. (1992). Identification of novel reduced pyridinium derivatives as synthetic cofactors for the enzyme DT diophorase (NAD(P)H dehydrogenase (quinone), EC 1.6.99.2). *Biochem. Pharmacol.* 44, 25–31. doi: 10.1016/0006-2952(92)90033-f
- Gao, H., Tiwari, M. K., Kang, Y. C., and Lee, J.-K. (2012). Characterization of H₂O-forming NADH oxidase from *Streptococcus pyogenes* and its application in l-rare sugar production. *Bioorg. Med. Chem. Lett.* 22, 1931–1935. doi: 10.1016/j.bmcl.2012.01.049
- Geueke, B., Riebel, B., and Hummel, W. (2003). NADH oxidase from *Lactobacillus brevis*: a new catalyst for the regeneration of NAD. *Enzyme Microbial. Technol.* 32, 205–211. doi: 10.1016/S0141-0229(02)00290-9
- Hentall, P. L., Flowers, N., and Bugg, T. D. H. (2001). Enhanced acid stability of a reduced nicotinamide adenine dinucleotide (NADH) analogue. *Chem. Commun.* 2098–2099. doi: 10.1039/B107634P
- Hernandez, K., Berenguer-Murcia, A., Rodrigues, R. C., and Fernandez-Lafuente, R. (2012). Hydrogen peroxide in biocatalysis. A dangerous liaison. *Curr. Org. Chem.* 16, 2652–2672. doi: 10.2174/138527212804004526
- Heux, S., Cachon, R., and Dequin, S. (2006). Cofactor engineering in *Saccharomyces cerevisiae*: expression of a H₂O-forming NADH oxidase and impact on redox metabolism. *Metab. Eng.* 8, 303–314. doi: 10.1016/j.ymben.2005.12.003
- Higuchi, M., Shimada, M., Yamamoto, Y., Hayashi, T., Koga, T., and Kamio, Y. (1993). Identification of two distinct NADH oxidases corresponding to H₂O₂-forming oxidase and H₂O-forming oxidase induced in *Streptococcus mutans*. *J. Gen. Microbiol.* 139, 2343–2351. doi: 10.1099/00221287-139-10-2343
- Hummel, W., and Riebel, B. (2003). Isolation and biochemical characterization of a new NADH oxidase from *Lactobacillus brevis*. *Biotechnol. Lett.* 25, 51–54. doi: 10.1023/a:1021730131633
- Jia, B., Park, S.-C., Lee, S., Pham, B. P., Yu, R., Le, T. L., et al. (2008). Hexameric ring structure of a thermophilic archaeon NADH oxidase that produces predominantly H₂O. *FEBS J.* 275, 5355–5366. doi: 10.1111/j.1742-4658.2008.06665.x
- Jiang, R., and Bommarius, A. S. (2004). Hydrogen peroxide-producing NADH oxidase (nox-1) from *Lactococcus lactis*. *Tetrahedron Asymmetry* 15, 2939–2944. doi: 10.1016/j.tetasy.2004.07.057

- Jiang, R., Riebel, B. R., and Bommarius, A. S. (2005). Comparison of alkyl hydroperoxide reductase (AhpR) and water-forming NADH oxidase from *Lactococcus lactis* ATCC 19435. *Adv. Synth. Catalysis* 347, 1139–1146. doi: 10.1002/adsc.200505063
- Kara, S., Schrittwieser, J. H., Hollmann, F., and Ansoerge-Schumacher, M. B. (2014). Recent trends and novel concepts in cofactor-dependent biotransformations. *Appl. Microbiol. Biotechnol.* 98, 1517–1529. doi: 10.1007/s00253-013-5441-5445
- Karrer, P., and Stare, F. J. (1937). N-Alkyl-o-dihydro-nicotinsäure-amide. *Helvetica Chimica Acta* 20, 418–423. doi: 10.1002/hlca.19370200167
- Kawasaki, S., Ishikura, J., Chiba, D., Nishino, T., and Niimura, Y. (2004). Purification and characterization of an H₂O-forming NADH oxidase from *Clostridium aminovalericum*: existence of an oxygen-detoxifying enzyme in an obligate anaerobic bacteria. *Arch. Microbiol.* 181, 324–330. doi: 10.1007/s00203-004-0659-653
- Knox, R. J., Friedlos, F., Jarman, M., Davies, L. C., Goddard, P., Anlezark, G. M., et al. (1995). Virtual cofactors for an *Escherichia coli* nitroreductase enzyme: relevance to reductively activated prodrugs in antibody directed enzyme prodrug therapy (ADEPT). *Biochem. Pharmacol.* 49, 1641–1647. doi: 10.1016/0006-2952(95)00077-d
- Knox, R. J., Jenkins, T. C., Hobbs, S. M., Chen, S. A., Melton, R. G., and Burke, P. J. (2000). Bioactivation of 5-(aziridin-1-yl)-2,4-dinitrobenzamide (CB 1954) by human NAD(P)H quinone oxidoreductase 2: a novel co-substrate-mediated antitumor prodrug therapy. *Cancer Res.* 60, 4179–4186.
- Laemmli, U. K. (1970). Cleavage of structural proteins during the assembly of the head of bacteriophage T4. *Nature* 227, 680–685. doi: 10.1038/227680a0
- Lountos, G. T., Jiang, R., Wellborn, W. B., Thaler, T. L., Bommarius, A. S., and Orville, A. M. (2006). The crystal structure of NAD (P)H oxidase from *Lactobacillus sanfranciscensis*: insights into the conversion of O₂ into two water molecules by the flavoenzyme. *Biochemistry* 45, 9648–9659. doi: 10.1021/bi060692p
- Lutz, J., Hollmann, F., Ho, T. V., Schnyder, A., Fish, R. H., and Schmid, A. (2004). Bioorganometallic chemistry: biocatalytic oxidation reactions with biomimetic NAD⁺/NADH co-factors and [Cp*₂Rh(bpy)H]⁺ for selective organic synthesis. *J. Organomet. Chem.* 689, 4783–4790. doi: 10.1016/j.jorganchem.2004.09.044
- Maid, H., Böhm, P., Huber, S. M., Bauer, W., Hummel, W., Jux, N., et al. (2011). Iron catalysis for in situ regeneration of oxidized cofactors by activation and reduction of molecular oxygen: a synthetic metalloporphyrin as a biomimetic NAD(P)H oxidase. *Angew. Chem. Int. Ed. Engl.* 50, 2397–2400. doi: 10.1002/anie.201004101
- Matsuda, T., Yamanaka, R., and Nakamura, K. (2009). Recent progress in biocatalysis for asymmetric oxidation and reduction. *Tetrahedron Asymmetry* 20, 513–557. doi: 10.1016/j.tetasy.2008.12.035
- Mauzerall, D., and Westheimer, F. H. (1955). 1-Benzyl-dihydro-nicotinamide—a model for reduced DPN. *J. Am. Chem. Soc.* 77, 2261–2264. doi: 10.1021/ja01613a070
- Park, J. T., Hirano, J.-I., Thangavel, V., Riebel, B. R., and Bommarius, A. S. (2011). NAD(P)H oxidase V from *Lactobacillus plantarum* (NoxV) displays enhanced operational stability even in absence of reducing agents. *J. Mol. Catalysis B Enzymatic* 71, 159–165. doi: 10.1016/j.molcatb.2011.04.013
- Paul, C. E., Arends, I. W. C. E., and Hollmann, F. (2014a). Is simpler better? Synthetic Nicotinamide cofactor analogues for redox chemistry. *ACS Catalysis* 4, 788–797. doi: 10.1021/cs4011056
- Paul, C. E., Churakova, E., Maurits, E., Girhard, M., Urlacher, V. B., and Hollmann, F. (2014b). In situ formation of H₂O₂ for P450 peroxxygenases. *Bioorg. Med. Chem.* 22, 5692–5696. doi: 10.1016/j.bmc.2014.05.074
- Paul, C. E., Gargiulo, S., Opperman, D. J., Lavandera, I., Gotor-Fernandez, V., Gotor, V., et al. (2013). Mimicking nature: synthetic nicotinamide cofactors for c-c bioreduction using enoate reductases. *Org. Lett.* 15, 180–183. doi: 10.1021/ol303240a
- Paul, C. E., Tischler, D., Riedel, A., Heine, T., Itoh, N., and Hollmann, F. (2015). Nonenzymatic regeneration of styrene Monooxygenase for catalysis. *ACS Catalysis* 5, 2961–2965. doi: 10.1021/acscatal.5b00041
- Poizat, M., Arends, I., and Hollmann, F. (2010). On the nature of mutual inactivation between Cp*₂Rh(bpy)(H₂O) (2⁺) and enzymes - analysis and potential remedies. *J. Mol. Catalysis B Enzymatic* 63, 149–156. doi: 10.1016/j.molcatb.2010.01.006
- Riebel, B. R., Gibbs, P. R., Wellborn, W. B., and Bommarius, A. S. (2003). Cofactor regeneration of both NAD(+) from NADH and NADP(+) from NADPH : NADH oxidase from *Lactobacillus sanfranciscensis*. *Adv. Synth. Catalysis* 345, 707–712. doi: 10.1002/adsc.200303039
- Rocha-Martin, J., Vega, D., Bolivar, J. M., Godoy, C. A., Hidalgo, A., Berenguer, J., et al. (2011). New biotechnological perspectives of a NADH oxidase variant from *Thermus thermophilus* HB27 as NAD⁺-recycling enzyme. *BMC Biotechnol.* 11:101. doi: 10.1186/1472-6750-11-101
- Rollin, J. A., Tam, T. K., and Zhang, Y. H. P. (2013). New biotechnology paradigm: cell-free biosystems for biomanufacturing. *Green Chem.* 15, 1708–1719. doi: 10.1039/C3GC40625C
- Rover, L. Jr., Fernandes, J. C. B., Neto, G. D. O., Kubota, L. T., Katekawa, E., and Serrano, S. L. H. P. (1998). Study of NADH stability using ultraviolet-visible spectrophotometric analysis and factorial design. *Anal. Biochem.* 260, 50–55. doi: 10.1006/abio.1998.2656
- Ryan, J. D., Fish, R. H., and Clark, D. S. (2008). Engineering cytochrome p450 enzymes for improved activity towards biomimetic 1,4-NADH-cofactors. *ChemBioChem* 9, 2579–2582. doi: 10.1002/cbic.200800246
- Schmidt, H.-L., Stöcklein, W., Danzer, J., Kirch, P., and Limbach, B. (1986). Isolation and properties of an H₂O-forming NADH oxidase from *Streptococcus faecalis*. *Eur. J. Biochem.* 156, 149–155. doi: 10.1111/j.1432-1033.1986.tb09560.x
- Studier, F. W. (2005). Protein production by auto-induction in high-density shaking cultures. *Protein Exp. Purif.* 41, 207–234. doi: 10.1016/j.pep.2005.01.016
- Takeda, J., Ohta, S., and Hirobe, M. (1987). Steric and electronic effects of methyl substituents at 2- and 6-positions on N-Benzyl-1,4-dihydro-nicotinamide. *Chem. Pharm. Bull.* 35, 2661–2667. doi: 10.1248/cpb.35.2661
- Tauber, K., Hall, M., Kroutil, W., Fabian, W. M. F., Faber, K., and Glueck, S. M. (2011). A highly efficient ADH-coupled NADH-recycling system for the asymmetric bioreduction of carbon-carbon double bonds using enoate reductases. *Biotechnol. Bioeng.* 108, 1462–1467. doi: 10.1002/bit.23078
- Tóth, K., Sedlak, E., Sprinzl, M., and Zoldak, G. (2008). Flexibility and enzyme activity of NADH oxidase from *Thermus thermophilus* in the presence of monovalent cations of Hofmeister series. *Biochim. Biophys. Acta* 1784, 789–795. doi: 10.1016/j.bbapap.2008.01.022
- Weckbecker, A., Gröger, H., and Hummel, W. (2010). "Regeneration of nicotinamide coenzymes: principles and applications for the synthesis of chiral compounds," in *Biosystems Engineering I*, eds C. Wittmann and R. Krull (Berlin: Springer), 195–242.
- Zhang, R.-Y., Qin, Y., Lv, X.-Q., Wang, P., Xu, T.-Y., Zhang, L., et al. (2011). A fluorometric assay for high-throughput screening targeting nicotinamide phosphoribosyltransferase. *Anal. Biochem.* 412, 18–25. doi: 10.1016/j.ab.2010.12.035
- Zhang, Y.-W., Tiwari, M. K., Gao, H., Dhiman, S. S., Jeya, M., and Lee, J.-K. (2012). Cloning and characterization of a thermostable H₂O-forming NADH oxidase from *Lactobacillus rhamnosus*. *Enzyme Microb. Technol.* 50, 255–262. doi: 10.1016/j.enzmictec.2012.01.009

Conflict of Interest Statement: The authors declare that the research was conducted in the absence of any commercial or financial relationships that could be construed as a potential conflict of interest.

Copyright © 2015 Nowak, Beer, Pick, Roth, Lommes and Sieber. This is an open-access article distributed under the terms of the Creative Commons Attribution License (CC BY). The use, distribution or reproduction in other forums is permitted, provided the original author(s) or licensor are credited and that the original publication in this journal is cited, in accordance with accepted academic practice. No use, distribution or reproduction is permitted which does not comply with these terms.

3.1.2 Characterization of Biomimetic Cofactors According to Stability, Redox Potentials, and Enzymatic Conversion by NADH Oxidase from *Lactobacillus pentosus*

In this publication, the synthetic nicotinamide cofactors MNAH, BNAH, P2NAH², and P3NAH³ were characterized in detail and conversion with *LpNox* was shown. Thus, the substrate spectrum and the usability of this biocatalyst were increased compared to the previous publication (see section 3.1.1).

The biomimetics contained the same nicotinamide moiety but differ in chain length. It was shown that P2NAH was most suitable, its stability being comparable with that of NADH. As far as the stability of the other biomimetics is concerned, it was less beneficial compared to the natural cofactor. Electrochemical analysis demonstrated that the oxidized forms of the studied biomimetic cofactors are thermodynamically stronger oxidants and weaker reducing agents than NAD⁺ and NADP⁺.

LpNox was able to convert all studied biomimetics with K_M for P2NAH of $0.44 \text{ mM} \pm 0.17 \text{ mM}$ with k_{cat} of $0.11 \text{ s}^{-1} \pm 0.01 \text{ s}^{-1}$ and K_M for P3NAH of $0.45 \text{ mM} \pm 0.11 \text{ mM}$ with k_{cat} of $0.195 \text{ s}^{-1} \pm 0.01 \text{ s}^{-1}$. According to the previous experiments, conversion with FAD and additionally a water-soluble iron-porphyrin catalyst was also successfully performed. FAD produces H₂O₂ as side product, whereas *LpNox* and the iron-porphyrin catalyst form innocuous water. Comparisons of the activities of *LpNox* and FAD showed opposite preferences for the biomimetics. FAD might react more rapidly with MNAH. Although P2NAH and P3NAH can theoretically be oxidized best according to their relative redox potentials, the steric hindrance that is associated with the conformation of these molecules in aqueous solution needs to be considered. This effect is not apparent with the enzymatic oxidation in the presence of *LpNox*. Here, the activities are better correlated to the relative redox potentials and this may be explained in terms of an extended conformation of the cofactors allowing easy access of the hydride. As a result, several strategies for regeneration of oxidized biomimetics were identified.

Claudia Nowak designed and conducted all experiments regarding the biomimetic cofactors among others including synthesis of the biomimetic molecules, assay development, conversion of biomimetics with *LpNox*, FAD, and the iron-porphyrin catalyst, measurement of side reaction products, and she wrote the manuscript. André Pick supported in designing the experiments and proofread the manuscript. Lénárd-István Csepei performed the electrochemical measurements. Claudia Nowak designed the research project and experimental approach guided by Volker Sieber.

Supporting Information to this manuscript can be found in the appendix.

² P2NA⁺ - 3-carbamoyl-1-phenethylpyridin-1-ium chloride

P2NAH - 1-phenethyl-1,4-dihydropyridine-3-carboxamide

³ P3NA⁺ - 3-carbamoyl-1-(3-phenylpropyl)pyridin-1-ium bromide

P3NAH - 1-(3-phenylpropyl)-1,4-dihydropyridine-3-carboxamide

Characterization of Biomimetic Cofactors According to Stability, Redox Potentials, and Enzymatic Conversion by NADH Oxidase from *Lactobacillus pentosus*

Claudia Nowak, André Pick, Lénárd-István Csepei, and Volker Sieber

ChemBioChem
2017

Reproduced with permission, license number 4376060529234
DOI: 10.1002/cbic.201700258

Characterization of Biomimetic Cofactors According to Stability, Redox Potentials, and Enzymatic Conversion by NADH Oxidase from *Lactobacillus pentosus*

Claudia Nowak,^[a] André Pick,^[a] Lénárd-István Csepei,^[b] and Volker Sieber^{*[a, b, c, d]}

Oxidoreductases are attractive biocatalysts that convert achiral substrates into products of higher value, but they are also for the most part dependent on nicotinamide cofactors. Recently, biomimetic nicotinamide derivatives have received attention as less costly alternatives to natural cofactors. However, recycling of biomimetics is still challenging because there are only limited opportunities. Here, we have characterized various biomim-

etic cofactors with regard to stability and redox potentials to find the best alternative to natural cofactors. Further, the cofactor spectrum of NADH oxidase from *Lactobacillus pentosus* (*LpNox*) could be expanded, and the enzymatic activity was also compared to activities with different small-molecule catalysts. As a result, we succeeded in identifying several strategies for regeneration of oxidized biomimetics.

Introduction

High degrees of chemo-, regio-, and stereoselectivity and environmentally friendly reaction conditions have paved the way for the use of biocatalysis in the production of high-quality chemicals.^[1] General concepts for whole-cell or cell-free biocatalysis have been established. Whereas whole-cell systems regenerate and reproduce nearly all reagents in closed reaction systems, undesired side pathways can reduce the final product yields. Alternatively, cell-free approaches can produce high-quality compounds by use of crude cell extracts or purified enzymes, thus eliminating side reactions. Moreover, new synthetic routes can be designed in combination with simpler systems and reaction control.^[2] Because most oxidoreductases depend on the stoichiometric use of cofactors as electron carriers—typically nicotinamide cofactors—an integrated efficient recycling system is crucial to allow process operation under economic conditions.^[3]

Enzymatic regeneration of oxidized cofactors can be achieved by using NADH oxidases.^[4] In these applications, the substrate oxygen is either partially reduced to hydrogen peroxide (H₂O₂) or completely reduced to water, depending on electron transfer within the enzyme.^[5] Because small amounts of H₂O₂ can decrease reaction rates,^[6] water-forming NADH oxidases are preferred in biotechnological applications. The NADH oxidases from *Lactobacillus brevis* or *Lactobacillus safranciscensis* were used, for example, for cofactor regeneration in different stereoselective reactions of alcohol dehydrogenases.^[7]

In addition to enzymatic recycling methods, electrochemical methods—such as direct anodic oxidation and indirect electrochemical regeneration—have been reported.^[8] Direct anodic oxidation requires enzymatic reactions that are capable of handling high oxidation power, which is necessary in the process but can also lead to undesired side reactions. This overpotential can be reduced by using mediators, but interactions of these mediators, cofactors, and enzymatic reactions need to be coordinated carefully.^[9] Also, light-driven cofactor regeneration with use of visible light and proflavine as photosensitizer can be applied.^[10]

Despite the use of efficient recycling systems, the instability and high cost of NAD(P)/H remain drawbacks of enzymatic oxidation/reduction reactions. In measures to address these disadvantages, semisynthetic or totally synthetic biomimetic cofactors are increasingly being investigated.^[2a] Semisynthetic biomimetics are derived from natural NAD(P)/H, whereas synthetic analogues can be prepared from nicotinamide and the appropriate alkyl halides,^[11] followed by reduction with sodium dithionite.^[12] Thanks to the resulting simplification of synthesis, the overall process costs can be reduced.^[11,13]

Biomimetic cofactors were initially described in studies of interactions between NAD(P)/H, enzymes, and substrates,^[12] and applications to biocatalysis are more recent. Among these, flavin-dependent enoate reductase from *Thermus scotoductus*

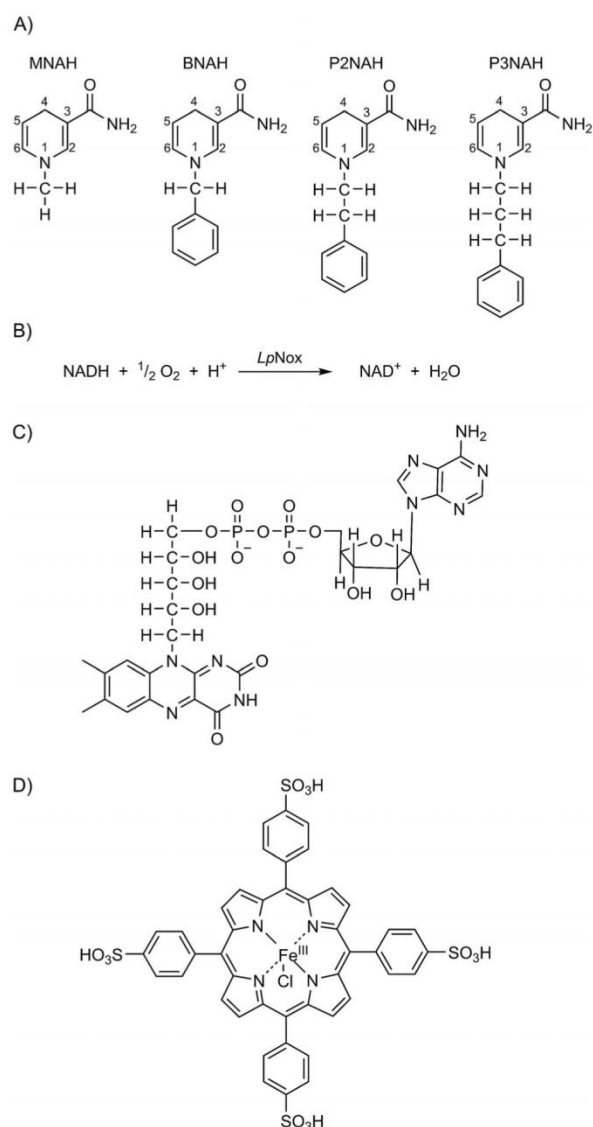
[a] C. Nowak, A. Pick, Prof. Dr. V. Sieber
Technical University of Munich
Department of Life Science Engineering, Straubing Center of Science
Schulgasse 16, 94315 Straubing (Germany)
E-mail: sieber@tum.de

[b] Dr. L.-I. Csepei, Prof. Dr. V. Sieber
Fraunhofer Institute for Interfacial Engineering and Biotechnology IGB
Bio, Electro and Chemocatalysis BioCat, Straubing Branch
Schulgasse 11a, 94315 Straubing (Germany)
E-mail: volker.sieber@igb.fraunhofer.de

[c] Prof. Dr. V. Sieber
Technical University of Munich, Catalysis Research Center
Ernst-Otto-Fischer-Strasse 1, 85748 Garching (Germany)

[d] Prof. Dr. V. Sieber
The University of Queensland
School of Chemistry and Molecular Biosciences
68 Cooper Road, St. Lucia 4072 (Australia)

 Supporting information and the ORCID identification numbers for the authors of this article can be found under <https://doi.org/10.1002/cbic.201700258>.



Scheme 1. A) Various biomimetic cofactors active in B) conversions with *LpNox*, together with C) the chemical catalyst FAD, and D) an iron-porphyrin catalyst.^[29]

or cytochrome P450 BM-3 R966D/W1046S from *Bacillus megaterium* reportedly catalyze reactions in which 1-benzyl-1,4-dihydropyridine-3-carboxamide (BNAH) is involved.^[13a, 14]

Because of the presence of a flavin derivative bound in the enzyme, between the substrate and cofactor, the hydride is not directly transferred to the substrate (mediator-like system).^[11]

Recently, we described an NADH oxidase from *Lactobacillus pentosus* (*LpNox*)^[15] that displayed activity with two biomimetic cofactors: 1-methyl-1,4-dihydropyridine-3-carboxamide (MNAH) and BNAH. Here we have increased the potential applicability of *LpNox* by expanding the cofactor scope

(Scheme 1 A). Additionally, we have investigated the stabilities and redox potentials of various biomimetic cofactors.

Results and Discussion

Stabilities of biomimetic cofactors

Up to now, 3-carbamoyl-1-methylpyridinium iodide (MNA⁺) and, especially, BNA/H have been the most widely used biomimetic cofactors in biocatalysis applications.^[11] Generally, these can be synthesized with good yields by well-established procedures^[12] and are more cost-effective than their natural counterparts.^[2a]

Because the stability of biocatalysis strongly depends on the type of buffer, pH, and temperature, we investigated decomposition of reduced cofactors under varied conditions. For both cofactors, incubation in 100 mM potassium phosphate buffer resulted in the highest decomposition rate (*k*). In contrast, degradation of the same biomimetics was up to seven times slower in MOPS, HEPES, or Tris-HCl (100 mM, pH 7) than in potassium phosphate (Table 1). Alivisatos et al. suggested that NAD(P)H is inactivated by the addition of phosphate (from the buffer) at the dihydronicotinamide ring (5,6 double bond).^[16] Because NAD(P)H and these biomimetics share the nicotinamide moiety, the derivatives are likely attacked in a similar manner. Moreover, we assume that molecule stabilities likely depend on protection of the weak 5,6 double bond of the dihydronicotinamide after folding of the phenyl ring against the dihydronicotinamide, as described for the adenine ring in NAD(P)/H.^[17]

Because Tris-HCl provided the lowest decomposition rate, we analyzed the stability of cofactors in this buffer under varying conditions of pH and temperature (Figure 1). It is well known that NAD(P)H is stable under alkaline conditions and decomposes in acids following the addition of water to the 5,6 double bond of the dihydronicotinamide.^[18] This property could also be seen with biomimetic cofactors, because the rate constant for the deactivation of BNAH at pH 5.2 was about 80 times higher than that at pH 10. Comparisons of synthetic and natural derivatives showed that the low stability of NAD(P)H during processing and storage could not be circumvented by the use of BNAH/MNAH. Under these conditions, NADH was the most stable cofactor, and NADPH and BNAH had comparable stability, followed by MNAH.

On the basis of these results, we investigated two biomimetics containing either an ethyl chain (3-carbamoyl-1-phenethyl-

Table 1. Rate constants (*k*) for decomposition of biomimetic cofactors in different buffers (100 mM, pH 7).

Buffer	<i>k</i> [min ⁻¹]			
	MNAH	BNAH	P2NAH	P3NAH
potassium phosphate	(137.7 ± 3.9) × 10 ⁻⁴	(55.4 ± 3.4) × 10 ⁻⁴	(51.4 ± 1.2) × 10 ⁻⁴	(125.0 ± 5.6) × 10 ⁻⁴
MOPS	(61.1 ± 1.2) × 10 ⁻⁴	(21.4 ± 1.2) × 10 ⁻⁴	(26.4 ± 2.9) × 10 ⁻⁴	(57.2 ± 2.6) × 10 ⁻⁴
HEPES	(64.5 ± 3.5) × 10 ⁻⁴	(27.8 ± 2.1) × 10 ⁻⁴	(28.1 ± 0.6) × 10 ⁻⁴	(58.6 ± 5.6) × 10 ⁻⁴
Tris-HCl	(25.8 ± 1.2) × 10 ⁻⁴	(8.0 ± 1.2) × 10 ⁻⁴	(13.2 ± 2.0) × 10 ⁻⁴	(26.5 ± 1.2) × 10 ⁻⁴

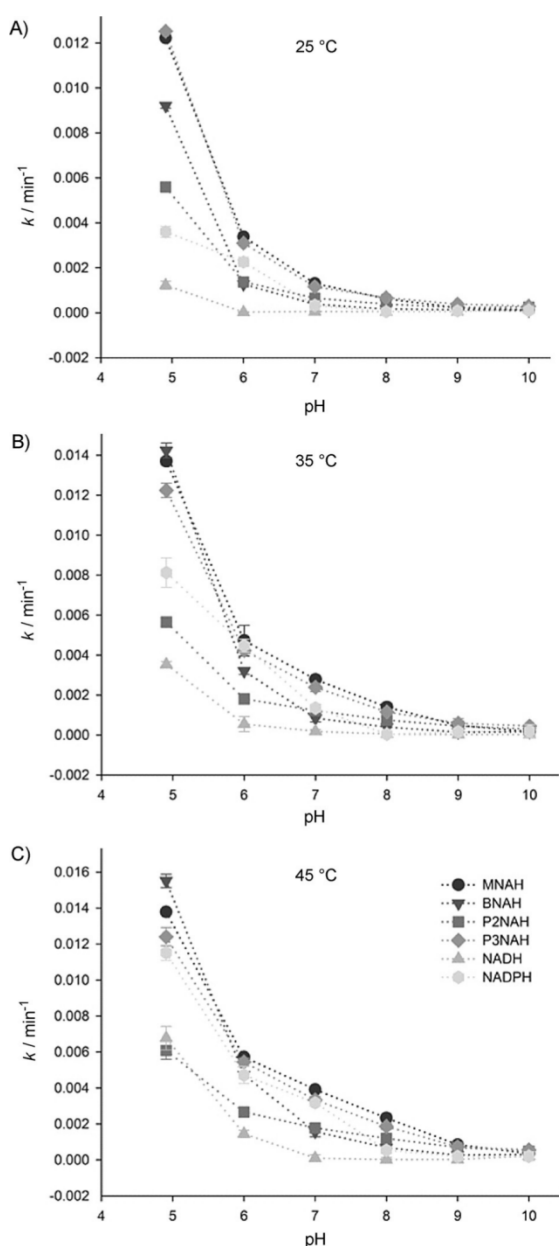


Figure 1. Effects of pH and temperature on rate constants (k) for decomposition of natural and biomimetic cofactors in 100 mM Tris-HCl.

pyridinium chloride, P2NA⁺; reduced: 1-phenethyl-1,4-dihydropyridine-3-carboxamide, P2NAH) or a propyl chain [3-carbamoyl-1-(3-phenylpropyl)pyridinium bromide, P3NA⁺; reduced: 1-(3-phenylpropyl)-1,4-dihydropyridine-3-carboxamide, P3NAH] connecting the nicotinamide and phenyl groups.^[19] The syntheses were analogous to those of MNA/H or BNA/H, respectively.^[20] We assumed that extension of the alkyl chain between nicotinamide and phenyl rings improves the stability of the molecule by opening the possibility of interactions between the two moieties while maintaining the activity with *LpNox*,

because the reactive part of the cofactor is unchanged. Investigations of these new biomimetics in various buffers showed that the lowest rate constant for decomposition was in 100 mM Tris-HCl, pH 7 (Table 1). In pH and temperature analyses, we found that the residues on the dihydronicotinamide ring had significant effects on stability (Figure 1). Generally, P3NAH was as unstable as MNAH and BNAH, whereas P2NAH was as stable as NADH, especially at increased temperatures and low pH. Therefore, the presence of the ethyl group in P2NAH might indeed enable more stable folding of the phenyl ring against the dihydronicotinamide than in BNAH and P3NAH, leading to better protection of the 5,6 double bond of the dihydronicotinamide (π - π stacking interactions) and interruption of the electron conjugation within the molecule (Figure S1 in the Supporting Information), which ultimately corresponds with better stability of the molecule. Thus, of the tested biomimetics, P2NAH was the only one that was competitive with the natural cofactor NADH. In spite of the efforts undertaken, higher stability was not achieved with degassed buffers, by incubation under reducing conditions [addition of dithiothreitol (DTT)], or by increasing ionic strength with sodium chloride or calcium chloride (Table S2).

Redox potentials

The electrochemical behavior of the biomimetic cofactors was evaluated by cyclic voltammetry with both oxidized and reduced forms. In accordance with the observations of Löw et al.,^[21] we also noted that a high anodic reversal potential (+950 to +1350 mV vs. Ag/AgCl) was required to allow observation of the characteristic reduction and oxidation peaks of the cofactors (Figure S3). Although we did not intend to investigate this requirement in this study, we noted that the anodic reversal potential was far larger than the usual $35/n$ mV (with n as the number of transferred electrons) past the peak potential that has been reported previously.^[22]

Reduction potentials of the natural cofactor references were also determined [NAD⁺ -329 ± 7 mV, NADP⁺ -309 ± 2 mV] and were in relatively good agreement with the generally accepted reduction potentials of -320 mV for NAD⁺ and -320 to -324 mV for NADP⁺ reported in the literature (Figures 2 and S3, Tables S4 and S5).^[11,23] However, these published

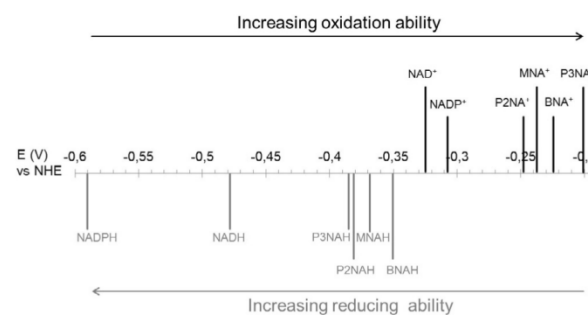


Figure 2. Ranking order of cathodic and anodic potentials in increasing order of cofactor reduction and oxidation abilities.

data are based on chemical equilibrium considerations^[24] or potentiometric determinations of equilibrium potential based on the Nernst equation.^[25] Both of these methods gave single values that are referred to as oxidation/reduction potentials. In contrast to the equilibrium methods, nonequilibrium methods (such as the cyclic voltammetry used here) give the potentials corresponding to both the reduction and the oxidation reactions.^[22,26] For an ideal electrochemically reversible redox couple the cathodic and anodic potentials and currents are approximately the same. After application of two reversibility criteria (difference between cathodic and anodic potentials and ratios of currents), we concluded that the reaction is electrochemically pseudo-reversible on the Pt electrode, potentially reflecting slow electron transfer and/or slow chemical reactions coupled with the electrochemical reaction.^[22,26] Examination of oxidation ability indicated that all the biomimetics are stronger oxidants than NAD⁺ or NADP⁺, with the strongest being P3NA⁺. In line with this, the resulting reduction ability was somewhat weaker than that of NADH and considerably weaker than that of NADPH, thus indicating that these biomimetics are thermodynamically less effective reducing agents than their natural counterparts.

Oxidation of biomimetic cofactors with *LpNox*

Recently, we described *LpNox*, a water-forming NADH oxidase from *L. pentosus*, and showed its activity in conjunction with MNAH and BNAH.^[15] Regeneration of P2NA⁺ and P3NA⁺ was now also tested with the FAD-dependent enzyme *LpNox* (Scheme 1B and C) and free FAD, and the results were compared with the previous measurements. Activity was detected for all combinations. Side product analyses revealed the formation of hydrogen peroxide (H₂O₂) in the presence of free FAD, whereas water was the product of *LpNox* for all biomimetics; this implies that all are subjected to the same mechanisms^[5] (Figure S6). Comparisons of the activities of *LpNox* and FAD showed opposite preferences for the biomimetics under investigation (Table 2). Specifically, FAD had the highest turnover

	TON		
	free FAD [min ⁻¹]	<i>LpNox</i> [min ⁻¹]	iron-porphyrin [min ⁻¹]
MNAH	2.23 ± 0.15 ^[15]	1.03 ± 0.10 ^[15]	0.50 ± 0.04
BNAH	0.97 ± 0.07 ^[15]	0.79 ± 0.01 ^[15]	0.15 ± 0.05
P2NAH	0.98 ± 0.04	2.43 ± 0.25	0.21 ± 0.02
P3NAH	1.03 ± 0.10	3.95 ± 0.12	0.21 ± 0.03

number (TON) with MNAH [(2.23 ± 0.15) min⁻¹], whereas its activities with P3NAH, P2NAH, and BNAH were identical [(1.03 ± 0.10) min⁻¹, (0.98 ± 0.04) min⁻¹, and (0.97 ± 0.07) min⁻¹, respectively]. With only one methyl group attached at the dihydronicotinamide ring MNAH is structurally smaller than the other biomimetics tested. Hence, in the absence of steric hindrances,

FAD might react more rapidly with MNAH, resulting in higher conversion than with the other biomimetics (Figure S1). Although P2NAH and P3NAH can theoretically be oxidized best, according to their relative redox potentials (Figure 2), the steric hindrance that is associated with the conformations of these molecules in aqueous solutions is also an important factor.

This effect is not apparent with the enzymatic oxidation in the presence of *LpNox*. Here the activities are better correlated to the relative redox potentials, and this could be explained in terms of an extended conformation of the cofactors, allowing easy access of the hydride.^[27] In contrast with the reaction with FAD, MNAH showed the lowest catalytic efficiency (k_{cat}/K_m) with *LpNox*. Hence, enlargement of the molecule with a phenyl group that provides more interactions in the cofactor binding site might be crucial for increasing catalytic efficiency (Table 3, Figures S7 and S8). BNAH, which is less flexible than

Table 3. Kinetic measurements for *LpNox* with the four biomimetic cofactors.

	K_m [mM]	v_{max} [mU mg ⁻¹]	k_{cat} [s ⁻¹]	k_{cat}/K_m [mM ⁻¹ s ⁻¹]
MNAH ^[15]	1.62 ± 0.48	166.03 ± 16.92	0.14 ± 0.01	0.09 ± 0.04
BNAH ^[15]	1.31 ± 0.42	198.85 ± 19.83	0.17 ± 0.02	0.13 ± 0.06
P2NAH	0.44 ± 0.17	127.31 ± 9.48	0.11 ± 0.01	0.28 ± 0.11
P3NAH	0.45 ± 0.11	224.92 ± 13.22	0.195 ± 0.01	0.49 ± 0.13

P2NAH or P3NAH, was better recognized and coordinated in *LpNox* than MNAH but was more poorly recognized than P2NAH/P3NAH. Because P2NAH has an additional methylene group and is slightly bigger and more flexible than BNAH, interactions of this biomimetic with the surrounding amino acids of *LpNox* were improved. Accordingly, the associated K_m value was decreased from 1.3 mM for BNAH to 0.4 mM for P2NAH. Moreover, further elongation with a methylene group, as in P3NAH, increased activity with the enzyme (127.3 mU mg⁻¹ for P2NAH to 224.9 mU mg⁻¹ for P3NAH), while the K_m value was retained in comparison with P2NAH. Consequently, k_{cat}/K_m was improved 5.4-fold after optimization of the biomimetic cofactor for biocatalysis. On examination of the structure of *LpNox*, modeling showed that the dihydronicotinamide ring of the cofactor is between the isoalloxazine part of FAD and the phenyl ring of the amino acid Tyr157, thus allowing stabilizing π - π stacking interactions. These interactions between the aromatic rings might strengthen the coordination of the reactive parts of the cofactors. Additionally, increasing length in the various biomimetics seems to be beneficial for a stabilizing network of van der Waals interactions and hydrogen bonds (Figure S8).^[28]

The iron-porphyrin catalyst described by Maid et al.^[29] might provide an alternative for the enzymatic regeneration of oxidized biomimetics (Scheme 1D). This water-soluble compound oxidizes NADH and forms H₂O as a side product; this represents an advantage over FAD, which forms H₂O₂. We therefore also tested the biomimetics with this catalyst and found the ensuing activities to be similar to those of FAD, with MNAH being converted best, followed by BNAH, P2NAH, and P3NAH (Table 2). This again demonstrates that accessibility of the nico-

tinamide ring is the major determinant for low-molecular-weight catalysts in comparison with enzymes.

Conclusion

Cofactor regeneration is an important issue for creating an environmentally friendly process. Additionally, the use of simple biomimetic cofactors can further reduce process costs.

We characterized various biomimetics with chains of increasing length, all containing the same nicotinamide moiety, and showed that P2NAH was most suitable, its stability being comparable with that of NADH.

Our investigations of electrochemical properties showed that the oxidized forms of the studied biomimetic cofactors are thermodynamically stronger oxidants and weaker reducing agents than NAD^+ and NADP^+ . However, the redox potentials are thermodynamic properties whereas the enzymatic reactivity is determined by the kinetics, which in turn depend on the steric and electronic properties.

The FAD-dependent enzyme *LpNox* efficiently oxidized all of the studied biomimetics. Although the chemical compound FAD or the water-soluble iron-porphyrin catalyst could be used as alternatives, the former produces H_2O_2 as a side product, whereas the latter and *LpNox* produce innocuous water. Furthermore, *LpNox* might be advantageous because activity could be improved by using enzyme engineering.

Experimental Section

Reagents: All chemicals were purchased from Sigma–Aldrich, Merck, or Carl Roth. All columns used for protein purification were from GE Healthcare.

Synthesis of oxidized and reduced biomimetics: The synthetic procedures were adapted from former procedures.^[12] MNAH and BNAH, as well as P2NAH and P3NAH, were synthesized as described previously.^[15,19,20]

Stability measurements: The stabilities of the reduced biomimetics were tested in different buffers under various conditions. The reduced biomimetics were dissolved in DMSO before use (final DMSO concentration 5%). MNAH, BNAH, P2NAH, and P3NAH were measured at 358 nm with a Multiskan or Varioskan spectrophotometer (ThermoFisher Scientific) or an Epoch2C spectrophotometer (BioTek). All measurements were performed in triplicate. The following extinction coefficients were used: for MNAH, $\epsilon = 5.9 \text{ L mmol}^{-1} \text{ cm}^{-1}$, for BNAH, $\epsilon = 7.4 \text{ L mmol}^{-1} \text{ cm}^{-1}$, for P2NAH, $\epsilon = 3.9 \text{ L mmol}^{-1} \text{ cm}^{-1}$, and for P3NAH, $\epsilon = 8.3 \text{ L mmol}^{-1} \text{ cm}^{-1}$.^[20]

Reduced biomimetics were initially incubated at 25 °C with the following buffers: potassium phosphate (100 mM, pH 7), MOPS (100 mM, pH 7), Tris-HCl (100 mM, pH 7), and HEPES (100 mM, pH 7). Secondly, pH and temperature profiles were recorded, and reduced cofactors were incubated in Tris-HCl (100 mM) at pH 4.9, 6, 7, 8, 9, and 10 at 25, 35 or 45 °C. Rate constants for deactivation were obtained by calculating the first-order rate constants (extent of reaction vs. time).^[30]

Furthermore, the effects of variations in Tris-HCl (100 mM, pH 8) were evaluated: degassed buffer, DTT (5 mM), NaCl (5 mM), and CaCl_2 (5 mM) at 25 °C.

Measurements of redox potentials: To determine the redox potentials of biomimetic cofactors, cyclic voltammetric (CV) experiments were performed with a conventional three-electrode arrangement consisting of a working electrode (Pt disk with 2 mm diameter), a counter electrode (graphite rod with 2 mm diameter), and a reference electrode (Ag/AgCl, 3 M Cl^-). The electrolyte solution contained both reduced and oxidized forms of the cofactor dissolved at 5 mM in DMSO/ H_2O (9:1, v/v) that was buffered with Tris (100 mM, pH 7), and Na_2SO_4 (40 mM) was used as a support electrolyte. The natural cofactors— NAD^+/NADH and $\text{NADP}^+/\text{NADPH}$ —were used as references for comparison of biomimetic redox potentials. Before experiments, the electrolytes were deaerated by argon bubbling. Cyclic voltammograms were recorded at sweep rate of 30 mV s^{-1} , starting from 0.0 V towards cathodic polarization. The values of the upper and lower reversal potentials were chosen in such a way as to achieve well-shaped and reproducible peaks. At least two CV curves were recorded for each cofactor pair. Representative CV curves are shown in Figure S3. To enable direct comparisons with published data, the cathodic and anodic peak potentials were converted into potentials versus a normal hydrogen reference electrode and are listed in Table S4. The difference between cathodic and anodic peak potentials indicates that the reaction is electrochemically pseudo-reversible on the working electrode ($\Delta E_p = E_{p,c} - E_{p,a} \geq 59/n \text{ mV}$, n is the number of transferred electrons). The criteria for peak current ratios ($0 < -I_{p,a}/I_{p,c} < 1$, Table S4)^[22,26] confirmed the pseudo-reversibility for MNAH/MNAH, BNAH/BNAH, P2NAH⁺/P2NAH, P3NAH⁺/P3NAH, and NAD^+/NADH and almost full reversibility for the $\text{NADP}^+/\text{NADPH}$ redox couple.

NADH oxidase from *L. pentosus* (*LpNox*): All experiments with *LpNox* were adapted and repeated from previously described procedures.^[15] For kinetic measurements the following values were used: P2NAH $\lambda_{\text{ex}} = 384 \text{ nm}$, $\lambda_{\text{em}} = 434 \text{ nm}$; P3NAH $\lambda_{\text{ex}} = 382 \text{ nm}$, $\lambda_{\text{em}} = 440 \text{ nm}$.

Determination of activity with Fe-porphyrin catalyst: The chemical catalyst 5,10,15,20-tetrakis-(4-sulfonatophenyl)-porphyrin- Fe^{III} chloride was obtained from PorLab (order number PL00832617). Subsequently, reduced cofactor (0.5 mM) was incubated with catalyst (0.05 mM) in Tris-HCl (100 mM, pH 8) at 25 °C, and the reaction was monitored at 358 nm.

Modeling of *LpNox*: Phyre2^[31] was used for structural modeling of *LpNox* (GenBank: CCB83530.1) and 3DLigandSite^[32] for FAD binding. Cofactor was modeled into *LpNox* by use of the crystal structure of glutathione reductase from *Escherichia coli* (PDB ID: 1GET)^[33] as described for NADH oxidase from *L. brevis*.^[34] YASARA (version 13.9.8) was used for energy minimization. Visualization and modeling of the biomimetics in the structure were done with PyMol Molecular Graphics System, Schrödinger, LLC.

Abbreviations for natural cofactors

NAD^+ : nicotinamide adenine dinucleotide, NADH: reduced nicotinamide adenine dinucleotide, NADP^+ : nicotinamide adenine dinucleotide phosphate, NADPH: reduced nicotinamide adenine dinucleotide phosphate.

Acknowledgements

Claudia Nowak was funded by the Bavarian State Ministry of Economic Affairs and Media, Energy and Technology and the COST action CM1303 Systems Biocatalysis. We would like to

thank Barbara Beer for her support in proofreading of the manuscript.

Conflict of Interest

The authors declare no conflict of interest.

Keywords: biomimetic cofactors · enzyme catalysis · NADH · oxidoreductases · redox chemistry

- [1] a) T. Matsuda, R. Yamanaka, K. Nakamura, *Tetrahedron: Asymmetry* **2009**, *20*, 513–557; b) R. C. Simon, F. G. Mutti, W. Kroutil, *Drug Discovery Today Technol.* **2013**, *10*, e37–e44; c) R. A. Sheldon, *Green Chem.* **2017**, *19*, 18–43.
- [2] a) J. A. Rollin, T. K. Tam, Y. H. P. Zhang, *Green Chem.* **2013**, *15*, 1708–1719; b) Y. H. P. Zhang, J. B. Sun, J. J. Zhong, *Curr. Opin. Biotechnol.* **2010**, *21*, 663–669.
- [3] a) A. Weckbecker, H. Gröger, W. Hummel, in *Biosystems Engineering I, Vol. 120* (Eds.: C. Wittmann, R. Krull), Springer, Berlin, **2010**, pp. 195–242; b) K. Tauber, M. Hall, W. Kroutil, W. M. F. Fabian, K. Faber, S. M. Glueck, *Biotechnol. Bioeng.* **2011**, *108*, 1462–1467.
- [4] H. Wu, C. Y. Tian, X. K. Song, C. Liu, D. Yang, Z. Y. Jiang, *Green Chem.* **2013**, *15*, 1773–1789.
- [5] G. T. Lountos, R. Jiang, W. B. Wellborn, T. L. Thaler, A. S. Bommarius, A. M. Orville, *Biochemistry* **2006**, *45*, 9648–9659.
- [6] K. Hernandez, A. Berenguer-Murcia, R. C. Rodrigues, R. Fernandez-La Fuente, *Curr. Org. Chem.* **2012**, *16*, 2652–2672.
- [7] a) B. Geueke, B. Riebel, W. Hummel, *Enzyme Microb. Technol.* **2003**, *32*, 205–211; b) B. R. Riebel, P. R. Gibbs, W. B. Wellborn, A. S. Bommarius, *Adv. Synth. Catal.* **2003**, *345*, 707–712.
- [8] F. Hollmann, A. Schmid, *Biocatal. Biotransform.* **2004**, *22*, 63–88.
- [9] C. I. Fort, L. C. Cotet, G. L. Turdean, V. Danciu, *Stud. Univ. Babeş-Bolyai Chem.* **2015**, *60*(3), 215–224.
- [10] D. H. Nam, C. B. Park, *ChemBioChem* **2012**, *13*, 1278–1282.
- [11] C. E. Paul, I. W. C. E. Arends, F. Hollmann, *ACS Catal.* **2014**, *4*, 788–797.
- [12] a) P. Karrer, F. J. Stare, *Helv. Chim. Acta* **1937**, *20*, 418–423; b) D. Mauzerall, F. H. Westheimer, *J. Am. Chem. Soc.* **1955**, *77*, 2261–2264.
- [13] a) C. E. Paul, S. Gargiulo, D. J. Opperman, I. Lavandera, V. Gotor-Fernandez, V. Gotor, A. Taglieber, I. W. C. E. Arends, F. Hollmann, *Org. Lett.* **2013**, *15*, 180–183; b) Y. Okamoto, V. Kohler, C. E. Paul, F. Hollmann, T. R. Ward, *ACS Catal.* **2016**, *6*, 3553–3557.
- [14] J. D. Ryan, R. H. Fish, D. S. Clark, *ChemBioChem* **2008**, *9*, 2579–2582.
- [15] C. Nowak, B. C. Beer, A. Pick, T. Roth, P. Lommes, V. Sieber, *Front. Microbiol.* **2015**, *6*, 957.
- [16] S. G. A. Alivisatos, G. Abraham, F. Ungar, *Nature* **1964**, *203*, 973–975.
- [17] N. J. Oppenheimer, L. J. Arnold, N. O. Kaplan, *Proc. Natl. Acad. Sci. USA* **1971**, *68*, 3200–3205.
- [18] A. G. Anderson, G. Berkelhammer, *J. Am. Chem. Soc.* **1958**, *80*, 992–999.
- [19] a) R. J. Knox, T. C. Jenkins, S. M. Hobbs, S. Chen, R. G. Melton, P. J. Burke, *Cancer Res.* **2000**, *60*, 4179–4186; b) M. E. Brewster, A. Simay, K. Czako, D. Winwood, H. Farag, N. Bodor, *J. Org. Chem.* **1989**, *54*, 3721–3726.
- [20] C. Nowak, A. Pick, P. Lommes, V. Sieber, *ACS Catal.* **2017**, *7*, 5202–5208.
- [21] S. A. Löw, I. M. Löw, M. J. Weissenborn, B. Hauer, *ChemCatChem* **2016**, *8*, 911–915.
- [22] A. J. Bard, L. R. Faulkner, *Electrochemical Methods: Fundamentals and Applications*, 2 ed., Wiley, New York, **2001**.
- [23] H. K. Chenault, G. M. Whitesides, *Appl. Biochem. Biotechnol.* **1987**, *14*, 147–197.
- [24] a) J. A. Olson, C. B. Anfinsen, *J. Biol. Chem.* **1953**, *202*, 841–856; b) F. L. Rodkey, *J. Biol. Chem.* **1955**, *213*, 777–786.
- [25] a) F. L. Rodkey, J. A. Donovan, Jr., *J. Biol. Chem.* **1959**, *234*, 677–680; b) F. L. Rodkey, *J. Biol. Chem.* **1959**, *234*, 188–190.
- [26] P. T. Kissinger, W. R. Heineman, *J. Chem. Educ.* **1983**, *60*, 702–706.
- [27] O. Carugo, P. Argos, *Proteins Struct. Funct. Bioinf.* **1997**, *28*, 10–28.
- [28] A. M. Lesk, *Curr. Opin. Struct. Biol.* **1995**, *5*, 775–783.
- [29] H. Maid, P. Bohm, S. M. Huber, W. Bauer, W. Hummel, N. Jux, H. Groger, *Angew. Chem. Int. Ed.* **2011**, *50*, 2397–2400; *Angew. Chem.* **2011**, *123*, 2445–2448.
- [30] B. M. Anderson, C. D. Anderson, *J. Biol. Chem.* **1963**, *238*, 1475–1478.
- [31] L. A. Kelley, S. Mezulis, C. M. Yates, M. N. Wass, M. J. E. Sternberg, *Nat. Protoc.* **2015**, *10*, 845–858.
- [32] M. N. Wass, L. A. Kelley, M. J. E. Sternberg, *Nucleic Acids Res.* **2010**, *38*, W469–W473.
- [33] P. R. E. Mittl, A. Berry, N. S. Scrutton, R. N. Perham, G. E. Schulz, *Protein Sci.* **1994**, *3*, 1504–1514.
- [34] D. V. Titov, V. Cracan, R. P. Goodman, J. Peng, Z. Grabarek, V. K. Mootha, *Science* **2016**, *352*, 231–235.

Manuscript received: May 13, 2017

Accepted manuscript online: July 27, 2017

Version of record online: August 25, 2017

3.2 Enzymatic Reduction of Nicotinamide Biomimetic Cofactors Using an Engineered Glucose Dehydrogenase: Providing a Regeneration System for Artificial Cofactors

In this publication, the regeneration of reduced biomimetic cofactors MNAH, BNAH, P2NAH, and P3NAH was shown using glucose dehydrogenase from *Sulfolobus solfataricus* (*SsGDH*) and an enzyme-coupled process was devised.

During screening of various commercially and non-commercially available regeneration enzymes, wild-type *SsGDH* was the only biocatalyst with which activity with biomimetics could be detected. Comparison of the various crystal structures and homology models showed that the nucleotide binding site of *SsGDH* appears to be very open and only in this enzyme, in the inner end two phenylalanine residues could be found performing potentially beneficial π - π stacking interactions with the nicotinamide ring.

Based on these results and on further analysis of the *SsGDH* cofactor binding site, a strategy for enzyme engineering was developed resulting in the double mutant *SsGDH* Ile192Thr/Val306Ile, which had ten-fold increased activity with P2NA⁺ (K_M 8.16 mM \pm 0.62 mM, k_{cat} 42.1 s⁻¹ \pm 0.81 s⁻¹). These results offer a promising starting point for understanding and identifying factors that influence cofactor binding and for expanding and optimizing the use of biomimetics.

As proof of concept, a regeneration/production process was devised, in which the thermostable enzyme enoate reductase from *Thermus scotoductus* and the mutant *SsGDH* Ile192Thr/Val306Ile used the biomimetic P2NA/H as a cofactor to produce 2-methylbutanal. However, internally bound natural nicotinamide cofactor, which could not be completely removed during protein purification, was in the first place a strong interfering factor. Thus, the addition of a third enzyme to create a sink for NAD(P)/H was necessary to obtain full conversion of 10 mM substrate within 12 h based on biomimetic cofactors. Although currently available enzymes still prefer natural cofactors, further enzyme engineering of *TsER*, and *SsGDH* in particular, may lead to further improvements in activity with biomimetics and technical feasibility. Compared with the chemical rhodium complex and metalloproteins, the opportunity to further evolve and improve *SsGDH* is a major advantage.

Claudia Nowak designed and conducted all experiments regarding the biomimetic cofactors among others including synthesis of the biomimetic molecules, activity measurements of various enzymes, development of the enzyme engineering, characterization of wild-type as well as mutant *SsGDH* and she wrote the manuscript. André Pick supported in designing the experiments and proofread the manuscript. Petra Lommes supported synthesis of biomimetic cofactors. Claudia Nowak designed the research project and experimental approach guided by Volker Sieber.

Supporting Information to this manuscript can be found in the appendix.

Enzymatic Reduction of Nicotinamide Biomimetic Cofactors Using an
Engineered Glucose Dehydrogenase: Providing a Regeneration System for
Artificial Cofactors

Claudia Nowak, André Pick, Petra Lommes, and Volker Sieber

ACS Catalysis
2017

Reprinted with permission from ACS Catal. 2017, 7, 8, 5202-5208.

Copyright (2017) American Chemical Society.

DOI: 10.1021/acscatal.7b00721

Enzymatic Reduction of Nicotinamide Biomimetic Cofactors Using an Engineered Glucose Dehydrogenase: Providing a Regeneration System for Artificial Cofactors

Claudia Nowak,[†] André Pick,[†] Petra Lommes,[†] and Volker Sieber^{*,†,‡,§}

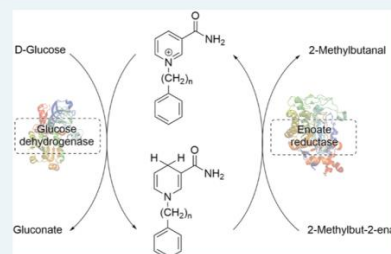
[†]Department of Life Science Engineering, Straubing Center of Science, Technical University of Munich, Schulgasse 16, 94315 Straubing, Germany

[‡]TUM Catalysis Research Center, Ernst-Otto-Fischer-Straße 1, 85748 Garching, Germany

 Supporting Information

ABSTRACT: The increasing demand for chiral compounds supports the development of enzymatic processes. Dehydrogenases are often the enzymes of choice due to their high enantioselectivity combined with broad substrate acceptance. However, their requirement on costly NAD(P)/H as cofactor has sparked interest in the development of biomimetic derivatives that are easy to synthesize and, therefore, less expensive. Until now, few reactions with biomimetics have been described and regeneration is limited to nonenzymatic means, which are not suitable for incorporation and in situ approaches. Herein, we describe a regeneration enzyme, glucose dehydrogenase from *Sulfolobus solfataricus* (SsGDH), and demonstrate its activity with different biomimetics with the structure nicotinamide ring-alkyl chain-phenyl ring. Subsequent enzyme engineering resulted in the double mutant SsGDH Ile192Thr/Val306Ile, which had a 10-fold higher activity with one of the biomimetics compared with the wild-type enzyme. Using this engineered variant in combination with an enoate reductase from *Thermus scotoductus* resulted in the first enzyme-coupled regeneration process for biomimetic cofactor without ribonucleotide or ribonucleotide analogue and full conversion of 10 mM 2-methylbut-2-enal with 1-phenethyl-1,4-dihydropyridine-3-carboxamide as cofactor.

KEYWORDS: biomimetic cofactors, cofactor regeneration, enzyme catalysis, glucose dehydrogenase, enoate reductase



INTRODUCTION

Cofactor regeneration is an important issue for reactions of oxidoreductases.^{1,2} In particular, dehydrogenases that are dependent on nicotinamide cofactors are used to biotechnologically perform various reactions with high enantioselectivity.³ However, the stoichiometric use of nicotinamide adenine dinucleotide (NAD⁺; reduced: dihydro nicotinamide adenine dinucleotide, NADH) or nicotinamide adenine dinucleotide phosphate (NADP⁺; reduced: dihydro nicotinamide adenine dinucleotide phosphate, NADPH) is too expensive for technical applications.⁴ Therefore, an efficient recycling system is essential,⁵ and the constant supply of regenerated cofactor and removal of the product can also help to shift the reaction equilibrium.⁶ Various strategies for cofactor recycling have been developed. The most common method involves the addition of a second enzyme and a sacrificial substrate.⁶ Formate dehydrogenase (FDH) and glucose dehydrogenase (GDH) are often used as both conversions are nearly irreversible and the substrates are inexpensive.^{7–9} For example, FDH was used industrially for the ton-scale production of *tert*-leucine with leucine dehydrogenase.¹⁰ Alternatively, a second substrate can be used alone in regeneration and production reactions that are performed by the same enzyme.⁶ Isopropanol and acetone are common cosubstrates for reactions that are catalyzed by alcohol dehydrogenases.¹¹ In addition, internal regeneration of the

cofactor can be achieved using multistep processes.⁶ For example, such “closed loop” reactions were used for the enzymatic synthesis of ketones and cleavage of lignin.^{12–14}

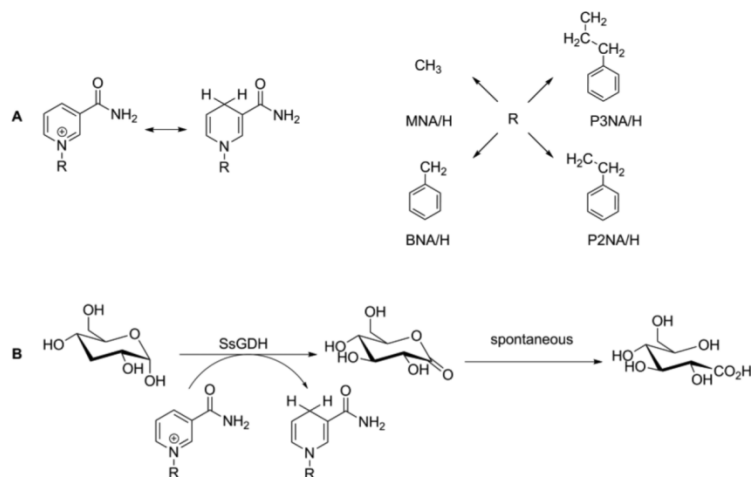
Recently, biomimetic nicotinamide derivatives have been suggested to further reduce the cost of cofactors. Molecules like 1-benzyl-1,4-dihydropyridine-3-carboxamide (BNAH) are structurally less complex than NAD(P)H and are easier to synthesize.⁴ Accordingly, BNAH has been successfully used as a hydride donor for cytochrome P450 monooxygenase¹⁵ as well as enoate reductase reactions.¹⁶ However, standard enzymatic methods for regeneration of the reduced form are not suitable for these biomimetic cofactors. Instead, regeneration reactions are mainly performed using chemical complexes or as lately reported using artificial metalloproteins. Lutz et al. used a rhodium catalyst to regenerate BNAH, which was added to the hydroxylation reaction of 2-hydroxybiphenyl with 2-hydroxybiphenyl 3-monooxygenase.¹⁷ This recycling system was also applied to the conversion of *p*-nitrophenoxydecanoic acid with BNAH and P450 BM-3 R966D/W1046S from *Bacillus megaterium* (P450 BM-3 R966D/W1046S).¹⁵ Current disadvantages of this system/process include instability and

Received: March 6, 2017

Revised: May 17, 2017

Published: June 29, 2017

Scheme 1. Conversion of the Present Biomimetic Cofactors (A) by SsGDH (B)



mutual inactivation of chemical catalysts and enzymes.² Recently, Okamoto et al. reported *in situ* regeneration of various biomimetic cofactors with artificial metalloproteins based on streptavidin variants and a biotinylated iridium cofactor. Total turnover numbers of 2000 were achieved.¹⁸ Further, the Zhao group showed activity of various enzymes *in vitro* and *in vivo* using artificial cofactors with variation at the adenosine moiety by exchanging the adenosine for cytosine or flucytosine.^{19,20}

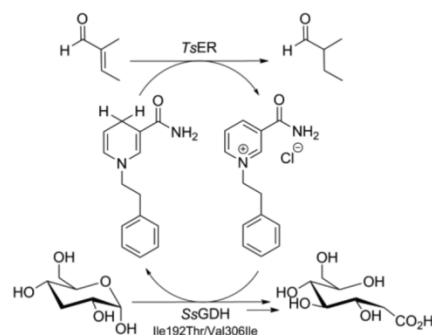
Looking at the success of enzymatic regeneration for the natural cofactors, we were interested in establishing an enzymatic regeneration system for biomimetic cofactors solely based on the nicotinamide moiety of the natural counterparts without ribonucleotide or ribonucleotide analogue. In general, enzymatic conversions performed with such biomimetic cofactors are far less efficient than those with native cofactors.²¹ Because structural similarities of biomimetic and natural derivatives are lacking, appropriate coordination and binding of biomimetics in nucleotide binding sites differ, with novel networks of hydrogen bonds and van der Waals interactions.²² All enzymes that have been shown to be active with these simple biomimetics so far have a second cofactor, flavin adenine mononucleotide (FAD) or flavin mononucleotide (FMN), tightly bound to the enzyme,^{15,16,21,23} which reportedly facilitate hydride transfer.²⁴

In the present study, we describe the glucose dehydrogenase from *Sulfolobus solfataricus* (SsGDH)²⁵ in connection with different described and so far in this context undescribed biomimetic cofactors (Scheme 1). Additionally, we report the first enzymatic regeneration and reaction process based on the conversion of such simple a biomimetic cofactor and devised an enzyme-coupled process with biomimetic cofactors (Scheme 2).

RESULTS AND DISCUSSION

Reduction of Biomimetic Cofactors. In contrast to the regeneration of NAD(P)H, which is most commonly performed enzymatically, enzymes for reducing biomimetics have not been described, and their reduction is currently performed using chemical complexes.^{17,18} For activity measurements of different enzymes, we synthesized various biomimetic cofactors all containing the same reactive nicotinamide group

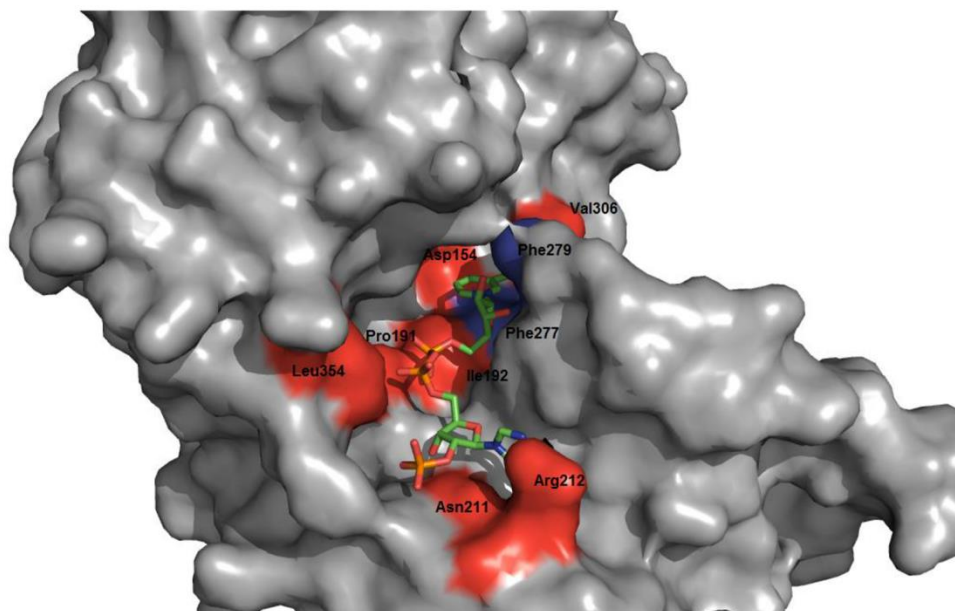
Scheme 2. Enzyme-Coupled Biomimetic Cofactor Regeneration by SsGDH for the Production of 2-Methylbutanal by TsER



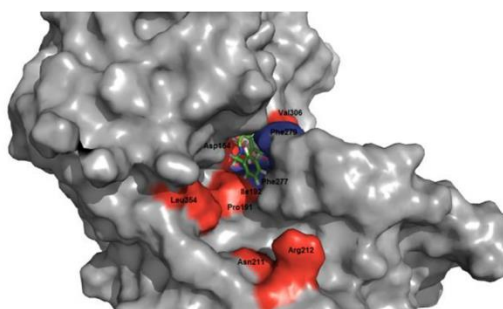
(Scheme 1A). 3-Carbamoyl-1-methylpyridinium iodide (MNA⁺; 1-methyl-1,4-dihydropyridine-3-carboxamide, MNAH) and especially BNA/H (BNA⁺: 1-benzyl-3-carbamoylpyridinium chloride) are the most widely used biomimetic cofactors in biocatalysis applications.²⁴ Additionally, we synthesized biomimetics, which are in this context undescribed cofactors, with an ethyl chain 3-carbamoyl-1-phenethylpyridinium chloride (P2NA⁺; 1-phenethyl-1,4-dihydropyridine-3-carboxamide, P2NAH)²⁶ or a propyl chain 3-carbamoyl-1-(3-phenylpropyl)pyridinium bromide (P3NA⁺; 1-(3-phenylpropyl)-1,4-dihydropyridine-3-carboxamide, P3NAH)²⁷ connecting the nicotinamide and phenyl group. We assumed that extension of the alkyl chain between nicotinamide and the phenyl ring increases flexibility, allowing better coordination within the cofactor binding site. Generally, all molecules can be synthesized with good yields using well-established procedures^{28,29} and as such can be supplied more cost-effective than their natural counterparts.⁴

We tested the commercially available common recycling enzymes formate dehydrogenase from *Candida boidinii* (FDH), glucose-6-phosphate dehydrogenase from *Saccharomyces cerevisiae* (G6PDH), and glucose dehydrogenase from *Thermoplasma acidophilum* (TaGDH). No activity with the present biomimetics could be detected. The same was found for the highly active and stable glucose dehydrogenase E170 K/Q252L

A



B



C

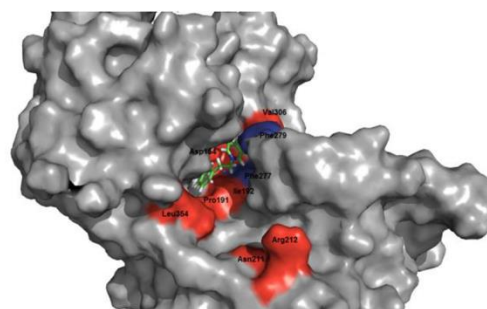


Figure 1. Visualization of the cofactor binding site of wild-type SsGDH with (A) NADP⁺, (B) BNA⁺, and (C) P2NA⁺. The crystal structure of SsGDH containing the cofactor NADP⁺ (PDB: 2CDA) was used as SsGDH has a dual cofactor specificity and computational experiments with NAD⁺ did not show any significant differences.

from *Bacillus subtilis* (BsGDH E170 K/Q252L)³⁰ and glucose dehydrogenase *Bacillus megaterium* (BmGDH-IV).³¹ BmGDH-IV shares a high sequence similarity with BsGDH E170 K/Q252L but is less active. Finally, glucose dehydrogenase from *Sulfolobus solfataricus* (SsGDH)³⁵ was the only enzyme tested, which showed activity with three of four biomimetics (Scheme 1B).

In order to explain the different behavior in biomimetic cofactor utilization of the tested enzymes, we compared the nucleotide binding site from crystal structures and homology models. All enzymes contain the typical Rossmann fold,³² a variation of the common GXGXXG motif,^{33,34} and binding of NAD(P)/H is based on a network of hydrogen bonds and van der Waals interactions.²² Thus, the nucleotide binding sites have a similar structure, but the amino acid composition is different, as the sequence identity of the enzymes was only about 20% (see the Supporting Information, Table S1). Looking at the crystal structure of SsGDH, the nucleotide binding site appears to be very open, and in the inner end two

phenylalanine residues, Phe277 and Phe279, can be found performing π - π -stacking interactions with the nicotinamide ring (Figure 1, see the Supporting Information, Figure S2).³⁵ These contacts between the aromatic molecules could not be found in the nucleotide binding sites of the other enzymes. TaGDH has one phenylalanine at a similar position (Phe275),^{36,37} but in BmGDH-IV^{31,38} or BsGDH E170 K/Q252L^{30,39} no aromatic amino acids in this orientation were found. The same applies for FDH. Additionally, the cofactor binding groove of FDH appears to be narrow compared to that of SsGDH, which reduces the number of possible binding positions of the biomimetic.⁴⁰ We assume that the phenylalanine residues play a potential role in binding of the biomimetics, which could be evaluated when introducing the amino acid in one of the other regeneration enzymes or substituting Phe277 and Phe279 in SsGDH with nonaromatic amino acids. Nonetheless, the rest of cofactor binding plays also an important role in coordination and binding of the biomimetic and has to be evaluated carefully.

Table 1. Kinetic Measurements of SsGDH Wild-Type and Variants with NAD⁺, BNA⁺, P2NA⁺, and P3NA⁺^a

		BNA ⁺ k_{cat} and $k_{\text{cat}}/K_{\text{m}} \times 10^{-3}$	P2NA ⁺ k_{cat} and $k_{\text{cat}}/K_{\text{m}} \times 10^{-3}$	P3NA ⁺ k_{cat} and $k_{\text{cat}}/K_{\text{m}} \times 10^{-3}$	NAD ⁺
SsGDH ⁴⁸	K_{m} [mM]	10.24 ± 1.66	16.33 ± 4.09	11.32 ± 3.27	0.43 ± 0.03
	k_{cat} [s ⁻¹]	1.60 ± 0.08	3.96 ± 0.36	0.96 ± 0.09	6.79 ± 1.40
	$k_{\text{cat}}/K_{\text{m}}$ [mM ⁻¹ s ⁻¹]	0.16 ± 0.03	0.24 ± 0.08	0.09 ± 0.03	15.94 ± 4.33
SsGDH Ile192Thr	K_{m} [mM]	14.78 ± 1.10	15.26 ± 0.82	12.76 ± 1.64	0.36 ± 0.03
	k_{cat} [s ⁻¹]	0.89 ± 0.02	3.03 ± 0.05	0.76 ± 0.03	2.83 ± 0.05
	$k_{\text{cat}}/K_{\text{m}}$ [mM ⁻¹ s ⁻¹]	0.06 ± 0.01	0.20 ± 0.01	0.06 ± 0.01	7.78 ± 0.73
SsGDH Ile192Val	K_{m} [mM]	13.02 ± 1.35	13.87 ± 0.96	11.57 ± 2.65	0.47 ± 0.05
	k_{cat} [s ⁻¹]	2.46 ± 0.07	3.98 ± 0.08	1.26 ± 0.10	2.86 ± 0.08
	$k_{\text{cat}}/K_{\text{m}}$ [mM ⁻¹ s ⁻¹]	0.19 ± 0.03	0.29 ± 0.03	0.11 ± 0.03	6.13 ± 0.84
SsGDH Val306Gly	K_{m} [mM]	8.76 ± 0.00	11.84 ± 1.16	10.29 ± 2.69	2.64 ± 0.24
	k_{cat} [s ⁻¹]	0.78 ± 0.04	0.47 ± 0.01	0.23 ± 0.02	1.62 ± 0.07
	$k_{\text{cat}}/K_{\text{m}}$ [mM ⁻¹ s ⁻¹]	0.09 ± 0.00	0.04 ± 0.00	0.02 ± 0.01	0.61 ± 0.08
SsGDH Val306Ile	K_{m} [mM]	13.15 ± 1.53	7.07 ± 0.72	5.13 ± 0.94	0.86 ± 0.08
	k_{cat} [s ⁻¹]	1.45 ± 0.06	4.42 ± 0.10	0.90 ± 0.04	8.38 ± 0.27
	$k_{\text{cat}}/K_{\text{m}}$ [mM ⁻¹ s ⁻¹]	0.11 ± 0.02	0.63 ± 0.08	0.18 ± 0.04	9.74 ± 1.24
SsGDH Ile192Thr/ Val306Gly	K_{m} [mM]	1.67 ± 0.26	4.35 ± 0.45	2.53 ± 0.68	0.41 ± 0.05
	k_{cat} [s ⁻¹]	1.74 ± 0.04	2.54 ± 0.04	1.84 ± 0.06	0.08 ± 0.00
	$k_{\text{cat}}/K_{\text{m}}$ [mM ⁻¹ s ⁻¹]	1.04 ± 0.19	0.58 ± 0.07	0.73 ± 0.22	0.19 ± 0.03
SsGDH Ile192Thr/Val306Ile	K_{m} [mM]	5.49 ± 0.32	8.16 ± 0.62	4.10 ± 0.60	0.17 ± 0.02
	k_{cat} [s ⁻¹]	9.00 ± 0.12	42.17 ± 0.81	6.97 ± 0.19	0.95 ± 0.02
	$k_{\text{cat}}/K_{\text{m}}$ [mM ⁻¹ s ⁻¹]	1.64 ± 0.12	5.17 ± 0.49	1.70 ± 0.30	5.65 ± 0.76

^aValues k_{cat} and $k_{\text{cat}}/K_{\text{m}}$ for BNA⁺, P2NA⁺, P3NA⁺, and the corresponding standard deviation times 10⁻³.

Kinetic Measurements of Wild-Type SsGDH. Comparing the biomimetic cofactors, the highest catalytic efficiency in the oxidation of D-glucose with SsGDH was found with P2NA⁺, for which k_{cat} was increased ($3.96 \times 10^{-3} \pm 0.36 \times 10^{-3} \text{ s}^{-1}$) compared to that of BNA⁺ ($1.60 \times 10^{-3} \pm 0.08 \times 10^{-3} \text{ s}^{-1}$) or P3NA⁺ ($0.96 \times 10^{-3} \pm 0.09 \times 10^{-3} \text{ s}^{-1}$; Table 1). Hence, elongation of the alkyl chain between the nicotinamide group and the phenyl group may lead to better positioning in the cofactor binding site, yet to the cost of a lower binding affinity, as the K_{m} for P2NA⁺ was almost doubled compared to BNA⁺ and P3NA⁺. The present biomimetics all lack the adenine dinucleotide moiety that is part of the natural cofactor NADH. Sicsic et al. discovered that the addition of adenosine or adenosine-5' phosphate to enzymatic reactions increases the activity of horse liver alcohol dehydrogenase with nicotinamide mononucleotide or nicotinamide mononucleoside.⁴¹ In our experiments, the addition of 5 mM adenosine or adenosine-5' phosphate to the reaction of SsGDH with BNA⁺, P2NA⁺, or P3NA⁺ and D-glucose did not increase specific activity. Hence, an improved positioning of the biomimetic in the enzyme could not be supported by either. Additionally, no activity was observed when MNA⁺ was used as a cofactor. Interactions of the nicotinamide group and the enzyme may insufficiently position and stabilize the complex for hydride transfer.

Enzyme Engineering of SsGDH for Improved Biomimetic Cofactor Recognition. Improving the specific activity of recycling enzymes is important for efficient cofactor regeneration. Therefore, we improved the activity of SsGDH with the biomimetics using enzyme engineering. Using various computational tools and published data from Milburn et al.,³⁵ we identified seven positions in and surrounding the cofactor binding site as target for modification (Figure 1). The amino acids Phe277 and Phe279 were used to evaluate the data from docking experiments. After establishing a reliable screening system (Z' factor⁴² of 0.58 and 0.54 for wild-type landscape for BNA⁺ and P2NA⁺, respectively, see the Supporting Information

for details), the following positions were separately subjected to mutagenesis: Asp154, Pro191, Ile192, Asn211, Arg212, Val306, and Lys354 (see the Supporting Information, S8.7 and S8.8). Variation of Asp154, which resides in the catalytic domain but in a 5 Å surrounding of the biomimetic, could lead to indirect structural changes in the transfer of electrons from cofactor to substrate. Pro191 and Ile192 are found in the conserved GXGXXG (aa 188–193) motif, where the polar ribose and pyrophosphate of NAD(P)⁺ are positioned. Because these NAD(P)⁺ moieties are replaced by a hydrophobic phenyl ring and an alkyl chain in the biomimetics, mutations in this highly conserved area may result in new interactions that improve binding. Asn211, Arg212, and Lys354 are located in the extended nonreactive part of the cofactor binding site and are responsible for coordination of phosphate and adenosine of the natural cofactor. Because this function is no longer required, mutations may result in beneficial changes in the entrance of the cofactor binding site. Val306 is found besides the important amino acid Asn307, which acts as a linker between the cofactor and substrate. Hence, structural modifications may lead to changes that could improve the connection between substrate, Asn307, and cofactor. Because BNA⁺ is a standard in the literature and P2NA⁺ was found to be the most active with wild-type SsGDH, these two were used as cofactors in the present activity screening analyses. Improvements in activity were found only with variants with mutations in Ile192 or Val306. Sequencing demonstrated the presence of these four mutants: SsGDH Ile192Thr, SsGDH Ile192Val, SsGDH Val306Gly, and SsGDH Val306Ile. Due to the slightly higher activity of SsGDH Ile192Thr compared to that of SsGDH Ile192Val in screening analyses, we generated SsGDH Ile192Thr/Val306Gly and SsGDH Ile192Thr/Val306Ile double mutants.

Characterizations of these novel variants showed decreased activity with NAD⁺ compared to wild-type SsGDH but enhanced catalysis with the biomimetics, especially with

P2NA⁺ (Table 1, see the Supporting Information, Figure S3). Thus, the positions Ile192 and Val306 are of high importance for the recognition and coordination of biomimetics. In addition, the best results were obtained using the double mutant SsGDH Ile192Thr/Val306Ile: k_{cat} with P2NA⁺ was increased 10-fold ($42.17 \times 10^{-3} \pm 0.81 \times 10^{-3} \text{ s}^{-1}$) compared to wild-type SsGDH, with BNA⁺ and P3NA⁺ k_{cat} was improved 5.6 fold and 7.2 fold, respectively. Exchange of the nonpolar and large isoleucine with a smaller and more polar threonine, which could also act as a hydrogen donor and acceptor, supported binding interactions in combination with the mutation Val306Ile. Interestingly, the single mutant SsGDH Ile192Thr ($0.20 \times 10^{-3} \pm 0.01 \times 10^{-3} \text{ mM}^{-1} \text{ s}^{-1}$) behaved similarly to wild-type SsGDH ($0.24 \times 10^{-3} \pm 0.08 \times 10^{-3} \text{ mM}^{-1} \text{ s}^{-1}$), and although SsGDH Val306Ile already showed a 2.6 fold increased catalytic efficiency, this was further improved to $5.17 \times 10^{-3} \pm 0.49 \times 10^{-3} \text{ mM}^{-1} \text{ s}^{-1}$ in the double mutant SsGDH Ile192Thr/Val306Ile. These synergistic effects were also observed with SsGDH Ile192Thr/Val306Gly in the presence of BNA⁺ as cofactor. The single mutants SsGDH Ile192Thr and SsGDH Val306Gly, in which a hydrophobic amino acid was replaced with a small, neutral residue, showed activities that were less than or equal to wild-type SsGDH, but the combination resulted in better activity. Generally, comparing the various kinetic values NAD⁺ was still preferred by all SsGDH variants. More detailed information on the exact mechanism of improvements has to be obtained from crystallographic studies of the various mutants. Moreover, further mutagenesis experiments will facilitate the understanding of how biomimetics are coordinated in the cofactor binding site compared with NAD(P)⁺ and will identify the ensuing requirements.

Enzyme-Coupled Cofactor Regeneration. We wanted to create an enzyme-coupled process with enoate reductase from *Thermus scotoductus* (TsER)⁴³ based on the conversion of biomimetic cofactors. Generally, enoate reductases are used for the asymmetric reduction of C=C bonds and are known to have a high substrate promiscuity including for example α,β -unsaturated ketones, aldehydes, nitroalkenes, imides, or carboxylic acids. Thus, they can be applied in many reactions in chiral asymmetric synthesis.^{44,45} In addition, TsER is described to be active with various biomimetic cofactors.¹⁶ We analyzed the activity of TsER with BNAH and P2NAH and different substrates including cyclohex-2-en-1-one, cinnamaldehyde, and 2-methylbut-2-enal, which are known to be efficiently converted by the enzyme. Cyclohex-2-en-1-one was also converted by TsER using the biomimetics with high efficiency as shown by formation of phenol, demonstrating disproportionation of cyclohex-2-en-1-one instead of reduction and internal biomimetic recycling (Table 2). Because TsER had a higher

Table 2. Activity Measurements of TsER with Cyclohex-2-en-1-one^a

cofactor	cyclohex-2-en-1-one [mM]	cyclohexanone [mM]	phenol [mM]
BNAH	2.34 ± 0.10	4.43 ± 0.09	2.12 ± 0.01
P2NAH	6.13 ± 0.48	1.60 ± 0.19	2.36 ± 0.28
NADPH	5.75 ± 0.44	3.77 ± 0.19	0.46 ± 0.02

^aConcentrations of substrate and products are shown after 45 min for NADPH and 2.5 h for BNAH/P2NAH. Kinetic data for TsER toward cyclohex-2-en-1-one measured with NADPH are $K_{\text{m}} = 3.68 \pm 0.24 \text{ mM}$, $k_{\text{cat}} = 110.1 \text{ s}^{-1}$, and $k_{\text{cat}}/K_{\text{m}} = 3.1 \times 10^4 \text{ M}^{-1} \text{ s}^{-1}$.⁴⁹

activity with 2-methylbut-2-enal (formation of $9.56 \pm 2.2 \text{ mM}$ 2-methylbutanal) than with cinnamaldehyde (formation of $1.41 \pm 0.2 \text{ mM}$ 3-phenylpropanal), it was chosen for the reaction/regeneration process. In addition, P450 R966D/W1046S from *Bacillus megaterium* was tested, but decoupling instead of product formation was detected (see the Supporting Information, Table S4).

Thus, the production (TsER) and regeneration (SsGDH Ile192Thr/Val306Ile) reactions were combined to convert 10 mM 2-methylbut-2-enal with the biomimetic P2NA⁺ (Scheme 2). Full conversion was achieved (Figure 2, ●), and all controls

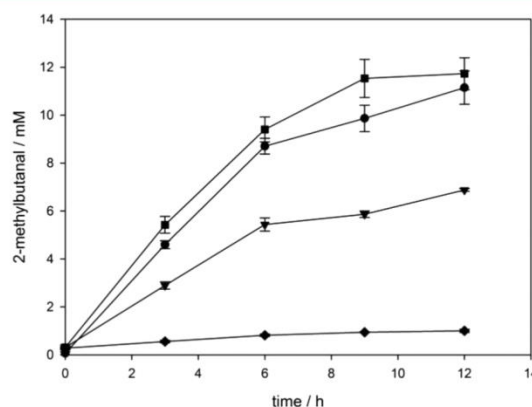


Figure 2. Conversion of 10 mM 2-methylbut-2-enal by TsER producing 2-methylbutanal in combination with SsGDH Ile192Thr/Val306Ile providing the cofactor P2NAH. The process was run in the absence of a futile cycle (●, reaction; ▼, control without biomimetic P2NA⁺) and in the presence of a futile cycle (■, reaction; ◆, control without biomimetic P2NA⁺). The control without cofactor shows the disturbing side reaction due to internal bound natural cofactor.

were negative except when only the biomimetic cofactor was omitted (Figure 2, ▼). Apparently, during incubation of the substrate 2-methylbut-2-enal with TsER, SsGDH Ile192Thr/Val306Ile and D-glucose without P2NA⁺, product was formed and reached 62% of the result of the complete reaction mixture that included P2NA⁺. We assumed that this side reaction was due to enzyme-bound natural cofactor, which already had been an issue in some original work with HLADH (see the Supporting Information S5).⁴⁶ Since the analysis of the enzyme-coupled process was disturbed by internally bound cofactor, we tried to further purify SsGDH Ile192Thr/Val306Ile as analyses showed this enzyme to be the dominant source of the natural cofactor contamination. To this end we have applied extensive dialysis of SsGDH, protein purification including partial unfolding at high temperatures (50 °C), incubation with an NADase, protein purification with Sepharose blue, which is supposed to specifically interact with the NAD-binding site, and even complete unfolding of the protein with 6 M guanidinium chloride and subsequent dialysis. Unfortunately, none of these attempts removed the undesired activity (data not shown). For our proof of concept, we included an NADH-specific futile cycle in the regeneration/production process. Lactate dehydrogenase from *Geobacillus stearothermophilus* (GstLDH)⁴⁷ was used to create a sink for NAD(P)/H because it has no activity with P2NA⁺, does not interact with any of the substrates of the other enzymes, and is highly active with its substrates pyruvate and NADH (see the

Supporting Information, Table S6). Activity with NADPH was also detected ($3.7 \pm 0.2 \text{ U mg}^{-1}$). Subsequently, the reaction was repeated after the same procedure including *GstLDH* and pyruvate, and full conversion of 10 mM 2-methylbut-2-enal was again detected (Figure 2, ■). Under these conditions, the contribution of the internally bound cofactor was strongly reduced to $1.00 \pm 0.07 \text{ mM}$ (Figure 2, ◆). Consequently, the production of 2-methylbutanal was almost entirely (90%) based on the conversion of P2NA/H. Moreover, comparison of reactions with and without the futile cycle indicated that the activities of *TsER* and *SsGDH Ile192Thr/Val306Ile* were not influenced, because the product formation followed the same course. The concentration of NAD/H in *SsGDH Ile192Thr/Val306Ile* was calculated to be approximately 50% of the enzyme. Consequently, internal natural bound cofactor plays an important role when creating enzyme-coupled biomimetic processes and needs to be evaluated carefully as it can lead to a misinterpretation of data. More enzyme engineering of both enzymes, *SsGDH* and *TsER*, is necessary to further increase the affinity of biomimetics.

To compare our system, *SsGDH Ile192Thr/Val306Ile*, to the artificial protein from Okamoto et al.,¹⁸ we calculated the total turnover number (TTN) from concentration of product divided by concentration of regeneration enzyme. TTN of 1183 was achieved for *SsGDH Ile192Thr/Val306Ile*. Additionally, the half-life of *SsGDH Ile192Thr/Val306Ile* was measured to be about 25 days (see the Supporting Information, Figure S7).

CONCLUSION

The use of biomimetic cofactors is a promising approach to further increase the economic viability of cell-free biotransformation. Reduced nicotinamide derivatives, such as BNAH, have recently been used with flavin-dependent oxidoreductases^{15,16} and are particularly attractive.

SsGDH enzymatically reduced the biomimetics BNA⁺, P2NA⁺, and P3NA⁺, and P2NA⁺ was the most suitable substrate. Enzyme engineering of the cofactor binding site of *SsGDH* resulted in the mutant *SsGDH Ile192Thr/Val306Ile*, which had 10-fold increased activity with P2NA⁺. *SsGDH* is the first and so far only enzyme not carrying a flavin coenzyme, which has been shown to be able to be used for reducing simple biomimetics not containing any ribonucleotide or analogous moiety. These results offer a promising starting point for understanding and identifying factors that influence cofactor binding and for expanding and optimizing the use of biomimetics.

In addition, as proof of concept we devised a regeneration/production process, in which the thermostable enzymes *TsER* and *SsGDH Ile192Thr/Val306Ile* used the biomimetic P2NA/H as a cofactor to produce 2-methylbutanal. Although currently available enzymes still prefer natural cofactors, further enzyme engineering of *TsER*, and *SsGDH* in particular, may lead to further improvements in activity with biomimetics and technical feasibility. Compared with the chemical rhodium complex and metalloproteins, the opportunity to further evolve and improve *SsGDH* is a major advantage. In addition, *SsGDH* is biocompatible and has higher process stability. A further general advantage of biomimetics is that they open the possibility to work with crude cell extracts without interference by cell metabolism, and side reactions may be minimized by specific activities for biomimetics.

ASSOCIATED CONTENT

Supporting Information

The Supporting Information is available free of charge on the ACS Publications website at DOI: 10.1021/acscatal.7b00721.

Experimental section as well as information on sequence identities and nucleotide binding sites of the regeneration enzymes, screening analyses; details in kinetics of *SsGDH* wild-type, *SsGDH* variants, and *GstLDH*; information on P450 BM-3; activity measurements of *HLADH*; and data on half-life of *SsDH Ile192Thr/Val306Ile*. (PDF)

AUTHOR INFORMATION

Corresponding Author

*E-mail: sieber@tum.de.

ORCID

Volker Sieber: 0000-0001-5458-9330

Notes

The authors declare no competing financial interest.

ACKNOWLEDGMENTS

C.N. was funded by the Bavarian State Ministry of Economic Affairs and Media, Energy and Technology and in part by the COST action CM1303 Systems Biocatalysis. We would like to thank Barbara Beer for her support in proofreading of the manuscript, Ioannis Zachos for his help in k_{deact} measurements, and Dr. Broder Rühmann for his advices in LC-UV-ESI-MS/MS measurements.

REFERENCES

- (1) Weckbecker, A.; Gröger, H.; Hummel, W. Regeneration of Nicotinamide Coenzymes: Principles and Applications for the Synthesis of Chiral Compounds. In *Biosystems Engineering I*; Wittmann, C., Krull, R., Eds.; Springer: Berlin, 2010; Vol. 120, pp 195–242.
- (2) Kara, S.; Schrittwieser, J. H.; Hollmann, F.; Ansorge-Schumacher, M. B. *Appl. Microbiol. Biotechnol.* **2014**, *98*, 1517–1529.
- (3) Simon, R. C.; Mutti, F. G.; Kroutil, W. *Drug Discovery Today: Technol.* **2013**, *10*, e37–e44.
- (4) Rollin, J. A.; Tam, T. K.; Zhang, Y. H. P. *Green Chem.* **2013**, *15*, 1708–1719.
- (5) Chenault, H. K.; Simon, E. S.; Whitesides, G. M. *Biotechnol. Genet. Eng. Rev.* **1988**, *6*, 221–270.
- (6) Hummel, W.; Groger, H. *J. Biotechnol.* **2014**, *191*, 22–31.
- (7) Faber, K. *Biotransformations in Organic Chemistry*, 6th ed.; Springer-Verlag: Berlin, 2011.
- (8) Hilt, W.; Pfeleiderer, G.; Fortnagel, P. *Biochim. Biophys. Acta, Protein Struct. Mol. Enzymol.* **1991**, *1076*, 298–304.
- (9) Wong, C.-H.; Drucekhammer, D. G.; Sweets, H. M. *J. Am. Chem. Soc.* **1985**, *107*, 4028–4031.
- (10) Kragl, U.; VasicRacki, D.; Wandrey, C. *Bioprocess Eng.* **1996**, *14*, 291–297.
- (11) Keinan, E.; Seth, K. K.; Lamed, R. *Ann. N. Y. Acad. Sci.* **1987**, *501*, 130–149.
- (12) Hofer, M.; Strittmatter, H.; Sieber, V. *ChemCatChem* **2013**, *5*, 3351–3357.
- (13) Reiter, J.; Strittmatter, H.; Wiemann, L. O.; Schieder, D.; Sieber, V. *Green Chem.* **2013**, *15*, 1373–1381.
- (14) Staudt, S.; Bornscheuer, U. T.; Menyess, U.; Hummel, W.; Gröger, H. *Enzyme Microb. Technol.* **2013**, *53*, 288–292.
- (15) Ryan, J. D.; Fish, R. H.; Clark, D. S. *ChemBioChem* **2008**, *9*, 2579–2582.
- (16) Paul, C. E.; Gargjulo, S.; Opperman, D. J.; Lavandera, I.; Gotor-Fernandez, V.; Gotor, V.; Taglieber, A.; Arends, I. W. C. E.; Hollmann, F. *Org. Lett.* **2013**, *15*, 180–183.

- (17) Lutz, J.; Hollmann, F.; Ho, T. V.; Schnyder, A.; Fish, R. H.; Schmid, A. *J. Organomet. Chem.* **2004**, *689*, 4783–4790.
- (18) Okamoto, Y.; Kohler, V.; Paul, C. E.; Hollmann, F.; Ward, T. R. *ACS Catal.* **2016**, *6*, 3553–3557.
- (19) Ji, D. B.; Wang, L.; Hou, S. H.; Liu, W. J.; Wang, J. X.; Wang, Q.; Zhao, Z. K. *B. J. Am. Chem. Soc.* **2011**, *133*, 20857–20862.
- (20) Wang, L.; Ji, D.; Liu, Y.; Wang, Q.; Wang, X.; Zhou, Y. J.; Zhang, Y.; Liu, W.; Zhao, Z. K. *ACS Catal.* **2017**, *7*, 1977–1983.
- (21) Nowak, C.; Beer, B. C.; Pick, A.; Roth, T.; Lommes, P.; Sieber, V. *Front Microbiol.* **2015**, *6*.
- (22) Lesk, A. M. *Curr. Opin. Struct. Biol.* **1995**, *5*, 775–783.
- (23) Knaus, T.; Paul, C. E.; Levy, C. W.; De Vries, S.; Mutti, F. G.; Hollmann, F.; Scrutton, N. S. *J. Am. Chem. Soc.* **2016**, *138*, 1033–1039.
- (24) Paul, C. E.; Arends, I. W. C. E.; Hollmann, F. *ACS Catal.* **2014**, *4*, 788–797.
- (25) Giardina, P.; Debiasi, M. G.; Derosa, M.; Gambacorta, A.; Buonocore, V. *Biochem. J.* **1986**, *239*, 517–522.
- (26) Knox, R. J.; Jenkins, T. C.; Hobbs, S. M.; Chen, S.; Melton, R. G.; Burke, P. *J. Cancer Res.* **2000**, *60*, 4179–4186.
- (27) Brewster, M. E.; Simay, A.; Czako, K.; Winwood, D.; Farag, H.; Bodor, N. *J. Org. Chem.* **1989**, *54*, 3721–3726.
- (28) Karrer, P.; Stare, F. *Helv. Chim. Acta* **1937**, *20*, 418–423.
- (29) Mauzerall, D.; Westheimer, F. H. *J. Am. Chem. Soc.* **1955**, *77*, 2261–2264.
- (30) Vazquez-Figueroa, E.; Chaparro-Riggers, J.; Bommarius, A. S. *ChemBioChem* **2007**, *8*, 2295–2301.
- (31) Nagao, T.; Mitamura, T.; Wang, X. H.; Negoro, S.; Yomo, T.; Urabe, I.; Okada, H. *J. Bacteriol.* **1992**, *174*, 5013–5020.
- (32) Rossmann, M. G.; Moras, D.; Olsen, K. W. *Nature* **1974**, *250*, 194–199.
- (33) Branden, C. I. Q. *Q. Rev. Biophys.* **1980**, *13*, 317–338.
- (34) Wierenga, R. K.; De Maeyer, M. C. H.; Hol, W. G. *Biochemistry* **1985**, *24*, 1346–1357.
- (35) Milburn, C. C.; Lamb, H. J.; Theodossis, A.; Bull, S. D.; Hough, D. W.; Danson, M. J.; Taylor, G. L. *J. Biol. Chem.* **2006**, *281*, 14796–14804.
- (36) Smith, L. D.; Budgen, N.; Bungard, S. J.; Danson, M. J.; Hough, D. W. *Biochem. J.* **1989**, *261*, 973–977.
- (37) John, J.; Crennell, S. J.; Hough, D. W.; Danson, M. J.; Taylor, G. L. *Structure* **1994**, *2*, 385–393.
- (38) Nishioka, T.; Yasutake, Y.; Nishiyama, Y.; Tamura, T. *FEBS J.* **2012**, *279*, 3264–3275.
- (39) Vazquez-Figueroa, E.; Yeh, V.; Broering, J. M.; Chaparro-Riggers, J. F.; Bommarius, A. S. *Protein Eng., Des. Sel.* **2008**, *21*, 673–680.
- (40) Schirwitz, K.; Schmidt, A.; Lamzin, V. S. *Protein Sci.* **2007**, *16*, 1146–1156.
- (41) Sicsic, S.; Durand, P.; Langrene, S.; Legoffic, F. *FEBS Lett.* **1984**, *176*, 321–324.
- (42) Zhang, J. H.; Chung, T. D. Y.; Oldenburg, K. R. *J. Biomol. Screening* **1999**, *4*, 67–73.
- (43) Opperman, D. J.; Piater, L. A.; van Heerden, E. *J. Bacteriol.* **2008**, *190*, 3076–3082.
- (44) Toogood, H. S.; Gardiner, J. M.; Scrutton, N. S. *ChemCatChem* **2010**, *2*, 892–914.
- (45) Stuermer, R.; Hauer, B.; Hall, M.; Faber, K. *Curr. Opin. Chem. Biol.* **2007**, *11*, 203–213.
- (46) Fish, R. H.; Lo, C. H. *Angew. Chem., Int. Ed.* **2002**, *41*, 478–481.
- (47) Barstow, D. A.; Clarke, A. R.; Chia, W. N.; Wigley, D.; Shannan, A. F.; Holbrook, J. J.; Atkinson, T.; Minton, N. P. *Gene* **1986**, *46*, 47–55.
- (48) Guterl, J.-K.; Garbe, D.; Carsten, J.; Steffler, F.; Sommer, B.; Reisse, S.; Philipp, A.; Haack, M.; Ruehmann, B.; Koltermann, A.; Kettling, U.; Brueck, T.; Sieber, V. *ChemSusChem* **2012**, *5*, 2165–2172.
- (49) Opperman, D. J.; Sewell, B. T.; Litthauer, D.; Isupov, M. N.; Littlechild, J. A.; van Heerden, E. *Biochem. Biophys. Res. Commun.* **2010**, *393*, 426–431.

4 Discussion and Prospects

4.1 Characterization and Optimization of Enzymes

Over the past years, there has been an increasing demand for the production of fine chemicals by oxidoreductases using cell-free biocatalysis (MATSUDA et al. 2009). Even though biomimetic cofactors have been known since the early part of the 20th century, their use for biotechnological processes is just at the beginning (PAUL & HOLLMANN 2016). Regarding these biotechnological applications, in which nicotinamide dependent enzymes are used, biomimetics hold the potential to decrease process costs and increase process stability (PAUL et al. 2013). In contrast to the regeneration of NAD(P)/H in an efficient reaction/regeneration process, which is most commonly performed enzymatically, the regeneration of biomimetics using enzymes has not yet been described.

4.1.1 NADH Oxidase from *Lactobacillus pentosus*

With NADH oxidase from *Lactobacillus pentosus* (*LpNox*), a FAD-dependent regeneration system for the natural cofactor NAD⁺, as well as the biomimetics MNA⁺, BNA⁺, P2NA⁺, and P3NA⁺ was identified.

First experiments showed that the content of the essential cofactor FAD in *LpNox* plays a major role in the activity of the enzyme with the biomimetic cofactors. Incubation of the enzyme with an excess amount of FAD and subsequent desalting resulted in fully activated *LpNox* that did not lose FAD during desalting or the activity tests and obviated the need of adding FAD to the reaction mixture, which is important when biomimetic cofactors are used (JIANG & BOMMARIUS 2004; JIANG et al. 2005; ROCHA-MARTIN et al. 2011; TOTH et al. 2008).

Following the approach of Paul *et al.* (PAUL et al. 2014b), the activity of the biomimetics MNAH, BNAH, P2NAH, and P3NAH was also tested with free FAD. Both, *LpNox* and free FAD, were able to oxidize all synthesized cofactors differing in the side products formed during catalysis. The chemical catalyst FAD produces H₂O₂ during oxidation (two hydride transfer), whereas the amount of H₂O₂ during *LpNox* catalysis is insignificant and so that it can be devised as a water-forming NADH oxidase (four electron transfer). Generally, formation of H₂O₂ should be avoided in a biocatalytic process as it can damage the enzymes and substrates that are involved (HERNANDEZ et al. 2012). To overcome this problem, an H₂O₂-degrading enzyme, namely catalase, might be added. However, with the addition of a further reaction component, the complexity of the system would be increased and all components need to be arranged for optimal performance. In contrast, if H₂O₂ is necessary for the product forming reaction like for example in P450 peroxygenase catalysis (PAUL et al. 2014b), than free FAD as regeneration system for the biomimetics might be the superior choice.

Looking at the activities of the catalysts with the investigated biomimetics, an opposite preference was identified. FAD was most active with MNAH, whereas the turnover numbers with BNAH, P2NAH, and P3NAH were low. MNAH is the smallest molecule with only one methyl group attached at the dihydro nicotinamide ring, thus, the steric hindrance is minimal and FAD might react rapidly with this cofactor. In contrast, the investigation of the redox potentials showed that P2NAH and P3NAH could theoretically be oxidized best but the steric hindrance, which is associated with the conformations, seems to be an important factor in the conversion with FAD. However, the use of *LpNox* as catalysts

showed that the increase in the size of the molecules provided more interactions in the cofactor binding site, which seems to be crucial for increasing catalytic efficiency. The more flexible biomimetics P2NAH and P3NAH were better recognized and coordinated than BNAH, which was more efficiently converted than MNAH. Thus, the additional methylene and the consequent increase in molecular size improved interactions within the cofactor binding site of *LpNox*.

This is in line with the observations made on the structural analysis of the homology model of *LpNox*. The increasing length of the alkyl chain and the phenyl group attached at the end of this chain seem to lead to the development of beneficial van der Waals interactions and hydrogen bonds, respectively. In addition, the dihydro nicotinamide ring of the cofactor appears to be in between the isoalloxazine part of FAD and the phenyl ring of the amino acid Tyr157 possibly resulting in stabilizing π - π stacking interactions. Accordingly, these interactions might improve the coordination of the reactive part of the molecule in the cofactor binding site.

In addition to *LpNox* and free FAD, another regeneration system for reduced cofactors, an iron-porphyrin catalyst (MAID et al. 2011), was investigated with the synthesized biomimetics. All biomimetics could be converted with the same preference as found for FAD: MNAH was oxidized best followed by BNAH, P2NAH, and P3NAH. These results proved that the accessibility of the nicotinamide ring is a major determinant for low-molecular-weight catalysts in comparison with enzymes.

To summarize, an evolvable regeneration enzyme for biomimetic cofactors was described with *LpNox*. Generally, the enzymatic activity with biomimetics compared to NADH needs to be improved and ideally the preference for the natural nicotinamide cofactors should be removed, if the enzyme is supposed to be applied in a biotechnological process only involving biomimetic cofactors. To do this, the crystal structure of *LpNox* with NADH and the biomimetics, respectively, will aid identifying amino acids for (semi-)rational mutagenesis. Positions that are important in NADH binding and in close distance to the biomimetics, respectively, can be targeted, whereas the stabilizing π - π stacking interactions should be maintained. Due to the great difference in molecular size of the natural and synthetic cofactors, multiple rounds of enzyme engineering might be necessary. Successful enzyme engineering of a water-forming NADH oxidase from *Streptococcus mutans* towards a dual cofactor specificity (NADH and NADPH) has been performed using a homology model and site directed mutagenesis. A positively charged amino acids for increased NADPH binding was introduced, but an aspartate residue at the C-terminus of the second β -strand of the $\beta\alpha\beta\alpha\beta$ region was maintained to facilitate binding of NADH (PETSCHACHER et al. 2014).

Another possibility could be the use of directed evolution by including error prone PCR in which random positions would be changed. This might be advantageous as amino acids might be varied that are not so important for biomimetic binding in the first place. However, the screening effort is considerably higher compared to the rational protein design and also various rounds of engineering may be necessary.

A further step could be that the information obtained from these experiments might be transferred to other NADH oxidases (or enzymes with similar characteristics), thereby accelerating the number of available enzymes with activity using biomimetic cofactors. Hence, the number of processes dependent on such regeneration enzymes might be expanded.

4.1.2 Glucose Dehydrogenase from *Sulfolobus solfataricus*

Within this work, various commercially (formate dehydrogenase from *Candida boidinii* [FDH], glucose-6-phosphate dehydrogenase from *Saccharomyces cerevisiae* [G6PDH], and glucose dehydrogenase from *Thermoplasma acidophilum* [TaGDH]) and non-commercially (glucose dehydrogenase E170K/Q252L from *Bacillus subtilis* [BsGDH E170K/Q252L] (VAZQUEZ-FIGUEROA et al. 2007), glucose dehydrogenase from *Bacillus megaterium* [BmGDH-IV] (NAGAO et al. 1992), and glucose dehydrogenase from *Sulfolobus solfataricus* (SsGDH) (GIARDINA et al. 1986)) regeneration enzymes were investigated for their activity with biomimetic cofactors. As a result, glucose dehydrogenase from *Sulfolobus solfataricus* was identified, which was the only tested enzyme that was naturally able to convert these simple biomimetic cofactors, albeit with very low activity.

Over the last few decades, various biocatalysts were characterized for their structure and amino acid composition of the nucleotide binding site. Although Rossmann *et al.* already described the structural similarity of this region in the 1970s, the diverse amino acid composition plays a crucial role in cofactor acceptance and binding (ROSSMANN 1976; ROSSMANN et al. 1974). Analyzing crystal structures and homology models of the tested enzymes proved that there were high structural similarities, as all biocatalysts have a typical Rossmann fold and a variation of the common GXGXXG motif. The cofactor binding site of SsGDH appears to be uncovered and open, in the inner end of which, two phenylalanine residues were found performing π - π stacking interactions with the nicotinamide ring of NAD(P)⁺. In TaGDH, one phenylalanine at a similar position could be detected, however, the activity with synthetic cofactors could not be measured leading to the conclusion that the π - π interaction found in SsGDH may be of strong influence. Accordingly, no aromatic residues in such an orientation were found in BmGDH-IV, BsGDH E170 K/Q252L, and FDH. Thus, enzyme engineering of the non-active NADH regeneration enzymes tested, in which these possibly beneficial phenylalanine residues are included, may clearly identify the role of the π - π stacking interactions.

However, the rest of the cofactor binding site also plays an essential role in biomimetic binding. Rollin *et al.* proposed the use of a module swap technique for cofactor specificity engineering as the cofactor binding motifs are highly conserved. Using this method, the entire cofactor binding domain is replaced resulting in a modified cofactor specificity (ROLLIN et al. 2013). This was already shown for the exchange of the NADP⁺-binding domain of an isocitrate dehydrogenase to get a NAD⁺-dependent enzyme (YAOI et al. 1996). Thus, wild-type or optimized cofactor binding site of SsGDH may be integrated in TaGDH (or any other enzyme) creating a biocatalyst, which is possibly able to use biomimetic cofactor for its enzymatic reaction. However, the tertiary structure of the engineered enzyme needs to be maintained so that the enzyme still folds properly and the interaction of the nicotinamide from the cofactor with the substrate *via* various amino acids is sustained.

Comparing the biomimetic cofactors, the highest catalytic efficiency in the oxidation of D-glucose with SsGDH was found with P2NA⁺, followed by BNA⁺, and P3NA⁺. No activity could be detected when MNA⁺ was added as the cofactor. Thus, the elongation of the alkyl chain and the addition of the phenyl group allowed active positioning in the cofactor binding site, yet at the cost of a lower binding affinity. To overcome the lack of the adenine dinucleotide moiety, which is important for coordination and binding of the cofactor, Sicsic *et al.* added adenosine or adenosine-5' phosphate to the reaction of HLADH with nicotinamide mononucleotide or nicotinamide mononucleoside resulting in increased

activity (SICSIC et al. 1984). If an improved positioning of the biomimetic in the enzyme had been supported, this would have been a simple method to quickly improve the turnover numbers of the reactions. Following the investigation, activity of *SsGDH* with BNA^+ , P2NA^+ , and P3NA^+ could not be increased (or even decreased). Under the condition used during the experiments, an effective coordination of the biomimetic and the supporting molecule was not possible or did not support the transfer of the hydride.

To improve the activity of *SsGDH* with the biomimetics, enzyme engineering was performed based on the information gained from crystal structure analysis and data published in literature (MILBURN et al. 2006). This was necessary as the activity of wild-type *SsGDH* was considerably lower when using biomimetics than with natural nicotinamide cofactors. Overall, the amino acids Phe277 and Phe279 that perform these potentially beneficial π - π stacking interactions were maintained and seven positions in the cofactor binding site were modified. Variation of *SsGDH* in the positions of Asp154, Asn211, Arg212, and Lys354 did not lead to improved activity or even decreased activity with the biomimetics. Asp154 resides in the catalytic domain but in a 5 Å surrounding of the biomimetic but indirect structural changes for an improved transfer of electrons from the cofactor to the substrate were not achieved. Asn211, Arg212, and Lys354 are located in the extended nonreactive part of the cofactor binding site and are responsible for the coordination of phosphate and adenosine of the natural cofactor. This function is not required anymore when biomimetics were used, but the introduced variations in these positions may have changed the inner cofactor binding site to such an extent that the cofactor cannot be coordinated properly. Pro191 and Ile192 are within the conserved GXGXXG motif, where the polar ribose and pyrophosphate of NAD(P)^+ are positioned. These NAD(P)^+ moieties are replaced by a hydrophobic phenyl ring and an alkyl chain in the biomimetics. Improved activity in variants with mutations in Ile192 was detected during screening analysis, whereas improved Pro191 variants were not found. Finally, the distance between Pro191 and the biomimetic was slightly increased compared to that of Ile192, potentially resulting in interactions with lower influences. However, specific engineering of Pro191 and Ile192 might be necessary to clearly define the roles in biomimetic binding as these amino acids are very close to each other. Increased activity with biomimetics was also found in Val306 variants. The amino acid is next to the important amino acid Asn307, which acts as a linker between the cofactor and substrate and the structural modifications lead to improved connection between these key components.

Sequencing demonstrated the presence of these four mutants: *SsGDH* Ile192Thr, *SsGDH* Ile192Val, *SsGDH* Val306Gly, and *SsGDH* Val306Ile. Due to a slightly higher activity of *SsGDH* Ile192Thr compared to that of *SsGDH* Ile192Val in screening analyses, *SsGDH* Ile192Thr/Val306Gly and *SsGDH* Ile192Thr/Val306Ile double mutants were constructed. Characterizations of these novel variants showed decreased activity with NAD^+ compared to wild-type *SsGDH*, but enhanced catalysis with the biomimetics, especially P2NA^+ . In addition, the best results were obtained using the double mutant *SsGDH* Ile192Thr/Val306Ile. Exchange of the nonpolar and large isoleucine with a smaller and more polar threonine in Ile192Thr, which could also act as a hydrogen donor and acceptor, supported binding interactions in combination with the mutation Val306Ile. During characterization of the single as well as double mutants, synergistic effects were observed since specific activity was further increased in the double mutants compared to the single mutants.

However, there are more positions in *SsGDH* that may be interesting for mutagenesis like Glu114 or Pro151 that were detected during docking analysis. These amino acids are not in the cofactor binding domain but in a 5 Å connection to the biomimetic cofactor potentially leading to indirect improvements of catalysis. Leu305 might also be of interest as the amino acid is in case of NAD(P)⁺ responsible for binding of the nicotinamide group. While, Thr41 also appeared to be interesting during docking analysis, Milburn *et al.* found that the mutation *SsGDH* Thr41Ala traps the substrate in the enzyme (MILBURN *et al.* 2006). Thus, a systematic approach in order to stepwise include variations in the cofactors binding site of *SsGDH* might lead to more clear information.

Scholtissek *et al.* subjected a conserved cysteine residue in the active site of Class III Old Yellow Enzymes OYERo2a from *Rhodococcus opacus* ICP to mutagenesis and constructed the mutants C25A, C25S, and C25G. According to the authors, the cofactors NADPH and BNAH were most efficiently converted by the wild-type enzyme and an increase in turnover frequency for the variants was only achieved for the natural cofactor. However, BNAH might represent an alternative cofactor for conversion including OYERo2a as no inhibitory effects were noticed and the biomimetic is more economical compared to NADPH (SCHOLTISSEK *et al.* 2018). Thus, further enzyme engineering here might also be needed in order to increase the applicability of biomimetic cofactors.

The results of the engineering of *SsGDH* also showed that preference and activity with NAD⁺ could be decreased, but not completely removed. However, small amounts of the natural nicotinamide cofactors disturb any reaction/regeneration process, which is supposed to be based on the conversion of biomimetics. Hence, further improvement of the enzyme is necessary. Moreover, crystallographic studies of the various mutants with the biomimetics as well as further mutagenesis experiments will facilitate the understanding of how biomimetics are coordinated in the cofactor binding site compared with NAD(P)⁺ and will identify the ensuing requirements. Using such a method, a decreased size of the cofactor binding site due to a smaller biomimetic cofactor in xenobiotic reductase A from *Pseudomonas putida* was described by Knaus *et al.* (KNAUS *et al.* 2015). A change in the conformation of the amino acid Trp302 was observed. As already described for *LpNox*, rational protein design or directed evolution including error prone PCR might be used, but the differences in screening effort need to be considered.

Overall, compared to metal catalysts, other chemical molecules, or non-enzymatic catalysts, which were described for the regeneration of biomimetic cofactors, enzymes like *SsGDH* hold the potential to be evolvable, hence, activity may be further improved.

4.2 Characterization and Optimization of Biomimetic Cofactors

Within this work, various biomimetic cofactors were tested: MNAH and BNAH are widely used in scientific literature, whereas P2NAH and P3NAH were undescribed in this context. Since the biomimetic cofactors might be used in a cell-free reaction system, the effect of pH, buffer, and temperature need to be evaluated.

Looking at the different buffers, MNAH, BNAH, P2NAH, and P3NAH showed the lowest stability in potassium phosphate buffer, whereas the rate of decomposition in MOPS, HEPES, or Tris-HCl was considerably lower resulting in a stabilizing effect. This is in line with the observations described for NAD(P)H following the mechanism that the phosphate from the potassium phosphate buffer is added

at the 5,6-double bond of the dihydro nicotinamide ring (ALIVISATOS et al. 1964). In addition, the weak 5,6-double bond is also responsible for the decomposition of the natural nicotinamide cofactors NAD(P)H as well as the tested biomimetics in acids. Thus, the molecular stability strongly depends on the protection of the weak 5,6-double bond. For NADH, it was observed that the adenine part was folded against the dihydro nicotinamide ring in order to shield this part (OPPENHEIMER et al. 1971). Due the reduced size of the tested biomimetics, this protection mechanism might not be available or the phenyl ring of BNA/H, P2NA/H, and P3NA/H might not mimic this molecular folding sufficiently. Hence, for the design of new biomimetic cofactors, an integration of functional groups might increase the stability of the weak 5,6-double bond. Following this, Hentall *et al.* found that an increased stability in aqueous buffers could be achieved by the introduction of a methyl group at C5, which improves the protection of the 5,6-double bond from protonation (HENTALL et al. 2001). Thus, the transferability of these results regarding an integration of such a “protection group” into the tested biomimetic MNA/H, BNA/H, P2NA/H, and P3NA/H might be of interest.

Comparing the stability of MNAH, BNAH, P2NAH, and P3NAH with the natural nicotinamide cofactors, P3NAH was as unstable as MNAH and BNAH, but P2NAH was found to be as stable as NADH in particular at higher temperature and lower pH. Accordingly, the ethyl group in P2NAH may lead to a more stable folding of the phenyl ring against the 5,6-double bond of the dihydro nicotinamide ring compared to BNAH and P3NAH including interruption of electron conjugation within the molecule. Thus, P2NAH was the only cofactor tested, which was competitive with NADH. Further analysis of the redox potentials of the biomimetic cofactors showed that the biomimetics are stronger oxidants than their natural counterparts. Subsequently, the reduction ability of the biomimetics is weaker compared to NAD(P)H indicating that MNAH/BNAH/P2NAH/P3NAH are thermodynamically less effective reducing agents.

Looking at the overall set up of an enzymatic process, the buffer, in which the enzyme is most active and in which the cofactor is as stable as possible, needed to be found and arranged; also accepting a decreased performance of one of the components. During the characterization of *LpNox*, the enzyme was found to be the most active in potassium phosphate buffer (with NADH as cofactor). However, the buffer Tris-HCl was finally used for the activity tests with the biomimetics since the stability of the cofactors was higher than in potassium phosphate buffer and the activity of *LpNox* was still acceptable.

Furthermore, MNA/H, BNA/H, P2NA/H, and P3NA/H can be prepared in a one step or two step syntheses, however, partly due to the costs of decreased stability. In contrast, the semi synthetic cofactor carba NAD has an excellent stability, but the production is expensive (SLAMA & SIMMONS 1988). For carba NAD, satisfactory enzymatic activity might be expected faster since this cofactor is closely related to NAD(P)H compared to the totally synthetic molecules. Thus, increased costs in synthesis with a probably higher stability or a more simple synthesis with possibly lower stability have to be weighed.

At the moment, there are various biomimetic cofactors molecules available for catalysis (ZACHOS et al. 2019). For example, Paul *et al.* designed a series of synthetic molecules in which the carboxamide group is changed and created butyl nicotinamide cofactors (PAUL et al. 2013). Löw and coworkers synthesized 1-phenyl-1,4-dihydro-nicotinamide and the variant 1-(4-hydroxyphenyl)-1,4-dihydro-nicotinamide (LOW et al. 2016). Hence, biomimetics may be optimized by introduction of various

groups, exchange of the specific atoms, or variation in chain length and chain type. Additional information from crystal structure analysis of the enzyme-biomimetic cofactor complex, activity test of various enzymes with biomimetics and results received from enzyme engineering might also give evidence on how the cofactor molecule could be precisely improved to further increase coordination and binding in the cofactor binding site of the enzyme in regard to hydrogen bonds and van der Waals interactions. Another point to consider during the planning and synthesis of new biomimetic molecules is the solubility of the reduced forms (OKAMOTO et al. 2016). Using the tested biomimetics MNAH, BNAH, P2NAH, or P3NAH, the addition of DMSO was necessary to ensure solubility of the cofactor, but not all enzymes might be able to tolerate such an amount of organic solvent. However, there is a great potential to create a high number of improved biomimetic cofactors.

4.3 Optimization of the Reaction/Regeneration Process

In order to prove the applicability of *SsGDH Ile192Thr/Val306Ile*, a reaction/regeneration process was set up in this work.

For the regeneration reaction, the improved *SsGDH Ile192Thr/Val306Ile* was used as the highest catalytic efficacy compared to the other variants was achieved during the characterization process. The reaction of interest was supposed to be performed by P450 R966D/W1046S from *Bacillus megaterium* (RYAN et al. 2008), but the enzyme was almost completely uncoupled with the cofactor P2NAH. The conversion of the cofactor was observed, but reduction of the substrate was not detected. Thus, redox equivalents get lost following the formation of water, hydrogen peroxide or superoxide ions. One of the reasons might be a too great distance between bound substrate and reactive species and the accessibility of water to the active center (LOIDA & SLIGAR 1993). Thus, the production enzyme was switched to *TsER*, which was also described to be active with various biomimetic cofactors (KNAUS et al. 2015; OKAMOTO et al. 2016; PAUL et al. 2013). Analysis of the activity of *TsER* with BNAH and P2NAH with various substrates showed that 2-methylbut-2-enal was most suitable as for example with cyclohex-2-en-1-one, disproportionation of the substrate instead of reduction and internal biomimetic recycling was detected.

Following this, the production (*TsER*) and regeneration (*SsGDH Ile192Thr/Val306Ile*) reactions were combined to convert 2-methylbut-2-enal with the biomimetic P2NA⁺ and full conversion was achieved. However, product was also detected in a reaction control containing the substrate, *TsER*, *SsGDH Ile192Thr/Val306Ile*, and D-glucose (without P2NA⁺) concluding that the natural cofactor was still bound in the regeneration enzyme *SsGDH Ile192Thr/Val306Ile*. This had already been an issue in some original work of HLADH (LO & FISH 2002; PAUL & HOLLMANN 2016). Only little information on the HLADH preparation of Lo *et al.* is known, but the false positive results may be attributed to such impurities with natural nicotinamide cofactor. The presence of natural nicotinamide cofactors in purified preparations of dehydrogenases is a known phenomenon. Schirwitz *et al.*, for example, demonstrated that NAD⁺ was present in approximately 50% of formate dehydrogenase preparations (from *Candida boidinii*) after purification, which could only be removed by extensive washing with 2 M sodium chloride (SCHIRWITZ et al. 2007). The internally bound cofactor may not have a consequence when a process with the natural nicotinamide cofactors is set up, however, it disturbs reactions, which are supposed to be based on the conversion of biomimetic cofactors. In a

reaction/regeneration process, only low concentration of natural cofactor is necessary to feign activity since it is recycled constantly and with high efficiency. The regeneration enzyme was the major source for the contamination, but various purification experiments on *SsGDH Ile192Thr/Val306Ile* failed to decrease the concentration of internally bound natural cofactor.

However, using *SsGDH Ile192Thr/Val306Ile* and without improved purification methods, a shunt need to be created around the reaction and regeneration reaction. Hence, an NADH-specific futile cycle using lactate dehydrogenase from *Geobacillus stearothermophilus* (*GstLDH*) was included in the process to create a sink for NAD(P)/H as the biocatalyst does not convert biomimetics nor interact with any of the substrates of the other enzymes. Subsequently, the reaction was repeated following the same procedure including *GstLDH* and pyruvate and full conversion of 2-methylbut-2-enal was detected again. However, under these conditions, the contribution of the internally bound cofactor was strongly reduced. Consequently, the production of 2-methylbutanal was almost entirely (90%) based on the conversion of P2NA/H. Moreover, comparison of reactions with and without the futile cycle indicated that the activities of *TsER* and *SsGDH Ile192Thr/Val306Ile* were not influenced as the product formation followed the same course. Comparison of the *SsGDH Ile192Thr/Val306Ile* with the artificial protein from Okamoto *et al.* (OKAMOTO *et al.* 2016) showed comparable total turnover numbers

Thus, with the addition of a NAD(P)/H specific futile cycle, it was proven that a reaction/regeneration process can be set up with cofactors analogous to processes actually developed for NAD(P)/H. However, regarding this combination of biocatalysts, enzyme engineering of both enzymes, *SsGDH* and *TsER*, is necessary to further increase the affinity for biomimetics. So far, a process using wild-type *TsER* and *SsGDH Ile192Thr/Val306Ile* might be set up when first the internally bound cofactor is used for catalysis until its decomposition and then a cheap biomimetic is added to continue the reaction/regeneration. Such a system is possible when the stability of the enzymes exceed the stability of the nicotinamide cofactors. With the increase in number of enzymes available for catalysis with biomimetic cofactors, more processes that were in the first place developed for NAD(P)/H might be reproduced and the usability of these synthetic molecules in industrial applications might be expanded.

5 References

- ACS American Chemical Society, International Historic Chemical Landmarks: Antoine-Laurent Lavoisier: The Chemical Revolution. Online: <http://www.acs.org/content/acs/en/education/whatischemistry/landmarks/lavoisier.html>. (accessed: 04.11.2018).
- Adler, E.; Hellström, H. and Von Euler, H. (1936): Zur Kenntnis der Reduktion der Co-Zymase. In: *Hoppe-Seyler's Zeitschrift für physiologische Chemie*, Vol. **242**, S. 225.
- Alivisatos, S. G. A.; Abraham, G. and Ungar, F. (1964): Non-enzymatic interactions of reduced coenzyme I with inorganic phosphate and certain other anions. In: *Nature*, Vol. **203**, 494, S. 973-975.
- Anderson, B. M. and Anderson, C. D. (1963): Effect of buffers on nicotinamide adenine dinucleotide hydrolysis. In: *Journal of Biological Chemistry*, Vol. **238**, 4, S. 1475-1478.
- Anderson, B. M.; Ciotti, C. J. and Kaplan, N. O. (1959): Chemical properties of 3-substituted pyridine analogues of diphosphopyridine nucleotide. In: *Journal of Biological Chemistry*, Vol. **234**, 5, S. 1219-1225.
- Anderson, B. M. and Kaplan, N. O. (1959): Enzymatic studies with analogues of diphosphopyridine nucleotide. In: *Journal of Biological Chemistry*, Vol. **234**, 5, S. 1226-1232.
- Ansell, R. J.; Dilmaghanian, S.; Stead, C. V. and Lowe, C. R. (1997): Synthesis and properties of new coenzyme mimics based on the artificial coenzyme Blue N-3. In: *Enzyme and Microbial Technology*, Vol. **21**, S. 327-334.
- Ansell, R. J. and Lowe, C. R. (1999): Artificial redox coenzymes: biomimetic analogues of NAD⁺. In: *Applied Microbiology and Biotechnology*, Vol. **51**, 6, S. 703-710.
- Ansell, R. J.; Small, D. A. P. and Lowe, C. R. (1999a): The interactions of artificial coenzymes with alcohol dehydrogenase and other NAD(P)(H) dependent enzymes. In: *Journal of Molecular Catalysis B: Enzymatic*, Vol. **6**, S. 111-123.
- Ansell, R. J.; Small, D. A. P. and Lowe, C. R. (1999b): Synthesis and properties of new coenzyme mimics based on the artificial coenzyme CL4. In: *Journal of Molecular Recognition*, Vol. **12**, 1, S. 45-56.
- Beer, B.; Pick, A. and Sieber, V. (2017): In vitro metabolic engineering for the production of alpha-ketoglutarate. In: *Metabolic Engineering*, Vol. **40**, S. 5-13.
- Bellamacina, C. R. (1996): The nicotinamide dinucleotide binding motif: A comparison of nucleotide binding proteins. In: *Faseb Journal*, Vol. **10**, 11, S. 1257-1269.
- Bertani, G. (1951): Studies on lysogenesis 1. The mode of phage liberation by lysogenic *Escherichia coli*. In: *Journal of Bacteriology*, Vol. **62**, 3, S. 293-300.
- Borst, N. (2016): SCHEMA-Rekombination von Cytochrom P450 Monooxygenasen der Enzymfamilie CYP101 und CYP102 zur Bereitstellung neuer Hydroxylaseaktivitäten. Ph.D. Thesis, Technical University of Munich, Straubing.
- Bradford, M. M. (1976): Rapid and sensitive method for quantitation of microgram quantities of protein utilizing principle of protein-dye binding. In: *Analytical Biochemistry*, Vol. **72**, 1-2, S. 248-254.

- Braun, F. (1887): Untersuchungen über die Löslichkeit fester Körper und die den Vorgang der Lösung begleitenden Volum- und Energieänderungen. In: *Zeitschrift für Physikalische Chemie*, Vol. **1**, S. 259-272.
- Braun, F. (1888): Ueber einen allgemeinen qualitativen Satz für Zustandsänderungen nebst einigen sich anschliessenden Bemerkungen, insbesondere über nicht eindeutige Systeme. In: *Annalen der Physik*, Vol. **269**, 2, S. 337-353.
- Burton, S. J.; Stead, C. V.; Ansell, R. J. and Lowe, C. R. (1996): An artificial redox coenzyme based on a triazine dye template. In: *Enzyme and Microbial Technology*, Vol. **18**, 8, S. 570-580.
- Campbell, E.; Meredith, M.; Minter, S. D. and Banta, S. (2012): Enzymatic biofuel cells utilizing a biomimetic cofactor. In: *Chemical Communications*, Vol. **48**, 13, S. 1898-1900.
- Codexis (2018): Codex® Ketoreductase (KRED) Screening Kit. Online: <https://www.codexis-estore.com/product-page/codex-ketoreductase-kred-screening-kit>. (accessed: 18.11.2018).
- Colowick, S. P.; Kaplan, N. O. and Ciotti, M. M. (1951): The reaction of pyridine nucleotide with cyanide and its analytical use. In: *Journal of Biological Chemistry*, Vol. **191**, 2, S. 447-459.
- De Wildeman, S. A.; Sonke, T.; Schoemaker, H. E. and May, O. (2007): Biocatalytic reductions: from lab curiosity to "first choice". In: *Accounts of Chemical Research*, Vol. **40**, S. 1260-1266.
- Dilmaghanian, S.; Stead, C. V.; Ansell, R. J. and Lowe, C. R. (1997): Synthesis and properties of a naphthalene-containing artificial redox coenzyme. In: *Enzyme and Microbial Technology*, Vol. **20**, S. 165-173.
- Eisner, U. and Kuthan, J. (1972): Chemistry of dihydropyridines. In: *Chemical Reviews*, Vol. **72**, 1, S. 1-42.
- Enders, D.; Voith, M. and Lenzen, A. (2005): The dihydroxyacetone unit - a versatile C-3 building block in organic synthesis. In: *Angewandte Chemie-International Edition*, Vol. **44**, 9, S. 1304-1325.
- Erickson, B.; Nelson, J. E. and Winters, P. (2012): Perspective on opportunities in industrial biotechnology in renewable chemicals. In: *Biotechnology Journal*, Vol. **7**, 2, S. 176-185.
- Fujii, T.; Fujii, Y.; Machida, K.; Ochiai, A. and Ito, M. (2009): Efficient biotransformations using *Escherichia coli* with tolC acraB mutations expressing cytochrome P450 genes. In: *Bioscience Biotechnology and Biochemistry*, Vol. **73**, 4, S. 805-810.
- Geddes, A.; Paul, C. E.; Hay, S.; Hollmann, F. and Scrutton, N. S. (2016): Donor-acceptor distance sampling enhances the performance of "Better than Nature" nicotinamide coenzyme biomimetics. In: *Journal of the American Chemical Society*, Vol. **138**, 35, S. 11089-11092.
- Geueke, B.; Riebel, B. and Hummel, W. (2003): NADH oxidase from *Lactobacillus brevis*: a new catalyst for the regeneration of NAD. In: *Enzyme and Microbial Technology*, Vol. **32**, 2, S. 205-211.
- Giardina, P.; Debiassi, M. G.; Derosa, M.; Gambacorta, A. and Buonocore, V. (1986): Glucose dehydrogenase from the thermoacidophilic archaebacterium *Sulfolobus solfataricus*. In: *Biochemical Journal*, Vol. **239**, 3, S. 517-522.
- Grogan, G. (2011): Cytochromes P450: exploiting diversity and enabling application as biocatalysts. In: *Current Opinion in Chemical Biology*, Vol. **15**, 2, S. 241-248.
- Gröger, H.; Hummel, W.; Borchert, S. and Krauß, M. (2012): Enzyme-catalyzed asymmetric reduction of ketones. In: *Enzyme Catalysis in Organic Synthesis*, Vol. **2**, S. 1037-1110.

- Guilbert, C. C. and Johnson, S. L. (1971): Isolation and characterization of fluorescent alkali product from diphosphopyridine nucleotide. In: *Biochemistry*, Vol. **10**, 12, S. 2313-2316.
- Guilbert, C. C. and Johnson, S. L. (1977): Investigation of open ring form of nicotinamide adenine-dinucleotide. In: *Biochemistry*, Vol. **16**, 2, S. 335-344.
- Guterl, J.-K.; Garbe, D.; Carsten, J.; Steffler, F.; Sommer, B.; Reisse, S.; Philipp, A.; Haack, M.; Ruedmann, B.; Koltermann, A.; Kettling, U.; Brueck, T. and Sieber, V. (2012): Cell-free metabolic engineering: production of chemicals by minimized reaction cascades. In: *ChemSusChem*, Vol. **5**, 11, S. 2165-2172.
- Hamilton, G. A. (2009): Mechanism of two- and four-electron oxidations catalyzed by some metalloenzymes. In: F. F. Nord and A. Meister (Hrsg.) *Advances in enzymology and related areas of molecular biology*. Interscience Publishers a division of John Wiley & Sons.
- Harden, A. and Young, W. J. (1906a): The alcoholic ferment of yeast-juice. In: *Proceedings of the Royal Society B: Biological Sciences*, Vol. **77**, 519, S. 405-420.
- Harden, A. and Young, W. J. (1906b): The alcoholic ferment of yeast-juice. Part II. - The cofermment of yeast-juice. In: *Proceedings of the Royal Society B: Biological Sciences*, Vol. **78**, 526, S. 369-375.
- Hentall, P. L.; Flowers, N. and Bugg, T. D. H. (2001): Enhanced acid stability of a reduced nicotinamide adenine dinucleotide (NADH) analogue. In: *Chemical Communications*, Vol., 20, S. 2098-2099.
- Hernandez, K.; Berenguer-Murcia, A.; Rodrigues, R. C. and Fernandez-Lafuente, R. (2012): Hydrogen peroxide in biocatalysis. A dangerous liaison. In: *Current Organic Chemistry*, Vol. **16**, 22, S. 2652-2672.
- Hoenes, J.; Heindl, D.; Horn, C. and Gaessler-Dietsche, C. (2007): Stabile NAD/NADH-Derivate. F.Hoffmann-La Roche AG / Roche Diagnostics GmbH. WO2007012494 A1.
- Hummel, W. and Gröger, H. (2014): Strategies for regeneration of nicotinamide coenzymes emphasizing self-sufficient closed-loop recycling systems. In: *Journal of Biotechnology*, Vol. **191**, S. 22-31.
- Hummel, W. and Riebel, B. (2003): Isolation and biochemical characterization of a new NADH oxidase from *Lactobacillus brevis*. In: *Biotechnology Letters*, Vol. **25**, 1, S. 51-54.
- Hutton, R. F. and Westheimer, F. H. (1958): N-Methyldihydronicotinamide. In: *Tetrahedron*, Vol. **3**, S. 73-77.
- Inoue, H.; Nojima, H. and Okayama, H. (1990): High-efficiency transformation of *Escherichia coli* with plasmids. In: *Gene*, Vol. **96**, 1, S. 23-28.
- Jennewein, S.; Rithner, C. D.; Williams, R. M. and Croteau, R. B. (2001): Taxol biosynthesis: taxane 13 alpha-hydroxylase is a cytochrome P450-dependent monooxygenase. In: *Proceedings of the National Academy of Sciences of the United States of America*, Vol. **98**, 24, S. 13595-13600.
- Ji, D. B.; Wang, L.; Hou, S. H.; Liu, W. J.; Wang, J. X.; Wang, Q. and Zhao, Z. K. B. (2011): Creation of bioorthogonal redox systems depending on nicotinamide flucytosine dinucleotide. In: *Journal of the American Chemical Society*, Vol. **133**, 51, S. 20857-20862.
- Jiang, R. and Bommarius, A. S. (2004): Hydrogen peroxide-producing NADH oxidase (nox-1) from *Lactococcus lactis*. In: *Tetrahedron: Asymmetry*, Vol. **15**, 18, S. 2939-2944.

- Jiang, R.; Riebel, B. R. and Bommarius, A. S. (2005): Comparison of alkyl hydroperoxide reductase (ahpr) and water-forming NADH oxidase from *Lactococcus lactis* ATCC 19435. In: *Advanced Synthesis & Catalysis*, Vol. **347**, 7-8, S. 1139-1146.
- Johannes, T. W.; Woodyer, R. D. and Zhao, H. M. (2007): Efficient regeneration of NADPH using an engineered phosphite dehydrogenase. In: *Biotechnology and Bioengineering*, Vol. **96**, 1, S. 18-26.
- Johnson, S. L. and Morrison, D. L. (1970): Substituent effects on pyridinium ring-opening reactions. Facile ring opening of 1-(N,N-dimethylcarbamoyl)nicotinamide cation. In: *Biochemistry*, Vol. **9**, 6, S. 1460-1470.
- Kaplan, N. O. and Ciotti, M. M. (1954): The 3-acetylpyridine analog of DPN. In: *Journal of the American Chemical Society*, Vol. **76**, 6, S. 1713-1714.
- Kaplan, N. O. and Ciotti, M. M. (1956): Chemistry and properties of the 3-acetylpyridine analogue of diphosphopyridine nucleotide. In: *Journal of Biological Chemistry*, Vol. **221**, 2, S. 823-832.
- Kaplan, N. O.; Ciotti, M. M. and Stolzenbach, F. E. (1956): Reaction of pyridine nucleotide analogues with dehydrogenases. In: *Journal of Biological Chemistry*, Vol. **221**, 2, S. 833-844.
- Kaplan, N. O.; Colowick, S. P. and Barnes, C. C. (1951): Effect of alkali on diphosphopyridine nucleotide. In: *Journal of Biological Chemistry*, Vol. **191**, 2, S. 461-472.
- Kara, S.; Schrittwieser, J. H.; Hollmann, F. and Ansorge-Schumacher, M. B. (2014): Recent trends and novel concepts in cofactor-dependent biotransformations. In: *Applied Microbiology and Biotechnology*, Vol. **98**, 4, S. 1517-1529.
- Karrer, P. and Stare, F. J. (1937): N-Alkyl-dihydro-nicotinsäureamide. In: *Helvetica Chimica Acta*, Vol. **20**, 1, S. 418-423.
- Keinan, E.; Seth, K. K. and Lamed, R. (1987): Synthetic applications of alcohol-dehydrogenase from *Thermoanaerobium brockii*. In: *Annals of the New York Academy of Sciences*, Vol. **501**, 1, S. 130-149.
- Knaus, T.; Paul, C. E.; Levy, C. W.; De Vries, S.; Mutti, F. G.; Hollmann, F. and Scrutton, N. S. (2015): Better than Nature: nicotinamide biomimetics that outperform natural coenzymes. In: *Journal of the American Chemical Society*, Vol. **138**, 3, S. 1033-1039.
- Koike, K.; Kobayashi, T.; Ito, S. and Saitoh, M. (1985): Purification and characterization of NADH oxidase from a strain of *Leuconostoc mesenteroides*. In: *Journal of Biochemistry*, Vol. **97**, 5, S. 1279-1288.
- Kroutil, W. and Rueping, M. (2014): Introduction to ACS catalysis virtual special issue on cascade catalysis. In: *ACS Catalysis*, Vol. **4**, 6, S. 2086-2087.
- Laemmli, U. K. (1970): Cleavage of structural proteins during the assembly of the head of Bacteriophage T4. In: *Nature*, Vol. **227**, S. 680-685.
- Lamble, H. J.; Heyer, N. I.; Bull, S. D.; Hough, D. W. and Danson, M. J. (2003): Metabolic pathway promiscuity in the archaeon *Sulfolobus solfataricus* revealed by studies on glucose dehydrogenase and 2-keto-3-deoxygluconate aldolase. In: *Journal of Biological Chemistry*, Vol. **278**, 36, S. 34066-34072.
- Le Chatelier, A.L. (1884): Sur un énoncé général des lois des équilibres chimiques. In: *Comptes Rendus*, Vol. **99**, S. 786-789.
- Levy, S. B. (1992): Dihydroxyacetone-containing sunless or self-tanning lotions. In: *Journal of the American Academy of Dermatology*, Vol. **27**, 6, S. 989-993.

- Liang, J.; Mundorff, E.; Voladri, R.; Jenne, S.; Gilson, L.; Conway, A.; Krebber, A.; Wong, J.; Huisman, G.; Truesdell, S. and Lalonde, J. (2010): Highly enantioselective reduction of a small heterocyclic ketone: biocatalytic reduction of tetrahydrothiophene-3-one to the corresponding (R)-alcohol. In: *Organic Process Research & Development*, Vol. **14**, 1, S. 188-192.
- Lin, B. X. and Tao, Y. (2017): Whole-cell biocatalysts by design. In: *Microbial Cell Factories*, Vol. **16**, 1, S. 106-117.
- Lo, C. H. and Fish, R. H. (2002): Biomimetic NAD⁺ models for tandem cofactor regeneration, horse liver alcohol dehydrogenase recognition of 1,4-NADH-derivatives and chiral synthesis. In: *Angewandte Chemie-International Edition*, Vol. **41**, 3, S. 478-481.
- Loida, P. J. and Sligar, S. G. (1993): Molecular recognition in cytochrome P-450: mechanism for the control of uncoupling reactions. In: *Biochemistry*, Vol. **32**, 43, S. 11530-11538.
- Lountos, G. T.; Jiang, R.; Wellborn, W. B.; Thaler, T. L.; Bommarius, A. S. and Orville, A. M. (2006): The crystal structure of NAD(P)H oxidase from *Lactobacillus sanfranciscensis*: insights into the conversion of O₂ into two water molecules by the flavoenzyme. In: *Biochemistry*, Vol. **45**, 32, S. 9648-9659.
- Low, S. A.; Low, I. M.; Weissenborn, M. J. and Hauer, B. (2016): Enhanced ene-reductase activity through alteration of artificial nicotinamide cofactor substituents. In: *ChemCatChem*, Vol. **8**, 5, S. 911-915.
- Lowry, O. H.; Passonneau, J. V. and Rock, M. K. (1961): The stability of pyridine nucleotides. In: *The Journal of Biological Chemistry*, Vol. **236**, 10, S. 2756-2759.
- Lutz, J.; Hollmann, F.; Ho, T. V.; Schnyder, A.; Fish, R. H. and Schmid, A. (2004): Bioorganometallic chemistry: biocatalytic oxidation reactions with biomimetic NAD⁺/NADH co-factors and [Cp*Rh(bpy)H]⁺ for selective organic synthesis. In: *Journal of Organometallic Chemistry*, Vol. **689**, 25, S. 4783-4790.
- Ma, S. K.; Gruber, J.; Davis, C.; Newman, L.; Gray, D.; Wang, A.; Grate, J.; Huisman, G. W. and Sheldon, R. A. (2010): A green-by-design biocatalytic process for atorvastatin intermediate. In: *Green Chemistry*, Vol. **12**, 1, S. 81-86.
- Maid, H.; Bohm, P.; Huber, S. M.; Bauer, W.; Hummel, W.; Jux, N. and Groger, H. (2011): Iron catalysis for in situ regeneration of oxidized cofactors by activation and reduction of molecular oxygen: a synthetic metalloporphyrin as a biomimetic NAD(P)H oxidase. In: *Angewandte Chemie-International Edition*, Vol. **50**, 10, S. 2397-2400.
- Mansson, M. O.; Larsson, P. O. and Mosbach, K. (1978): Covalent binding of an NAD analog to liver alcohol-dehydrogenase resulting in an enzyme-coenzyme complex not requiring exogenous coenzyme for activity. In: *European Journal of Biochemistry*, Vol. **86**, 2, S. 455-463.
- Matsuda, T.; Yamanaka, R. and Nakamura, K. (2009): Recent progress in biocatalysis for asymmetric oxidation and reduction. In: *Tetrahedron: Asymmetry*, Vol. **20**, 5, S. 513-557.
- Maurer, S. C.; Kuhnel, K.; Kaysser, L. A.; Eiben, S.; Schmid, R. D. and Urlacher, V. B. (2005): Catalytic hydroxylation in biphasic systems using CYP102A1 mutants. In: *Advanced Synthesis & Catalysis*, Vol. **347**, 7-8, S. 1090-1098.
- Mauzerall, D. and Westheimer, F. H. (1955): 1-Benzylidihydronicotinamide - a model for reduced DPN. In: *Journal of the American Chemical Society*, Vol. **77**, 8, S. 2261-2264.
- May, S. W. and Padgett, S. R. (1983): Oxidoreductase enzymes in biotechnology - current status and future potential. In: *Bio/Technology*, Vol. **1**, 8, S. 677-686.

- McLoughlin, S. B. and Lowe, C. R. (1997): An enzymatically active artificial redox coenzyme based on a synthetic dye template. In: *Enzyme and Microbial Technology*, Vol. **20**, 1, S. 2-11.
- Milburn, C. C.; Lambie, H. J.; Theodossis, A.; Bull, S. D.; Hough, D. W.; Danson, M. J. and Taylor, G. L. (2006): The structural basis of substrate promiscuity in glucose dehydrogenase from the hyperthermophilic archaeon *Sulfolobus solfataricus*. In: *The Journal of Biological Chemistry*, Vol. **281**, 21, S. 14796-14804.
- Mülhardt, C. (2009): *Der Experimentator: Molekularbiologie, Genomics*. Akademischer Verlag Spektrum.
- Müller, J. M. (2013): *Charakterisierung neuer 2-Keto-3-Desoxyglukonat Aldolasen für die zellfreie Biosynthese*. M.Sc. Thesis, Technical University of Munich, Straubing.
- Nagao, T.; Mitamura, T.; Wang, X. H.; Negoro, S.; Yomo, T.; Urabe, I. and Okada, H. (1992): Cloning, nucleotide-sequences, and enzymatic-properties of glucose-dehydrogenase isozymes from *Bacillus megaterium* IAM1030. In: *Journal of Bacteriology*, Vol. **174**, 15, S. 5013-5020.
- Niimura, Y.; Ohnishi, K.; Yarita, Y.; Hidaka, M.; Masaki, H.; Uchimura, T.; Suzuki, H.; Kozaki, M. and Uozumi, T. (1993): A flavoprotein functional as NADH oxidase from *amphibacillus-xylanus* ep01 - purification and characterization of the enzyme and structural-analysis of its gene. In: *Journal of Bacteriology*, Vol. **175**, 24, S. 7945-7950.
- Okamoto, Y.; Kohler, V.; Paul, C. E.; Hollmann, F. and Ward, T. R. (2016): Efficient in situ regeneration of NADH mimics by an artificial metalloenzyme. In: *ACS Catalysis*, Vol. **6**, 6, S. 3553-3557.
- Oppenheimer, N. J. (1982): *Chemistry and Solution - Conformation of the Pyridine Coenzyme* In: J. Everse; B. Anderson and Y. Kwan-Sa (Hrsg.) *The Pyridine Nucleotide Coenzymes*. Academic Press.
- Oppenheimer, N. J. (1994): NAD hydrolysis - chemical and enzymatic mechanisms. In: *Molecular and Cellular Biochemistry*, Vol. **138**, 1-2, S. 245-251.
- Oppenheimer, N. J.; Arnold, L. J. and Kaplan, N. O. (1971): Structure of pyridine nucleotides in solution. In: *Proceedings of the National Academy of Sciences of the United States of America*, Vol. **68**, 12, S. 3200-3205.
- Oppenheimer, N. J. and Kaplan, N. O. (1974): Structure of the primary acid rearrangement product of reduced nicotinamide adenine dinucleotide (NADH). In: *Biochemistry*, Vol. **13**, 23, S. 4675-4685.
- Pace, C. N.; Vajdos, F.; Fee, L.; Grimsley, G. and Gray, T. (1995): How to measure and predict the molar absorption-coefficient of a protein. In: *Protein Science*, Vol. **4**, 11, S. 2411-2423.
- Park, H. J.; Reiser, C. O. A.; Kondruweit, S.; Erdmann, H.; Schmid, R. D. and Sprinzl, M. (1992): Purification and characterization of a NADH oxidase from the thermophile *Thermus thermophilus* HB8. In: *European Journal of Biochemistry*, Vol. **205**, 3, S. 881-885.
- Paul, C. E.; Arends, I. W. C. E. and Hollmann, F. (2014a): Is simpler better? Synthetic nicotinamide cofactor analogues for redox chemistry. In: *ACS Catalysis*, Vol. **4**, 3, S. 788-797.
- Paul, C. E.; Churakova, E.; Maurits, E.; Girhard, M.; Urlacher, V. B. and Hollmann, F. (2014b): In situ formation of H₂O₂ for P450 peroxygenases. In: *Bioorganic & Medicinal Chemistry*, Vol. **22**, 20, S. 5692-5696.
- Paul, C. E.; Gargiulo, S.; Opperman, D. J.; Lavandera, I.; Gotor-Fernandez, V.; Gotor, V.; Taglieber, A.; Arends, I. W. C. E. and Hollmann, F. (2013): Mimicking nature: synthetic nicotinamide

- cofactors for C=C bioreduction using enoate reductases. In: *Organic Letters*, Vol. **15**, 1, S. 180-183.
- Paul, C. E. and Hollmann, F. (2016): A survey of synthetic nicotinamide cofactors in enzymatic processes. In: *Applied Microbiology and Biotechnology*, Vol. **100**, 11, S. 4773-4778.
- Paul, C. E.; Tischler, D.; Riedel, A.; Heine, T.; Itoh, N. and Hollmann, F. (2015): Nonenzymatic regeneration of styrene monooxygenase for catalysis. In: *ACS Catalysis*, Vol. **5**, 5, S. 2961-2965.
- Petschacher, B.; Staunig, N.; Muller, M.; Schurmann, M.; Mink, D.; De Wildeman, S.; Gruber, K. and Glieder, A. (2014): Cofactor specificity engineering of *Streptococcus mutans* NADH oxidase 2 for NAD(P)(+) regeneration in biocatalytic oxidations. In: *Computational and Structural Biotechnology Journal*, Vol. **9**, S. e201402005.
- Poizat, M.; Arends, Iwce and Hollmann, F. (2010): On the nature of mutual inactivation between Cp*Rh(bpy)(H₂O) (2+) and enzymes - analysis and potential remedies. In: *Journal of Molecular Catalysis B: Enzymatic*, Vol. **63**, 3-4, S. 149-156.
- Richter, M. (2013): Functional diversity of organic molecule enzyme cofactors. In: *Natural Product Reports*, Vol. **30**, 10, S. 1324-1345.
- Riebel, B. R.; Gibbs, P. R.; Wellborn, W. B. and Bommarius, A. S. (2003): Cofactor regeneration of both NAD(+) from NADH and NADP(+) from NADPH: NADH oxidase from *Lactobacillus sanfranciscensis*. In: *Advanced Synthesis & Catalysis*, Vol. **345**, 6-7, S. 707-712.
- Riedel, A.; Mehnert, M.; Paul, C. E.; Westphal, A. H.; van Berkel, W. J. H. and Tischler, D. (2015): Functional characterization and stability improvement of a 'thermophilic-like' ene-reductase from *Rhodococcus opacus* 1CP. In: *Frontiers in Microbiology*, Vol. **6**, S. 14.
- Rioz-Martinez, A.; Cuetos, A.; Rodriguez, C.; de Gonzalo, G.; Lavandera, I.; Fraaije, M. W. and Gotor, V. (2011): Dynamic kinetic resolution of alpha-substituted beta-ketoesters catalyzed by Baeyer-Villiger monooxygenases: access to enantiopure alpha-hydroxy esters. In: *Angewandte Chemie-International Edition*, Vol. **50**, 36, S. 8387-8390.
- Rocha-Martin, J.; Vega, D.; Bolivar, J. M.; Godoy, C. A.; Hidalgo, A.; Berenguer, J.; Guisan, J. M. and Lopez-Gallego, F. (2011): New biotechnological perspectives of a NADH oxidase variant from *Thermus thermophilus* HB27 as NAD⁺-recycling enzyme. In: *BMC Biotechnology*, Vol. **11**, S. 101.
- Roche (2009): Stabilisierung von Dehydrogenasen mit stabilen Coenzymen. F.Hoffmann-La Roche AG / Roche Diagnostics GmbH. EP 2 093 284 A1.
- Rollin, J. A.; Tam, T. K. and Zhang, Y. H. P. (2013): New biotechnology paradigm: cell-free biosystems for biomanufacturing. In: *Green Chemistry*, Vol. **15**, 7, S. 1708-1719.
- Ross, R. P. and Claiborne, A. (1992): Molecular-cloning and analysis of the gene encoding the NADH oxidase from *Streptococcus-faecalis* 10C1 - comparison with NADH peroxidase and the flavoprotein disulfide reductases. In: *Journal of Molecular Biology*, Vol. **227**, 3, S. 658-671.
- Rossmann, M. G. (1976): Molecular-structure of NAD. In: *Nature*, Vol. **262**, 5570, S. 726-726.
- Rossmann, M. G.; Moras, D. and Olsen, K. W. (1974): Chemical and biological evolution of a nucleotide-binding protein. In: *Nature*, Vol. **250**, 5463, S. 194-199.
- Ryan, J. D.; Fish, R. H. and Clark, D. S. (2008): Engineering cytochrome P450 enzymes for improved activity towards biomimetic 1,4-NADH-cofactors. In: *ChemBioChem*, Vol. **9**, 16, S. 2579-2582.

- Sattler, J. H.; Fuchs, M.; Tauber, K.; Mutti, F. G.; Faber, K.; Pfeffer, J.; Haas, T. and Kroutil, W. (2012): Redox self-sufficient biocatalyst network for the amination of primary alcohols. In: *Angewandte Chemie-International Edition*, Vol. **51**, 36, S. 9156-9159.
- Schelhorn, J. (2004): Die Nicotinamid-, Thymin- und Uracilkonzentration im Leichenblut - Ein Baustein zur Todeszeitschätzung bei fortgeschrittener Leichenliegezeit? Ph.D. Thesis, Friedrich-Schiller-Universität Jena, Jena.
- Schirwitz, K.; Schmidt, A. and Lamzin, V. S. (2007): High-resolution structures of formate dehydrogenase from *Candida boidinii*. In: *Protein Science*, Vol. **16**, 6, S. 1146-1156.
- Scholtissek, A.; Gadke, E.; Paul, C. E.; Westphal, A. H.; van Berkel, W. J. H. and Tischler, D. (2018): Catalytic performance of a class III Old Yellow Enzyme and its cysteine variants. In: *Frontiers in Microbiology*, Vol. **9**, S. 2410.
- Scholtissek, A.; Tischler, D.; Westphal, A. H.; van Berkel, W. J. H. and Paul, C. E. (2017): Old Yellow Enzyme - catalysed asymmetric hydrogenation: linking family roots with improved catalysis. In: *Catalysts*, Vol. **7**, 5, S. 130.
- Shafiee, A. and Hutchinson, C. R. (1987): Macrolide antibiotic biosynthesis - isolation and properties of 2 forms of 6-deoxyerythronolide-B hydroxylase from *Saccharopolyspora erythraea* (streptomyces, erythreus). In: *Biochemistry*, Vol. **26**, 19, S. 6204-6210.
- Shaked, Z. and Whitesides, G. M. (1980): Enzyme-catalyzed organic synthesis: NADH regeneration by using formate dehydrogenase. In: *Journal of the American Chemical Society*, Vol. **102**, 23, S. 7104-7105.
- Sharp, P. A.; Sugden, B. and Sambrook, J. (1973): Detection of 2 restriction endonuclease activities in *Haemophilus parainfluenzae* using analytical agarose-ethidium bromide electrophoresis. In: *Biochemistry*, Vol. **12**, 16, S. 3055-3063.
- Sheldon, R. A. and Woodley, J. M. (2018): Role of biocatalysis in sustainable chemistry. In: *Chemical Reviews*, Vol. **118**, 2, S. 801-838.
- Sicsic, S.; Durand, P.; Langrene, S. and Legoffic, F. (1984): A new approach for using cofactor dependent enzymes - example of alcohol-dehydrogenase. In: *Febs Letters*, Vol. **176**, 2, S. 321-324.
- Simon, R. C.; Mutti, F. G. and Kroutil, W. (2013): Biocatalytic synthesis of enantiopure building blocks for pharmaceuticals. In: *Drug Discovery Today: Technologies*, Vol. **10**, 1, S. 37-44.
- Slama, J. T. and Simmons, A. M. (1988): Carbanicotinamide adenine dinucleotide: synthesis and enzymological properties of a carbocyclic analogue of oxidized nicotinamide adenine dinucleotide. In: *Biochemistry*, Vol. **27**, 1, S. 183-193.
- Slama, J. T. and Simmons, A. M. (1989): Inhibition of NAD glycohydrolase and ADP-ribosyl transferase by carbocyclic analogues of oxidized nicotinamide adenine dinucleotide. In: *Biochemistry*, Vol. **28**, 19, S. 7688-7694.
- Steffler, F. (2014): Produktion und Entwicklung von Oxidoreduktasen für enzymatische Kaskadenreaktionen. Ph.D. Thesis, Technical University of Munich, Straubing.
- Studier, F. W. (2005): Protein production by auto-induction in high-density shaking cultures. In: *Protein Expression and Purification*, Vol. **41**, 1, S. 207-234.
- Stueckler, C.; Winkler, C. K.; Bonnekessel, M. and Faber, K. (2010): Asymmetric synthesis of (R)-3-hydroxy-2-methylpropanoate ('Roche Ester') and derivatives via biocatalytic C=C-bond reduction. In: *Advanced Synthesis & Catalysis*, Vol. **352**, 14-15, S. 2663-2666.

- Tachon, S.; Chambellon, E. and Yvon, M. (2011): Identification of a conserved sequence in flavoproteins essential for the correct conformation and activity of the NADH oxidase NoxE of *Lactococcus lactis*. In: *Journal of Bacteriology*, Vol. **193**, 12, S. 3000-3008.
- Theodossis, A.; Milburn, C. C.; Heyer, N. I.; Lambie, H. J.; Hough, D. W.; Danson, M. J. and Taylor, G. (2005): Preliminary crystallographic studies of glucose dehydrogenase from the promiscuous Entner-Doudoroff pathway in the hyperthermophilic archaeon *Sulfolobus solfataricus*. In: *Acta Crystallographica Section F Structural Biology and Crystallization Communications*, Vol. **61**, S. 112-115.
- Toth, K.; Sedlak, E.; Sprinzl, M. and Zoldak, G. (2008): Flexibility and enzyme activity of NADH oxidase from *Thermus thermophilus* in the presence of monovalent cations of Hofmeister series. In: *Biochimica Et Biophysica Acta*, Vol. **1784**, 5, S. 789-95.
- UniProt (Last modified December 5, 2014): Cofactor. Online: <https://www.uniprot.org/help/cofactor>. (accessed: 06.05.2018).
- Vazquez-Figueroa, E.; Chaparro-Riggers, J. and Bommarius, A. S. (2007): Development of a thermostable glucose dehydrogenase by a structure-guided consensus concept. In: *ChemBioChem*, Vol. **8**, 18, S. 2295-2301.
- Voet, Daniel; Voet, Judith G. and Pratt, Charlotte W. (2002): *Lehrbuch der Biochemie*. John Wiley & Sons, Inc.
- Von Euler, H.; Albers, H. and Schlenk, F. (1936): Chemische Untersuchungen an hochgereinigter Co-Zymase. In: *Hoppe-Seyler's Zeitschrift für physiologische Chemie*, Vol. **240**, S. 113-126.
- Wada, M.; Yoshizumi, A.; Noda, Y.; Kataoka, M.; Shimizu, S.; Takagi, H. and Nakamori, S. (2003): Production of a doubly chiral compound, (4R,6R)-4-hydroxy-2,2,6-trimethylcyclohexanone, by two-step enzymatic asymmetric reduction. In: *Applied and Environmental Microbiology*, Vol. **69**, 2, S. 933-937.
- Warburg, O. and Christian, W. (1931): Über Aktivierung der Robison'schen Hexose-Mono-Phosphorsäure in roten Blutzellen und die Gewinnung aktivierender Fermentlösungen. In: *Biochemische Zeitschrift*, Vol. **242**, S. 206-227.
- Warburg, O. and Christian, W. (1936): Pyridine as a functional group of dehydrated enzymes. In: *Biochemische Zeitschrift*, Vol. **286**, S. 142-142.
- Warburg, O.; Christian, W. and Griese, A. (1935): Wasserstoffübertragendes Co-Ferment, seine Zusammensetzung und Wirkungsweise. In: *Biochemische Zeitschrift*, Vol. **282**, S. 157-165.
- Weber, M. M. and Kaplan, N. O. (1956): Pyridine nucleotide analogs and the sulfhydryl nature of some FAD enzymes. In: *Science*, Vol. **123**, 3202, S. 844-845.
- Westheimer, F. H. (1962): Mechanisms related to enzyme catalysis. In: *Advances in Enzymology and Related Subjects of Biochemistry*, Vol. **24**, S. 441-482.
- Wierenga, R. K.; De Maeyer, M. C. H. and Hol, W. G. J. (1985): Interaction of pyrophosphate moieties with alpha-helices in dinucleotide-binding proteins. In: *Biochemistry*, Vol. **24**, 6, S. 1346-1357.
- Winkelhausen, E. and Kuzmanova, S. (1998): Microbial conversion of D-xylose to xylitol. In: *Journal of Fermentation and Bioengineering*, Vol. **86**, 1, S. 1-14.
- Wong, C.-H. and Whitesides, G. M. (1981): Enzyme-catalyzed organic synthesis: NAD(P)H cofactor regeneration by using glucose 6-phosphate and the glucose-6-phosphate dehydrogenase from *Leuconostoc mesenteroides*. In: *Journal of the American Chemical Society*, Vol. **103**, 16, S. 4890-4899.

- Wu, H.; Tian, C. Y.; Song, X. K.; Liu, C.; Yang, D. and Jiang, Z. Y. (2013): Methods for the regeneration of nicotinamide coenzymes. In: *Green Chemistry*, Vol. **15**, 7, S. 1773-1789.
- Yaoi, T.; Miyazaki, K.; Oshima, T.; Komukai, Y. and Go, M. (1996): Conversion of the coenzyme specificity of isocitrate dehydrogenase by module replacement. In: *Journal of Biochemistry*, Vol. **119**, 5, S. 1014-1018.
- Zachos, I. ; Nowak, C. and Sieber, V. (2019): Biomimetic cofactors and methods for their recycling. In: *Current Opinion in Chemical Biology*, Vol. **49**, S. 59-66.
- Zhang, Y.; Gao, F.; Zhang, S. P.; Su, Z. G.; Ma, G. H. and Wang, P. (2011): Simultaneous production of 1,3-dihydroxyacetone and xylitol from glycerol and xylose using a nanoparticle-supported multi-enzyme system with in situ cofactor regeneration. In: *Bioresource Technology*, Vol. **102**, 2, S. 1837-1843.
- Zhang, Y. H. P. (2010): Production of biocommodities and bioelectricity by cell-free synthetic enzymatic pathway biotransformations: challenges and opportunities. In: *Biotechnology and Bioengineering*, Vol. **105**, 4, S. 663-677.
- Zhao, H. M. and van der Donk, W. A. (2003): Regeneration of cofactors for use in biocatalysis. In: *Current Opinion in Biotechnology*, Vol. **14**, 6, S. 583-589.

6 Appendix

6.1 Supporting Information - A water-forming NADH oxidase from *Lactobacillus pentosus* suitable for the regeneration of synthetic biomimetic cofactors



Supplementary Material

A water-forming NADH oxidase from *Lactobacillus pentosus* suitable for synthetic biomimetic cofactors

Claudia Nowak^{1, 2}, Barbara Beer^{1, 2}, André Pick¹, Teresa Roth¹, Petra Lommes¹, Volker Sieber^{1*}

¹ Chair of Chemistry of Biogenic Resources, Straubing Centre of Science, Department Life Science Engineering, Technische Universität München, Straubing, Germany

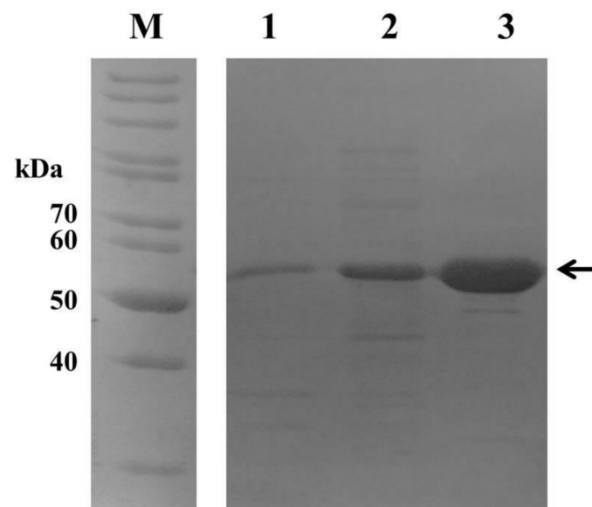
² Both authors contributed equally

* **Correspondence:** Corresponding Author, Prof. Dr. Volker Sieber, Chair of Chemistry of Biogenic Resources, Straubing Centre of Science, Department Life Science Engineering, Technische Universität München, Schulgasse 16, D-94315 Straubing, sieber@tum.de

Supplementary Material



Supplementary Figure 1. Multiple sequence alignment of NADH oxidases. Amino acid sequences of *Lactobacillus pentosus* (Uniprot ID I8R785), *Lactobacillus sanfranciscensis* (Uniprot ID Q9F1X5), *Lactobacillus brevis* (Uniprot ID M5AB03), and *Lactococcus lactis* (Uniprot ID A2RIB7) were aligned using Clustal Omega (Sievers et al., 2011). The secondary structure assignment and the binding site for FAD/ADP of Nox from *L. sanfranciscensis* (PDB ID: 2CDU) is depicted above the alignment. The catalytically active Cys42 is marked in a red box.



Supplementary Figure 2: SDS-PAGE of *LpNox* purification. Lane 1: insoluble fraction of the cell lysate, lane 2: soluble fraction of the cell lysate, lane 3: *LpNox* after purification. *LpNox* (arrow) is mainly found in the soluble fraction of the lysed cells. *LpNox* could be purified to >95 % homogeneity.

References

- Sievers, F., Wilm, A., Dineen, D., Gibson, T.J., Karplus, K., Li, W., Lopez, R., McWilliam, H., Remmert, M., Söding, J., Thompson, J.D., and Higgins, D.G. (2011). Fast, scalable generation of high-quality protein multiple sequence alignments using Clustal Omega. *Molecular Systems Biology* 7, 539-539. doi: 10.1038/msb.2011.75.

6.2 Supporting Information - Characterization of Biomimetic Cofactors According to Stability, Redox Potentials, and Enzymatic Conversion by NADH Oxidase from *Lactobacillus pentosus*

CHEMBIOCHEM

Supporting Information

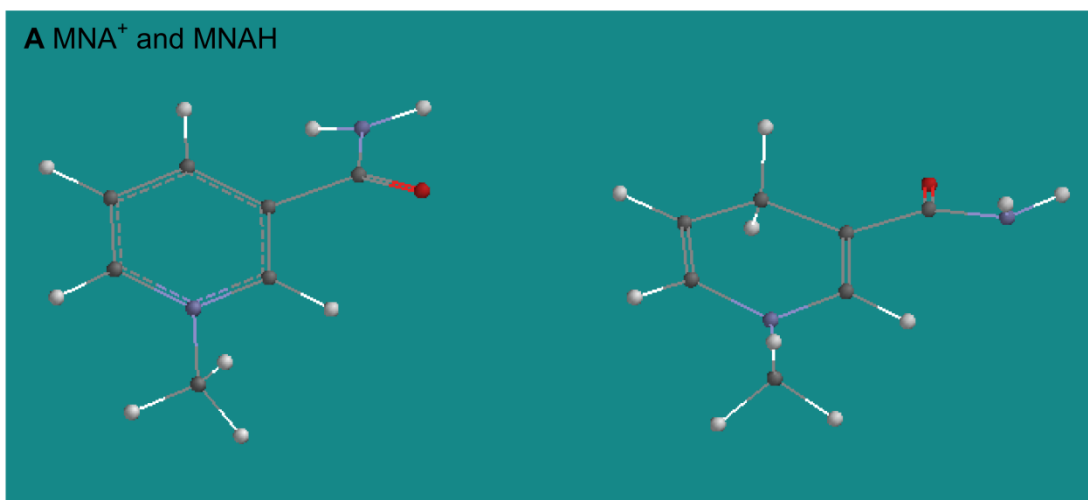
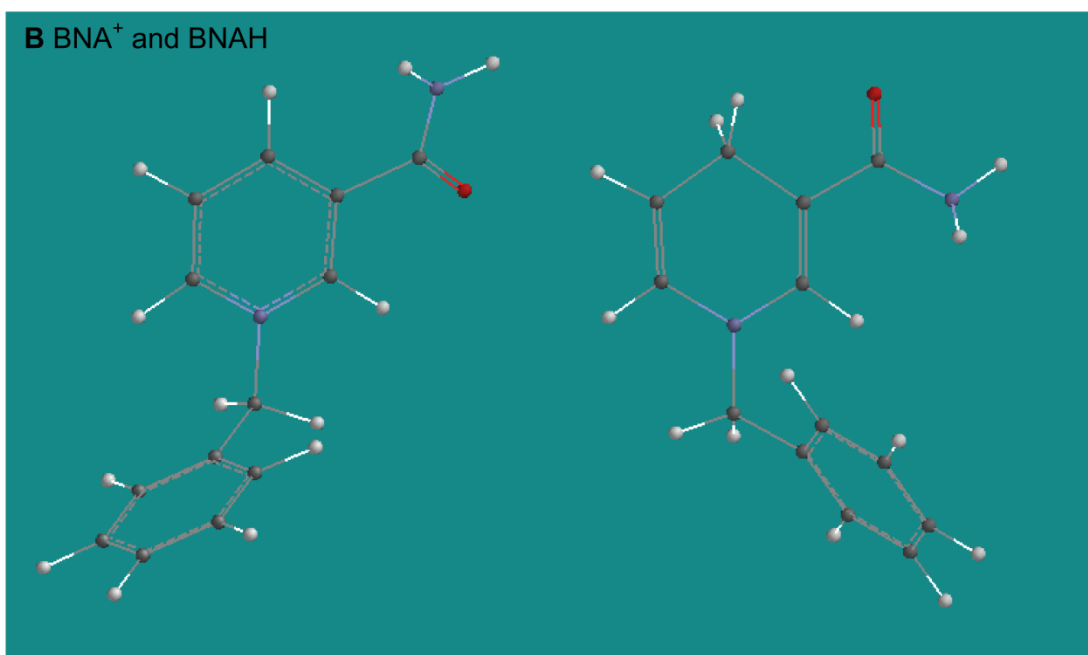
Characterization of Biomimetic Cofactors According to Stability, Redox Potentials, and Enzymatic Conversion by NADH Oxidase from *Lactobacillus pentosus*

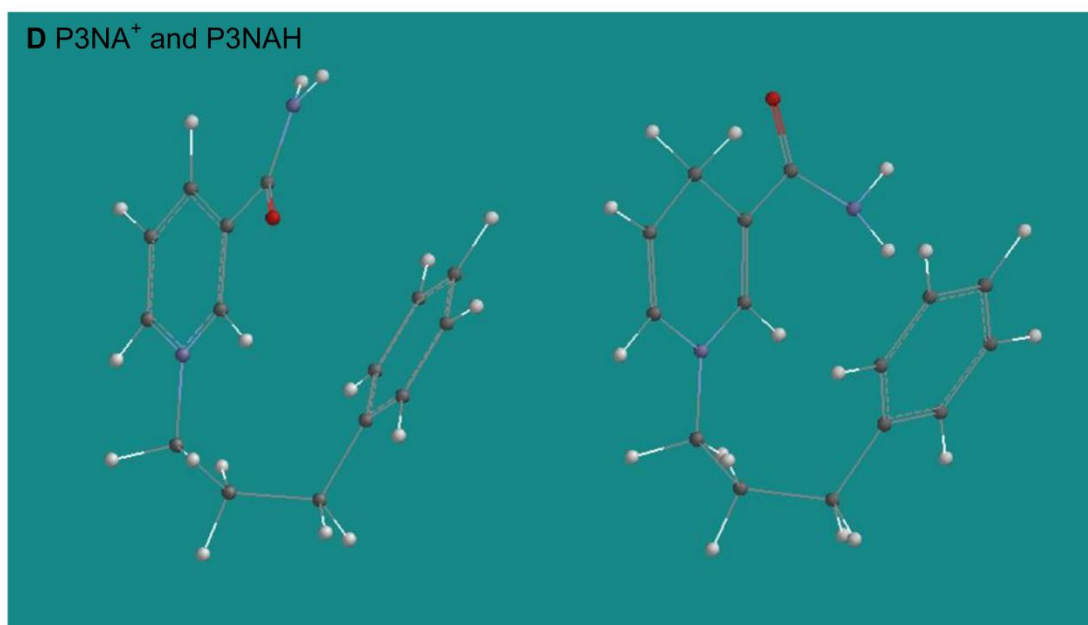
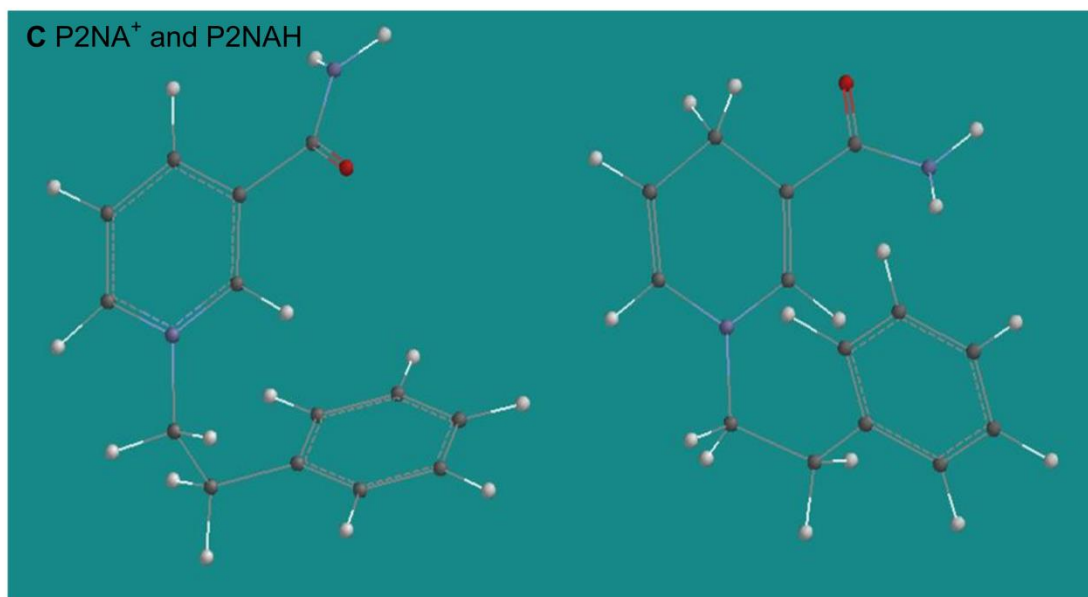
Claudia Nowak,^[a] André Pick,^[a] Lénárd-István Csepei,^[b] and Volker Sieber*^[a, b, c, d]

cbic_201700258_sm_miscellaneous_information.pdf

Table of Contents

- S1.** Modeling of the biomimetic cofactors **A** MNA⁺ and MNAH, **B** BNA⁺ and BNAH, **C** P2NA⁺ and P2NAH, and **D** P3NA⁺ and P3NAH (molecular structures were optimized using the DFT method pBD-DN* starting from the lowest energy conformer 6-31G* structure).
- S2.** Determination of rate constants (k) of deactivation in 100 mM Tris-HCl pH 8 with different variations.
- S3.** Cyclic voltammograms of biomimetic and natural cofactors.
- S4.** Cathodic and anodic potentials of the natural and biomimetic cofactors and peak current ratios.
- S5.** Comparison of various redox potentials of NAD⁺/NADH and NADP⁺/NADPH.
- S6.** Side product analyses of reactions of FAD and *LpNox* with biomimetic cofactors.
- S7.** Kinetic measurements of *LpNox* with the biomimetics P2NAH and P3NAH.
- S8.** Visualization of NADH, FAD and the biomimetic cofactors in the cofactor binding site of *LpNox* including detailed view in the coordination of the dihydro nicotinamide ring.

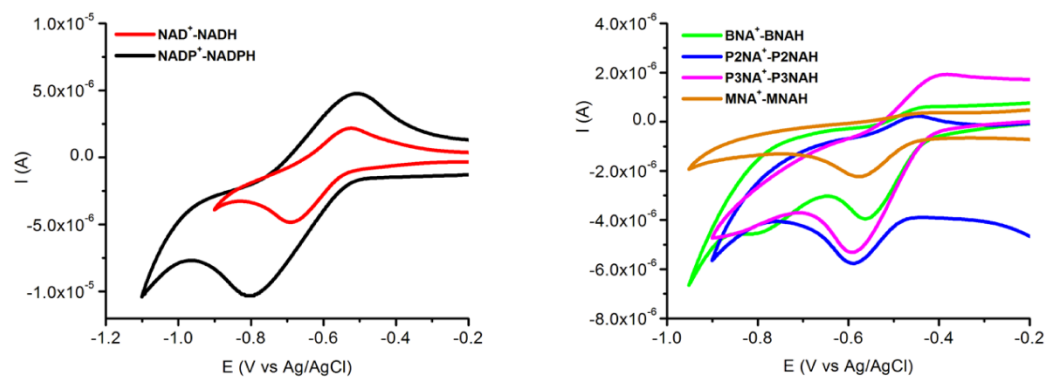
A MNA^+ and MNAH **B** BNA^+ and BNAH 



S1. Modeling of the biomimetic cofactors **A** MNA⁺ and MNAH, **B** BNA⁺ and BNAH, **C** P2NA⁺ and P2NAH, and **D** P3NA⁺ and P3NAH (molecular structures were optimized using the DFT method pBD-DN* starting from the lowest energy conformer 6-31G* structure).^[1]

S2. Determination of rate constants (k) of deactivation in 100 mM Tris-HCl pH 8 with different variations.

	k min^{-1}			
	MNAH	BNAH	P2NAH	P3NAH
without treatment	$8.20 \cdot 10^{-4}$ $\pm 0.19 \cdot 10^{-4}$	$9.15 \cdot 10^{-4}$ $\pm 0.79 \cdot 10^{-4}$	$6.79 \cdot 10^{-4}$ $\pm 0.06 \cdot 10^{-4}$	$7.91 \cdot 10^{-4}$ $\pm 0.19 \cdot 10^{-4}$
degassed	$10.27 \cdot 10^{-4}$ $\pm 0.70 \cdot 10^{-4}$	$8.63 \cdot 10^{-4}$ $\pm 1.52 \cdot 10^{-4}$	$7.72 \cdot 10^{-4}$ $\pm 1.53 \cdot 10^{-4}$	$7.41 \cdot 10^{-4}$ $\pm 1.48 \cdot 10^{-4}$
DTT	$30.79 \cdot 10^{-4}$ $\pm 1.39 \cdot 10^{-4}$	$23.79 \cdot 10^{-4}$ $\pm 0.73 \cdot 10^{-4}$	$12.66 \cdot 10^{-4}$ $\pm 0.84 \cdot 10^{-4}$	$31.67 \cdot 10^{-4}$ $\pm 0.56 \cdot 10^{-4}$
NaCl	$8.94 \cdot 10^{-4}$ $\pm 0.80 \cdot 10^{-4}$	$7.69 \cdot 10^{-4}$ $\pm 1.51 \cdot 10^{-4}$	$6.84 \cdot 10^{-4}$ $\pm 0.50 \cdot 10^{-4}$	$7.49 \cdot 10^{-4}$ $\pm 0.15 \cdot 10^{-4}$
CaCl ₂	$7.80 \cdot 10^{-4}$ $\pm 0.30 \cdot 10^{-4}$	$7.91 \cdot 10^{-4}$ $\pm 0.38 \cdot 10^{-4}$	$7.88 \cdot 10^{-4}$ $\pm 1.56 \cdot 10^{-4}$	$9.29 \cdot 10^{-4}$ $\pm 3.26 \cdot 10^{-4}$



S3. Cyclic voltammograms of natural and biomimetic cofactors.

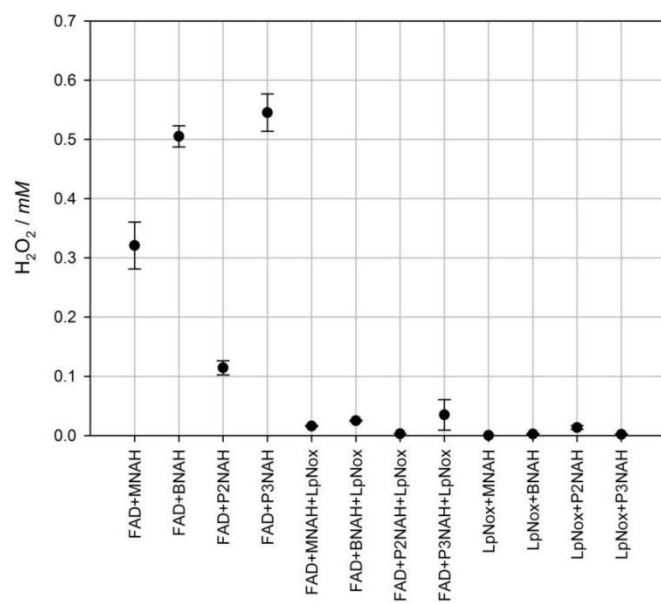
S4. Cathodic and anodic potentials of the natural and biomimetic cofactors and peak current ratios.

	$E_{p,cathodic}$ <i>mV</i> vs NHE	$E_{p,anodic}$ <i>mV</i> vs NHE	$-I_{p,a}/I_{p,c}$
MNA ⁺ /MNAH	-369 ± 2	-238 ± 2	0.16 ± 0.02
BNA ⁺ /BNAH	-339 ± 1	-227 ± 1	0.26 ± 0.06
P2NA ⁺ /P2NAH	-381 ± 1	-249 ± 3	0.44 ± 0.05
P3NA ⁺ /P3NAH	-384 ± 1	-202 ± 8	0.65 ± 0.06
NAD ⁺ /NADH	-479 ± 5	-325 ± 7	0.83 ± 0.01
NADP ⁺ /NADPH	-590 ± 2	-309 ± 2	0.94 ± 0.01

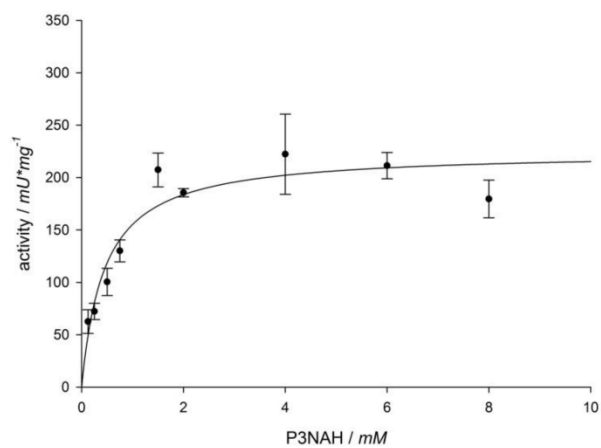
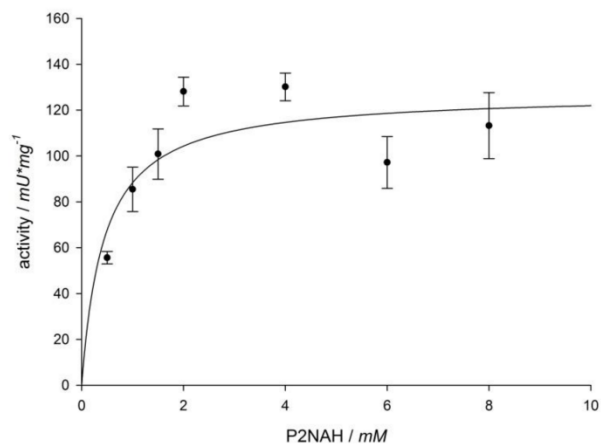
S5. Comparison of various redox potentials of NAD⁺/NADH and NADP⁺/NADPH.

Redox potentials NAD ⁺ /NADH <i>mV</i>	Redox potentials NADP ⁺ /NADPH <i>mV</i>	Method	Reference
-320	-324	chemical equilibrium considerations	Burton <i>et. al.</i> 1953 ^[2]
	-283	chemical equilibrium considerations	Olson <i>et. al.</i> 1953 ^[3]
-323		chemical equilibrium considerations	Rodkey <i>et. al.</i> 1955 ^[4]
-362		Titration (pH 8.37)	Rodkey <i>et. al.</i> 1955 ^[4]
-318		chemical equilibrium considerations, interpolated to pH 7	Rodkey <i>et. al.</i> 1955 ^[4]
-308		electrochemical equilibrium considerations, interpolated to pH 7	Rodkey <i>et. al.</i> 1959 ^[b]
	-307	potentiometric titration, interpolated to pH 7	Rodkey <i>et. al.</i> 1959 ^[6]
-325 ± 7 ^[a]	-309 ± 2 ^[a]	cyclic voltammetry	current work

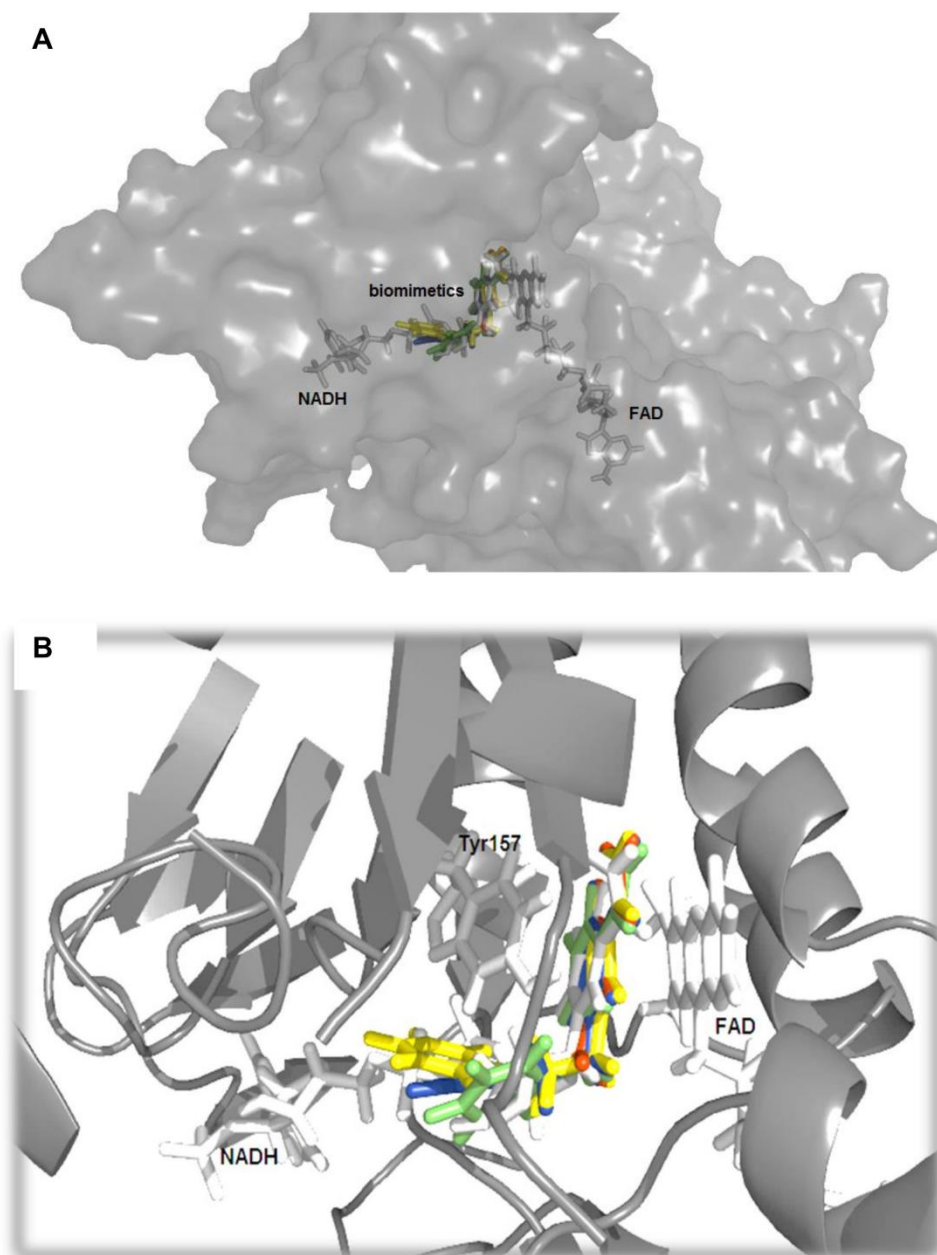
[a] anodic potentials



S6. Side product analyses of reactions of FAD and *LpNox* with biomimetic cofactors.



S7. Kinetic measurements of *LpNox* with the biomimetics P2NAH and P3NAH.



S8. Visualization of NADH, FAD and the biomimetic cofactors (MNAH: red, BNAH: green, P2NAH: blue, P3NAH: yellow) in the cofactor binding site of *LpNox* (**A**) including detailed view in the coordination of the dihydronicotinamide ring (**B**).

References

- [1] E. G. Lewars, *Computational Chemistry*, 2 ed., Springer Netherlands, **2011**.
- [2] K. Burton, T. H. Wilson, *Biochem. J.* **1953**, *54*, 86-94.
- [3] J. A. Olson, C. B. Anfinsen, *J. Biol. Chem.* **1953**, *202*, 841-856.
- [4] F. L. Rodkey, *J. Biol. Chem.* **1955**, *213*, 777-786.
- [5] F. L. Rodkey, *J. Biol. Chem.* **1959**, *234*, 188-190.
- [6] F. L. Rodkey, J. A. Donovan, *J. Biol. Chem.* **1959**, *234*, 677-680.

6.3 Supporting Information - Enzymatic Reduction of Nicotinamide Biomimetic Cofactors Using an Engineered Glucose Dehydrogenase: Providing a Regeneration System for Artificial Cofactors

Supporting Information

Enzymatic Reduction of Nicotinamide Biomimetic Cofactors Using an Engineered Glucose Dehydrogenase – Providing a Regeneration System for Artificial Cofactors

Claudia Nowak[†], André Pick[†], Petra Lommes[†], Volker Sieber^{†‡}*

[†]Technical University of Munich, Department of Life Science Engineering, Straubing Center of Science, Schulgasse 16, 94315 Straubing (Germany)

[‡] TUM Catalysis Research Center, Ernst-Otto-Fischer-Straße 1, 85748 Garching (Germany)

Table of Contents

Table S1. Sequence identity of different regeneration enzymes including glucose dehydrogenase from *Thermoplasma acidophilum* (TaGDH), glucose dehydrogenase *Bacillus megaterium* (BmGDH-IV), glucose-6-phosphate dehydrogenase from *Saccharomyces cerevisiae* (G6PDH), formate dehydrogenase from *Candida boidinii* (FDH), and glucose dehydrogenase E170K/Q252L from *Bacillus subtilis* (BsGDH E170K/Q252L) compared to SsGDH wild-type.

Figure S2. Nucleotide binding groove of the different regeneration enzymes with NAD(P)⁺: **A** glucose dehydrogenase from *Thermoplasma acidophilum* (TaGDH), **B** glucose dehydrogenase *Bacillus megaterium* (BmGDH-IV), **C** formate dehydrogenase from *Candida boidinii* (FDH), and **D** glucose dehydrogenase E170K/Q252L from *Bacillus subtilis* (BsGDH E170K/Q252L).

Table S3. Kinetic measurements of SsGDH wild-type and variants with NAD⁺, BNA⁺, P2NA⁺, and P3NA⁺: **A** SsGDH wild-type, **B** SsGDH Ile192Thr, **C** SsGDH Ile192Val, **D** SsGDH Val306Gly, **E** SsGDH Val306Ile, **F** SsGDH Ile192Thr/Val306Gly, and **G** SsGDH Ile192Thr/Val306Ile.

Table S4. Activity measurements of P450 BM-3 R966D/W1046S with oleic acid.

S5. Activity measurements of HLADH.

Table S6. Kinetic measurements of GstLDH with pyruvate/L-lactate and NADH/NAD⁺.

Figure S7. Half-life measurements of SsGDH Ile192Thr/Val306Ile.

S8. Experimental Section

Figure S9. NMR of **A** P2NA⁺, **B** P2NAH, **C** P3NA⁺, and **D** P3NAH.

Table S1. Sequence identity of different regeneration enzymes including glucose dehydrogenase from *Thermoplasma acidophilum* (*TaGDH*), glucose dehydrogenase *Bacillus megaterium* (*BmGDH-IV*), glucose-6-phosphate dehydrogenase from *Saccharomyces cerevisiae* (*G6PDH*), formate dehydrogenase from *Candida boidinii* (*FDH*), and glucose dehydrogenase E170K/Q252L from *Bacillus subtilis* (*BsGDH* E170K/Q252L) compared to *SsGDH* wild-type.

Enzyme	Sequence identity compared to <i>SsGDH</i>
<i>TaGDH</i>	35.5 %
<i>BmGDH-IV</i>	23.2 %
<i>G6PDH</i>	21.3 %
<i>FDH</i>	21.1 %
<i>BsGDH</i> E170K/Q252L	20.6 %

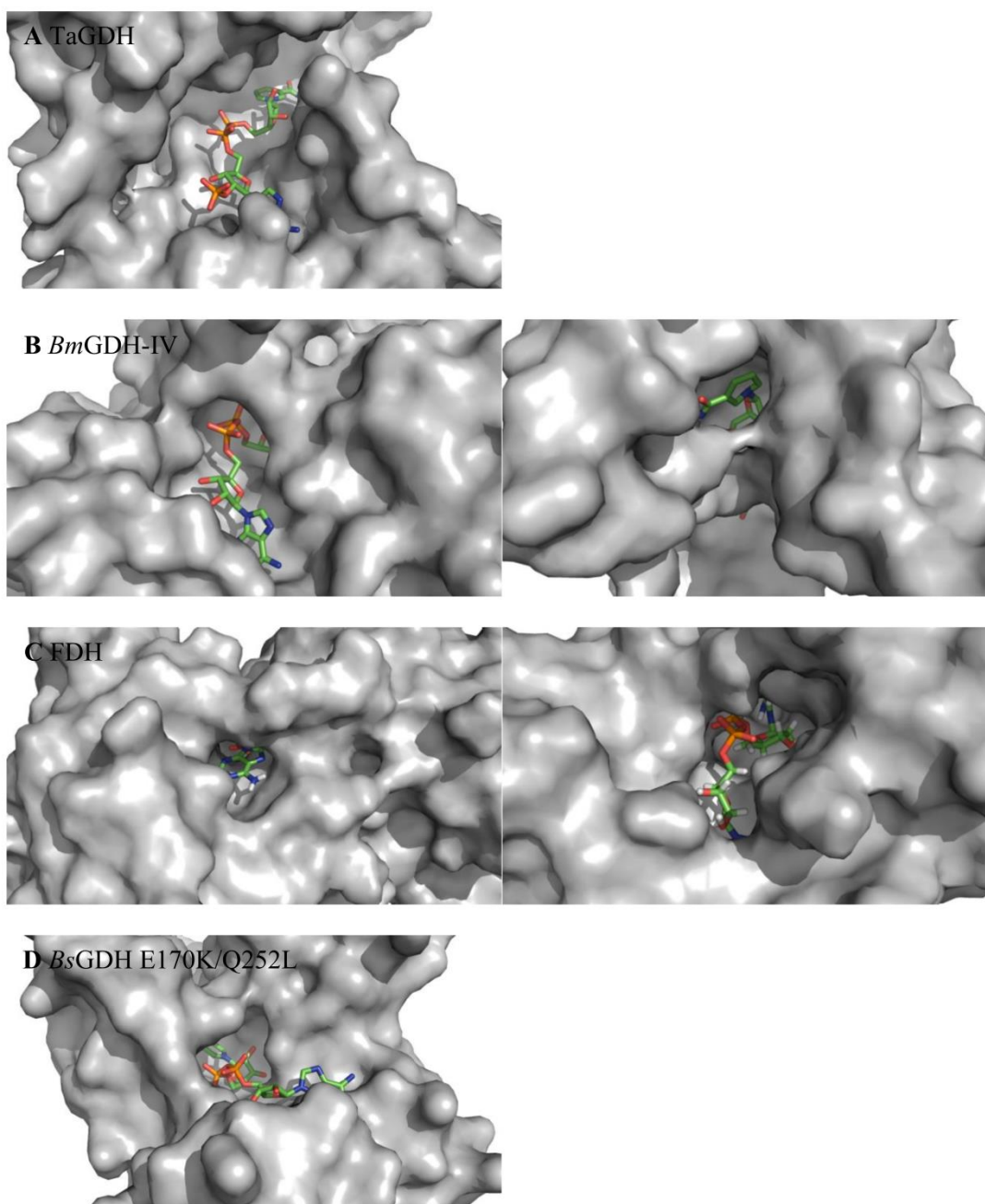
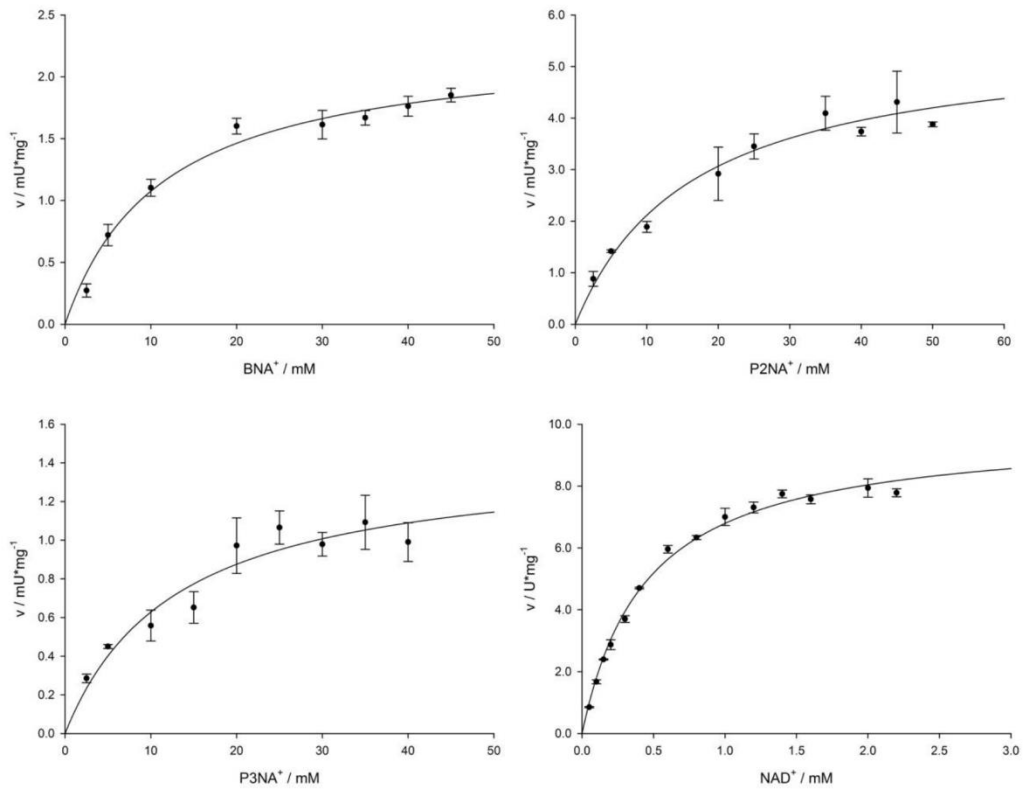
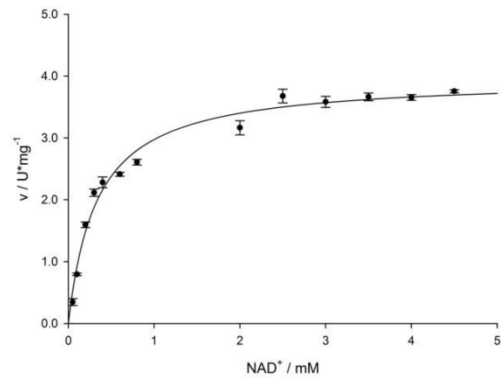
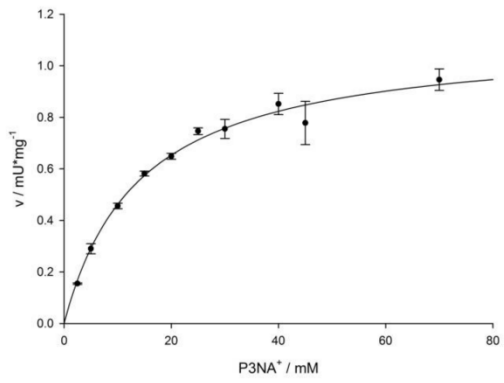
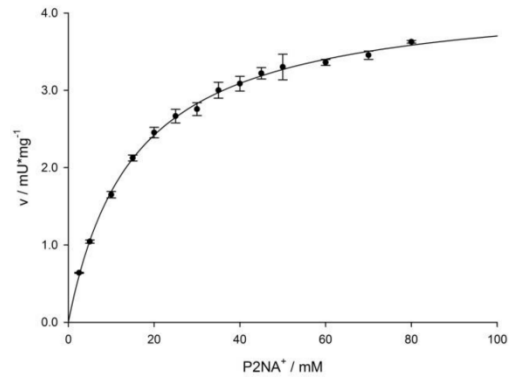
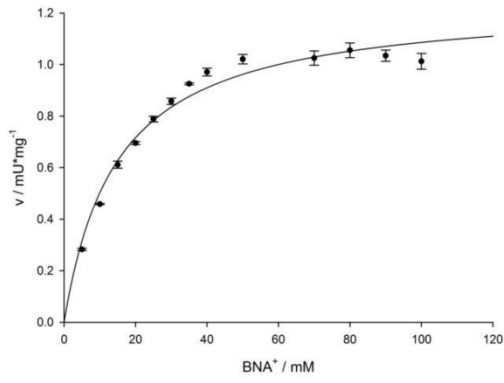


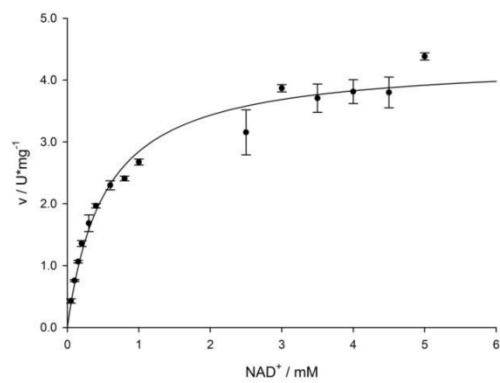
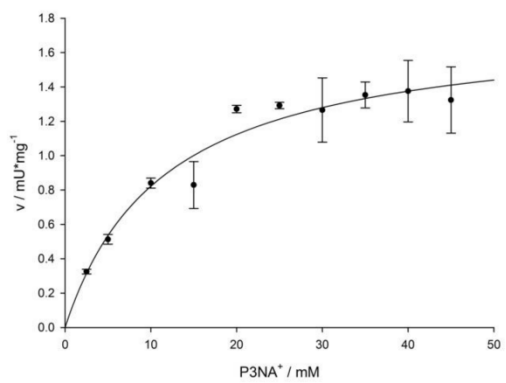
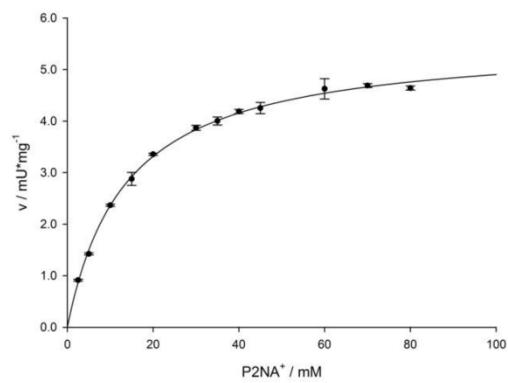
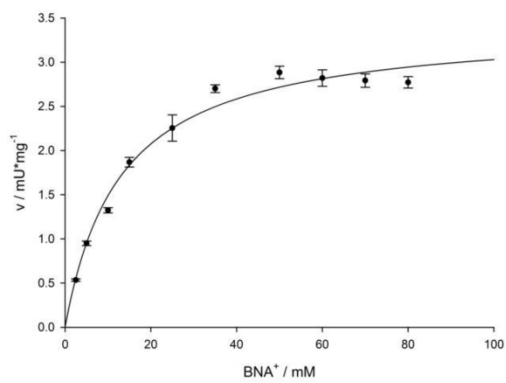
Figure S2. Nucleotide binding groove of the different regeneration enzymes with NAD(P)⁺: **A** glucose dehydrogenase from *Thermoplasma acidophilum* (*TaGDH*), **B** glucose dehydrogenase *Bacillus megaterium* (*BmGDH-IV*), **C** formate dehydrogenase from *Candida boidinii* (*FDH*), and **D** glucose dehydrogenase E170K/Q252L from *Bacillus subtilis* (*BsGDH E170K/Q252L*).

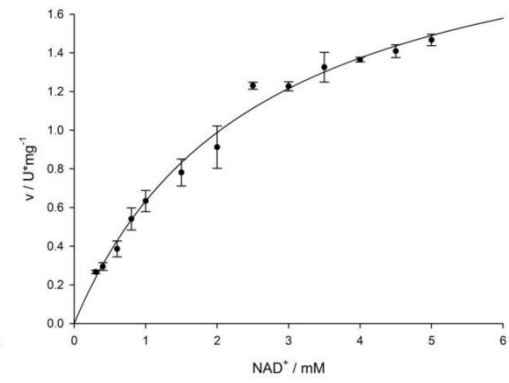
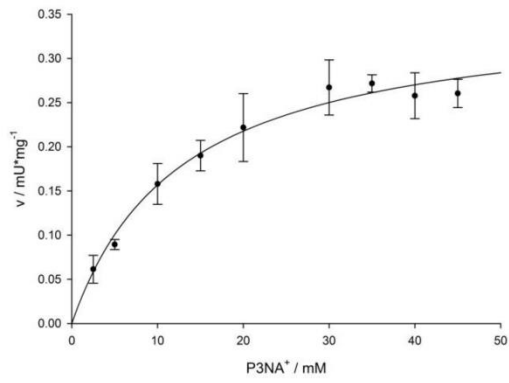
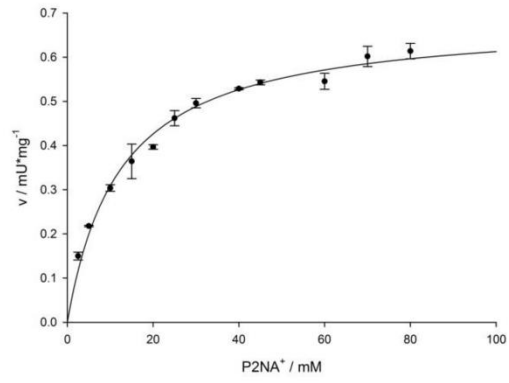
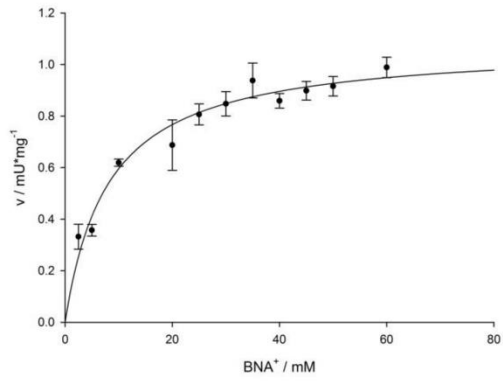
A SsGDH wild-type

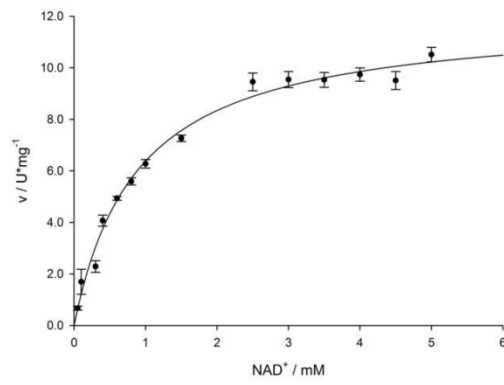
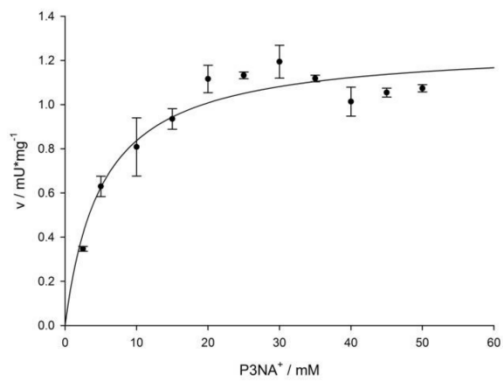
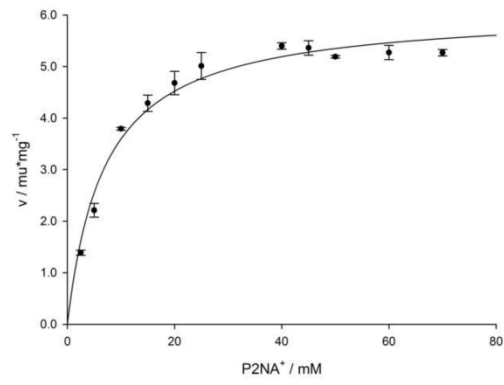
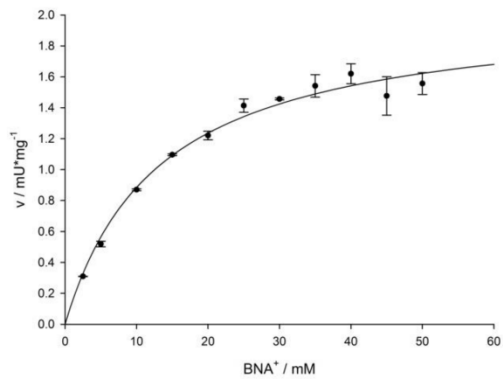


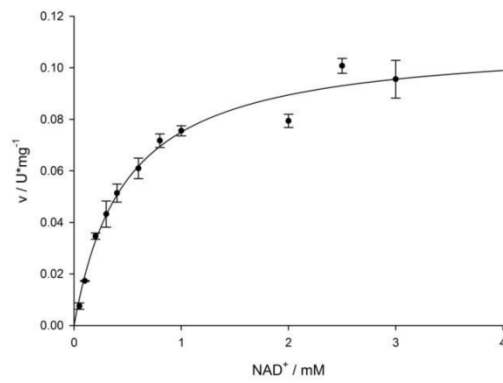
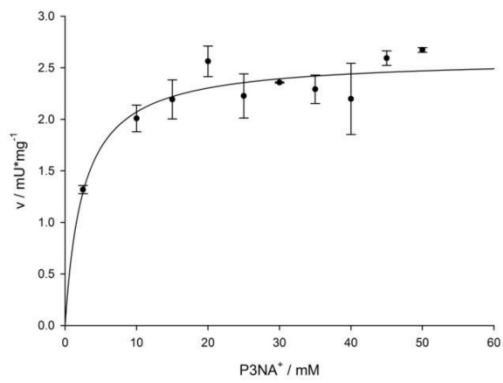
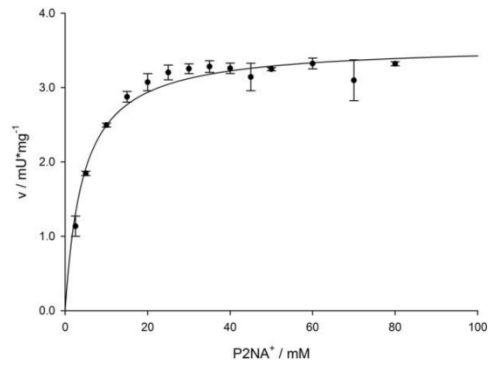
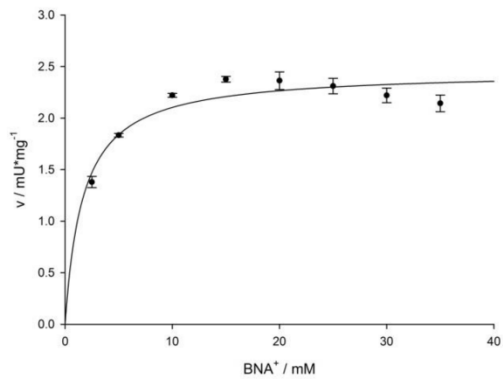
B *Ss*GDH Ile192Thr

C SsGDH Ile192Val



D *Ss*GDH Val306Gly

E *Ss*GDH Val306Ile

F *Ss*GDH Ile192Thr/Val306Gly

G *SsGDH* Ile192Thr/Val306Ile

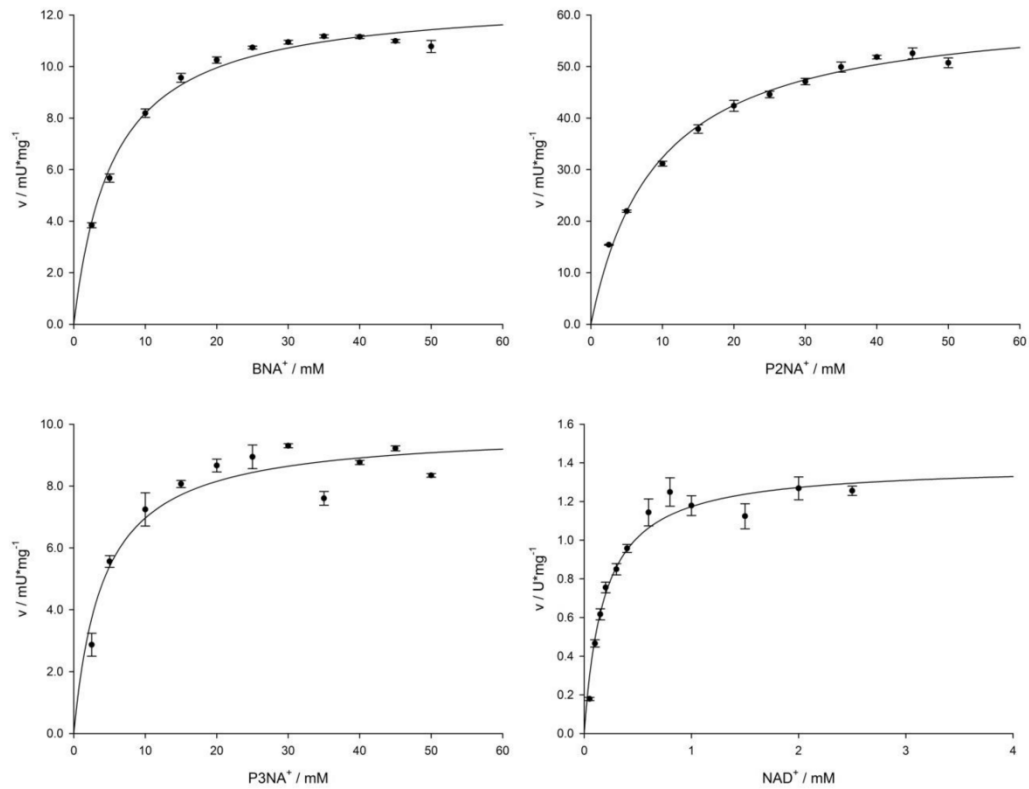


Figure S3. Kinetic measurements of *SsGDH* wild-type and variants with NAD^+ , BNA^+ , P2NA^+ , and P3NA^+ : **A** *SsGDH* wild-type, **B** *SsGDH* Ile192Thr, **C** *SsGDH* Ile192Val, **D** *SsGDH* Val306Gly, **E** *SsGDH* Val306Ile, **F** *SsGDH* Ile192Thr/Val306Gly, and **G** *SsGDH* Ile192Thr/Val306Ile.

Additional discussion:

The mutations of Asn211, Arg212 and Lys354 let to decreased enzyme activities with the present biomimetics. Hence, the access to the inner cofactor binding site may have been changed to such an extent that the cofactor cannot be coordinated properly. Additionally, Asp154 substitution resulted in inactive variants. Because this amino acid is in the catalytic domain but is

close to the cofactor, structural changes may disturb the connection between substrate and cofactor. Even though Pro191 is in the GXGXXG motif next to Ile192, which mutation resulted in variants with higher activity, no Pro191 variants were an improvement on the wild-type enzyme. Finally, the distance between Pro191 and the biomimetic was increased compared to that of Ile192, potentially resulting in interactions with lower influences.

Additionally, the activities of double mutants with NAD^+ were lowest, which could be expected due to the major structural differences between cofactor molecules. K_m values for NAD^+ and the variants *SsGDH* Val306Gly and *SsGDH* Val306Ile were greater than that of the wild-type enzyme. Interestingly, K_m values for double mutants were again decreased to wild-type levels for *SsGDH* Ile192Thr/Val306Gly and even further to smaller values for *SsGDH* Ile192Thr/Val306Ile showing antagonistic influences of the mutations.

Table S4. Activity measurements of P450 BM-3 R966D/W1046S with oleic acid.

Ryan *et al.* showed that the double mutant P450 BM-3 R966D/W1046S converted p-nitrophenoxydecanoic acid while oxidizing BNAH.¹ Subsequently, we attempted to transfer this activity to the substrate oleic acid and use P2NAH as a cofactor. However, whereas conversion of P2NAH was observed photometrically, no reduction of the substrate was detected in GC analyses. Therefore, we assumed that the enzyme was almost completely uncoupling with the cofactor P2NAH. The table shows the substrate concentrations after 75 min of reaction time.

Cofactor	Remaining oleic acid ^[a] [mM]	Remaining oleic acid ^[b] [mM]
BNAH	0.09 ± 0.002	0.28 ± 0.01
P2NAH	0.36 ± 0.03	0.39 ± 0.01
NADH	0.03 ± 0.01	0.23 ± 0.01

[a] reaction conditions: 0.4 mM oleic acid, 0.6 mM cofactor;

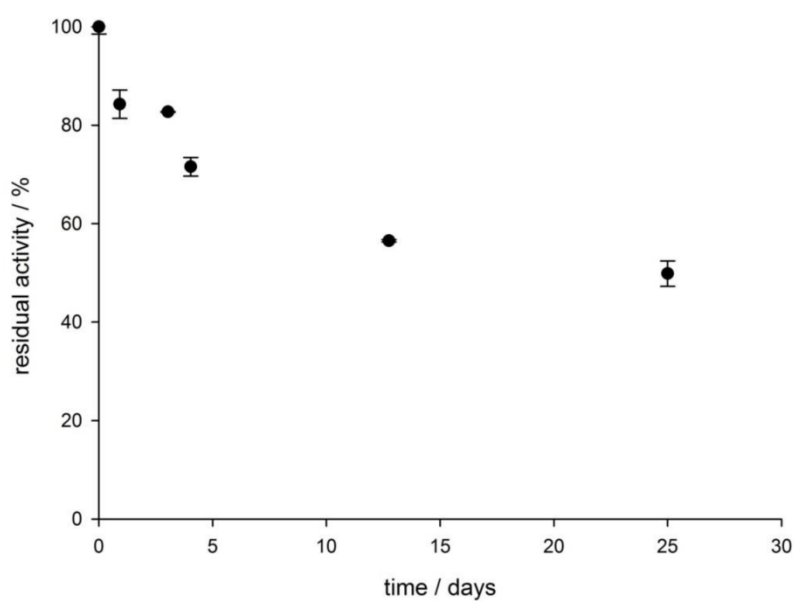
[b] reaction conditions: 0.4 mM oleic acid, 0.2 mM cofactor

S5. Activity measurements of HLADH.

The presence of natural nicotinamide cofactors in even purified preparations of dehydrogenases is a known phenomenon. Schirwitz *et al*, for example, demonstrated that NAD^+ was present in approximately 50 % of formate dehydrogenase preparations (from *Candida boidinii*) after purification, which could only be removed by extensive washing with 2 M NaCl.² Accordingly, horse liver alcohol dehydrogenase (HLADH) had been earlier described to efficiently convert BNA/H with various substrates.³ In a first approach for cofactor regeneration, *Ts*ER, 2-methylbut-2-enal, HLADH, propan-2-ol, and BNA^+ were combined. We had to discover, that the negative control, where the biomimetic was omitted, also showed product formation (data not shown). Hence, we investigated activity of HLADH in detail with 2-pentanol/2-pentanone. Reaction conditions were analogous with Lo *et al*. but neither the oxidation of 2-pentanol nor the reduction of 2-pentanone could be detected. The decrease of absorption in the reduction reaction was similar to the instability of the reduced biomimetic cofactor under these reaction conditions. These results have also been proven before by Paul *et al*.⁴ Only little information on the enzyme preparation of Lo *et al*. is known and the false positive results may be attributed to impurities with natural nicotinamide cofactor in the enzyme preparation. In the reaction/regeneration process only low concentrations of natural cofactor is necessary to feign activity, since it is recycled constantly and with high efficiency.

Table S6. Kinetic measurements of *Gst*LDH with pyruvate/L-lactate and NADH/NAD⁺.

	K_m [mM]	v_{max} [U*mg ⁻¹]	k_{cat} [s ⁻¹]	k_{cat}/K_m [mM ⁻¹ *s ⁻¹]
Pyruvate	6.1 ± 0.8	156.3 ± 5.8	90.6 ± 3.4	14.9 ± 2.5
L-Lactate	99.6 ± 3.7	7.4 ± 0.1	4.3 ± 0.1	4.3*10 ⁻² ± 0.2*10 ⁻²
NADH	0.6 ± 0.1	195.2 ± 8.3	113.2 ± 4.8	188.7 ± 34.6
NAD	1.3 ± 0.1	5.6 ± 0.1	3.3 ± 0.1	2.5 ± 0.3

**Figure S7.** Half-life measurements of SsGDH Ile192Thr/Val306Ile.

S8. Experimental Section

S8.1 Reagents

All chemicals were purchased from Sigma-Aldrich, Merck, or Carl Roth. All columns used for protein purification were from GE Healthcare (Munich, Germany). *Pfu*Ultra High-fidelity DNA polymerase was obtained from Agilent (Waldbronn, Germany) and DNaseI was from Serva (Heidelberg, Germany). Oligonucleotides were synthesized by biomers.net (Ulm, Germany). The commercially available enzymes formate dehydrogenase from *Candida boidinii* (product number F8649), glucose dehydrogenase from *Thermoplasma acidophilum* (product number G5909), glucose-6-phosphate dehydrogenase from *Saccharomyces cerevisiae* (product number G6378), and horse liver alcohol dehydrogenase (product number 55689) were also obtained from Sigma-Aldrich.

S8.2 Synthesis of Oxidized and Reduced Biomimetics

The synthetic procedures were adapted from former procedures.⁵⁻⁶ MNA/H and BNA/H were synthesized as described previously.⁷

P2NA⁺⁸: Nicotinamide (40 mmol) was dissolved in 40 mL acetonitrile and heated to reflux. Subsequently, 40 mmol (2-chloroethyl)benzene was added, and the reaction mixture was stirred under reflux for 115 h. After cooling to room temperature, 50 mL of diethyl ether was added, and the precipitate was filtered and washed twice with diethyl ether. The product was purified using soxhlet extraction with ethyl acetate. C₁₄H₁₅ClN₂O; white solid; yield: 31 %; ¹H NMR (400 MHz, D₂O) δ 8.9 (s, 1H), 8.7 (d, 1H), 8.6 (d, 1H), 7.9 (d, 1H), 7.2 (m, 3H), 7.0 (m, 2H), 4.8 (t, 2H), 3.2 (t, 2H).

P3NA⁺⁹: Nicotinamide (40 mmol) was dissolved in 50 mL acetonitrile while heating to reflux. Subsequently, (3-bromopropyl)benzene (40 mmol) was added, and the reaction mixture was stirred under reflux for 67 h. After cooling to room temperature, 50 mL diethyl ether was added, and the precipitate was filtered and washed twice with diethyl ether. C₁₅H₁₇BrN₂O; white solid; yield: 82 %; ¹H NMR (400 MHz, DMSO) δ 9.5 (s, 1H), 9.3 (d, 1H), 8.9 (d, 1H), 8.6 (s, 1H), 8.2 (m, 2H), 7.2 (m, 5H), 4.7 (t, 2H), 2.6 (m, 2H), 2.3 (m, 2H).

P2NAH/P3NAH⁸⁻⁹: P2NA⁺ (2.8 mmol)/P3NA⁺ (2.7 mmol) was dissolved in 250 mL of water at 40 °C under an argon atmosphere. Sodium carbonate (24 mmol) and sodium bicarbonate (30 mmol) were then added to the reaction mixture, sodium dithionite (14 mmol) was added in portions, and the mixture was stirred for another 30 min at 40 °C. Cooling to room temperature resulted in an oily liquid. The crude product was extracted three times with dichloromethane, combined organic phases were washed once with water and dried over sodium sulphate and the solvent was removed by rotary evaporation. P2NAH C₁₄H₁₆N₂O; yellow solid; yield: 71 %; ¹H NMR (400 MHz, CDCl₃) δ 7.2 (m, 5H), δ 7.0 (s, 1H), 5.6 (m, 1H), 5.2 (s, 2H), 4.7 (m, 1H), 3.3 (t, 2H), 3.1 (m, 2H), 2.8 (t, 2H); P3NAH C₁₅H₁₈N₂O; yellow solid, yield: >99 %; ¹H NMR (400 MHz, CDCl₃) δ 7.2 (m, 6H), 5.7 (m, 1H), 5.5 (s, 2H), 4.7 (m, 1H), 3.1 (m, 4H), 2.6 (m, 2H), 1.8 (m, 2H).

S8.3 Strains, Plasmids, and Expression

Plasmid construction (pCBR-CHis-SsGDH) for SsGDH was generated preciously.¹⁰ For the preparation of genomic DNA from *Bacillus megaterium* DSM 319, *Bacillus subtilis* DSM 402 and *Geobacillus stearothermophilus* ATCC 7953 the protocol of Saha *et al.* was used.¹¹ The gene encoding for gdhIV of *Bacillus megaterium* (BmGDH-IV) was cloned into pET22b with a

C-terminal His-tag (GenBank™ BAA01476.1).¹² The gene of the glucose dehydrogenase of *Bacillus subtilis* (*BsGDH*) was cloned into pACYC-Duet1 without any His-tag. Subsequently, two substitutions were introduced using QuikChange® Site-Directed Mutagenesis and the variant *BsGDH* E170K/Q252L described by Vázquez-Figueroa *et al.* was generated.¹³ The gene encoding for P450 BM-3 R966D/W1046S was cloned into a pET28a vector and the two substitutions were introduced using QuikChange® Site-Directed Mutagenesis.¹⁴ The gene encoding lactate dehydrogenase of *Geobacillus stearothermophilus* (*GstLDH*) was cloned into a pET28a vector with an N-terminal His-tag.¹⁵ *E.coli* BL21 (DE3) was transformed with the generated constructs.

Expression was done using the same protocol. A preculture was done in 150 mL of LB medium containing 30 $\mu\text{g}\cdot\text{mL}^{-1}$ kanamycin (*SsGDH*, *BmGDH-IV*, *GstLDH*) or 34 $\mu\text{g}\cdot\text{mL}^{-1}$ chloramphenicol (*BsGDH* E170K/Q252L) at 37 °C overnight. Expression culture was inoculated 1:100 into 1 L Zym5052 medium¹⁶ containing 100 $\mu\text{g}\cdot\text{mL}^{-1}$ kanamycin (*SsGDH*, *BmGDH-IV*, *GstLDH*) or 34 $\mu\text{g}\cdot\text{mL}^{-1}$ chloramphenicol (*BsGDH* E170K/Q252L) and was incubated for 24 h at 37 °C. Cells were harvested by centrifugation.

To express P450 BM-3 R966D/W1046S construct, cells were pre-cultured in 50 mL of LB medium with 30 $\mu\text{g}\cdot\text{mL}^{-1}$ kanamycin at 37 °C overnight. The expression culture (1 L LB medium containing 30 $\mu\text{g}\cdot\text{mL}^{-1}$ kanamycin) was inoculated to OD₆₀₀ of 0.1, incubated at 37 °C, and was then induced at OD₆₀₀ of 0.6 with 0.25 mM isopropyl β -D-1-thiogalactopyranoside (IPTG). Subsequently, cultures were incubated at 16 °C overnight and cells were harvested by centrifugation.¹⁷

The vector containing enoate reductase from *Thermus scotoductus* (*TsER*)¹⁸ was a kind gift from Dr. Diederik J. Opperman. For expression a preculture of transformed *E.coli* BL21 (DE3)

containing *TsER* was done in 25 mL of LB medium containing $100 \mu\text{g}\cdot\text{mL}^{-1}$ ampicillin. The expression culture was then inoculated to OD_{600} of 0.1 in 1 L LB medium containing $100 \mu\text{g}\cdot\text{mL}^{-1}$ ampicillin at 37°C . At OD_{600} 0.6 cells were induced with 1 mM IPTG and were incubated for an additional 4 h at 37°C . Cells were harvested by centrifugation.

S8.4 Purification

Harvested cells containing *SsGDH* or *BmGDH-IV* were resuspended in 100 mM HEPES containing 20 mM imidazole pH 7.4 (binding buffer). After incubation with 2.5 mM MgCl_2 and $10 \mu\text{g}\cdot\text{mL}^{-1}$ DNaseI for 20 min, cells were disrupted using a Basic-Z Cell Disrupter (IUL Constant Systems). Cell debris was then removed by centrifugation at 4°C for 1 h at 20000 rpm, and the supernatant of *SsGDH* or *BmGDH-IV* was applied to an IMAC affinity resin column 5 mL HisTrapTM FF. After washing with binding buffer, the target protein was eluted with 70 % 100 mM HEPES containing 500 mM imidazole pH 7.4. The eluted protein was desalted using a HiPrepTM 26/10 desalting column with 100 mM HEPES pH 7.4.

Purification of P450 BM-3 R966D/W1046S was performed using the same procedure with 50 mM potassium phosphate pH 7.5 containing 300 mM sodium chloride as the binding buffer, 50 mM potassium phosphate pH 7.5 containing 300 mM sodium chloride and 500 mM imidazole as elution buffer and 50 mM potassium phosphate pH 7.5 as the desalting buffer. Proteins were eluted with 40 % elution buffer.¹⁷ For purification of *GstLDH*, 20 mM Tris-HCl pH 8 containing 20 mM imidazole as binding buffer, 20 mM Tris-HCl pH 8 containing 500 mM imidazole as elution buffer (70 % for elution), and 20 mM Tris-HCl pH 8 for desalting was used.¹⁹

The harvested cells containing *BsGDH* E170K/Q252L were resuspended in 100 mM HEPES pH 7.4. After cell disruption (as described above), the lysate was incubated at 70°C for 1 h.

Afterwards 2.5 mM MgCl₂ and 10 μg*mL⁻¹ DNaseI were added and incubated for 20 min at room temperature. The insoluble fraction was removed by centrifugation (40 min, 4 °C, 20000 rpm) and the supernatant was applied to the HiPrep™ 26/10 column using 100 mM HEPES pH 7.4 buffer.

Harvested *TsER* cell were resuspended in 50 mM MOPS-NaOH²⁰ pH 7 containing 5 mM NaCl. Cells were then disrupted with ultrasonication and the solution was incubated at 70 °C for 30 min. After centrifugation at 4 °C for 1 h at 20000 rpm, supernatant containing *TsER* was subjected to gel filtration using HiPrep™ 26/10 desalting column with 50 mM MOPS-NaOH pH 7 containing 5 mM NaCl.

Aliquots of purified proteins were subjected to 12 % SDS gel electrophoresis,²¹ and protein concentration of *SsGDH* was determined photometrically (Nanophotometer, Implen) with the following parameters: molecular weight 42.6 kDa, extinction coefficient 49.77 M⁻¹*cm⁻¹.²² Protein concentrations of the other enzymes were measured using Bradford assay (Roti®-nanoquant, Carl Roth).

S8.5 Activity Measurements of Different Recycling Enzymes

Activity measurements of formate dehydrogenase (0.7 mg*mL⁻¹) and different glucose dehydrogenases (0.1 mg*mL⁻¹) were carried out in 100 mM Tris-HCl pH 8 containing 5 mM NAD(P)⁺ or 50 mM oxidized biomimetic and 10 mM D-glucose or sodium formate, respectively. The activity of the glucose-6 phosphate dehydrogenase (2.5 U*mL⁻¹) was measured with 6.7 mM D-glucose 6-phosphate. Reactions were monitored at 358 nm (biomimetics) and 340 nm (NADH) for 1 h at 37 °C.

S8.6 Structural Comparison of Different Recycling Enzymes

Sequence alignment was done with PRALINE multiple sequence alignment tool²³ and Clustal-Omega²⁴⁻²⁵. The following sequences were used: *Ss*GDH (PDB: 2CDA), FDH (PDB: 5DN9), *Ta*GDH (GenbankTM CAA42450.1), *Bm*GDH-IV (PDB: 3AUT), *Bs*GDH (NCBI: NP_388275), G6PDH (GenbankTM AAA34619.1). For structural modelling of *Ta*GDH and *Bs*GDH Phyre2²⁶ and for ligand binding 3DLigandSite²⁷ were used. Visualization was done with PyMol Molecular Graphics System, Schrödinger, LLC.

S8.7 Site Directed Mutagenesis

Positions for site directed mutagenesis were selected by evaluating of the data reported by Milburn *et al.*²⁸ and by docking of *Ss*GDH (PDB: 2CDA) with biomimetic cofactors (energy minimized with Chem3DPro 12.0) using YASARA version 13.9.8 (standard macro: dock_run; www.yasara.org). Docking was performed over the whole protein and within a 5 Å simulation cell around Phe279. Visualization was performed using PyMol Molecular Graphics System, Schrödinger, LLC.

A modification of QuikChangeTM Site Directed Mutagenesis was performed as described by Wang *et al.*²⁹ All primers are listed below. To construct mutagenesis libraries, two separate PCRs (each 50 µL) were prepared with forward primer and reverse primer, respectively: 50 ng of template plasmid DNA, 3 U of *Pfu*Ultra High-fidelity DNA polymerase, 5 µL of 10x *Pfu* buffer, 1 µL of dNTPs (each 10 mM), and 8 µL of 10 mM primer. PCR was run at 95 °C for 3 min, followed by four cycles at 95 °C for 45 s, 55 °C for 60 s, and 72 °C for 380 s. Subsequently, 25 µL of each PCR mixture were combined, and 3 U of *Pfu*Ultra High-fidelity DNA polymerase were added for further 18 cycles of PCR under the same conditions. Afterwards 25 µL PCR

reactions were incubated with 20 U *DpnI* at 37 °C for 1.5 h. Chemically competent *E.coli* NEB Turbo were then transformed with 10 µL of digested PCR mixtures. The high quality of generated libraries was verified by sequencing three clones per library (GATC Biotech, Cologne, Germany). Colonies were washed from LB-agar plates (at least 100 for each library) with 2 mL of LB medium. After centrifugation (5 min, 13.000 rpm), pellets were used for plasmid extraction with GeneJET Plasmid Miniprep Kit (ThermoFisher Scientific).

Double mutants were created according to the procedure described above using pCBR-CHis-SsGDH Ile192Thr as a template.

Primer name	Sequence 5' → 3'
Asp154_forward	CTGGCACAGCCGCTGGCANN K ATTGAAAAATCCATTGAAG
Asp154_reverse	CTTCAATGGATTTTTCAATM N NTGCCAGCGGCTGTGCCAG
Pro191_forward	CTGGTTGTTGGCACCGGT N NKATTGGTGTCTGTTTACC
Pro191_reverse	GGTAAACAGAACACCAATM N NACCGGTGCCAACAACCAG
Ile192_forward	GGTTGTTGGCACCGGTCCG N NKGGTGTCTGTTTACCCTGC
Ile192_reverse	GCAGGGTAAACAGAACACCM N NCGGACCGGTGCCAACAACC
Asn211_forward	GGAAGTTTGGATGGCANN K CGTCGTGAACCGACCG
Asn211_reverse	CGGTCCGTTACGACGM N NTGCCATCCAAACTTCC
Arg212_forward	GGAAGTTTGGATGGCAAAT N NKCGTGAACCGACCGAAGTTG
Arg212_reverse	CAACTTCGGTCGGTTCACGM N NATTTGCCATCCAAACTTCC
Val306_forward	CCATTATTGGCCTG N NKAATGGTCAGAAACCGCATTTTC
Val306_reverse	GAAAATGCGGTTTCTGACCATTM N NCAGGCCAATAATGG
Lys354_forward	GCTGAAAGTGCTGCGTGA N NKGAACATGGCGAAATC
Lys354_reverse	GATTTCGCCATGTT C M N NTTACGCAGCACTTTCAGC

Val306Gly_forward	CCATTATTGGCCTGGGCAATGGTCAGAAACCGCATTTTC
Val306Gly_reverse	GAAAATGCGGTTTCTGACCATTGCCAGGCCAATAATGG
Val306Ile_forward	CCATTATTGGCCTGATTAATGGTCAGAAACCGCATTTTC
Val306Ile_reverse	GAAAATGCGGTTTCTGACCATTAATCAGGCCAATAATGG

S8.8 Screening

Electro competent *E.coli* BL21 (DE3) cells were transformed with mutagenesis libraries. Single colonies were transferred into 96 deep-well plates containing 1.2 mL LB and 30 $\mu\text{g}\cdot\text{mL}^{-1}$ kanamycin and were then incubated at 37 °C for 20 h. Expression cultures containing 1.2 mL Zym5052 medium¹⁶ with 100 $\mu\text{g}\cdot\text{mL}^{-1}$ kanamycin were inoculated with 120 μL of preculture and were then incubated for 24 h at 37 °C. Additionally, 50 μL aliquots of precultures were mixed with 50 μL of 60 % glycerol and were stored at -80 °C. Activity assays were performed with 200 μL aliquots of the expression cultures after transfer to a 96 well U-bottom microtiter plate. After centrifugation (15 min, 4 °C, 4000 rpm), the supernatants were discarded, and the cells were frozen at -20 °C. Pellets were resuspended in 100 μL of cell-lysis solution (2.5 $\text{mg}\cdot\text{mL}^{-1}$ lysozyme, and 0.1 $\text{mg}\cdot\text{mL}^{-1}$ DNaseI in 100 mM Tris-HCl pH 8) and were incubated at 37 °C for 2 h. After heat incubation in a water bath (70 °C for 30 min), disrupted cells were centrifuged at 4 °C for 30 min at 4000 rpm. Measurements of photometric activity were performed at 358 nm for 1 h at 45 °C following the addition of 70 μL of supernatant to 130 μL master mixes containing 77 mM BNA⁺ or P2NA⁺ and 3.1 mM D-glucose in 100 mM Tris-HCl pH 8. Analyses were performed by calculating increases of absorption over time. Variants with residual activity greater than the wild-type enzyme plus standard deviation were considered hits. Prior to mutagenesis library screening, evaluations of wild-type landscape were

performed by calculating of the Z' factors.³⁰ Controls included empty vector controls, medium controls, and wild-type controls.

S8.9 Determination of Extinction Coefficients

Various concentrations of reduced biomimetic cofactor were weighed-in, diluted in DMSO, and measured at 358 nm in cuvettes (in triplicate). The following extinction coefficients of biomimetics were determined: MNAH, $\epsilon=5.9 \text{ L}\cdot\text{mmol}^{-1}\cdot\text{cm}^{-1}$; BNAH, $\epsilon=7.4 \text{ L}\cdot\text{mmol}^{-1}\cdot\text{cm}^{-1}$; P2NAH, $\epsilon=3.9 \text{ L}\cdot\text{mmol}^{-1}\cdot\text{cm}^{-1}$; and P3NAH, $\epsilon=8.3 \text{ L}\cdot\text{mmol}^{-1}\cdot\text{cm}^{-1}$.

S8.10 Kinetic Parameters

Kinetic measurements of wild-type *SsGDH* and variants were performed in 100 mM Tris-HCl pH 8 with 5 mM D-glucose and varying cofactor concentrations at 45 °C for 60 min. Data were fitted to Michaelis-Menten equations using SigmaPlot 11.0. (Systat Software). All measurements were performed in triplicate. Controls lacked enzyme, D-glucose, or cofactor. One unit of enzyme activity was defined as the amount of protein that oxidized 1 μmol of cofactor/min at 45 °C.

S8.11 Detection of Reaction Products of *SsGDH*

HPLC product analyses (gluconate) were performed as described by Guterl *et al.*¹⁰

S8.12 Measurement of Half-life of *Ss*GDH Ile192Thr/Val306Ile

Briefly, the enzyme (1.025 mg*mL⁻¹) was incubated in desalting buffer at 45 °C. Activity was measured in 100 mM Tris-HCl pH 8 containing 0.1025 mg*mL⁻¹ enzyme, 5 mM D-glucose, and 50 mM P2NA⁺ and reaction was monitored at 358 nm.

S8.13 Activity Measurements of P450 BM-3 R966D/W1046S

P450 BM-3 R966D/W1046S (0.057 mg*mL⁻¹) was incubated with 0.4 mM oleic acid and 0.6 mM NADH/BNAH/P2NAH or with 0.4 mM oleic acid and 0.2 mM NADH/BNAH/P2NAH in 100 mM Tris-HCl pH 8. DMSO concentrations were maintained at less than 5 %. Reactions were followed at 340 nm (NADH) and 358 nm (BNAH/P2NAH) and were incubated at 37 °C for 75 min. Controls lacked either enzyme or substrate. Extraction and measurement procedures were variations of an in-house protocol.³¹ 500 µL of the sample was acidified with 100 µL of 1 M HCl and 1 mL of tert-butyl methyl ether (MTBE) was added. Mixtures were then incubated for at least 1 h on a rocking shaker. After filtration of the organic layer, 150 µL aliquots of sample were derivatized using 50 µL N-methyl-N-(trimethylsilyl) trifluoroacetamide (MSTFA). Decreases in substrate concentrations were monitored using GC-FID and were quantified using X-calibur.

Compound	Description
GC	Trace GC Ultra, Thermo Fisher Scientific, USA Autosampler TriPlus Flame ionization detector (FID)

Column	Rxi®-5Sil MS (RESTEK) Length: 30 m Diameter: 0.25 mm Film thickness: 0.25 µm
Carrier gas	Helium, constant flow 0.8 mL*min ⁻¹
Oven	Start: 90 °C for 3.5 min Ramp / °C*min ⁻¹ ; end temperature / °C; hold time / min #1 45 °C*min ⁻¹ ; 220 °C; 2 min #2 45 °C*min ⁻¹ ; 280 °C, 2 min #3 60 °C*min ⁻¹ ; 330 °C, 1.5 min
Injector	Temperature: 340 °C Split: 16 mL*min ⁻¹ Injection volume: 4 µL
FID	Temperature: 340 °C

S8.14 Activity Measurements of *Ts*ER with Cyclohex-2-en-1-one

*Ts*ER (0.023 mg*mL⁻¹ for NADPH; 0.23 mg*mL⁻¹ for BNAH/P2NAH) was incubated with 10 mM cyclohex-2-en-1-one and 5 mM NADPH/BNAH/P2NAH in 100 mM Tris-HCl pH 8. DMSO concentrations were maintained at less than 5 %. The reaction was monitored at 340 nm for NADPH and was incubated for 45 min at 45 °C. The reaction mixture containing BNAH/P2NAH as a cofactor was incubated at 45 °C for 2.5 h. Controls lacked either enzyme or substrate. Samples (500 µL) were extracted using 3x1 mL MTBE and 200 µL aliquots of the organic layers were used for GC-MS measurements. Decreases of substrate concentrations and

increases in product concentrations were detected using GC-MS. To identify peaks, sample references and the National Institute of Standards and Technology (NIST) library were used.

Compound	Description
GC	Trace GC Ultra, Thermo Fisher Scientific, USA Autosampler TriPlus MS Trace DSQ
Column	BPX5 (SGE Analytical Science) Length: 30 m Diameter: 0.25 mm Film thickness: 0.25 μm
Carrier gas	Helium, constant flow 0.8 mL*min ⁻¹
Oven	Start: 50 °C for 5 min Ramp / °C*min ⁻¹ ; end temperature / °C; hold time / min #1 10 °C*min ⁻¹ ; 110 °C; 0 min #2 25 °C*min ⁻¹ ; 220 °C, 2 min
Injector	Temperature: 250 °C Split: 10 mL*min ⁻¹ Injection volume: 1 μL
FID	Temperature: 200 °C
MS	Transfer line: 250 °C Ion source: 250 °C Start time: 4 min

Ionization energy: 70 eV

Mass range: m/z 50-650

S8.15 Activity Measurements of *Ts*ER with 2-Mehtylbut-2-enal and Cinnamaldehyde

*Ts*ER (0.013 mg*mL⁻¹) was incubated with 10 mM 2-mehtylbut-2-enal and cinnamaldehyde, respectively, and 10 mM NADPH in 100 mM Tris-HCl pH 8. Reaction mixtures were incubated at 45 °C for 5 h. Controls lacked either enzyme or substrate and analyses was performed as described below.

S8.16 Detection of 2-Methylbutanal and 3-Phenylpropanal

2-Methylbutanal and 3-phenylpropanal were detected using LC-UV-ESI-MS/MS according to the protocol of Rühmann *et al.*³² Briefly, 25 µL reaction mixtures were added to 96-well-PCR microtiter plates with 75 µL of derivatization reagent (0.1 M methanolic-PMP-solution: 0.4 % ammonium hydroxide solution 2:1), and were mixed and sealed with a TPE cap mat. After centrifugation for 2 min at 2000 x g, plates were incubated at 70 °C for 100 min. Subsequently, 20 µL aliquots of cooled solution were transferred to a 96-well microtiter plate and 130 µL aliquots of 19.23 M acetic acid in 50 % methanol and 50 % water were added. Plates were then sealed using a 96-well silicon cap mats. Methodical variations from the protocol included temperature, gradient, mass, and retention time. Specifically, the temperature of the autosampler was set to 25 °C and the gradient was adapted to the products. The mobile phase B started at 5 %, was increased to 40 % within 5 min, and was then held for 2 min. The content of phase B was further increased to 50 % over 2 min, was held constant for 0.5 min, and was then decreased to 5 % over 0.3 min and was held for 2.2 min. The m/z value for 2-methylbutanal was 417 and

the retention time was 8.3 min. The m/z value for 3-phenylpropanal was 465 and the retention time was 8.6 min.

S8.17 Activity Measurements of Horse Liver Alcohol Dehydrogenase (HLADH)

HLADH activity was measured according to Lo *et al.*³ For the oxidation reaction 2 U/mL HLADH was incubated in 16 mM 2-pentanol and 16 mM oxidized cofactor in 100 mM potassium phosphate pH 7.0 at 37 °C. The reduction reaction was measured using 2 U/mL HLADH, 16 mM 2-pentanone, and 0.5 mM reduced cofactor in 100 mM potassium phosphate pH 7.0 at 37 °C. The reactions were monitored at 340 nm and 358 nm. Controls lacked enzymes, substrates or cofactor.

S8.18 Reaction-/Regeneration process

To convert 2-methylbut-2-enal, 0.025 mg*mL⁻¹ *TsER*, 0.36 mg*mL⁻¹ *SsGDH* Ile192Thr/Val306Ile, and 50 mM P2NA⁺ in 100 mM Tris-HCl pH 8 (degassed) were incubated for 1 h at 45 °C with shaking at 600 rpm. Subsequently, the substrates 2-methylbut-2-enal (10 mM) and 20 mM D-glucose were added, and the reaction progressed at 45 °C with shaking at 600 rpm. Samples were then taken within 12 h, and were directly derivatized and neutralized. In further experiments, reactions were repeated as described above with 10 mM pyruvate and 0.001 mg*mL⁻¹ *GstLDH* (added before pre incubation). Controls lacked enzymes, substrates or cofactor.

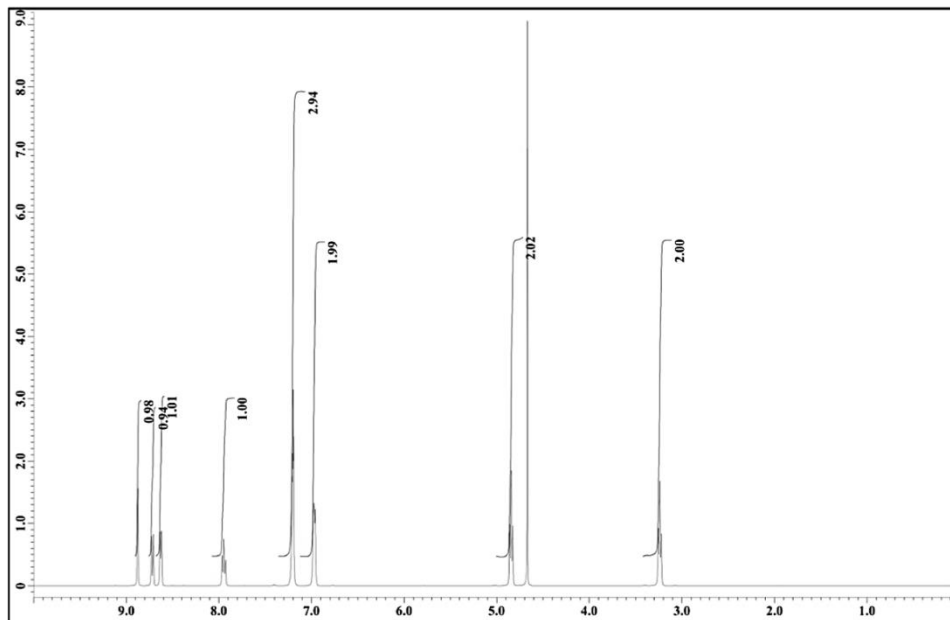
S8.19 Activity Measurement of *Gst*LDH with P2NA/H

The activity of *Gst*LDH with P2NA/H was measured using pyruvate and L-lactate. *Gst*LDH (0.317 mg*mL⁻¹) was incubated with 0.5 mM P2NAH and 10 mM pyruvate in 100 mM Tris-HCl pH 8. The activity of *Gst*LDH was measured with 50 mM P2NA⁺ and 10 mM L-lactate in 100 mM Tris-HCl pH 8. The reaction was monitored at 358 nm at 45 °C. Controls lacked the enzyme, substrate, or cofactor.

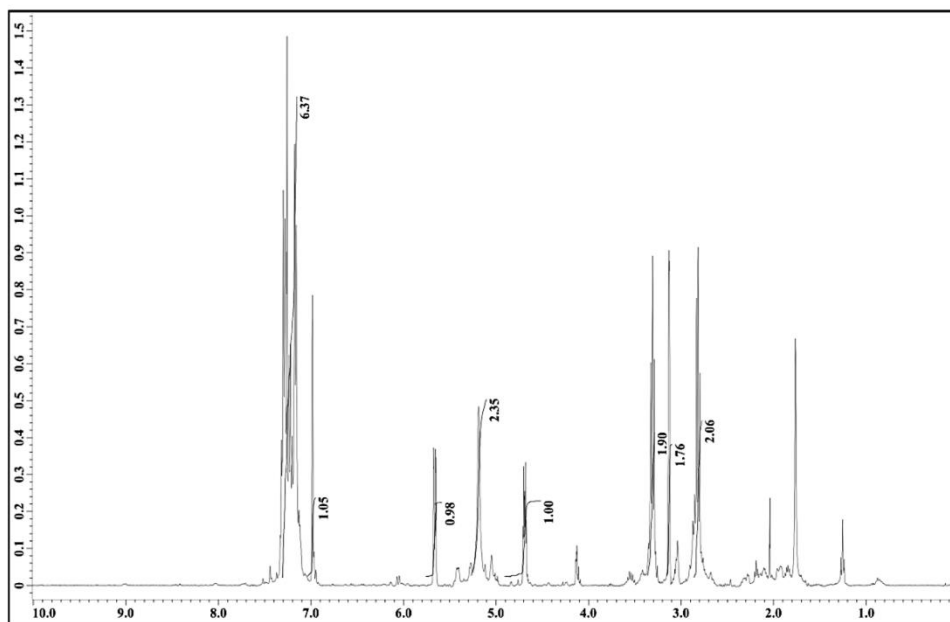
S8.20 Kinetic Measurements of *Gst*LDH

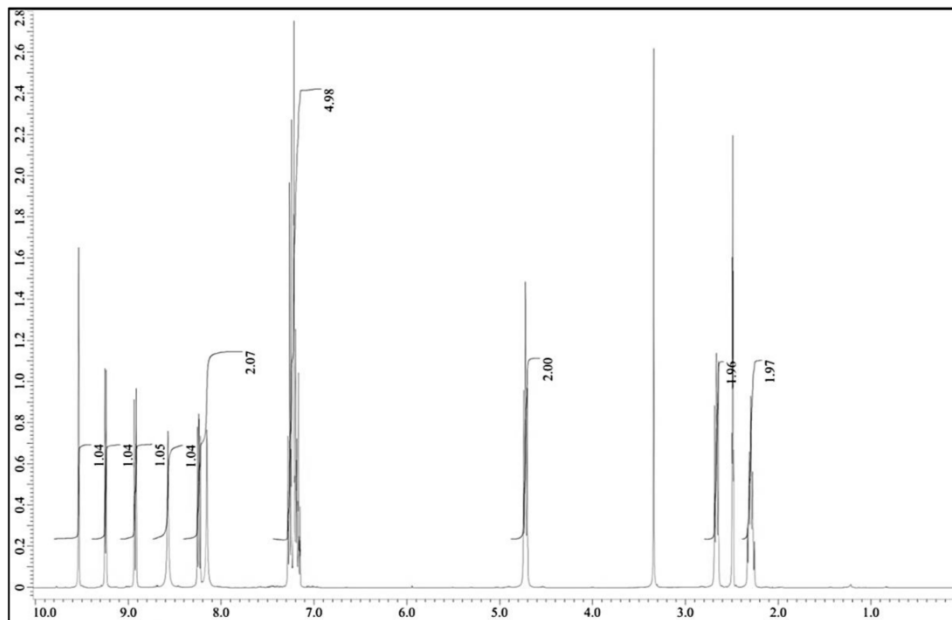
Kinetic measurements were performed in 100 mM Tris-HCl pH 8 at 45 °C for 30 min with (1) 0.5 mM NADH and varying pyruvate concentrations, (2) 5 mM NAD⁺ and varying L-lactate concentrations, (3) 60 mM pyruvate and varying NADH concentrations and (4) 100 mM L-lactate and varying NAD⁺ concentrations. The extinction coefficient used for NADH was 6.22 L*mmol⁻¹*cm⁻¹. Data were fitted to Michaelis-Menten equations using SigmaPlot 11.0. (Systat Software). All measurements were performed in triplicate. Controls lacked the enzyme, substrate, or cofactor. One unit of enzyme activity was defined as the amount of protein that converted 1 μmol of cofactor/min at 45 °C.

The activity of *Gst*LDH with NADPH (2 mM) and pyruvate (60 mM) was measured in 100 mM Tris-HCl pH 8 at 45 °C. The reaction was monitored at 340 nm and the extinction coefficient for NADPH was 6.22 L*mmol⁻¹*cm⁻¹.

P2NA⁺

P2NAH



P3NA⁺

P3NAH

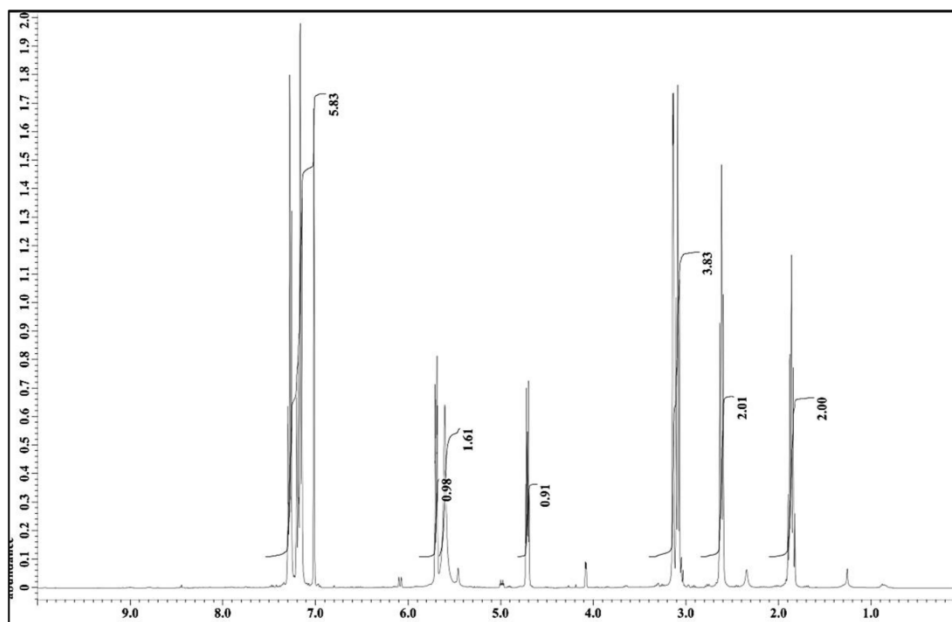


Figure S9. NMR of **A** P2NA⁺, **B** P2NAH, **C** P3NA⁺, and **D** P3NAH.

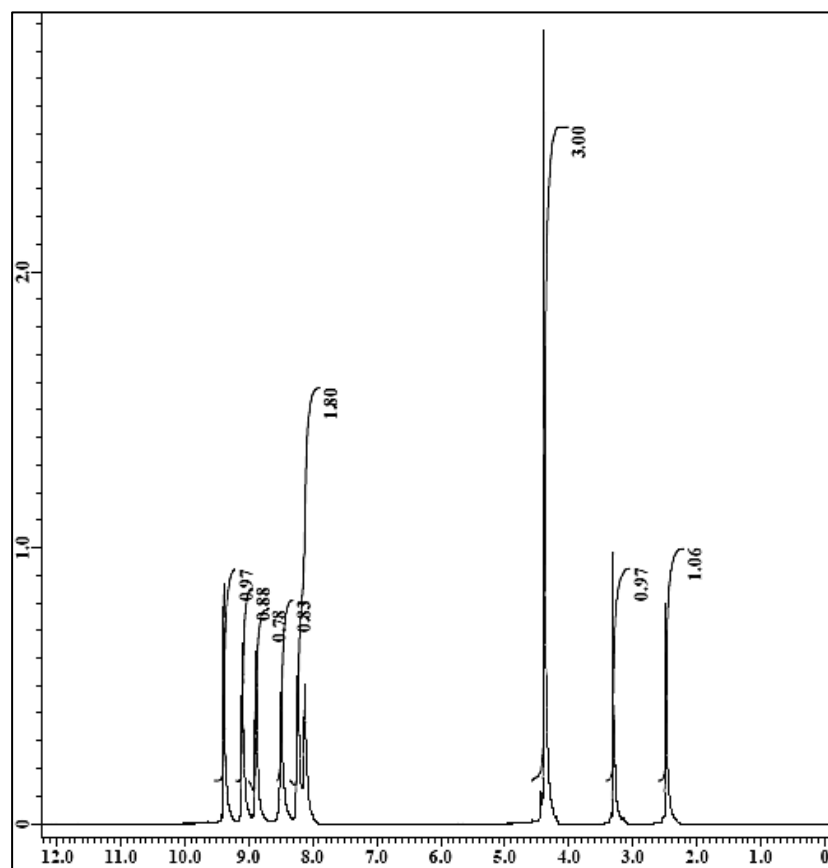
- (1) Ryan, J. D.; Fish, R. H.; Clark, D. S. *ChemBioChem* **2008**, *9*, 2579-2582.
- (2) Schirwitz, K.; Schmidt, A.; Lamzin, V. S. *Protein Sci.* **2007**, *16*, 1146-1156.
- (3) Fish, R. H.; Lo, C. H. *Angew. Chem. Int. Ed.* **2002**, *41*, 478-481.
- (4) Paul, C. E.; Hollmann, F. *Appl. Microbiol. Biotechnol.* **2016**, *100*, 4773-4778.
- (5) Mauzerall, D.; Westheimer, F. H. *J. Am. Chem. Soc.* **1955**, *77*, 2261-2264.
- (6) Karrer, P.; Stare, F. J. *Helv. Chim. Acta* **1937**, *20*, 418-423.
- (7) Nowak, C.; Beer, B. C.; Pick, A.; Roth, T.; Lommes, P.; Sieber, V. *Front Microbiol.* **2015**, *6*.
- (8) Knox, R. J.; Jenkins, T. C.; Hobbs, S. M.; Chen, S.; Melton, R. G.; Burke, P. J. *Cancer Res.* **2000**, *60*, 4179-4186.
- (9) Brewster, M. E.; Simay, A.; Czako, K.; Winwood, D.; Farag, H.; Bodor, N. *J. Org. Chem.* **1989**, *54*, 3721-3726.
- (10) Guterl, J.-K.; Garbe, D.; Carsten, J.; Steffler, F.; Sommer, B.; Reisse, S.; Philipp, A.; Haack, M.; Ruehmann, B.; Koltermann, A.; Kettling, U.; Brueck, T.; Sieber, V. *ChemSusChem* **2012**, *5*, 2165-2172.
- (11) Saha, S. K.; Uma, L.; Subramanian, G. *World J. Microbiol. Biotechnol.* **2005**, *21*, 877-881.
- (12) Nagao, T.; Mitamura, T.; Wang, X. H.; Negoro, S.; Yomo, T.; Urabe, I.; Okada, H. *J. Bacteriol.* **1992**, *174*, 5013-5020.
- (13) Vazquez-Figueroa, E.; Chaparro-Riggers, J.; Bommarius, A. S. *ChemBioChem* **2007**, *8*, 2295-2301.
- (14) Maurer, S. C.; Kuhnel, K.; Kaysser, L. A.; Eiben, S.; Schmid, R. D.; Urlacher, V. B. *Adv. Synth. Catal.* **2005**, *347*, 1090-1098.
- (15) Barstow, D. A.; Clarke, A. R.; Chia, W. N.; Wigley, D.; Sharman, A. F.; Holbrook, J. J.; Atkinson, T.; Minton, N. P. *Gene* **1986**, *46*, 47-55.
- (16) Studier, F. W. *Protein Expression Purif.* **2005**, *41*, 207-234.
- (17) Borst, N. SCHEMA-Rekombination von Cytochrom P450 Monooxygenasen der Enzymfamilie CYP101 und CYP102 zur Bereitstellung neuer Hydroxylaseaktivitäten. Ph.D. Thesis, Technical University of Munich, Straubing, 2016.
- (18) Opperman, D. J.; Piater, L. A.; van Heerden, E. *J. Bacteriol.* **2008**, *190*, 3076-3082.
- (19) Müller, J. M. M.Sc. Thesis, Technical University of Munich, Straubing, 2013.
- (20) Knaus, T.; Paul, C. E.; Levy, C. W.; De Vries, S.; Mutti, F. G.; Hollmann, F.; Scrutton, N. S. *J. Am. Chem. Soc.* **2015**, *138*, 1033-1039.
- (21) Laemmli, U. K. *Nature* **1970**, *227*, 680-685.
- (22) Steffler, F. Produktion und Entwicklung von Oxidoreduktasen für enzymatische Kaskadenreaktionen. Ph.D. Thesis, Technical University of Munich, Straubing, 2014.
- (23) Heringa, J. *Comput. Chem.* **1999**, *23*, 341-364.
- (24) Sievers, F.; Wilm, A.; Dineen, D.; Gibson, T. J.; Karplus, K.; Li, W.; Lopez, R.; McWilliam, H.; Remmert, M.; Söding, J.; Thompson, J. D.; Higgins, D. G. *Mol. Syst. Biol.* **2011**, *7*.
- (25) Goujon, M.; McWilliam, H.; Li, W. Z.; Valentin, F.; Squizzato, S.; Paern, J.; Lopez, R. *Nucleic Acids Res.* **2010**, *38*, W695-W699.
- (26) Kelley, L. A.; Mezulis, S.; Yates, C. M.; Wass, M. N.; Sternberg, M. J. E. *Nat. Protocols* **2015**, *10*, 845-858.
- (27) Wass, M. N.; Kelley, L. A.; Sternberg, M. J. E. *Nucleic Acids Res.* **2010**, *38*, W469-W473.

-
- (28) Milburn, C. C.; Lamble, H. J.; Theodossis, A.; Bull, S. D.; Hough, D. W.; Danson, M. J.; Taylor, G. L. *J. Biol. Chem.* **2006**, 281, 14796-14804.
- (29) Wang, W. Y.; Malcolm, B. A. *Biotechniques* **1999**, 26, 680-682.
- (30) Zhang, J. H.; Chung, T. D. Y.; Oldenburg, K. R. *J. Biomol. Screening* **1999**, 4, 67-73.
- (31) Rimmel, N. *Selektive ω -Oxidation aliphatischer Substrate - Charakterisierung von Monooxygenasen und Etablierung einer Biotransformationsplattform*. Ph.D. Thesis, Technical University of Munich, Straubing, 2016.
- (32) Rühmann, B.; Schmid, J.; Sieber, V. *J. Chromatogr. A* **2014**, 1350, 44-50.

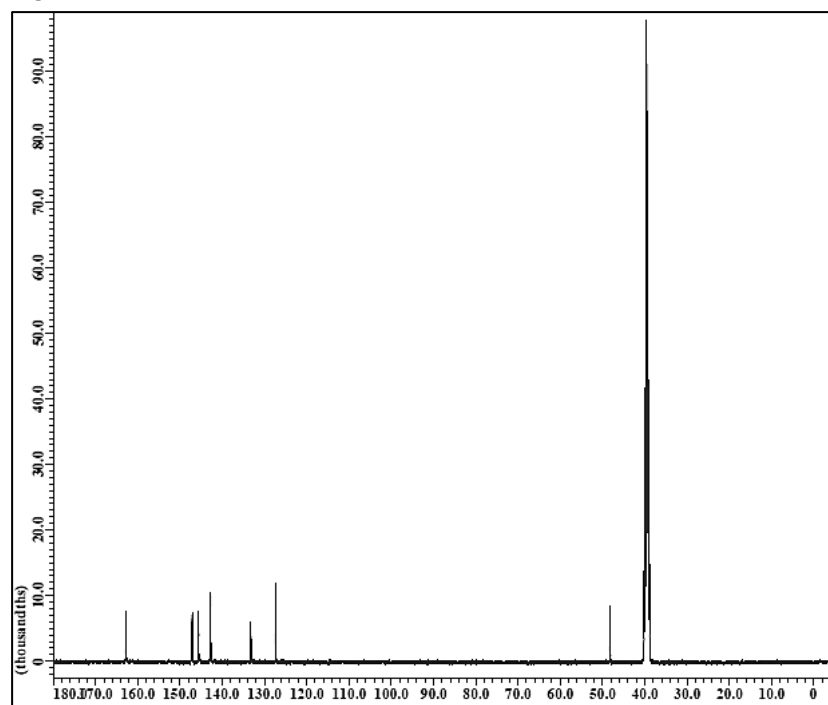
6.4 NMR of Biomimetic Cofactors

MNA⁺

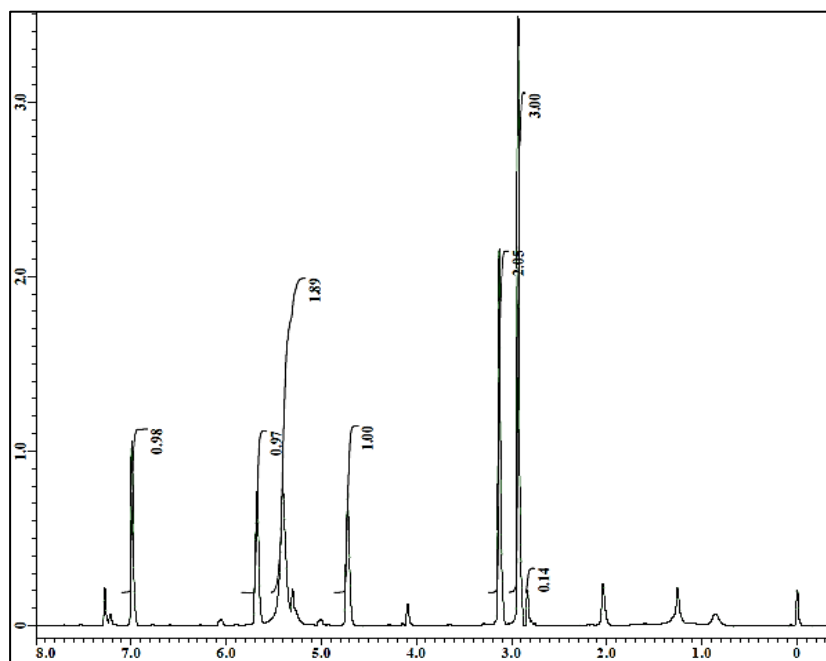
¹H

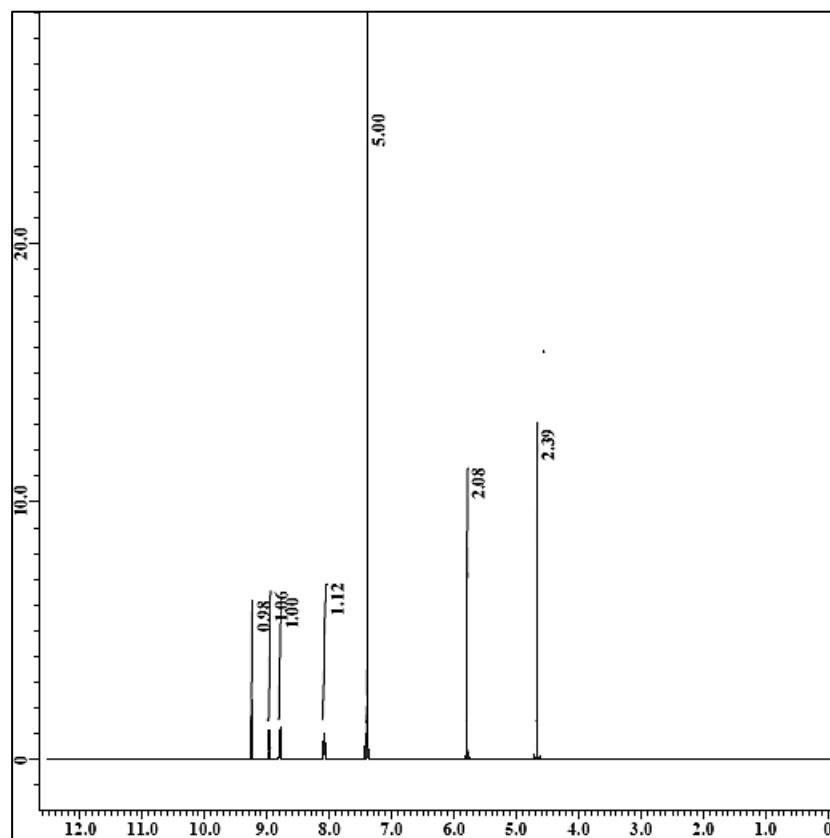
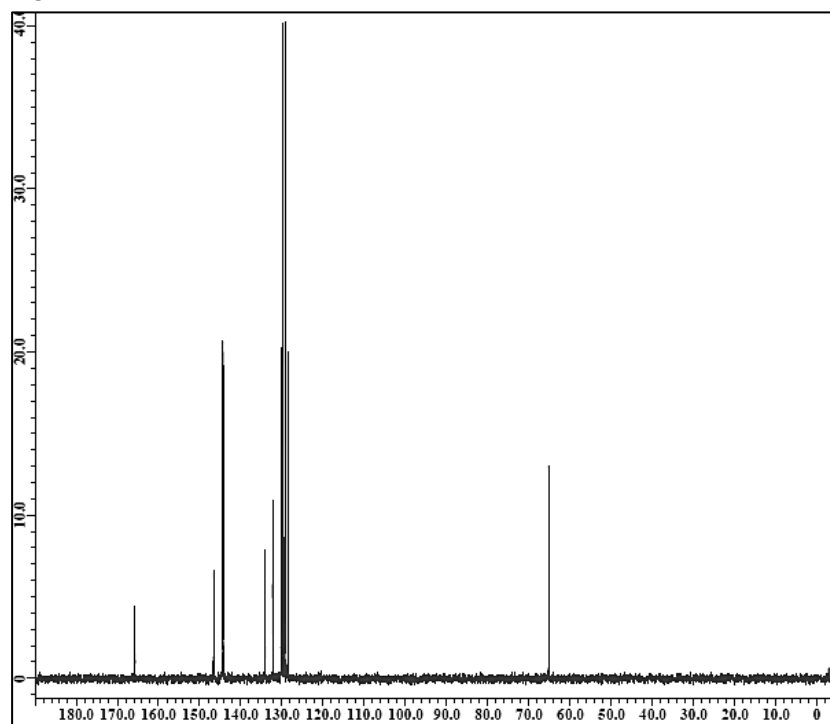


¹³C

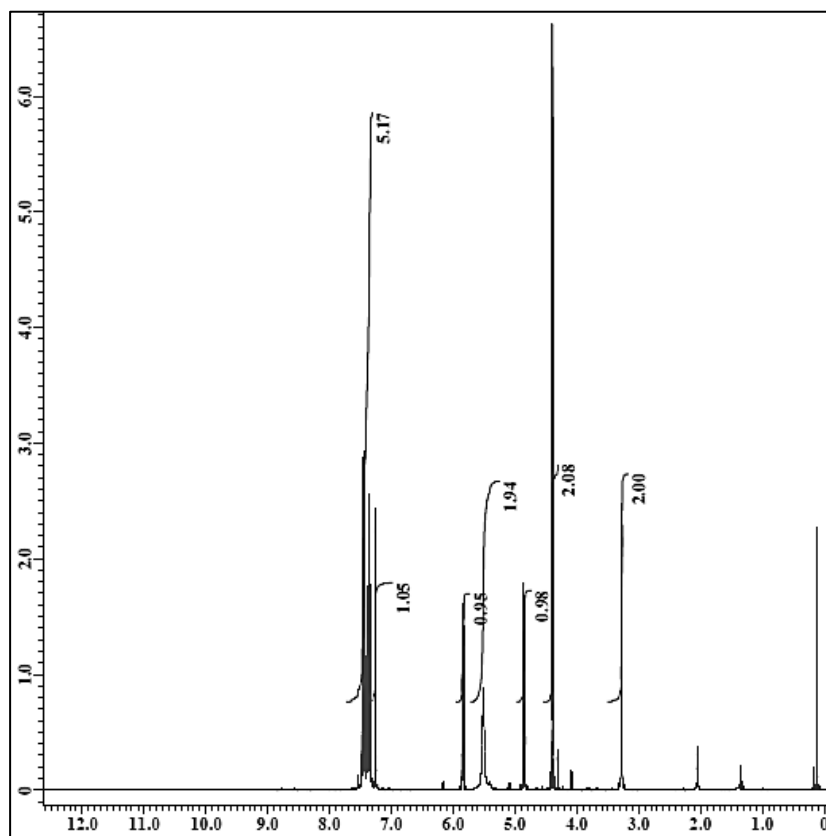
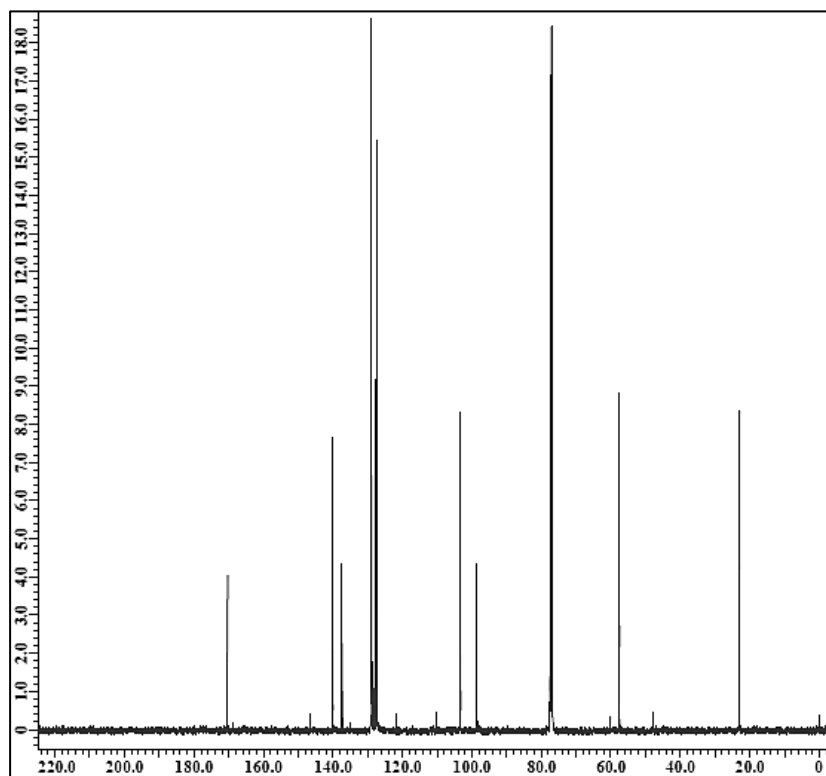


MNAH

 ^1H 

BNA⁺¹H¹³C

BNAH

 ^1H  ^{13}C 

6.5 List of Enzymes Additionally Investigated for the Activity with Biomimetic Cofactors

Table 11: Enzyme tested for activity with biomimetic cofactors within this work for which an activity was not detected.

Enzyme	Organism
Alanine dehydrogenase	<i>Bacillus subtilis</i>
Alanine dehydrogenase	<i>Thermus thermophiles</i>
Alcohol dehydrogenase CH yihu	<i>Escherichia coli</i>
Alcohol dehydrogenase yqhd	<i>Escherichia coli</i>
Alcohol dehydrogenase adhP	<i>Escherichia coli</i>
Alcohol dehydrogenase yjgb	<i>Escherichia coli</i>
Alcohol dehydrogenase LND/VKD/DIN/SNC/NND/CND	<i>Escherichia coli</i>
Alcohol dehydrogenase	<i>Geobacillus stearothermophilus</i>
Aldehyde dehydrogenase Alda	<i>Escherichia coli</i>
Aldehyde dehydrogenase SAD	<i>Escherichia coli</i>
Aldehyde dehydrogenase	<i>Thermoplasma acidophilum</i>
Butandiol dehydrogenase	<i>Bacillus cereus</i>
Lactate dehydrogenase (Serva order number: 27415.01)	<i>Porcine heart</i>
Uronate dehydrogenase	<i>Agrobacterium tumefaciens</i>
Uronate dehydrogenase	<i>Oceanicola granulosus</i>
Uronate dehydrogenase	<i>Streptomyces viridochromeogenes</i>
Xylose dehydrogenase	<i>Caulobacter crescentus</i>

Activity measurements of the different enzymes were carried out in 100 mM Tris-HCl pH 8 containing 5 mM NAD(P)⁺ or 15-50 mM oxidized biomimetic / 0.5-0.75 mM reduced cofactor and 5 mM substrate. Controls lacked enzyme, substrate, or cofactor. Reactions were monitored 358 nm (biomimetics) and 340 nm (NADH) for 1 h at 25 °C for 60 min. All enzymes were available at the Chair of Chemistry of Biogenic Resources (Technical University of Munich).

7 Abbreviations

%	Percent
Å	Ångstrom
°C	Degree Celsius
€	Euro
ϵ_{280}	Extinction Coefficient
μg	Microgram
μL	Microliter
μm	Micrometer
μM	Micromolar / Micromole per Liter
μmol	Micromole
A_{260}	Absorption at 260 nm
A_{280}	Absorption at 280 nm
ADH	Alcohol Dehydrogenase
Ala	Alanine
AlaDH	Alanine Dehydrogenase
AIDH	Glyceraldehyde Dehydrogenase
ALS	Acetolactate Synthase
APS	Ammonium Persulfate
Arg (One letter code: R)	Arginine
Asn (One letter code: N)	Asparagine
Asp (One letter code: D)	Aspartic Acid
BLAST	Basic Local Alignment Search Tool
<i>BmGDH-IV</i>	Glucose Dehydrogenase from <i>Bacillus megaterium</i>
Bn	Benzyl
BNA/H	1-Benzyl Nicotinamide and 1-Benzyl-1,4-dihydro Nicotinamide
BNA ⁺	1-Benzyl Nicotinamide
BNAH	1-Benzyl-1,4-dihydro Nicotinamide
bp	Base Pairs
<i>BsGDH E170K/Q252L</i>	Glucose Dehydrogenase E170K/Q252L from <i>Bacillus subtilis</i>
c	Concentration
¹³ C NMR	Carbon Nuclear Magnetic Resonance
carba NAD	Carba Nicotinamide Adenine Dinucleotide
Carl Roth	Carl Roth GmbH & Co. KG
CAS	Chemical Abstract Service
CO ₂	Carbon Dioxide
Cys (One letter code: C)	Cysteine
d	Optical Path Length
DA	Dalton
ddH ₂ O	Double Distilled Water
DHAD	Dihydroxy Acid Dehydratase

DNA	Deoxyribonucleic Acid
EC	Enzyme Class
<i>E. coli</i>	<i>Escherichia coli</i>
EDTA	Ethylenediaminetetraacetic Acid
<i>ee</i>	Enantiomeric Excess
ExPASy	ProtParam Tool
f	Dilution factor
FAD	Flavin Adenine Dinucleotide
FADH ₂	Dihydro Flavin Adenine Dinucleotide
FDH	Formate Dehydrogenase; especially Formate Dehydrogenase from <i>Candida boidinii</i>
FMN	Flavin Mononucleotide
g	Gram
G6P	Glucose-6-phosphate
G6PDH	Glucose-6-phosphate Dehydrogenase; especially Glucose-6-phosphate Dehydrogenase from <i>Saccharomyces cerevisiae</i>
GC	Gas Chromatography
GDH	Glucose Dehydrogenase
Glc	D-Glucose
Gln (One letter code: Q)	Glutamine
Glu (One letter code: E)	Glutamic Acid
GlucD	Glucarate Dehydratase
Gly (One letter code: G)	Glycine
<i>Gst</i> LDH	Lactate Dehydrogenase from <i>Geobacillus stearothermophilus</i>
h	Hour
¹ H NMR	Proton Nuclear Magnetic Resonance
H ₂ O	Water
H ₂ O ₂	Hydrogen Peroxide
HCl	Hydrochloric Acid
HCO ₂ ⁻	Hydrogencarbonate
HCOONH ₄	Ammonium Formate
HEPES	4-(2-Hydroxyethyl)-1-Piperazineethanesulfonic Acid
His (One letter code: H)	Histidine
HLADH	Horse Liver Alcohol Dehydrogenase
HPLC	High Performance Liquid Chromatography
Ile	Isoleucine
KARI	Ketolacid Reductoisomerase
<i>k</i> _{cat}	Catalytic Constant
<i>k</i> _{cat} / <i>K</i> _m	Catalytic Efficiency
kDA	Kilo Dalton
KDC	2-Ketoacid Decarboxylase
KDGA	2-Keto-3-Desoxygluconate Aldolase

KdgD	5-Keto-4-Deoxyglucarate Dehydratase
KgsalDH	Aldehyde Dehydrogenase
K_m	Michaelis–Menten Constant
kV	Kilovolt
L (unit)	Liter
L-Ala	L-Alanine
Leu (One letter code: L)	Leucine
LeuDh	Leucine Dehydrogenase
<i>Lp</i> Nox	NADH Oxidase from <i>Lactobacillus pentosus</i>
Lys (One letter code: K)	Lysine
M	Molar / Mole per Liter
mA	Milliampere
m_{DNA}	DNA used for Transformation
Mg	Milligram
min	Minute
mL	Milliliter
mM	Millimolar / Millimole per Liter
mmol	Millimole
MNA/H	N-Methyl Nicotinamide and N-Methyl-1,4-dihydro Nicotinamide
MNA ⁺	N-Methyl Nicotinamide
MNAH	N-Methyl-1,4-dihydro Nicotinamide
mol	Mole
MOPS	3-(N-Morpholino)Propanesulfonic Acid
ms	Millisecond
MS	Mass-spectrometer
MW	Molecular Weight
Na ₂ S ₂ O ₄	Sodium Dithionite
NaCN	Soidum Cyanide
NAD(P)/H	Nicotinamide Adenine Dinucleotide (Phosphate) and Dihydro Nicotinamide Adenine Dinucleotide (Phosphate)
NAD/H	Nicotinamide Adenine Dinucleotide and Dihydro Nicotinamide Adenine Dinucleotide
NAD ⁺	Nicotinamide Adenine Dinucleotide
NADH	Dihydro Nicotinamide Adenine Dinucleotide
NADP/H	Nicotinamide Adenine Dinucleotide Phosphate and Dihydro Nicotinamide Adenine Dinucleotide Phosphate
NADP ⁺	Nicotinamide Adenine Dinucleotide Phosphate
NADPH	Dihydro Nicotinamide Adenine Dinucleotide Phosphate
NCBI	National Center for Biotechnology Information
$n_{Colonies}$	Number of Colonies
NH ₃	Ammonia
nm	Nanometer

nmol	Nanomole
NMR	Nuclear Magnetic Resonance
NOX	NADH Oxidase
O ₂	Molecular Oxygen
OD	Optical Density
OTf	Triflate
OYE	Old Yellow Enzyme
OYERo2a	Old Yellow Enzyme OYERo2a from <i>Rhodococcus opacus</i> 1CP
P2NA/H	3-Carbamoyl-1-phenethylpyridin-1-ium Chloride and 1-Phenethyl-1,4-dihydropyridine-3-carboxamide
P2NA ⁺	3-Carbamoyl-1-phenethylpyridin-1-ium Chloride
P2NAH	1-Phenethyl-1,4-dihydropyridine-3-carboxamide
P3NA/H	3-Carbamoyl-1-(3-phenylpropyl)pyridin-1-ium bromide and 1-(3-phenylpropyl)-1,4-dihydropyridine-3-carboxamide
P3NA ⁺	3-Carbamoyl-1-(3-phenylpropyl)pyridin-1-ium Bromide
P3NAH	1-(3-Phenylpropyl)-1,4-dihydropyridine-3-carboxamide
P450-BM3	Cytochrome P450 from <i>Bacillus megaterium</i>
P450cam	Cytochrome P450 from <i>Pseudomonas putida</i>
PCR	Polymerase Chain Reaction
PDB	RCSB Protein Data Bank
PDC	Pyruvate Decarboxylase
Phe	Phenylalanine
PHYRE ²	Protein Homology / analogY Recognition Engine V 2.0
PLP	Pyridoxal5'-phosphate
ppm	Chemical Shift in Parts Per Million
Pro	Proline
rpm	Rounds per Minute
s	Second
SDS	Sodium Dodecyl Sulfate
SDS-PAGE	Sodium Dodecyl Sulfate Polyacrylamide Gel Electrophoresis
Ser (One letter code: S)	Serine
Serva	Serva Electrophoresis GmbH
SsGDH	Glucose Dehydrogenase from <i>Sulfolobus solfataricus</i>
StyA1	Styrene Monooxygenase StyA1 from <i>Rhodococcus opacus</i> 1CP
StyB	Styrene Monooxygenase StyB from <i>Rhodococcus opacus</i> 1CP
TAE	Tris-Acetate-EDTA
TaGDH	Glucose Dehydrogenase from <i>Thermoplasma acidophilum</i>
TBADH	Alcohol Dehydrogenase from <i>Thermoanaerobacter brockii</i>
T _E	Transformation efficiency
Thr	Threonine
TMS	Tetramethylsilane
Tris	Tris(hydroxymethyl)aminomethane

Tris-HCl	Tris Puffer – pH adjusted with Hydrochloric Acid
Trp (One letter code: W)	Tryptophan
TsER	Enoate Reductase from <i>Thermus scotoductus</i>
TSP	Trimethylsilylpropanoic Acid
Tyr	Tyrosine
U	Unit / Enzyme Activity $\mu\text{mol}/\text{min}$
UDH	Uronate Dehydrogenase
UHPLC	Ultra High Performance Liquid Chromatography
UV	Ultraviolet
v/v	Volume per Volume
v/w	Volume per Weight
Val	Valine
v_{max}	Maximum Reaction Rate
VWR	VWR International GmbH
w/v	Weight per Volume
w/w	Weight per Weight
YASARA	Yet Another Scientific Artificial Reality Application

8 List of Figures

Figure 1: A) The natural nicotinamide cofactors, NADH and NADPH, are composed of a nicotinamide moiety, a ribose, a pyrophosphate, and an adenosine. NADP/H is phosphorylated at C2 of the riboside compared to NAD/H. B) The C4 of the nicotinamide moiety releases or accepts the hydride, respectively.....	8
Figure 2: The Rossmann fold of glucose dehydrogenase from <i>Sulfolobus solfataricus</i> (MILBURN et al. 2006) contains three β -sheets and two α -helices (green colour). The first three β -sheets are connected by α -helices. Additionally, this pattern is duplicated. The GXGXXG motif is highlighted in yellow. Additionally, NAD(P)/H binds an extended conformation and the orientation including hydrogen bonds and van der Waals interactions is similar in a classical cofactor binding domain.	9
Figure 3: A) Acid catalyzed decomposition of NAD(P)H. B) Degradation of NAD(P) ⁺ under alkaline conditions. (HENTALL et al. 2001; OPPENHEIMER 1982; OPPENHEIMER 1994; OPPENHEIMER & KAPLAN 1974).	10
Figure 4: Interaction of NADH with phosphate (from the buffer) following cofactor degradation. (ALIVISATOS et al. 1964).....	11
Figure 5: Dynamic kinetic resolution applying a Baeyer-Villiger monooxygenase for the synthesis of α -hydroxy esters. Cofactor regeneration was achieved with glucose-6-phosphate (G6P) and glucose-6-phosphate dehydrogenase (G6PDH). (RIOZ-MARTINEZ et al. 2011; SIMON et al. 2013)	12
Figure 6: Alcohol dehydrogenase catalyzed redox reaction for the introduction of an alcohol group in the overall synthesis to atorvastatin. Cofactor regeneration was achieved with D-glucose (Glc) and glucose dehydrogenase (GDH). (MA et al. 2010; SIMON et al. 2013)	13
Figure 7: Alcohol dehydrogenase dependent reaction to (R)-tetrahydrothiophene-3-ol for the overall synthesis of sulopenem. (LIANG et al. 2010; SIMON et al. 2013)	13
Figure 8: Ene reductase catalyzed reaction for the overall synthesis of α -tocopherol or antibiotics. Cofactor regeneration was achieved with D-glucose (Glc) and glucose dehydrogenase (GDH). (SIMON et al. 2013; STUECKLER et al. 2010).....	14
Figure 9: One pot reaction combining various enzymes for the bioamination of primary alcohols. The coenzyme pyridoxal 5'-phosphate (PLP) need to be additionally added for the animation reaction. (SATTLER et al. 2012).....	14
Figure 10: Multi-step reaction cascade for the overall synthesis of ethanol or isobutanol, respectively. The following enzymes were used: glucose dehydrogenase (GDH), dihydroxy acid dehydratase (DHAD), 2-keto-3-desoxygluconate aldolase (KDGA), glyceraldehyde dehydrogenase (AIDH), pyruvate decarboxylase (PDC), alcohol dehydrogenase (ADH), acetolactate synthase (ALS), ketolacid reductoisomerase (KARI), and 2-ketoacid decarboxylase (KDC).(GUTERL et al. 2012)....	15
Figure 11: Multistep synthesis combining various enzymes for the synthesis of α -ketoglutarate. The following enzymes were used: uronate dehydrogenase (UDH), glucarate dehydratase (GlucD), 5-keto-4-deoxyglucarate dehydratase (KdgD), aldehyde dehydrogenase (KgsalDH), and NADH oxidase (NOX). (BEER et al. 2017).....	16
Figure 12: Biomimetic cofactors synthesized in the beginning of the 20 th century. (KARRER & STARE 1937)	16
Figure 13: General synthesis of oxidized and reduced biomimetic cofactors. (PAUL et al. 2013).....	17
Figure 14: Investigation of various semi-synthetic nicotinamide cofactors with variations at C3 of the nicotinamide ring. (ANDERSON et al. 1959)	17
Figure 15: By replacing the ribotide oxygen with a methylene, the more stable biomimetic carba NAD was designed. (SLAMA & SIMMONS 1988; SLAMA & SIMMONS 1989)	18
Figure 16: Synthetic cofactor developed by Ansell and coworkers that was most active with HLADH. (ANSELL et al. 1999a; ANSELL et al. 1999b)	19
Figure 17: Process developed by Lo and Fish using a HLADH catalyzed reaction for the synthesis of a chiral alcohol. (LO & FISH 2002).....	19
Figure 18: The P450 mutant was able to use BNAH as the cofactor. Regeneration was done with a rhodium catalysts. (RYAN et al. 2008)	20
Figure 19: Conversion of various biomimetic cofactors by enoate reductase. (PAUL et al. 2013).....	21

Figure 20: Comparison of styrene catalyzed reactions using NADH or BNAH as cofactor, respectively. (PAUL et al. 2015).....	21
Figure 21: Variation of Trp302 position depending on the size of the cofactor. The conformation for the natural cofactors is indicated in red and for the biomimetic cofactor (BNA/H) is colored in blue. (KNAUS et al. 2015).....	22
Figure 22: A) Scheme of an enzyme-coupled cofactor regeneration. B) Application of GDH for the cofactor regeneration in the overall synthesis to actinol. (HUMMEL & GRÖGER 2014; WADA et al. 2003).....	24
Figure 23: Synthesis of <i>tert</i> L-leucine from trimethylpyruvic acid by LeuDH. FDH was used for cofactor regeneration. (GRÖGER et al. 2012; SHAKED & WHITESIDES 1980).....	24
Figure 24: A) Scheme of a substrate-coupled cofactor regeneration. B) Synthesis of the desired chiral alcohol and acetone in the regeneration reaction using an ADH as production as well as regeneration enzyme. (HUMMEL & GRÖGER 2014; KEINAN et al. 1987)	26
Figure 25: Scheme of a reaction-internal cofactor regeneration. (HUMMEL & GRÖGER 2014).....	26
Figure 26: <i>Ss</i> GDH catalyzed reaction using D-glucose as substrate with NAD(P) ⁺ as cofactor. (MILBURN et al. 2006)	27
Figure 27: Various sugars for which an activity with <i>Ss</i> GDH was tested. (LAMBLE et al. 2003).....	27
Figure 28: Water-forming NADH oxidase (NOX) catalyzed reaction with the cofactor NADH resulting in H ₂ O as side product.	28

9 List of Tables

Table 1: Overview on costs of NAD(P)/H (obtained from Carl Roth GmbH & Co. KG online on 10.11.2018)...	12
Table 2: Listing of the equipment used in this work.	31
Table 3: Listing of the software and databases used in this work.	33
Table 4: Overview of chemicals used in this work in detail.	34
Table 5: Listing of enzymes used in this work.	37
Table 6: Listing of kits and standards used in this work.	38
Table 7: Listing of antibiotics used in this work.	39
Table 8: Listing of bacterial strains that were used in this work.	40
Table 9: Listing of plasmids used in this work.	40
Table 10: Chemical solvents used for NMR analysis with significant signals including tetramethylsilane (TMS) at 0 ppm or trimethylsilylpropanoic acid (TSP) at 0 ppm.	46
Table 11: Enzyme tested for activity with biomimetic cofactors within this work for which an activity was not detected.	148

Curriculum vitae

Claudia Nowak

geboren am 26.11.1987 in Wismar



- Aug. 1998 – Juli 2007** **Große Stadtschule Geschwister-Scholl-Gymnasium, Wismar, Deutschland**
Abschluss: Allgemeine Hochschulreife
Durchschnittsnote: 1,3
- Okt. 2007 – Okt. 2011** **Ernst-Moritz-Arndt-Universität Greifswald, Deutschland**
Grundstudium: Biochemie
Hauptstudium: Biochemie mit den Schwerpunkten Biotechnologie & Enzymkatalyse unter der Leitung von Prof. Dr. Bornscheuer und Genetik unter der Leitung von Prof. Dr. Hammerschmidt
- Okt. 2011 – Juni 2012** **Diplomarbeit an der Universität Oviedo, Spanien**
Thema der Diplomarbeit: „Chemoenzymatic Synthesis of Optically Active Diastereomeric Amines“
- Juni 2012** **Abschluss als Diplom-Biochemikerin (Note: 2,1)**
- Okt. 2012 – Juli 2016** **Promotion an der Technischen Universität München, Deutschland**
Lehrstuhl für Chemie Biogener Rohstoffe unter der Leitung von Prof. Dr. Sieber
Thema der Doktorarbeit: Entwicklung von Nikotinamid-Adenin-Dinukleotid-Derivaten und deren enzymatische Umsetzung
- seit Aug. 2017** **Wissenschaftlicher Mitarbeiter (Pharmacovigilance Advisor) bei Dr. Ebeling & Assoc. GmbH, Hamburg, Deutschland**

Danksagung

Ich möchte all den lieben Menschen danken, die an dem Gelingen dieser Dissertation mitgewirkt haben:

Ein besonderer Dank gilt Prof. Volker Sieber, für seine ausgiebige Unterstützung. Ich danke dir für die Anleitung, die Kritik und die kritischen Fragen, wenn es auf meiner Forschungsreise einmal nicht mehr voranging. Vielen Dank für deine Zeit und Mühen, die du in meine Arbeit investiert hast.

Ein großes Dankeschön möchte ich an Prof. Zollfrank richten, der sich bereit erklärt hat, das Koreferat zu übernehmen und sich die Zeit genommen hat, ein Gutachten zu verfassen. Ebenfalls möchte ich Prof. Gaderer danken, für die Bereitschaft sich an meiner Dissertationskommission zu beteiligen.

Lieber André, liebe Barbara, ohne euch hätte ich manchmal kein Licht am Ende des Tunnels gesehen. Danke für die offenen Ohren, das Lachen, die konstruktive Kritik und die vielen Ideen, die mir immer wieder den nötigen Aufschwung gegeben haben. Liebe Petra, ich danke dir, dass du mir immer mit Rat und Tat zur Seite gestanden hast. Lieber Broder, lieber Jochen, ihr habt das Team komplett gemacht.

Ein großer Dank geht an alle Mitdoktoranden sowie alle Mitarbeiterinnen und Mitarbeiter am Lehrstuhl für die außerordentlich gute Zusammenarbeit, sowie die kleinen und großen Hilfestellungen.

Nina und Sabine sowie all meinen Lieblingsstraubingern (Franz, Fini, Wolfi, Toni, Bernhard, Mika, Janne, Marcel, Johanna, Nadine, Sepp, Lea...) danke ich für eine einzigartige Freizeit, die ich in Straubing mit euch haben durfte. Ich werde Niederbayern nie vergessen!

Liebe Annina, wie hast du es so schön gesagt: Freundschaft ist eine Seele in zwei Körpern. Danke, dass es dich gibt!

Ganz besonderer Dank gilt meinen Eltern und meiner Schwester, die immer an mich geglaubt haben und mich auf meinem Weg bedingungslos unterstützt und bestärkt haben. Von Herzen: Danke für alles!